

**Solid mould surface characteristics in relation to chocolate  
adhesion and the influence of processing conditions.**

Esther Leonie Keijbets

*Submitted in accordance with the requirements for the degree of Doctor in Philosophy*

The University of Leeds  
School of Food Science and Nutrition  
September 2009

*The candidate confirms that the work submitted is her own and that appropriate credit has been given where reference has been made to the work of others.*

*This copy has been supplied on the understanding that it is copyright material and that no quotation from the thesis may be published without proper acknowledgement.*

## ACKNOWLEDGEMENTS

This thesis is the result of four years of research at the Procter Department of Food Science (now School of Food Science and Nutrition) of the University of Leeds, UK, and could not have been accomplished without the invaluable support of a number of people. First of all I would like to express my sincere gratitude to Dr. Jianshe Chen and Prof. Eric Dickinson for their supervision, involvement, constructive discussions and critical feedback which have guided me through this research. I am also extremely grateful to my industrial sponsor, Nestlé PTC York, and in particular to Dr. Joselio Vieira, Dr. Mark Fowler and Dr. Jeremy Hargreaves for valuable discussions and support throughout this research.

I would like to give special acknowledgements to Mike Leadbeater (Nestlé PTC) for allowing me to use his incredible knowledge regarding the materials used in this research as well as for his technical support and collaboration, to Ilaria Ferrari (Nestlé PTC) for the generation of the C-Cell data, and to Derek Harvey, Jean-Francois Favey, David Coleman and Denise Godson for their commitment, technical advice and hard work during the pilot plant (aeration) trials.

I am grateful to Dr. Hugo Christenson (University of Leeds) for introducing the concepts of contact angle and surface tension measurements, and to Barneby Hoare for initial work on the surface energy determination of chocolate. I would like to thank all the members of staff and research students from the Procter Department of Food Science, and in particular the Colloids group, for their discussions and collaborations. Most of all Mr Phillip Nelson, for designing and building pieces of equipment without which this research would not have been possible. To Paul, Stuart, Betty, Ian and Dave I would like to say thank you for both technical and moral support.

Without the silent support and encouragement of friends and family these past four years would not have been the exciting but challenging journey that it was. Thank you Janine, Thomas, Hassan, Georgious and Joe, for your friendship and many social Friday's. Laureline, you are not only an (ex-) colleague but also a great friend and I have enjoyed sharing many interesting discussions and both glorious and disappointing moments. To my hockey team I have to say thank you for sticking with me during the last couple of months and having faith in me.

Dan is er alleen nog familie die ik wil bedanken. Henriette en Daaf voor hun ondersteuning en begrip tijdens de afgelopen vier jaar. Henriette en Kersten voor de telefoontjes, opbeurende kaartjes en het medeleven op afstand maar toch dichtbij. Papa en mama, voor jullie zijn bijna geen woorden. Bedankt voor alle hulp, het eindeloze leeswerk en de correcties en vooral het altijd er zijn. En dan Lars, ik denk niet dat ik dit zonder jouw had kunnen bereiken. Samen met mij heb jij dit bereikt, en ik ben je dan ook extreem dankbaar voor alle geduld, schoonmaak partijen, maaltijden en gewoon je vriendschap.



## ABSTRACT

Crystallization of cocoa butter in the correct polymorphic form (Form V) leads to a volumetric contraction of tempered chocolate during solidification and aids in the ease of the demoulding process. Specific steps during chocolate bar manufacturing may result in an increased adhesion between chocolate and mould surface, causing intermittent problems in demoulding.

Adhesion is an important physical phenomenon commonly observed in many food-related situations. With respect to chocolate adhesion it is expected that the balance of the adhesion force between the chocolate and the mould and the cohesion force within the chocolate itself determines the stickiness at the chocolate–mould interface during demoulding. The research presented investigated the effect of surface thermodynamics and processing conditions on the observed extent of adhesion of (aerated) chocolate to four different mould materials (quartz glass, stainless steel, polycarbonate, and polytetrafluoroethylene (PTFE)). Surface energy of solid mould materials was calculated from experimental surface tension and contact angle data. An experimental set-up build around a Texture Analyser was developed for the experimental surface adhesion force determination, using a simple separation test between the solidified chocolate and a mould probe. Process conditions specific to the moulding and demoulding phases of the commercial chocolate manufacturing process have been investigated using this set-up.

Surface energy (thermodynamics) has been shown to be the major factor controlling the adhesion between chocolate and a mould material. Chocolate–mould adhesion can be minimized if the total surface energy of the mould material is  $< 30 \text{ mN m}^{-1}$ , and the electron donor component  $\sim 15 \text{ mN m}^{-1}$ . High surface energy materials are assumed to produce more compact crystal networks with a resulting increase in crystal–crystal interactions being responsible for difficulties demoulding. Processing parameters had a significant impact on the crystallization and solidification processes, and are therefore regarded as the key determining factors of chocolate–mould interactions. Demoulding can be optimised by pre-heating the mould under controlled environmental conditions (% RH, 25–30 °C) and by applying a cooling temperature of 10–15 °C.

Significant differences were observed between standard and aerated chocolate systems. It was shown that aeration lowers the cohesive or mechanical strength of the chocolate sample, consequently reducing the surface adhesion. Possible mechanisms proposed to impact surface adhesion of aerated chocolate, are the heat transfer coefficient of the mould material and the presence of water vapour at the mould surface which interacts with the CO<sub>2</sub> gas used for the chocolate aeration. Edible coatings can reduce the surface adhesion, but often have negative effects on chocolate surface characteristics. Further optimisation is required before edible coatings can be applied as a surface modification technique.

# CONTENTS

<b>CHAPTER 1 INTRODUCTION .....</b>	<b>1</b>
1.1    OBJECTIVE AND STRATEGY.....	1
1.2    OUTLINE OF THESIS .....	3
<b>CHAPTER 2 LITERATURE REVIEW .....</b>	<b>4</b>
2.1    CHOCOLATE .....	4
2.1.1    History of chocolate .....	4
2.1.2    Chocolate ingredients.....	5
2.1.2.1    Cocoa butter.....	6
2.1.2.2    Sugar.....	7
2.1.2.3    Milk components .....	8
2.1.2.4    Other components .....	10
2.1.2.4.1    Surfactants or surface active agents .....	10
2.1.2.4.2    Flavouring agents .....	12
2.1.3    Crystallization .....	13
2.1.3.1    Nucleation .....	15
2.1.3.1.1    Primary Homogeneous Nucleation.....	15
2.1.3.1.2    Primary Heterogeneous Nucleation.....	16
2.1.3.1.3    Secondary Nucleation.....	18
2.1.3.2    Fat crystallization .....	18
2.1.3.2.1    Cocoa butter polymorphism .....	19
2.1.3.2.2    Cocoa butter crystallization.....	22
2.1.3.2.3    Cocoa butter microstructure .....	26
2.1.3.3    Chocolate crystallization.....	28
2.1.3.3.1    Chocolate microstructure .....	31
2.1.4    Processing.....	36
2.1.4.1    Tempering or pre-crystallization.....	37
2.1.4.2    Moulding, cooling and demoulding.....	39
2.1.4.2.1    Chocolate moulding .....	40
2.1.4.2.2    Chocolate cooling.....	41
2.1.4.2.3    Chocolate demoulding.....	42

2.2	ADHESION .....	45
2.2.1	Adhesion versus stickiness.....	45
2.2.2	Cohesion and adhesion.....	46
2.2.3	Theories of adhesion .....	47
2.2.4	Molecular adhesion .....	50
2.3	SURFACE FREE ENERGY.....	52
2.3.1	Thermodynamics.....	52
2.3.1.1	<i>Gibbs dividing plane</i> .....	54
2.3.1.2	<i>Thermodynamics of interfaces</i> .....	56
2.3.1.3	<i>Adsorption at the solid surface</i> .....	57
2.3.2	Solid surface free energy.....	58
2.3.2.1	<i>Surface tension</i> .....	60
2.3.2.2	<i>Contact angle</i> .....	61
2.3.2.2.1	Wetting or spreading .....	64
2.3.2.2.2	Thermodynamics of wetting.....	64
2.4	THERMODYNAMICS VS PRACTICAL ADHESION .....	67
<b>CHAPTER 3 MATERIALS AND METHODS.....</b>		<b>70</b>
3.1	INTRODUCTION.....	70
3.2	MATERIALS .....	70
3.2.1	Chocolate systems.....	70
3.2.1.1	<i>Cocoa butter</i> .....	71
3.2.1.2	<i>Dark chocolate</i> .....	72
3.2.1.3	<i>Milk chocolate</i> .....	73
3.2.2	Solid mould materials.....	73
3.2.2.1	<i>Polycarbonate</i> .....	74
3.2.2.2	<i>Stainless steel</i> .....	75
3.2.2.3	<i>Polytetrafluoroethylene (PTFE)</i> .....	76
3.2.2.4	<i>Quartz glass</i> .....	76
3.2.1	Contact angle liquids.....	77
3.2.2	Thin film coating formulation.....	78
3.2.2.1	<i>Hydrocolloids</i> .....	78
3.2.2.2	<i>Lipids</i> .....	79
3.2.2.3	<i>Plasticizers</i> .....	80

3.3	METHODS .....	81
3.3.1	Surface energy determination.....	82
3.3.1.1	<i>Surface tension of liquids</i> .....	82
3.3.1.2	<i>Contact angles on solid surfaces</i> .....	84
3.3.1.3	<i>Surface energy of solid surfaces</i> .....	86
3.3.1.3.1	Zisman critical surface tension approach .....	87
3.3.1.3.2	Fowkes surface tension component approach .....	88
3.3.1.3.3	Owens and Wendt geometric mean approach .....	89
3.3.1.3.4	Van Oss, Chaudhury and Good approach .....	90
3.3.1.3.5	Della Volpe and Siboni modified acid–base approach .....	91
3.3.1.3.6	Equation of state (EQS) approach .....	92
3.3.1.4	<i>Work of Adhesion</i> .....	93
3.3.1.5	<i>Wetting Envelope</i> .....	93
3.3.2	Chocolate–mould adhesion determination.....	94
3.3.2.1	<i>Probe geometry development</i> .....	96
3.3.2.2	<i>Experimental adhesion force</i> .....	98
3.3.2.3	<i>Chocolate crystallization</i> .....	101
3.3.2.4	<i>Cohesive–adhesive failure</i> .....	102
3.3.2.5	<i>Chocolate processing conditions</i> .....	103
3.3.2.6	<i>Chocolate and mould parameters</i> .....	106
3.3.3	Moisture sorption .....	109
3.3.4	Aeration of chocolate .....	110
3.3.4.1	<i>Experimental adhesion force of aerated chocolate systems</i> .....	112
3.3.4.2	<i>Physical characterisation of aerated chocolate systems</i> .....	112
3.3.4.3	<i>Structural characterisation of aerated chocolate systems</i> .....	113
3.3.5	Thin film coating preparation.....	114
3.3.5.1	<i>Hydrocolloid coatings</i> .....	115
3.3.5.2	<i>Lipid coatings</i> .....	116
3.3.5.3	<i>Plasticizer and multicomponent coatings</i> .....	117
3.3.6	Solid surface topology.....	117

**CHAPTER 4 SURFACE ENERGY INVESTIGATION OF CHOCOLATE ADHESION TO SOLID MOULD MATERIALS..... 118**

4.1	INTRODUCTION.....	118
4.2	MATERIALS AND METHODS.....	118

4.2.1	Materials.....	118
4.2.2	Methods.....	119
4.3	RESULTS.....	120
4.3.1	Surface tension .....	120
4.3.1.1	<i>Surface tension components</i> .....	120
4.3.1.2	<i>Surface tension of chocolate systems</i> .....	121
4.3.1.3	<i>Relation between surface tension and temperature</i> .....	124
4.3.2	Contact angle.....	126
4.3.2.1	<i>Advancing contact angle of probe liquids on mould surfaces</i> .....	126
4.3.2.2	<i>Advancing contact angle of probe liquids on chocolate surfaces</i> .....	128
4.3.2.3	<i>Advancing contact angles of model chocolate systems</i> .....	131
4.3.2.4	<i>Relation between contact angle and temperature</i> .....	132
4.3.2.5	<i>Contact angle hysteresis</i> .....	133
4.3.2.5.1	<i>Surface microstructure</i> .....	133
4.3.3	Surface energy of solid mould materials.....	134
4.3.3.1	<i>Semi-empirical approaches</i> .....	135
4.3.3.2	<i>Van Oss, Chaudhury and Good approach</i> .....	137
4.3.3.3	<i>Temperature</i> .....	140
4.3.4	Surface energy of chocolate .....	143
4.3.4.1	<i>Effect of crystallization</i> .....	143
4.3.4.2	<i>Effect of ingredients</i> .....	145
4.3.4.3	<i>Effect of cooling temperature</i> .....	148
4.3.5	Wetting envelope.....	150
4.3.6	Adhesion of chocolate to mould surfaces.....	151
4.3.6.1	<i>Experimental surface adhesion</i> .....	151
4.3.6.2	<i>Surface hydrophilicity</i> .....	156
4.3.6.3	<i>Work of adhesion</i> .....	158
4.3.7	Comparison of the total surface energy and surface adhesion .....	159
4.4	DISCUSSION.....	163
4.5	CONCLUSIONS .....	165
	<b>CHAPTER 5 PROCESSING CONDITIONS AND THEIR EFFECT ON CHOCOLATE DEMOULDING. ....</b>	<b>166</b>
5.1	INTRODUCTION.....	166

5.2	MATERIALS AND METHODS.....	167
5.2.1	Materials.....	167
5.2.2	Methods.....	167
5.3	RESULTS.....	169
5.3.1	Ingredients.....	169
5.3.1.1	<i>Surface tension</i> .....	171
5.3.2	Contact time.....	173
5.3.3	Mould surface temperature.....	177
5.3.4	Cooling temperature.....	180
5.3.5	Relative humidity.....	184
5.3.5.1	<i>Cisorp</i> .....	187
5.3.6	Cleaning methods.....	188
5.3.6.1	<i>Cleaning procedures</i> .....	189
5.3.6.2	<i>Non-cleaning</i> .....	192
5.3.7	Mould roughness.....	195
5.3.7.1	<i>Surface microstructure</i> .....	198
5.4	DISCUSSION.....	199
5.5	CONCLUSIONS.....	201

**CHAPTER 6 THE EFFECT OF AERATION ON CHOCOLATE DEMOULDING**

.....**202**

6.1	INTRODUCTION.....	202
6.2	METHODS.....	203
6.2.1	Materials.....	203
6.2.2	Methods.....	203
6.3	RESULTS.....	203
6.3.1	Effect of aeration.....	203
6.3.2	Effect of different mould materials.....	207
6.3.3	Comparison of aerated dark and milk chocolate.....	213
6.3.4	Effect of bubble size.....	214
6.3.4.1	<i>CO<sub>2</sub> gas</i> .....	214
6.3.4.2	<i>N<sub>2</sub> gas</i> .....	217

6.3.4.3	<i>Microstructure</i> .....	220
6.4	DISCUSSION.....	224
6.5	CONCLUSIONS .....	226
<b>CHAPTER 7 CHOCOLATE ADHESION TO POLYCARBONATE SURFACES COATED WITH A THIN FILM.....</b>		<b>227</b>
7.1	INTRODUCTION.....	227
7.2	METHODS .....	228
7.2.1	Materials.....	228
7.2.2	Methods.....	228
7.3	RESULTS.....	229
7.3.1	One component coatings .....	229
7.3.1.1	<i>Hydrocolloids</i> .....	229
7.3.1.2	<i>Lipids</i> .....	232
7.3.2	Effect of concentration .....	234
7.3.2.1	<i>CMC concentration</i> .....	235
7.3.2.2	<i>Grindsted Acetem concentration</i> .....	238
7.3.3	Two component coatings .....	240
7.3.3.1	<i>Hydrocolloid and plasticizers</i> .....	241
7.3.3.2	<i>Hydrocolloid and lipid</i> .....	244
7.3.4	Three component coatings.....	246
7.3.5	Chocolate composition .....	249
7.4	DISCUSSION.....	250
7.5	CONCLUSIONS .....	252
<b>CHAPTER 8 CONCLUDING REMARKS.....</b>		<b>253</b>
8.1	SUMMARY OF THE MAIN RESULTS.....	253
8.2	PRACTICAL APPLICATION .....	256
8.3	FUTURE WORK.....	257
<b>REFERENCES.....</b>		<b>258</b>
<b>PUBLICATIONS .....</b>		<b>275</b>

## LIST OF FIGURES

<b>Figure 1.1</b> Schematic representation of the effect of processing on the demoulding stage.....	2
<b>Figure 2.1.</b> Nucleation mechanisms (Hartel, 2001; Mullin, 2001).....	15
<b>Figure 2.2.</b> Heterogeneous nucleation at the surface of a catalytic impurity (Walstra, 2003). ..	17
<b>Figure 2.3</b> Free activation energy of nucleation change ( $\Delta G_n^\#$ ) for the three main polymorphs, whereby $\Delta G_n^\#$ represents the free energy barrier that must be exceeded before stable nuclei can be formed (Awad and Marangoni, 2006). .....	19
<b>Figure 2.4</b> Qualitative isothermal phase-transition scheme of static cocoa butter. ....	21
<b>Figure 2.5</b> Crystallization events occurring within the bulk during solidification of cocoa butter (Dimick, 1999; Himawan et al., 2006). ....	24
<b>Figure 2.6</b> Phase transition scheme of cocoa butter (van Malsen et al., 1999).....	25
<b>Figure 2.7</b> Structural hierarchy of the crystallization process and the formation of the fat crystal network (Narine and Marangoni, 2005). ....	27
<b>Figure 2.8</b> Schematic representation of the microstructure of liquid dark chocolate obtained after conching and the stabilizing effect of a surface active agent, e.g. lecithin (adapted from Beckett, 2008) (not at scale).....	32
<b>Figure 2.9</b> Schematic representation of the microstructure of a crystallized and solidified dark chocolate sample (not at scale). ....	35
<b>Figure 2.10</b> Schematic diagram of the chocolate manufacturing process (adapted from Beckett, 2008). ....	37
<b>Figure 2.11</b> Time-temperature profile for milk chocolate (Talbot, 1999a; Afoakwa et al., 2007). ....	38
<b>Figure 2.12</b> Chocolate moulding, cooling and demoulding. ....	39
<b>Figure 2.13</b> Cooling and expansion curves of untempered chocolate (Nelson, 1999). ....	43
<b>Figure 2.14</b> Suspected direction of shrinkage depending on the cooling direction (Pinschower, 2003). ....	44
<b>Figure 2.15</b> Diagram illustrating the concepts of work of cohesion $W_c$ and work of adhesion $W_a$ (McGuire, 2005). ....	46
<b>Figure 2.16</b> Schematic overview of different types of adhesion forces that exist at various distances when two spheres are pulled apart (Kendall, 2001). ....	50
<b>Figure 2.17</b> Adhesion at the molecular level.....	51
<b>Figure 2.18</b> Representation of an interface, $\sigma$ , according to Gibbs (left), consisting of two phases, $\alpha$ and $\beta$ separated by thin boundary layer, and according to Guggenheim (right), where an extended interphase with a volume is present (Butt et al., 2003)..	55
<b>Figure 2.19</b> Visualization of the principle of Gibbs adsorption for a solid-gas system (Schrader, 2003). ....	58



<b>Figure 2.20</b>	Attractive forces between molecules at the surface region and in the bulk of a liquid which are responsible for the surface tension (Shaw, 1992). .....	61
<b>Figure 2.21</b>	A schematic representation of a liquid drop placed on a solid surface.....	62
<b>Figure 2.22</b>	The contact angle as a force balance, where $\cos \theta$ results from the equilibrium between the energy of cohesion within the liquid and the energy of adhesion between the liquid and solid surface.....	63
<b>Figure 2.23</b>	Three kinds of wetting, thermodynamically defined (Lyklema, 2000).....	65
<b>Figure 2.24</b>	Effect of solid surface free energy on bacterial adhesion, Baier curve (left), and on protein adhesion (right), respectively (Zhao, 2004).....	69
<b>Figure 3.1</b>	Polycarbonate chemical structure. ....	74
<b>Figure 3.2</b>	PTFE chemical structure.....	76
<b>Figure 3.3</b>	Surface tension determination via the Wilhelmy plate method (KRÜSS GmbH, 2009).....	83
<b>Figure 3.4</b>	Overview of the contact angle apparatus designed specifically for this research.....	84
<b>Figure 3.5</b>	Schematic representation of advancing, $\theta_a$ , and receding, $\theta_r$ , contact angles (KRÜSS GmbH, 2009).....	85
<b>Figure 3.6</b>	Critical surface tension according to Zisman.....	87
<b>Figure 3.7</b>	Linear Owens and Wendt relationship.....	89
<b>Figure 3.8</b>	Wetting envelope diagram. ....	94
<b>Figure 3.9</b>	Probe geometries developed specifically for the experimental adhesion force determination, based on the forces involved in the commercial chocolate demoulding process. ....	96
<b>Figure 3.10</b>	Experimental set-up used for the assessment of the effect of different probe geometries.....	97
<b>Figure 3.11</b>	Experimental surface adhesion as affected by probe geometry. ....	97
<b>Figure 3.12</b>	Schematic representation of the procedure and conditions of the surface adhesion measurements. ....	98
<b>Figure 3.13</b>	Photograph showing the modified Peltier chamber with the Texture Analyser. ....	99
<b>Figure 3.14</b>	Plot of the force against time, as obtained by the Texture Analyser.....	100
<b>Figure 3.15</b>	Surface adhesion as affected by the level of chocolate crystallization. ....	101
<b>Figure 3.16</b>	Schematic representation of the three different failure mechanisms specified in this research, i.e. cohesive, cohesive–adhesive and adhesive failure. ....	102
<b>Figure 3.17</b>	Experimental set-up developed to measure the effect of processing conditions on the surface adhesion force.....	104
<b>Figure 3.18</b>	Revolution 2 (ChocoVision) chocolate tempering device. ....	105
<b>Figure 3.19</b>	Force against time profile obtained for a surface penetration (5 mm depth) test of chocolate at both the chocolate–mould and chocolate–air surfaces. ....	107

<b>Figure 3.20</b>	Visualization of the measurement principle of the Tri-GLOSSmaster by determining the angular reflection at three angles (Sheen Instruments, 2003).....	108
<b>Figure 3.21</b>	Operating principle of the Cisorp moisture sorption analyser (Mangel, 2007). ...	109
<b>Figure 3.22</b>	Operating principle of the vacuum box.....	110
<b>Figure 3.23</b>	Operating principle of a positive pressure aeration system. ....	111
<b>Figure 3.24</b>	Images obtained for the structural characterisation of aerated chocolate using C-Cell.....	113
<b>Figure 3.25</b>	Operating principle of the thin film coating preparation. ....	114
<b>Figure 4.1</b>	Surface tension as affected by total cocoa solids content. ....	122
<b>Figure 4.2</b>	Surface tension as a function of temperature. ....	125
<b>Figure 4.3</b>	Negative interactions observed between certain probe liquids and solid mould surfaces. ....	128
<b>Figure 4.4</b>	Contact angles of cocoa butter ( ☒ ) and palm olein ( ☐ ), as affected by solid mould surfaces. ....	131
<b>Figure 4.5</b>	Surface microstructure of the solid mould materials. ....	134
<b>Figure 4.6.</b>	The total surface energy of different mould materials calculated using various empirical approaches. ....	136
<b>Figure 4.7</b>	Total surface energy, $\gamma_s^{\text{tot}}$ , of the different mould materials according to the Lifshits–van der Waals / acid–base or van Oss, Chaudhury and Good approach.....	138
<b>Figure 4.8</b>	Surface free energy components of the different solid mould surfaces according to the Lifshitz–van der Waals / acid–base method of van Oss, Chaudhury and Good. ....	140
<b>Figure 4.9</b>	The effect of temperature on the total surface energy, $\gamma_s^{\text{tot}}$ . ....	141
<b>Figure 4.10</b>	The effect of temperature on the dispersive or Lifshitz–van der Waals component (A), the polar or Lewis acid–base component (B), the electron acceptor component (C) and the electron donor component (D) of the total surface energy. ....	142
<b>Figure 4.11</b>	Total surface energy of dark chocolate as affected by crystallization. ....	144
<b>Figure 4.12</b>	Surface energy components of dark chocolate as affected by crystallization, calculated according to the Lifshitz–van der Waals / acid–base method developed by van Oss, Chaudhury and Good. ....	145
<b>Figure 4.13</b>	Total surface energy of chocolate as affected by chocolate composition.....	146
<b>Figure 4.14</b>	Surface energy components of chocolate as affected by chocolate composition, calculated according to the Lifshitz–van der Waals / acid–base method developed by van Oss, Chaudhury and Good. ....	147
<b>Figure 4.15</b>	Total surface energy of dark chocolate as affected by cooling temperature.....	148
<b>Figure 4.16</b>	Surface energy components of dark chocolate as affected by cooling temperature, calculated according to the Lifshitz–van der Waals / acid–base method developed by van Oss, Chaudhury and Good. ....	149

<b>Figure 4.17</b> Wetting envelopes with 0° contour for the four solid mould materials based on the Owens and Wendt approach. ....	150
<b>Figure 4.18</b> Surface adhesion as affected by different solid mould materials.....	152
<b>Figure 4.19</b> The effect of different mould materials on the amount of residues after probe separation (A), the hardness of the solidified chocolate samples (B), the difference of surface glossiness (C) and the difference of contact angle (D) of the mould surfaces before and after chocolate contact. ....	154
<b>Figure 4.20</b> Images of a polycarbonate mould surfaces before (A) and after contact with chocolate (B – D) (scale 1:0.34). ....	155
<b>Figure 4.21</b> Surface hydrophilicity as affected by different mould materials. ....	156
<b>Figure 4.22</b> Surface adhesion as a function of surface hydrophilicity. ....	157
<b>Figure 4.23</b> Surface adhesion as a function of the work of adhesion. ....	158
<b>Figure 4.24</b> Work of adhesion as a function of total surface energy. ....	159
<b>Figure 4.25</b> Surface adhesion as a function of total surface energy. ....	160
<b>Figure 4.26</b> Surface adhesion of different chocolate systems as a function of the surface free energy components, according to the Lifshitz–van der Waals / Lewis acid–base approach.....	161
<b>Figure 4.27</b> Relation between chocolate microstructure and solid surface free energy, evolvment upon cooling.....	164
<b>Figure 5.1</b> Surface adhesion as affected by total cocoa solids content.....	169
<b>Figure 5.2</b> The effect of total cocoa solids content on the amount of residues after probe separation (A), and the hardness of the solidified chocolate samples (B). ....	170
<b>Figure 5.3</b> Surface tension as affected by the total cocoa solids content. ....	172
<b>Figure 5.4</b> Surface adhesion as a function of surface tension for a set of chocolate samples with varying total cocoa solids content.....	173
<b>Figure 5.5</b> Surface adhesion of dark chocolate as a function of contact time. ....	174
<b>Figure 5.6</b> The effect of contact time on the amount of residues after probe separation (A), the hardness of the solidified chocolate samples (B), the difference of surface glossiness (C) and the difference of contact angle (D) of the polycarbonate mould surface before and after chocolate contact. ....	175
<b>Figure 5.7</b> Evolvment of microstructure with contact time. ....	177
<b>Figure 5.8</b> Surface adhesion of dark chocolate as a function of mould surface temperature. ...	178
<b>Figure 5.9</b> The effect of mould surface temperature on the amount of residues after probe separation (A), the hardness of the solidified chocolate samples (B), the difference of surface glossiness (C) and the difference of contact angle (D) of the polycarbonate mould surface before and after chocolate contact.....	179
<b>Figure 5.10</b> Surface adhesion of dark chocolate as a function of cooling temperature.....	181

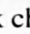
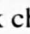
<b>Figure 5.11</b>	The effect of cooling temperature on the amount of residues after probe separation (A), the hardness of the solidified chocolate samples (B), the difference of surface glossiness (C) and the difference of contact angle (D) of the polycarbonate mould surface before and after chocolate contact.....	182
<b>Figure 5.12</b>	Schematic representation of the effect of cooling temperature on the chocolate microstructure.....	183
<b>Figure 5.13</b>	Surface adhesion of dark chocolate as a function of environmental relative humidity.....	185
<b>Figure 5.14</b>	Schematic representation of the effect of vapour adsorption at the mould surface.....	185
<b>Figure 5.15</b>	The effect of environmental relative humidity on the amount of residues after probe separation (A), the hardness of the solidified chocolate samples (B), the difference of surface glossiness (C) and the difference of contact angle (D) of the polycarbonate mould surface before and after chocolate contact.....	186
<b>Figure 5.16</b>	Moisture uptake by a polycarbonate mould surface as a function of environmental relative humidity at 30°C.....	188
<b>Figure 5.17</b>	Surface adhesion of dark chocolate as affected by different cleaning procedures.	190
<b>Figure 5.18</b>	The effect of different cleaning procedures on the amount of residues after probe separation (A), the hardness of the solidified chocolate samples (B), the difference of surface glossiness (C) and the difference of contact angle (D) of the polycarbonate mould surface before and after chocolate contact.....	191
<b>Figure 5.19</b>	Contact angle of water on polycarbonate mould surfaces treated with water, detergent, rinsing aid or a combination of detergent and rinsing aid, respectively, both before and after contact with a dark chocolate sample.....	192
<b>Figure 5.20</b>	Evolution of the surface adhesion of dark chocolate if the mould surface is not cleaned between measurements, together with a visualization of the mould and chocolate surfaces.....	193
<b>Figure 5.21</b>	The effect of non-cleaning of the mould surface between measurements on the amount of residues after probe separation (A), the hardness of the solidified chocolate samples (B), the difference of surface glossiness (C) and the difference of contact angle (D) of the polycarbonate mould surface before and after chocolate contact.....	194
<b>Figure 5.22</b>	Surface adhesion of dark chocolate as affected by mould surface roughness. ....	196
<b>Figure 5.23</b>	The effect of mould surface roughness on the amount of residues after probe separation (A), the hardness of the solidified chocolate samples (B), the difference of surface glossiness (C) and the difference of contact angle (D) of the polycarbonate mould surface before and after chocolate contact.....	197



<b>Figure 5.24</b> Surface microstructure of a polycarbonate mould surface with roughness 0 and with roughness 42.....	198
<b>Figure 6.1</b> Comparison of the surface adhesion of an aerated and a non-aerated milk chocolate system.....	204
<b>Figure 6.2</b> Comparison of an aerated and a non-aerated milk chocolate system with respect to the amount of residues after probe separation (A), and the hardness of the solidified chocolate samples (B).....	205
<b>Figure 6.3</b> Images (scale 1:0.34) of the aerated chocolate (A) and the mould surface (B) after the experimental surface adhesion force determination.....	206
<b>Figure 6.4</b> Surface adhesion of an aerated milk chocolate system as affected by different mould materials.....	207
<b>Figure 6.5</b> The effect of aeration on the amount of residues after probe separation (A), and the hardness of the solidified aerated chocolate samples (B). ....	208
<b>Figure 6.6</b> Images showing the surfaces of commercial mould materials after contact with aerated chocolate samples, obtained via the vacuum box aeration.....	209
<b>Figure 6.7</b> Surface adhesion of an aerated (■) and a non-aerated (□) milk chocolate system as a function of surface energy. ....	210
<b>Figure 6.8</b> Schematic representation of the relation between heat conductivity and demoulding of aerated chocolate systems. ....	212
<b>Figure 6.9</b> Comparison of the surface adhesion of an aerated dark and an aerated milk chocolate system. ....	213
<b>Figure 6.10</b> Comparison of an aerated dark and an aerated milk chocolate system on the amount of residues after probe separation (A), and the hardness of the solidified chocolate samples (B). ....	214
<b>Figure 6.11</b> Surface adhesion as a function of CO <sub>2</sub> gas hold-up.....	215
<b>Figure 6.12</b> The effect of CO <sub>2</sub> aeration on the amount of residues after probe separation (A), and the hardness of the solidified chocolate samples (B). ....	216
<b>Figure 6.13</b> Surface adhesion as a function of N <sub>2</sub> gas hold-up.....	218
<b>Figure 6.14</b> The effect of N <sub>2</sub> aeration on the amount of residues after probe separation (A), and the hardness of the solidified chocolate samples (B).....	219
<b>Figure 6.15</b> Number of cells per surface area as a function of gas hold-up of both CO <sub>2</sub> (■) and N <sub>2</sub> (●) aerated milk chocolate systems. ....	220
<b>Figure 6.16</b> Average cell diameter as a function of gas hold-up of both CO <sub>2</sub> (■) and N <sub>2</sub> (●) aerated milk chocolate systems.....	221
<b>Figure 6.17</b> Cross-sections representing the microstructure of milk chocolate samples at varying CO <sub>2</sub> gas hold-up values. ....	222
<b>Figure 6.18</b> Cross-sections representing the microstructure of milk chocolate sample at varying N <sub>2</sub> gas hold-up values. ....	222



<b>Figure 6.19</b> Number of cells per surface area (○) and cell diameter (■) as a function of surface adhesion of CO <sub>2</sub> aerated chocolate systems.....	223
<b>Figure 7.1</b> Visualization of a stand-alone 1.0% CMC coating formed on a solid polycarbonate substrate.....	229
<b>Figure 7.2</b> Surface adhesion of dark chocolate as affected by the type of hydrocolloid coating.....	230
<b>Figure 7.3</b> The effect of different types of hydrocolloids on the amount of residues after probe separation (A), the hardness of the solidified chocolate samples (B), the difference of surface glossiness (C) and the water contact angle (D).....	231
<b>Figure 7.4</b> Surface adhesion of dark chocolate as affected by different types of lipid coating.....	232
<b>Figure 7.5</b> The effect of different types of lipids on the amount of residues after probe separation (A), the hardness of the solidified chocolate samples (B), the difference of surface glossiness (C) and the water contact angle (D).....	233
<b>Figure 7.6</b> Visualization of the chocolate surfaces after contact with a clean polycarbonate surface, or a Grindsted Acetem, or Dimodan, or cocoa butter coating.....	234
<b>Figure 7.7</b> Surface adhesion as a function of CMC concentration.....	235
<b>Figure 7.8</b> The effect of CMC concentration on the amount of residues after probe separation (A), the hardness of the solidified chocolate samples (B), the difference of surface glossiness (C) and the water contact angle (D).....	236
<b>Figure 7.9</b> Visualization of the stick-slip behaviour observed when determining the advancing water contact angle on a 0.5% CMC coating.....	237
<b>Figure 7.10</b> Surface adhesion as a function of Grindsted Acetem concentration.....	238
<b>Figure 7.11</b> Visualization of the chocolate and mould surfaces coated with GA after contact.....	239
<b>Figure 7.12</b> The effect of Grindsted Acetem concentration on the amount of residues after probe separation (A), the hardness of the solidified chocolate samples (B), the difference of surface glossiness (C) and the water contact angle (D).....	240
<b>Figure 7.13</b> Surface adhesion as affected by plasticizer type and concentration, for a 2-component coating with 0.1% CMC as the 1 <sup>st</sup> component.....	241
<b>Figure 7.14</b> Visualization of a chocolate and mould surface coated with 1.0% sucrose, after contact.....	242
<b>Figure 7.15</b> The effect of plasticizer type and concentration of a 2 component coating system with 0.1% CMC on the amount of residues after probe separation (A), the hardness of the solidified chocolate samples (B), the difference of surface glossiness (C) and the water contact angle (D).....	243
<b>Figure 7.16</b> Surface adhesion as a function of Grinsted Acetem concentration, for a 2-component coating with 0.1% CMC as the 1 <sup>st</sup> component.....	245

<b>Figure 7.17</b> The effect of Grindsted Acetem concentration of a 2-component coating system with 0.1% CMC on the amount of residues after probe separation (A), the hardness of the solidified chocolate samples (B), the difference of surface glossiness (C) and the water contact angle (D).....	246
<b>Figure 7.18</b> Surface adhesion as affected by the 3-component coating composition.....	247
<b>Figure 7.19</b> The effect of composition of a 3 component coating system on the amount of residues after probe separation (A), the hardness of the solidified chocolate samples (B), the difference of surface glossiness (C) and the water contact angle (D). .....	248
<b>Figure 7.20</b> Surface adhesion as affected by different 1-component coating systems in combination with a dark chocolate (  ) or a milk chocolate (  ) system. ....	249

## LIST OF TABLES

<b>Table 2.1</b> Typical chocolate formulations (Jackson, 1999; Rousseau, 2007).....	5
<b>Table 2.2</b> Properties of milk powders and their influence on chocolate properties (Liang & Hartel, 2004).....	9
<b>Table 2.3.</b> Effect of the contact angle, $\theta$ , and factor, $\phi$ , on the free energy of nucleation, $\Delta G$ (Mullin, 2001).....	18
<b>Table 2.4</b> Overview of the physical properties of the polymorphic forms of cocoa butter (adapted from Talbot, 1999a and Rousseau, 2007). ....	20
<b>Table 3.1</b> Composition (%) of chocolate systems. ....	71
<b>Table 3.2</b> Specification of pure pressed cocoa butter (De Zaan, 2006).....	72
<b>Table 3.3</b> Mechanical and thermal properties of solid mould materials (Brydson, 1999; Wyatt et al., 1998; NVON-commissie, 1998). ....	73
<b>Table 3.4</b> Characteristic chemical composition of type 316 austenitic stainless steel (British Stainless Steel Association, 2007). ....	75
<b>Table 3.5</b> Characteristics of probe liquids used for surface tension and contact angle determinations (Acros Organics, 2009; Sigma-Aldrich, 2009). ....	77
<b>Table 4.1</b> Experimental and literature surface tension data (Good, 1992; van Oss, 2006; Della Volpe, 2004; Lyklema, 2000).....	120
<b>Table 4.2</b> Literature values for the liquid surface tension of chocolate systems (Mastrantonakis, 2004; Haedelt, 2005). ....	123
<b>Table 4.3</b> Literature values for the liquid surface tension of fatty acids and vegetable oils (Allen et al., 1999, Chumpitaz et al., 1999).....	124
<b>Table 4.4</b> The average advancing contact angles, $\theta_{adv}$ , and standard deviations obtained when placing the individual probe liquids on the four mould materials at room temperature. ....	127
<b>Table 4.5</b> The average advancing contact angles, $\theta_{adv}$ , and standard deviations obtained when placing the individual probe liquids on a dark chocolate surface and the impact of crystallization.....	129
<b>Table 4.6</b> The average advancing contact angles, $\theta_{adv}$ , obtained when placing the individual probe liquids on chocolate surfaces and the impact of ingredients. ....	130
<b>Table 4.7</b> The average advancing contact angles, $\theta_{adv}$ , obtained when placing the individual probe liquids on dark chocolate surfaces and the impact of cooling conditions.....	130
<b>Table 4.8</b> Effect of temperature on the advancing contact angle, $\theta_{adv}$ .....	132
<b>Table 4.9</b> Contact angle hysteresis, $H$ , of water, diiodomethane and formamide on the four different mould materials.....	133
<b>Table 4.10</b> Surface free energy data of different types of stainless steel found in literature....	139
<b>Table 5.1</b> Overview of processing conditions used for each individual experiment. ....	168



<b>Table 6.1</b> Heat conductivity values of a selection of gases and liquids / food systems at 20 °C (Singh and Heldman, 2001). .....	211
<b>Table 6.2</b> Density and gas hold-up of aerated milk chocolate systems in relation to the CO <sub>2</sub> processing pressure. ....	215
<b>Table 6.3</b> Density and gas hold-up of aerated milk chocolate systems in relation to the N <sub>2</sub> processing pressure. ....	218
<b>Table 7.1</b> Effect of sucrose addition on the surface glossiness. ....	244

# CHAPTER 1

## INTRODUCTION

### 1.1 OBJECTIVE AND STRATEGY

Commercial chocolate manufacturing is a continuously evolving process, and with the ever increasing product output it is essential to have a good understanding of the manufacturing process and processing conditions, and how they impact on chocolate characteristics. Focus thereby should not only be on the quality aspect, but on physical and organoleptic characteristics as well. An important example in this case is the adhesion of products during processing, which is a substantial ongoing problem in the food industry in general. During chocolate manufacturing the processes of moulding and demoulding are particularly prone to adhesion problems, leading to surface defects, production losses and increasing processing costs due to equipment cleaning.

Moulding is one of the final stages of the chocolate manufacturing process, where tempered chocolate is deposited in moulds and subsequently cooled. During cooling the polymorphic cocoa butter crystallises and the chocolate solidifies. In the subsequent demoulding stage, the solidified chocolate bars are removed from the moulds. This demoulding process is affected by two mechanisms: 1) the adhesive force between chocolate and the mould surface, and 2) the state of crystallization of the fat phase of the chocolate. Crystallization of cocoa butter in the correct polymorphic form (Form V) leads to a volumetric contraction of the tempered chocolate during solidification and aids in the ease of the demoulding process. Specific steps during chocolate bar manufacturing may result in an increased adhesion between chocolate and mould surface, as is visualized in Figure 1.1, causing intermittent problems in demoulding. Chocolate residues staying behind on the mould surface after demoulding are responsible for poor product appearance as they result in defects on the chocolate surface and consequent low consumer acceptance, production losses, and increased processing costs due to equipment cleaning.

The main objectives of this research were to gain an understanding of the mechanisms that cause the sticking (adhesion) of (aerated) chocolate to the mould materials, and to identify determining factors.

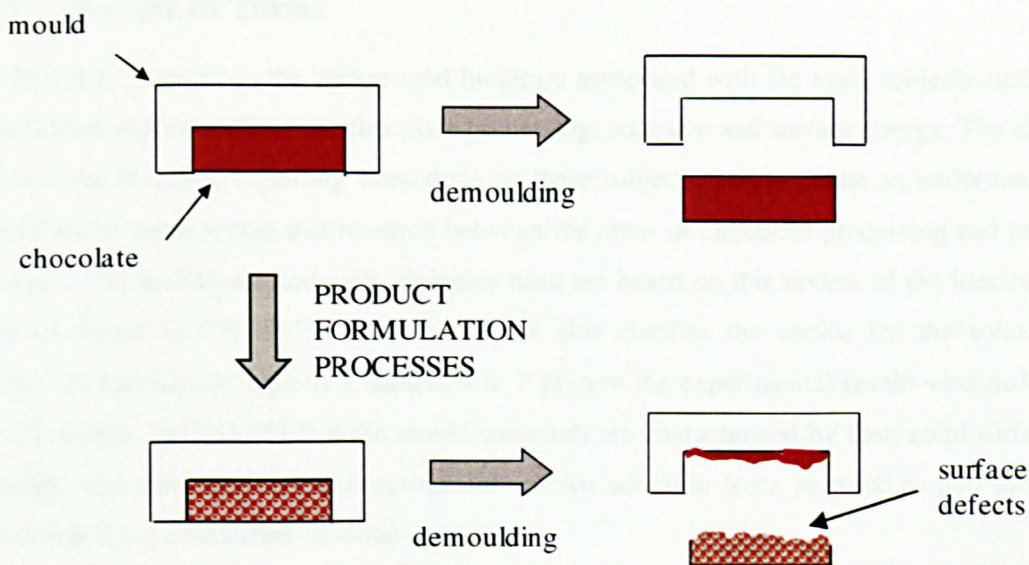


**Figure 1.1** Schematic representation of the effect of processing on the demoulding stage.

Based on the assumption that the extent of formation of chocolate deposits on a mould surface during demoulding will depend on the balance between the adhesion force (between the chocolate and the mould surface) and the cohesion force (within the chocolate itself), two different strategies are proposed to achieve a greater ease of chocolate demoulding: either by decreasing the surface adhesion between chocolate and mould surface, or by increasing the cohesion force of chocolate. The latter strategy is, of course, not the manufacturer's preferred choice, because it implies modifying the (desirable) texture and sensory properties of the chocolate product. Focus in this research is therefore on a method to minimize the adhesion force between chocolate and mould surface.

Two different approaches are applied to enhance the understanding of the interactions taking place at the chocolate–mould interface:

- Establishing relationships between the thermodynamic work of adhesion and the observed extent of adhesion of chocolate to a range of mould materials;
- Establishing relationships between processing conditions and the level of adhesion of chocolate to the mould surface during demoulding, with particular interest in processing conditions used during the moulding and cooling stages of the chocolate manufacturing process.

## **1.2 OUTLINE OF THESIS**

CHAPTER 2 describes the background literature associated with the main subjects studied: fat nucleation and crystallization, chocolate processing, adhesion and surface energy. The aim is to review the literature regarding work done on these subjects, and to create an understanding of correlations made within this research between the areas of chocolate processing and materials science. The techniques and methodologies used are based on this review of the literature, and are discussed in CHAPTER 3. This chapter also clarifies the choice for the solid mould materials and liquids applied. Chapters 4 to 7 present the experimental results obtained during this research. In CHAPTER 4 the mould materials are characterised by their solid surface free energy, and correlated to the experimental surface adhesion force required to pull the mould materials from a solidified chocolate sample.

CHAPTER 5 subsequently determined the impact of chocolate processing conditions on this surface adhesion force, which is a measure of the ease of chocolate demoulding. One processing parameter whose impact on demoulding is reviewed in more detail in CHAPTER 6 is aeration. Particular interest is given to the effect of bubble size and microstructure of aerated milk chocolate systems. The final results chapter, CHAPTER 7, discusses the use of edible coatings placed at the chocolate–mould interface as a technique to reduce the surface adhesion and improve demoulding properties. CHAPTER 8 correlates the results presented in the previous chapters and discusses the implications of these on chocolate manufacturing along with possible ideas for future research.

## **CHAPTER 2**

### **LITERATURE REVIEW**

#### **2.1 CHOCOLATE**

In 2006 and 2007 the average UK manufacturing sales of cocoa, chocolate and sugar confectionery was £ 3.5 billion (PRODCOM, 2008), being responsible for around 6.3% of the total turnover in the UK food and drink industry (ADAS, 2007). After Switzerland, the UK has the second highest consumption of chocolate in the world, with an average consumption of 9.97 kg per person (CAOBISCO, 2006). Sales figures indicate that the growth of the confectionery market is slowing down, which is considered to be caused by the increasing demand for healthy products. The trend observed within the chocolate industry is an increase in sales of dark chocolate, due to the health benefits associated with cocoa. Within the UK market, there are three major chocolate manufacturing companies, Nestlé Rowntree, Mars/Masterfoods and Cadbury Trebor Bassett. New product development is focussed on brand extension increasing variation, rather than the development of completely new concepts (ADAS, 2007). A good understanding of the ingredients and the processing conditions used is essential for the chocolate manufacturer to maintain its position within the confectionery market.

##### **2.1.1 History of chocolate**

The discovery of cacao, and indirectly chocolate, is ascribed to the Maya's in Mexico: "And so they were happy over the provisions of the good mountain, filled with sweet things, ... thick with pataxte and cacao, ..." (Anonymous, 2002). In turn, the Aztecs are held responsible for the cultivation of the cacao tree. Literally, *Theobroma cacao* means "food of the gods", and this emphasizes the position of the cacao bean in the history of the early Southern and Central American civilisations. To both the Mayas and the Aztecs the cacao bean served many different purposes, ranging from social and religious purposes to its use as currency (Dhoedt, 2008). However, its main use was in Xocoatl, a drink prepared from cocoa beans, vanilla and chilli. Research by Pucciarelli and Grivetti (2008) stresses the importance of this chocolate drink also as a medicine in early North America.

Columbus was the first European to discover the cocoa bean on his travels in 1502, but it was Don Cortez who introduced them in Europe in 1528. The cocoa bean was an expensive commodity, making it an exclusive privilege of the rich, and limiting its consumption (Dhoedt, 2008). The traditional cocoa drink was modified by Spanish monks, adding components such as honey, vanilla and sugar cane, creating the foundations for the chocolate recipe as it is known nowadays. Solid chocolate, however, was not developed until the 19<sup>th</sup> century. Due to the fact

that the whole cocoa bean was used for the traditional cocoa drink, it was a very fatty product (Minifie, 1989). In 1828 Coenraad Johannes Van Houten invented the cocoa press, enabling the separation of cocoa solids from cocoa butter, consequently creating a lower fat cocoa powder (~ 23% fat). The Industrial Revolution was responsible for the mechanisation of the production process, leading to the production of the first solid chocolate bar in 1847 by Joseph Fry. Fry used liquid cocoa butter rather than warm water to mix sugar and chocolate powder and produce a dry, grainy solid chocolate product. Addition of condensed milk, invented by Henri Nestlé, in combination with extra sugar, evolved in the production of the first solid milk chocolate by Daniel Peter in 1876 in Switzerland. In order to improve the manufacturing process and create a smoother and better tasting chocolate, Rodolphe Lindt, in 1880, developed the conche (Beckett, 1999b). Since then, the chocolate manufacturing process has undergone various changes for the purposes of either improved oral experience (flavour and texture) or increased productivity to meet increasing demands for chocolate products.

### 2.1.2 Chocolate ingredients

The main ingredients of chocolate are cocoa butter, cocoa solids and sugar, together with milk solids in the case of milk chocolate (Fryer & Pinschower, 2000). Depending on the manufacturer and the variety, different chocolate compositions can be obtained using the main ingredients. Table 2.1 gives a basic overview of typical chocolate formulations. Knowledge of the main chocolate ingredients is essential to understand the chemistry of the product and interactions within the food matrix.

**Table 2.1 Typical chocolate formulations (Jackson, 1999; Rousseau, 2007).**

Component	Typical percentage of component in			
	Milk chocolate	Dark chocolate	Bittersweet chocolate	White chocolate
Cocoa mass (cocoa solids and cocoa butter)	11.8	39.6	60.7	-
Added cocoa butter	20.0	11.8	2.6	23.0
Sugar	48.7	48.1	36.3	46.5
Lecithin	0.4	0.4	0.3	0.5
Flavour compounds (e.g. salt and vanillin)	0.1	0.1	0.2	
Whole milk powder	19.1	-	-	30.0
Total fats	31.5	36.4	35.4	

### 2.1.2.1 *Cocoa butter*

In order for a product to be called chocolate, the FAO and WHO require the product to be composed of, on a dry matter basis, minimum 35% total cocoa solids, of which at least 18% shall be cocoa butter and 14% fat-free cocoa solids (Codex Alimentarius, 2003). Cocoa butter is the fat obtained through pressing of the cocoa liquor / mass, which in turn is a result of the grinding of cocoa nibs, a part of the cocoa bean. On average, 55% of the cocoa bean is made up of cocoa butter, whilst the other 45% consists of solid material, cellulose, proteins and carbohydrates. An essential step in the flavour development of the cocoa components is the roasting of the cocoa nibs, resulting in a reduction in the acidity of the cocoa beans and the formation of the characteristic colour and chocolate notes of cocoa solids (Beckett, 2008). The typical cocoa aroma is mainly a result of non-enzymatic or Maillard browning, the chemical reaction between reducing sugars and amino acids.

Cocoa butter is composed of a mixture of 40-50 different triacylglycerols (TAG) and trace compounds, with three fatty acids, i.e. palmitic, oleic and stearic acid, accounting for approximately 95% of the total cocoa butter composition. The three main TAG in cocoa butter, which dominate the crystallization and phase transformations, are 1,3-palmitoyl-2-oleoylglycerol (POP) (15%), 1-palmitoyl-2-oleoyl-3-stearoylglycerol (POSt) (35%), and 1,3-stearoyl-2-oleoylglycerol (StOSt) (23%) (Schenk and Peschar, 2004). The composition and quality of cocoa butter, however, depends on the cocoa variety and the manufacturing process used for the fat extraction. Deshelling of cocoa beans before pressing improves the quality of the final cocoa butter product. For milk chocolate, however, an extra deodorization step is required to produce a milder flavour. Use of the whole beans, results in the incorporation of shell fat, which is known to negatively affect the flavour and setting properties of the cocoa butter (Meursing and Zijderfeld, 1999). This requires an additional manufacturing step, called refining, to ensure the reduction of free fatty acids and the removal of a number of polar components, e.g. glycolipids, phosphatides and mucilaginous substances (Dimick, 1999).

The relatively large amount of saturated TAG in refined cocoa butter causes the fat to show similarities with pure compounds with respect to its thermal and structural properties (Loisel et al., 1998b). According to Loisel et al. (1998a) approximately 13% corresponds to polyunsaturated and 3% to trisaturated TAG. Thermal and structural behaviour of cocoa butter is characterized by the TAG composition. Johnston (1972) mentions the resistance to oxidation, as a result of the low amount of polyunsaturated TAG, in combination with the absence of off-flavours, caused by either fat-splitting enzymes or chemical oxidation. The solidification behaviour and physical properties of cocoa butter are determined by its fatty acid composition. Long chain, saturated fatty acids account for approximately 1–2% of the cocoa butter composition, and have a high melting temperature. Short chain and/or unsaturated fatty acids, on the other hand, have much lower melting temperatures (Awad and Marangoni, 2006).

Being a mixture of TAG, cocoa butter is partly liquid at room temperature, caused by the presence of 5-20% of low melting TAG (Beckett, 2008).

### 2.1.2.2 Sugar

A general description of chocolate is given in the Codex Standard for Chocolate and Chocolate Products (Codex Alimentarius, 2003): “... shall be prepared from cocoa and cocoa materials with sugars and may contain sweeteners, milk products, flavouring substances and other food ingredients”. This definition clearly states the importance of sugar as one of the major ingredients of chocolate together with cocoa and cocoa materials. The main function of sugar is to deliver sweetness, which is especially important in dark chocolate recipes which are relatively bitter. General levels of sugar used in the production of different types of chocolate can be found in Table 2.1. A limit for the inclusion of sugar is not given, but it has been mentioned that small changes in sugar inclusion level (1-2%) significantly affect the product and economic costs, while a 5% increase of the sugar level results in the development of changes in the flavour profile (Jackson, 1999).

According to Beckett (2008), chocolate traditionally contained approximately 50% sugar, but the requirements for low caloric and sugar-free products have affected the types and level of sugars that are used. Originally, predominantly crystalline sucrose (saccharose,  $C_{12}H_{22}O_{11}$ ), a disaccharide consisting of the monosaccharides glucose and fructose, was used. When using amorphous sugar, there is an increased risk of moisture uptake, influencing the viscosity of the final chocolate through formation of sticky aggregates, and absorption of flavour compounds, affecting the sensory characteristics of the chocolate. Furthermore, the microstructure of sucrose is critical with respect to bloom formation. The use of crystalline sugar has been observed to instigate bloom formation, whereas amorphous sugar did not (Fryer and Pinschower, 2000). An important sugar present in cow's milk and consequently milk chocolate is lactose.

Other sugars and/or sugar substitutes are often used to replace the sucrose in the chocolate recipe. The monosaccharides glucose and fructose are usually not used as single components as they are hygroscopic, rapidly absorbing moisture from the air, causing the sugar particles to stick together and increase the viscosity of the chocolate. Glucose and lactose have been used to replace sucrose, especially in milk chocolate recipes. Lactose, a disaccharide of glucose and galactose, has a low sweetening power compared to sucrose. However, lactose positively contributes to the sensory characteristics of milk chocolate, through the formation of a mild caramelized flavour, as a result of its participation in the Maillard reaction. Sugar substitutes are sugar alcohols, e.g. xylitol, sorbitol, isomalt, mannitol and lactitol. They can be used for the manufacturing of specific chocolate products, e.g. low-caloric and sugar-free.



Due to differences in physical, chemical or physiological composition, sugar alcohols cannot always be used in the manufacturing of chocolate products.

The physical properties of sugar particles determine their behaviour when dispersed in a continuous fat phase. The presence of moisture at the sugar particle surface results in the formation of particle aggregates, increasing the friction and apparent viscosity. According to Krüger (1999), the particle size of sugars should lie between 6 and 30  $\mu\text{m}$  to optimise the rheological and textural properties of the chocolate. Afoakwa et al. (2007) observed different crystalline network structures and inter-particle interaction strengths depending on the particle size distribution of sugar and cocoa solids in dark chocolate, consequently affecting the mechanical properties. Addition of sugar particles also influences the crystallization of cocoa butter, by acting as a heterogeneous nucleation agent. In a cocoa butter / sugar mixture lower melting points were observed compared to plain cocoa butter, indicating that the presence of sugar particles preferentially promotes the formation of lower melting polymorphs (Dhonsi & Stapley, 2006).

### *2.1.2.3 Milk components*

For a product to be called milk chocolate the Codex Standard requires it to contain at least 2.5-3.5 % milk fat and 12-14 % total milk solids (Codex Alimentarius, 2003). White chocolate contains similar amounts of milk fat and milk solids, but there is no addition of cocoa solids. The addition of milk solids to chocolate creates a product that is significantly different from a physical and sensory, as well as processing point of view compared to dark chocolate. Pure (liquid) milk is not used during chocolate manufacturing, as the high moisture content negatively influences the rheological properties of the chocolate. Whole milk, on average, has 13.5% solids, consisting of approximately 3.4% protein, 4.6% fat, 4.7% lactose and 0.7% minerals (Haylock and Dodds, 1999). Several techniques are used to obtain milk powder from the whole milk, resulting in a number of powders with similar composition but varying physical characteristics, e.g. roller-dried and spray-dried whole milk powders and high-fat powders (Liang and Hartel, 2004).

Milk fat is essential for the characteristic texture and flavour of milk chocolate. Compared to dark chocolate, milk chocolate is relatively soft in texture and mouthfeel, which is due to the fact that milk fat is mainly liquid (15-20% solid) at room temperature (Afoakwa et al., 2007). However, a minimum solid fat content of 45% in the finished product is required, in order to obtain the desired physical properties, indicating that it is impossible to use only milk fat for the manufacturing of chocolate products. Milk fat is compatible with cocoa butter in all proportions, without changing the polymorphism of cocoa butter (Haylock and Dodds, 1999). Milk fat contains different amounts of high (> 50°C), medium (35-40°C) and low (> 15°C) melting

fractions. These different fractions are chemically distinct, consisting mainly of different levels of saturated and unsaturated fatty acids. Cocoa butter TAGs are thermodynamically compatible with the high melting fraction TAGs, and incompatible with the medium melting TAGs (Awad and Marangoni, 2006). Overall, as the milk fat and cocoa butter solids are thermodynamically incompatible, they crystallize individually. Induced by molecular geometric constraints, the formation of mixed crystals of cocoa butter and milk fat triglycerides is inhibited, causing a decrease in the melting point of the mixture below that of the individual components (Awad and Marangoni, 2006). A consequence of the lower tempering temperatures is that the setting or crystallization rate of the milk chocolate is slowed down (Liang and Hartel, 2004), resulting in a decrease in hardness. Finally, a negative side effect of the use of milk fat is its limited shelf life, as it is prone to oxidation and lipolysis, enzymatic break down of fats by lipases. On the other hand, a resistance to fat bloom exists as a result of the inclusion of free milk fat.

Depending on the characteristics of the milk powders, different finished products are obtained. The properties of milk powders affecting chocolate characteristics and determining their use in chocolate manufacturing include free fat content, particle size, particle size distribution and particle size structure, specific fat pore surface, air inclusion or vacuole volume, moisture content, and milk protein content and type (Liang and Hartel, 2004; Keogh et al., 2003).

**Table 2.2 Properties of milk powders and their influence on chocolate properties (Liang & Hartel, 2004).**

<b>Properties of milk powder</b>	<b>Properties of chocolate or processing conditions</b>
Particle size and distribution	Flow properties
Particle shape	Refining operations (particle size distribution)
Surface characteristics of particles	Tempering conditions (cocoa butter crystallization)
“Free” fat level	Hardness / Snap
Particle density	Bloom stability
Flavour attributes	Flavour attributes

Table 2.2 gives an overview of some of these characteristics of milk powders and how they affect the chocolate properties and/or processing conditions. Review of these specific properties of milk powders by Liang and Hartel (2004) has identified the free milk fat available to mix with the cocoa butter and the particle characteristics as the most important properties influencing the characteristics of milk chocolate, although there is not a clearly defined mechanism. As discussed previously in this chapter, addition of milk fat requires lower

tempering temperatures in order to promote nucleation of cocoa butter, as the milk fat inhibits cocoa butter crystallization. Besides influencing the tempering conditions, the free milk fat level also influences the rheological properties of the chocolate (Liang and Hartel, 2004). Milk fat reduces the yield stress and plastic viscosity, through a combination of reducing the dispersed phase volume and the particle size distribution. Depending on the type of milk powder used, e.g. skim milk powder or full cream milk powder, the amount of free milk fat available to react with the particles and the cocoa butter varies, resulting in different amounts of fat aiding the flow properties. In order for chocolate to flow, the particles must pass by one another, and the ease with which this happens depends on the viscosity of the system and the particle characteristics. Processing techniques used for the milk powder production define the particle characteristics as well as flavour characteristics (Beckett, 2008).

#### *2.1.2.4 Other components*

The Codex Standard for Chocolate (Codex Alimentarius, 2003) lists a large number of additives which are allowed within chocolate products within the limits specified: acidity regulators, emulsifiers, flavouring agents, sweeteners, glazing agents, antioxidants, colours, bulking agents and processing aids. Their use is in general regulated by Good Manufacturing Practice (GMP). Most important categories are the emulsifiers or surfactants and the flavouring agents, which will be discussed in slightly more detail below.

##### *2.1.2.4.1 Surfactants or surface active agents*

As will be discussed in section 2.1.3.3.1, chocolate is a colloidal system consisting of solid particles dispersed in a continuous fat phase. The lyophobic sugar particles are immiscible with the lipophilic cocoa butter molecules, creating a system that is thermodynamically not in equilibrium and will phase separate on storage. For the creation of a stable system, the use of surfactants or emulsifiers is required. The two main surfactants used in chocolate manufacturing are lecithin and polyglycerol-polyricinoleate (PGPR). Although there are many other surfactants, sometimes more generally called emulsifiers, e.g. sorbitan esters, sucrose dipalmitate and calcium-stearoyl lactoyl lactate, they often are not as efficient in reducing the yield value of the chocolate mixture (Beckett, 2008). Within the chocolate mixture, the positioning of the surfactant or emulsifier at the sugar / cocoa butter interface is responsible for a reduction in viscosity. By attaching its hydrophilic head to the sugar surface and leaving its hydrophobic tail in the continuous cocoa butter phase, the surfactant aids the flow behaviour of the chocolate mixture. As the surfactant covers the sugar particle surface, agglomeration of sugar particles is reduced as well as interparticle interactions (Götz et al., 2005). Although a significant decrease in viscosity can be obtained by the addition of low levels of surfactant,

thickening of the chocolate takes place when sufficiently high surfactant concentrations are used. At these concentrations, the surfactants will not only be present at the hydrophilic / lipophilic interfaces, but also dissolved in the fat phase either as single molecules, or by forming micelles or a bilayer around the sugar particles. The enlargement of the specific surface area of sugar molecules, in combination with the larger number of particles present in the continuous fat phase is responsible for the increase in viscosity, e.g. thickening of the chocolate. A final advantage of the use of surfactants is their application as antibloom agents, as they reduce the crystallization rate of cocoa butter (Götz et al., 2005). Specific surfactants may not deliver the required efficiency with respect to viscosity reduction, but they may alter the setting rate, surface gloss and/or bloom formation rate in chocolate products (Beckett, 2008). The use of combinations or mixtures of different surfactants in chocolate manufacturing is therefore not unusual.

- Lecithin.

Lecithin is a complex mixture of neutral lipids (triglycerides, sterols and fatty acids) and polar lipids (phospholipids and sugar- or glycolipids) (Götz et al., 2005), isolated mainly from soybean and egg yolk. The major glycerol phospholipids, derived from phosphatidic acid, present within raw soybean lecithin are phosphatidyl ethanolamine (PE), phosphatidyl inositol (PI) and phosphatidyl choline (PC) (Belitz et al., 2004).

Composition of lecithin varies, depending on origin, raw material quality and manufacturing processes. Some suppliers have developed a standardized product, as the effect of individual phospholipids on viscosity varies, e.g. PC significantly reduces plastic viscosity of some dark chocolates whereas PI and PE are less effective than standard lecithin (Chevalley, 1999). As lecithin is present within cocoa beans and milk, traces of lecithin will always be present within chocolate even if it is not included as a surfactant (Afoakwa et al., 2007).

According to Chevalley (1999), a similar reduction in viscosity is obtained by addition of 0.1–0.3% lecithin as would be obtained by addition of 10 times that amount of cocoa butter. However, thickening occurs at a concentration of 0.3–0.5%. The viscosity reducing effect of lecithin is particularly related to its strong binding to the sugar particle surface, where it was initially believed to be present in the form of a monolayer. The particle size distribution is important for the concentration of lecithin, as smaller sugar particles will increase the effective surface area and require an increased concentration of lecithin to cover all surfaces. Research by Ziegler et al. (2003), however, has shown that lecithin adsorbs in multilayers on the surface of both sugar and cocoa particles, where it aids in dispersing aggregates and helps reduce the viscosity.

An additional functional characteristic of lecithin is the fact that it enhances toleration of higher moisture levels within chocolate products (Afoakwa et al., 2007).

It has also been observed that the efficiency of lecithin depends on the time of addition

to the chocolate mass. Addition too early in the production process, whilst mixing and grinding are still being conducted, will increase the risk that the lecithin is absorbed onto the cocoa particle where it cannot reduce the viscosity (Chevalley, 1999). At the same time, exposure for long time periods to relatively high temperatures negatively affects lecithin efficiency.

- Ammonium phosphatide or YN

Ammonium phosphatide or YN, also called the synthetic lecithin, is obtained from partially hardened rapeseed oil through glycerolysis, phosphorylation and neutralization. It has a similar composition and efficiency as soybean lecithin (Chevalley, 1999). YN is actually even more effective at low concentrations, and in combination with its neutral flavour and (safe) non-GMO status it is a very popular replacer of soybean lecithin. At concentrations above 0.5% both lecithin and YN decrease the plastic viscosity of chocolate. In addition, YN does not affect the yield stress as a result of which there is no optimum dosage (Götz et al., 2005).

- Polyglycerol-Polyricinoleate or PGPR

Polyglycerol-Polyricinoleate or PGPR is another synthetic emulsifier. The application of PGPR in chocolate products is well known, and is mainly based on the effect of PGPR on the yield stress. In comparison to lecithin, PGPR can halve the yield value of chocolate at a concentration of 0.2% (Beckett, 2008). It is believed that the high efficiency of PGPR is a result of its higher molecular weight compared to lecithin, enhancing the steric stabilization mechanism and increasing the continuous phase volume fraction (Afoakwa et al, 2007). At these low levels of inclusion PGPR shows only a minimal effect on the plastic viscosity of the chocolate (Götz et al., 2005). Inclusion of 0.5-1.0% eliminates the flow point of chocolate, turning it into a Newtonian liquid with rapid setting properties. As a result of this behaviour, in industrial chocolate manufacturing mixtures of PGPR and lecithin are commonly used in order to produce a product with the optimum flow properties.

#### 2.1.2.4.2 Flavouring agents

Chocolate flavour is, to a large extent, determined by the processing techniques used. One of the key steps in the flavour and aroma development is the roasting of the cocoa beans, which ensures the development of flavour compounds that enhance the taste and aroma of the finished chocolate. The final flavour depends on the time and temperature of roasting, as well as on the origin and quality of the cocoa beans used, as discussed by Jackson (1999) and Dimick and Hoskin (1999). Another important processing step in relation to the flavour development is the conching process, where undesirable volatile acidic components are removed from the chocolate mass. Finally, the ingredients present within the chocolate recipe play an important role in the

flavour development. Sugar not only contributes sweetness, it also offsets the bitterness of cocoa solids. It can furthermore take part in the Maillard reaction with milk protein at elevated temperatures to create a milk caramelized flavour.

Flavour additions in chocolate manufacturing generally aim to enhance a characteristic flavour, rather than masking it. The main flavour additive commonly used is vanilla (natural flavour) or vanillin (artificial flavour), which gives a creamy note. Another commonly used flavour additive is salt, which enhances clean crispy notes (Jackson, 1999). Other flavour additives, e.g. spices, nutmeg and cinnamon, are added to chocolate to create a more specific flavour.

### **2.1.3 Crystallization**

Walstra (2003) describes a crystal as a solid state material with closely packed building entities, as a result of which the free energy of the material is at minimum. The presence of crystals in food products impacts food quality and organoleptic properties like texture, mouthfeel, physical stability and consistency. In the specific case of chocolate, the cooling sensation perceived upon eating of a piece of chocolate is a result of the endothermic reaction taking place in the mouth. Energy released as a result of the temperature difference between the chocolate and the mouth is adsorbed by the chocolate, melting the fat / cocoa butter crystals present. Crystallization is the process whereby a crystalline lattice structure is formed (Hartel, 2001), in this case from the liquid fat present in the chocolate mixture. Three (Awad and Marangoni, 2006; Lawler and Dimick, 2002) and sometimes four (Hartel, 2001; Walstra, 2003) stages have been defined within the crystallization process:

- **Supercooling**

For crystallization to take place, a phase change is required. This can be obtained by cooling the liquid cocoa butter below its equilibrium melting point. Below this temperature the free energy of the solid (crystalline) phase is lower than that of the liquid fat phase, driving crystallization. The deviation in temperature of the environment below the melting point of cocoa butter (equilibrium phase transition temperature) is defined as the level of supercooling.

- **Nucleation**

Once a certain level of supercooling has been achieved, crystal nuclei are formed. Nucleation can be defined as the transition from a metastable to a more stable phase, where the liquid state molecules rearrange through a cluster formation into a crystalline lattice. The nucleation rate is defined as the rate of formation of critical nuclei in the melt per unit time and unit volume.

In the case of fat crystallization the monoglyceride content significantly impacts the nucleation rate by forming catalytic impurities. Nucleation will be further discussed in section 2.1.3.1.

- Crystal growth

The nuclei formed during the nucleation stage continue to grow, through diffusion of the crystallizing molecule from the melt toward the solid–liquid interface of the growing crystal surface, until equilibrium is attained. Only molecules with a suitable configuration, e.g. size, shape and orientation, will be able to attach to a specific crystal surface. Two main factors drive crystal growth: the degree of supercooling and the viscosity of the melt, which controls the mobility of the molecules and consequently the rate of diffusion. Crystal size and shape are determined by the temperature and/or degree of supercooling. Relatively low supercooling results in the formation of (large) spherulites, and eventually a more open (spherical) crystalline structure, whereas increasing the degree of supercooling will increase the crystal growth rate, forming smaller crystals and a more compact crystalline structure.

- Recrystallization

While the crystallization process progresses, a moment exists where the degree of supercooling is reduced until equilibrium is obtained. At that stage the melt has been transformed into a stable (crystalline) system. However, even after reaching equilibrium reorganisations within the crystalline structure have been observed during long-term storage, in order to minimize the energy of the system. An increase in critical crystal size causes small crystals to dissolve, whilst large crystals continue to grow; this is defined as Ostwald ripening. Recrystallization also includes the transition of polymorphic forms as a result of storage temperature and time, e.g. fat bloom in chocolate products can be caused by a solid-state transition from Form V to Form VI polymorphs.

According to Timms (1997), the partition between crystal nucleation and growth is very thin, and these stages often occur simultaneously. Whilst the temperature is reduced to obtain the right degree of supercooling, the first nuclei will be formed, hence inducing nucleation and successive growth of the original nuclei. Chemical composition (recipe) and processing conditions like temperature, cooling rate and shear are the main drivers of fat crystallization. By controlling heat, mass and momentum transfer rates, the crystal size and consequently the texture and organoleptic characteristics of the cocoa butter system can be kept constant.

### 2.1.3.1 Nucleation

According to Hartel (2001), nucleation is the most important stage within the crystallization process. Without the formation of the required amount of nuclei at the appropriate time, it is impossible to obtain the desired crystalline structure. In other words, nuclei are essential as they act as centres of crystallization. Nucleation commences either through agitation, mechanical shock, friction or extreme pressures in the melt (Mullin, 2001).

Nucleation can be through different mechanisms, related to the driving factor responsible for nuclei formation. The overview in Figure 2.1 defines two main mechanisms of nucleation, primary and secondary. Primary nucleation can be further subdivided into homogeneous and heterogeneous nucleation. Lawler and Dimick (2002) suggested chemical nucleation as a third mechanism, based on observations made within the area of polymer science. There is some debate, however, as to whether this refers to chemical induction of heterogeneous nuclei or rather chemical nucleation resulting in the addition of solid heterogeneous nuclei.

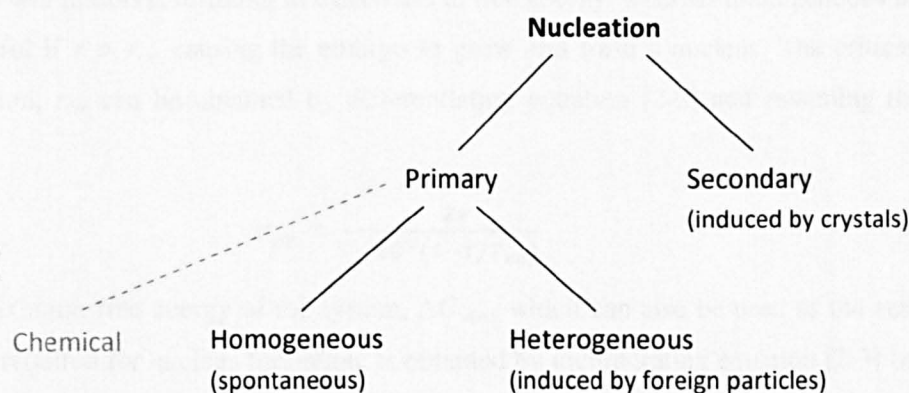


**Figure 2.1. Nucleation mechanisms (Hartel, 2001; Mullin, 2001).**

#### 2.1.3.1.1 Primary Homogeneous Nucleation

Primary homogeneous nucleation takes place in a homogeneous system, where no phase boundaries exist. Depending on the conditions, molecules can orientate themselves to form nuclei spontaneously (Walstra, 2003). Sufficient supercooling of the melt is required to ensure that the rate of association is greater than the rate of dissociation, resulting in the formation of a cluster of molecules of critical size to be called a nucleus (Hartel, 2001). The formation of such a cluster is relatively simple in a liquid, by association of solute or vapour molecules. In a solid, an additional complexity is that the molecules need to attain a mutual orientation as those of the crystals, in order to form a cluster. An embryo is a cluster of molecules which is smaller than a nucleus, and which easily re-dissolves. Upon aggregation of the molecules, two opposing mechanisms take place. First of all, nucleation is favoured by the release of heat as a result of the aggregation process. Secondly, the aggregated cluster has an increased surface area,



requiring energy to overcome the surface tension or pressure. If the energy resulting from the heat of crystallization exceeds the amount of energy required to overcome the surface energy, stable nuclei will be formed (Timms, 1997). The excess free energy of a spherical embryo,  $\Delta G_{emb}$ , with radius  $r$  is given by equation [2-1], in comparison to the excess free energy of a similar volume of phase  $\alpha$ :

$$\Delta G_{emb} = \frac{4}{3}\pi r^3 \Delta G^V + 4\pi r^2 \Delta G^S, \quad [2-1]$$

where  $\Delta G^V$  is the free energy change of the material, expressed per unit volume, and  $\Delta G^S$  is the interfacial free energy per unit surface area between the two phases, equalling the interfacial tension,  $\gamma$ . At low temperature differences the assumption is made that the interfacial tension is independent of temperature, and equation [2-1] can be rearranged into

$$\Delta G_{emb} = \frac{4}{3}\pi r^3 \Delta G^V \left(1 - \frac{T}{T_{eq}}\right) + 4\pi r^2 \gamma. \quad [2-2]$$

One of the parameters driving the nucleation process is the embryo radius,  $r$ . If  $r < r_{cr}$ , the embryo will dissolve, resulting in a decrease in free energy, whereas homogeneous nucleation is successful if  $r > r_{cr}$ , causing the embryo to grow and form a nucleus. The critical radius for nucleation,  $r_{cr}$ , can be obtained by differentiating equation [2-2] and assuming that  $\Delta G_{emb} = \Delta G_{max}$ :

$$r_{cr} = -\frac{2\gamma}{\Delta G^V(1-T/T_{eq})}. \quad [2-3]$$

The maximum free energy of the system,  $\Delta G_{max}$ , which can also be used as the activation free energy required for nucleus formation, is obtained by incorporating equation [2-3] into equation [2-2]:

$$\Delta G_{max} = \frac{16\pi\gamma^3}{3[\Delta G^V(1-T/T_{eq})]^2} = \frac{4}{3}\pi r_{cr}^2 \gamma. \quad [2-4]$$

As the level of supercooling required to initiate nucleation is considerable, homogeneous nucleation is sparse and is only observed in chemically pure systems (Walstra, 2003).

#### 2.1.3.1.2 Primary Heterogeneous Nucleation

Primary heterogeneous nucleation is induced by catalytic impurities at temperatures above the homogeneous nucleation temperature,  $T_{hom}$ . Catalytic impurities are small (foreign) particles or surfaces, whose character depends on the composition and purity of the melt (Walstra, 2003). The degree of supercooling required for heterogeneous nucleation is lower than that required for homogenous nucleation, consequently reducing the activation free energy associated with the formation of a critical nucleus under heterogeneous conditions,  $\Delta G'_{max}$  (Mullin, 2001).

Equation [2-5] describes the relation between homogeneous and heterogeneous nucleation, where factor  $\phi$  has a value less than unity.

$$\Delta G'_{max} = \phi \Delta G_{max} \quad [2-5]$$

Heterogeneous nucleation can be induced by either a small (foreign) particle, or a solid surface. In both cases, the driving factor is the angle of contact between the surface of the crystalline deposit and that of the catalytic impurity,  $\theta$ , which is schematically shown in Figure 2.2. The concept of contact angle will be discussed in more detail in section 2.3.2.2, but is mainly determined by the interfacial tension,  $\gamma$ . According to the Young's equation [2-30], a balance of forces exists at the point where three phases meet. In this case that applies to the point where the surface of the catalytic impurity, the crystalline deposit and the melt (liquid continuous phase) meet.

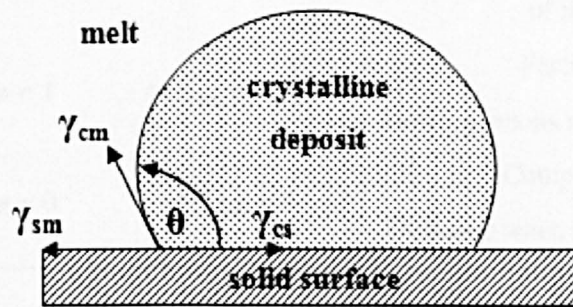


**Figure 2.2. Heterogeneous nucleation at the surface of a catalytic impurity (Walstra, 2003).**

The contact angle,  $\theta$ , is dependent on the balance between the interfacial tensions,  $\gamma$ , of the three phases: catalytic impurity or solid (s), melt (m) and crystalline deposit (c).

Crystalline deposit will form an embryo due to the presence of a solid surface, if  $\cos \theta$  is finite:

$$\cos \theta = \frac{\gamma_{sm} - \gamma_{cs}}{\gamma_{cm}} \quad [2-6]$$

where  $\gamma_{sm}$ ,  $\gamma_{cs}$  and  $\gamma_{cm}$  are the surface tensions of the solid–melt, crystal–solid and crystal–melt interfaces, respectively.

An embryo formed spontaneously (homogeneous), and an embryo formed as a result of an impurity (heterogeneous) only have the same curvature if the level of supercooling is the same in both systems (Walstra, 2003). From Figure 2.2 it can be observed that a “heterogeneous” embryo will have a lower volume in this situation. Factor  $\phi$  (see equation [2-5]) is obtained by dividing the volume of a “heterogeneous” embryo by that of a sphere of the same radius:

$$\phi = \frac{(2 + \cos \theta)(1 - \cos \theta)^2}{4} \quad [2-7]$$

Due to the fact that the energy required for the formation of “heterogeneous” embryos is lower than that required for “homogeneous” nucleation, heterogeneous nucleation is more commonly observed in food systems (Awad and Marangoni, 2006).

The relation between contact angle and the nucleation mechanisms is summarized in Table 2.3. Heterogeneous nucleation is favoured at relatively low contact angles (Timms, 1997).

**Table 2.3. Effect of the contact angle,  $\theta$ , and factor,  $\phi$ , on the free energy of nucleation,  $\Delta G$  (Mullin, 2001).**

Contact angle $\theta$	Factor $\phi$	Free energy of nucleation $\Delta G$	Comments
$\theta = 180^\circ$	$\phi = 1$	$\Delta G'_{\max} = \Delta G_{\max}$	Non-affinity between the crystalline deposit and the surface of the catalytic impurity. Homogeneous and heterogeneous nucleation require the same free energy of nucleation.
$0 < \theta < 180^\circ$	$\phi < 1$	$\Delta G'_{\max} < \Delta G_{\max}$	Partial affinity. Heterogeneous nucleation is preferred.
$\theta = 0^\circ$	$\phi = 0$	$\Delta G'_{\max} = 0$	Complete affinity. Obtained when seed crystals are used.

#### 2.1.3.1.3 Secondary Nucleation

Secondary nucleation can only occur when crystals are already present in a system, i.e. after primary nucleation has taken place. Due to shear or another external force, e.g. a scraped surface heat exchanger used during ice-cream manufacturing, growing crystals are fractured. The size of the fractured crystal determines whether secondary nucleation will occur. If the fractured crystal is below the critical nucleus size, it will re-dissolve. Otherwise, stable crystal nuclei are present, which induce crystal (secondary) nucleation and growth (Lawler and Dimick, 2002). According to Walstra (2003), the phenomenon described here is not *true secondary nucleation*, where a nucleus is formed in the vicinity of a crystal at the same phase, rather than at the surface.

#### 2.1.3.2 Fat crystallization

Fat crystallization is an important characteristic of many food products, where the fat crystals are responsible for a number of important properties, e.g. mechanical and eating properties, physical stability and visual appearance (Walstra, 2003). However, the characteristics of fats and oils make the crystallization process extremely complex. Fats are polymorphic, i.e. they contain triglycerides with the same composition which can exist in more than one crystal form or configuration (Lawler and Dimick, 2002). The three major crystal forms are:  $\alpha$ , or hexagonal

packing,  $\beta'$ , or orthorhombic perpendicular packing, and  $\beta$ , or triclinic parallel packing. They vary in melting point and crystal stability, with  $\alpha$  crystals having the lowest, and  $\beta$  crystals having the highest melting point and stability, respectively (Blaurock, 1999). As the free energy of nucleation,  $\Delta G_{\max}$ , is higher for the  $\beta$  polymorphic form, see Figure 2.3, triglycerides often crystallize initially in  $\alpha$  or  $\beta'$  structures. However, with time and at constant temperatures,  $\alpha$  and  $\beta'$  crystals transform into  $\beta$  crystals through solid-solid or solid-liquid-solid transformation mechanisms (Awad and Marangoni, 2006). Overall it can be concluded that polymorphism affects the crystallization rate, crystal size, crystal morphology, and degree of crystallinity (Awad and Marangoni, 2006).

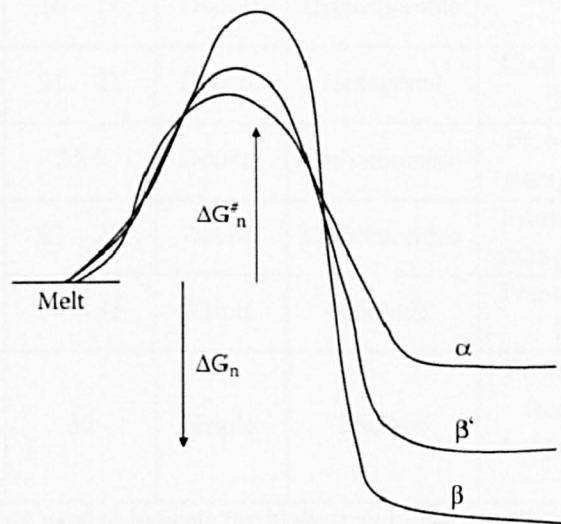


**Figure 2.3 Free activation energy of nucleation change ( $\Delta G_n^\#$ ) for the three main polymorphs, whereby  $\Delta G_n^\#$  represents the free energy barrier that must be exceeded before stable nuclei can be formed (Awad and Marangoni, 2006).**

Most fats are complex mixtures which are composed of a number of different triglycerides with various melting behaviours. The melting temperature of a triglyceride is determined by the length of the fatty acid chains, the number and configuration, e.g. cis or trans, of double bonds and the distribution of fatty acid residues (Walstra, 2003). As not all triglycerides can have the same composition, a mixture of different triglycerides, e.g. a fat, will have a melting range rather than a single melting point. Within a mixture of triglycerides, the melting temperature and the heat of crystallization of different triglycerides will be closely related, causing the higher melting triglycerides to dissolve in the lower melting ones.

#### 2.1.3.2.1 Cocoa butter polymorphism

Processing conditions and TAG composition of cocoa butter determine the crystal form, mainly by determining the packing arrangement during crystallization. For cocoa butter six different polymorphic forms have been identified, each with its own physical characteristics.

Despite many years of research, no uniform nomenclature exists. In general, either the convention of Wille and Lutton (1966), based on the Roman numbering system (I-VI) or the convention of Larsson (1966), based on the Greek nomenclature, is used. Table 2.4 summarizes the characteristics of the different cocoa butter polymorphs.

**Table 2.4 Overview of the physical properties of the polymorphic forms of cocoa butter (adapted from Talbot, 1999a and Rousseau, 2007).**

Form <sup>*1</sup>	Polymorph <sup>*2</sup>	Melting point [°C]	Chain packing	Molecular packing	Common means of development	Stability
I	$\beta_2$ or $\gamma$	16 – 18	Double	Orthorhombic	Rapid cool from melt	Unstable
II	$\alpha$	21 – 22	Double	Hexagonal	Cool from melt at 2 °C/min	Unstable
III	mixed	25.5	Double	Orthorhombic	From Form II on storage (5-10 °C)	Semi-stable
IV	$\beta_1$	27 – 29	Double	Orthorhombic	From Form III on storage (16-21 °C)	Semi-stable
V	$\beta_2$	34 – 35	Triple	Triclinic	Transformation of Form IV	Stable
VI	$\beta_1$	36	Triple	Triclinic	From Form V on storage (room temperature, long time)	Stable

<sup>a</sup> The subscripts 1 and 2 are used to indicate the highest and lowest melting form with similar crystal packing.

<sup>\*1</sup> As proposed by Wille and Lutton (1966)

<sup>\*2</sup> As proposed by Larsson (1966)

As mentioned earlier, processing conditions determine the polymorphic form of the cocoa butter phase formed. The main parameter affecting the formation of different polymorphic forms is the temperature during crystallization, although cooling rate and agitation rate are also known to have an effect (Hartel, 2001). A low temperature and fast cooling rate results in the formation of lower melting polymorphs, i.e. Form I and II, which are generally unstable and are with time transformed in higher melting polymorphs, i.e. Form III and IV (Arishima and Sato, 1989). These phase transitions are irreversible and are driven by temperature and time. The polymorphic form required during chocolate production is Form V, and the processing techniques required to obtain this form will be discussed in more detail in section 2.1.4.1. Upon storage Form V can transform into Form VI, which is generally associated with fat bloom and affects the sensorial properties of the product. The low melting cocoa butter polymorphs can be obtained directly through crystallization of totally molten cocoa butter, whereas the stable  $\beta$  polymorphs can only be obtained through transformation from  $\beta'$ .



Figure 2.4 shows an isothermal phase-transition scheme of cocoa butter under mechanically static conditions (Schenk and Peschar, 2004). The solidification temperature,  $T_p$ , has a significant impact on the initial polymorph obtained during cocoa butter solidification. At  $T_p \leq 20$  °C, the  $\alpha$  and  $\gamma$  ( $\beta_2$ ) polymorphs are obtained after a few minutes or seconds (depending on temperature), whilst at  $20 < T_p \leq 27$  °C solidification of the  $\beta'$  polymorphs decelerated to hours or days and at  $T_p \geq 28$  °C no solidification was perceived (van Malssen et al., 1999).

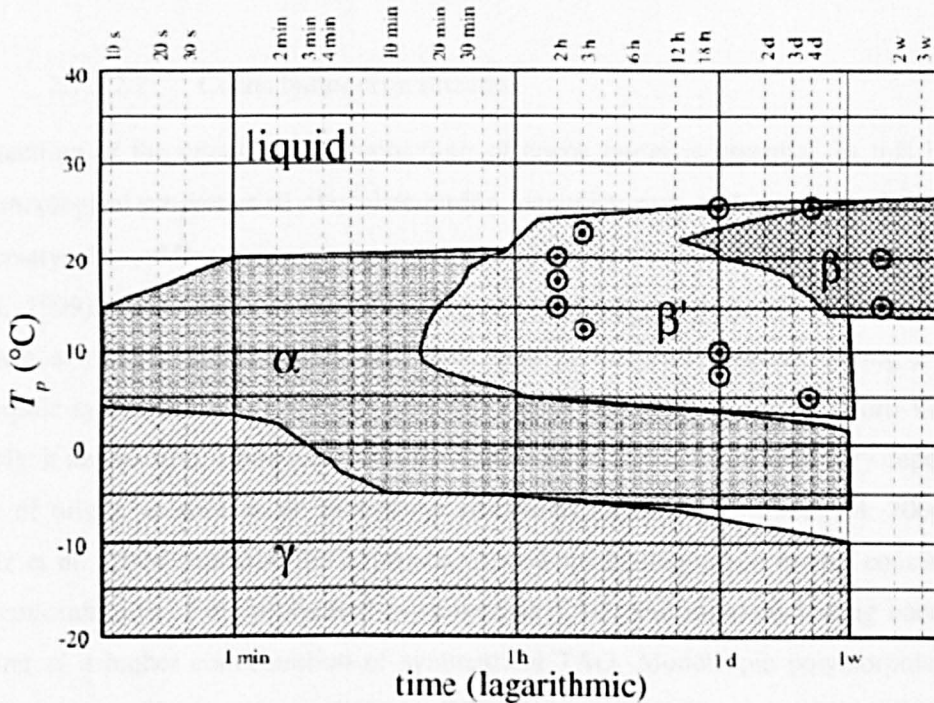


**Figure 2.4 Qualitative isothermal phase-transition scheme of static cocoa butter.**

**Solid phase present after isothermal crystallization time at  $T_p$  (Schenk and Peschar, 2004).**

An important discriminating factor for the different polymorphs is the molecular conformation or packing configuration, which in turn can be characterized by the distance between the fatty acid chains and the angle of tilt relative to the plane of the end methyl group (Talbot, 1999a). In general, fats can be classified by three main polymorphic forms with increasing thermodynamic stability:  $\alpha$ ,  $\beta'$  and  $\beta$ . The  $\alpha$  polymorph, which is the least stable configuration, has alkyl chains perpendicular to the end plane, resulting in a hexagonal symmetry. According to Rousseau (2007) they exist as small, fragile, transparent platelet crystals,  $\sim 5$   $\mu\text{m}$  in length, whereas the  $\beta'$  and  $\beta$  polymorphs exist as small delicate needles measuring 1-2  $\mu\text{m}$  and 50  $\mu\text{m}$  in length, respectively. The main difference between the  $\beta$  and  $\beta'$  structures are their angle of tilt relative to the end of plane of the molecules. Within the  $\beta'$  polymorph the angle of tilt is greater, with the fatty acid chains packed more perpendicular to each other, forming an orthorhombic structure. In the  $\beta$  structure the fatty acid chains are parallel, allowing a closer and more dense packing, a triclinic structure (Schenk and Peschar, 2004). The lamellar spacing and fatty acid arrangement of each polymorph can be identified by X-ray diffraction. Another parameter differentiating between the  $\beta$  and  $\beta'$  structure is the manner in which the triglycerides crystallize.

As can be observed from Table 2.4, the  $\beta'$  polymorph crystallizes in a double chain packing, whereas the  $\beta$  polymorph packs in a triple chain. Chain packing is defined as the distance between two subsequent methyl end planes. Triglyceride composition and the position of the double bond mainly determine the chain packing (Talbot, 1999a). All parameters discussed affect the crystallization and solidification characteristics of the cocoa butter, either direct or indirect.

#### 2.1.3.2.2 Cocoa butter crystallization

Understanding of the crystallization behaviour of cocoa butter is essential, as this behaviour affects rheological properties of chocolate during manufacturing, and consequently determines the viscosity, demoulding, snap, surface gloss and melting characteristics of the final product (Dimick, 1999). Cocoa butter is a complex mixture of triacylglycerols, of which approximately 75% have a uniform confirmation with oleic acid in the *sn*-2 position, giving a complex polymorphic system whose crystallization behaviour is not straight forward (Toro-Vazquez et al., 2004). It depends on, amongst others, the TAG composition, which may vary depending on country of origin, as well as on processing conditions (Awad and Marangoni, 2006). Toro-Vazquez et al. (2004) mention the existence of slow-nucleating cocoa butter, consisting of a higher concentration of di-unsaturated asymmetrical TAG, and rapid-nucleating cocoa butter, consisting of a higher concentration of symmetrical TAG. Monotropic polymorphism means that each polymorphic form has a different Gibbs free energy,  $G$ , and the polymorph with the lowest Gibbs free energy is thermodynamically the most stable one. As a result of the differences in Gibbs free energy, the less stable polymorphs transform to more stable polymorphic forms with time, as shown in Figure 2.4 (Himawan et al., 2006). As the Gibbs free energies of the different polymorphs do not cross below their melting points, each form can be obtained by crystallization as long as the rate of solid-state transformation is lower than that of crystallization (Sato, 1993).

Figure 2.5 shows the crystallization mechanisms taking place within a cocoa butter system in time. The crystallization process starts with supercooling of the liquid cocoa butter (melt), in order to induce a liquid-solid phase change resulting in the formation of primary crystals with characteristic polymorphism (Brunello et al., 2003). Both homogeneous and heterogeneous nucleation mechanisms, through the presence of endogenous plant materials acting as catalytic impurities, are responsible for this initial or primary crystallization stage, in which < 1% of the melt is solidified. It is possible to identify the crystals formed at different stages of the crystallization process through thermal and chemical analysis. The first (visible) cocoa butter crystals formed during a static crystallization process at 26-33°C were observed to contain POP, POSt and StOSt TAGs, and the concentration of StOSt was shown to increase with crystallization temperature (Sato & Koyano, 2001). Loisel et al. (1998a, 1998b) discuss the

segregation of cocoa butter by varying lipid families during crystallization, a process which is driven by the crystallization temperature. Nucleation is proposed to start with the complex lipids and trisaturated TAGs forming seed crystals if  $T_c > 26.2^\circ\text{C}$ , hypothesizing a fractionated crystallization process during cooling. Due to differences in solubility, saturated TAGs (SSS) segregate from other mono- and polyunsaturated TAGs upon crystallization, initiating crystallization of cocoa butter *via* the  $\alpha$  form. Secondary nucleation can take place once the initial crystals have been formed. This may result in the formation of multicomponent fat crystals (Dimick, 1999). According to Loisel et al. (1998a) the second nucleation step is driven by crystallization of monounsaturated TAGs (SUS). Nucleation is followed by a crystal growth stage and finally the formation of a continuous three-dimensional crystal network. According to DeMan (1999), the degree of supercooling determines whether nucleation or crystal growth predominates. At a temperature halfway between the melting temperature,  $T_m$ , and the glassy-state temperature,  $T_g$ , the crystallization rate is optimal, whereas close to  $T_m$  the degree of supercooling is low and crystal growth predominates, and close to  $T_g$  nucleation predominates. Crystal growth is favoured over the formation of the 3D network, as it requires less energy than is required for the aggregation and orientation of the melt molecules in a three-dimensional network. A heat- and mass-transfer-limited process is responsible for the aggregation of crystals, and growth continues until approximately 50–70% of the melt has been solidified (Dimick, 1999). The crystal size distribution depends on the nucleation rate and the rate of crystal growth, and is an important quality parameter in food systems. From a certain critical size fat crystals are detectable on the tongue and the amount and size of the crystals that are expected from a palatability point of view will depend on the product texture and the individual consumer (Himawan et al., 2006). The fat crystal size also affects the hardness of the cocoa butter system. Assuming that the solid fat content is the same for two products, the product with the smaller fat crystals is softer, more plastic, compared to the product with the larger fat crystals, which is harder (DeMan, 1999).

The aggregation or crystal nucleation and growth processes are responsible for an increase in the solid fraction or solid fat content (SFC) of the cocoa butter system. This process continues until the increase in solid fraction causes the individual crystals to come into contact with each other, slowing the crystal growth. At that stage, crystal-crystal interactions start to dominate (Himawan et al., 2006). Although there is some debate as to the exact mechanism, DeMan (1999) explains that van der Waals forces are responsible for keeping the crystal network together. Depending on the crystal size, van der Waals attractions are responsible for the aggregation of crystals, leading to the formation of crystal aggregates. Only at very low mutual distance some degree of repulsion may occur (Walstra et al., 2001). Post-crystallization processes taking place during storage affect the three-dimensional network that has been formed previously through aging of the bonds. Especially physical and/or mechanical properties of the fat, such as hardness and snap, have been observed to increase during storage (Himawan et al,



2006). One of the main mechanisms responsible for this increase is called sintering, which is the formation of solid bridges between crystals, consequently forming a network (DeMan, 1999; Himawan et al., 2006). The formation of a fat crystal network gives cocoa butter its plastic (physical) characteristics, i.e. external forces applied to the crystallized network cause the fat to deform or flow (Walstra et al., 2001).

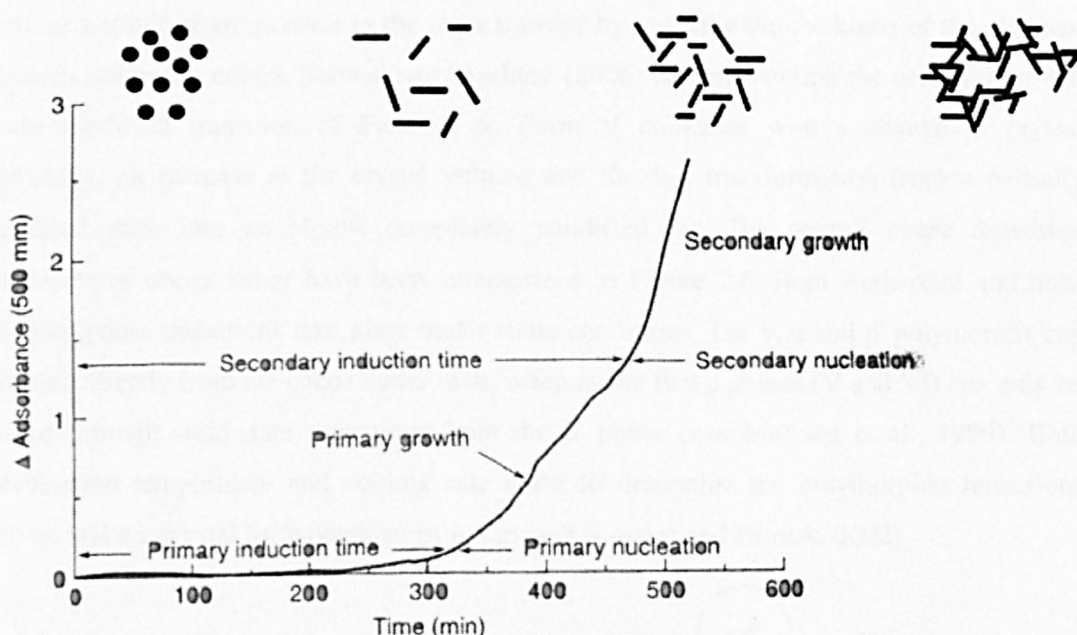


**Figure 2.5 Crystallization events occurring within the bulk during solidification of cocoa butter (Dimick, 1999; Himawan et al., 2006).**

The differences in free energy of activation for nucleation,  $\Delta G^\ddagger$ , between different polymorphic forms, as shown in Figure 2.3, cause triacylglycerols to crystallize initially in the unstable  $\alpha$  or  $\beta'$  form, before transforming into the stable  $\beta$  form through solid-solid or solid-liquid-solid mechanisms, depending on temperature and time (Awad and Marangoni, 2006). In the case of cocoa butter, several authors (Sonwai and Mackley, 2006; Mazzanti et al., 2004; van Malssen et al., 1999) have observed the initial crystallization of cocoa butter under static conditions into either  $\gamma$  or  $\alpha$  (Form II) polymorphs. Depending on time and cooling temperature, the crystals formed during the initial nucleation are transformed into the  $\beta'$  (Form IV) form, through a solid-state transition. According to Toro-Vazquez et al. (2004) this is followed by a nucleation and growth phase, in which additional  $\beta'$  crystals are developed directly from the melt. The transformation rate depends on the crystallization temperature, and at 20°C the transition is relatively fast. Eventually, the  $\beta'$  polymorphs will transform to the most stable  $\beta$  (Form V) polymorphs. As this transition requires a more intensive rearrangement of the crystal planes into an ordered and stable confirmation, this is the longest transformation process (Awad and Marangoni, 2006). However, the application of shear during the crystallization process induces a phase transition of cocoa butter from a less stable form, e.g. Form II ( $\alpha$ ), directly to the stable

Form V ( $\beta$ ) (Sonwai and Mackley, 2006). Stapley et al. (1999) mention three possible reasons why shear promotes the formation of Form V crystals: (i) shear aligns TAG molecules parallel to each other, increasing the possibility of interaction and nucleation events (primary nucleation); (ii) shear breaks up crystallites, increasing the number of seed crystals, initiating secondary nucleation; and (iii) shear force is responsible for a better overall mixing. A fourth mechanism has been proposed by Baichoo et al. (2006), who refer to the enhanced crystal growth as a result of an increase in the mass transfer by reducing the thickness of the stagnant film surrounding the nuclei. Sonwai and Mackley (2006) further mention the observation that the shear-induced transition of Form II to Form V coincides with a change in crystal morphology, an increase in the crystal volume and the fast transformation from a partially crystallized state into an almost completely solidified fat. The overall phase transition mechanisms of cocoa butter have been summarized in Figure 2.6. Both isothermal and non-isothermal phase transitions take place under static conditions. The  $\gamma$ ,  $\alpha$  and  $\beta'$  polymorphs can be formed directly from the cocoa butter melt, whereas the two  $\beta$  phases (V and VI) can only be obtained through solid-state transitions from the  $\beta'$  phase (van Malssen et al., 1999). Both crystallization temperature and cooling rate seem to determine the polymorphic transitions observed and the crystal form obtained from the melt (Lawler and Dimick, 2002).

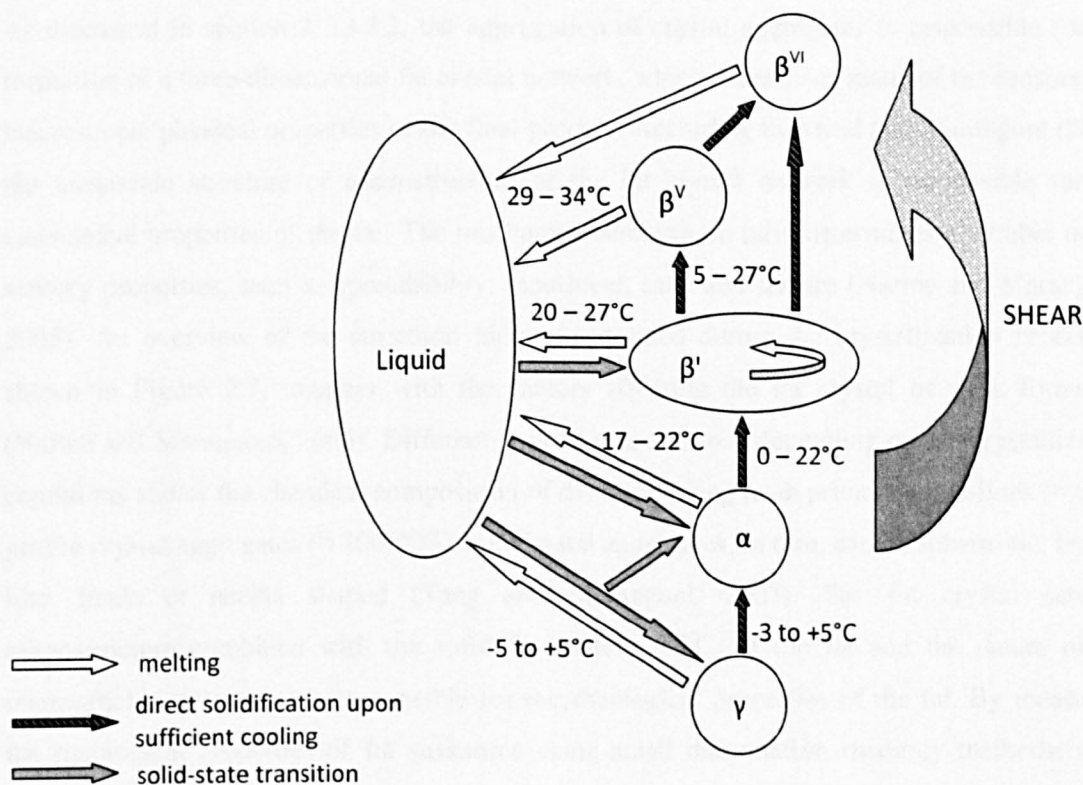


**Figure 2.6** Phase transition scheme of cocoa butter (van Malssen et al., 1999).

One of the major compound groups investigated in relation to the crystallization of cocoa butter are the phospholipids. By analyzing the composition of cocoa butter crystals formed at different stages of the crystallization process, Dimick (1999) found that the high-melting crystals formed

during the early stage of crystallization, consisted of large amounts of phospholipids and glycolipids. He proposed a mechanism whereby the polar lipids form a micelle or inverse hexagonal mesophase orientation, locking trace amounts of water in its core. These micelle act as crystal nuclei, onto which the high melting trisaturated TAGs, monounsaturated TAGs and the lowest-melting di-unsaturated TAGs, respectively, are loaded. Phospholipids present in cocoa butter are thus known as important compounds increasing the crystallization rate and enhancing the formation of  $\beta$  polymorphs (Lawler and Dimick, 2002).

By using the “memory” of the cocoa butter, it is possible to crystallize cocoa butter directly from the melt in any of the  $\beta$  phases. If a sample of cocoa butter, solidified in the  $\beta$  phase, is heated just above its melting end point, it does not lose all structural information about the crystalline state. As a result, upon cooling, the cocoa butter re-crystallizes into the  $\beta$  phase (Schenk and Peschar, 2004). In contrast to crystallization induced by seeding, where Form V cocoa butter or TAGs are added, the structural information or crystal-packing information responsible for crystallization in the stable  $\beta$  phase is present in the memory of the melt.

#### 2.1.3.2.3 Cocoa butter microstructure

As discussed in section 2.1.3.2.2, the aggregation of crystal aggregates is responsible for the formation of a three-dimensional fat crystal network, which determines many of the sensory and macroscopic physical properties of the final product. According to Awad and Marangoni (2006) the mesoscale structure or microstructure of the fat crystal network is responsible for the mechanical properties of the fat. The mechanical strength, in turn, determines a number of the sensory properties, such as spreadability, mouthfeel, snap and texture (Narine and Marangoni, 2005). An overview of the structural hierarchy defined during the crystallization process is shown in Figure 2.7, together with the factors affecting the fat crystal network formation (Narine and Marangoni, 2005). Different structures are formed depending on the crystallization conditions and/or the chemical composition of the fat, ranging from primary crystallites ( $\approx 0.5$ - $1 \mu\text{m}$ ) to crystal aggregates ( $\approx 100$ - $200 \mu\text{m}$ ). Crystal aggregates, in turn, can be spherulitic, feather like, blade or needle shaped (Tang and Marangoni, 2007). The fat crystal network microstructure combined with the solid fat content (SFC) of the fat and the nature of the interparticle interactions is responsible for the rheological properties of the fat. By measuring the rheological properties of fat structures using small deformation rheology methods, more information is obtained regarding the mechanical properties of the fat crystal network. Combining these results with microscopy analysis, e.g. polarized light microscopy, allows the determination of the effect of the fat microstructure on the mechanical properties (Tang and Marangoni, 2007).

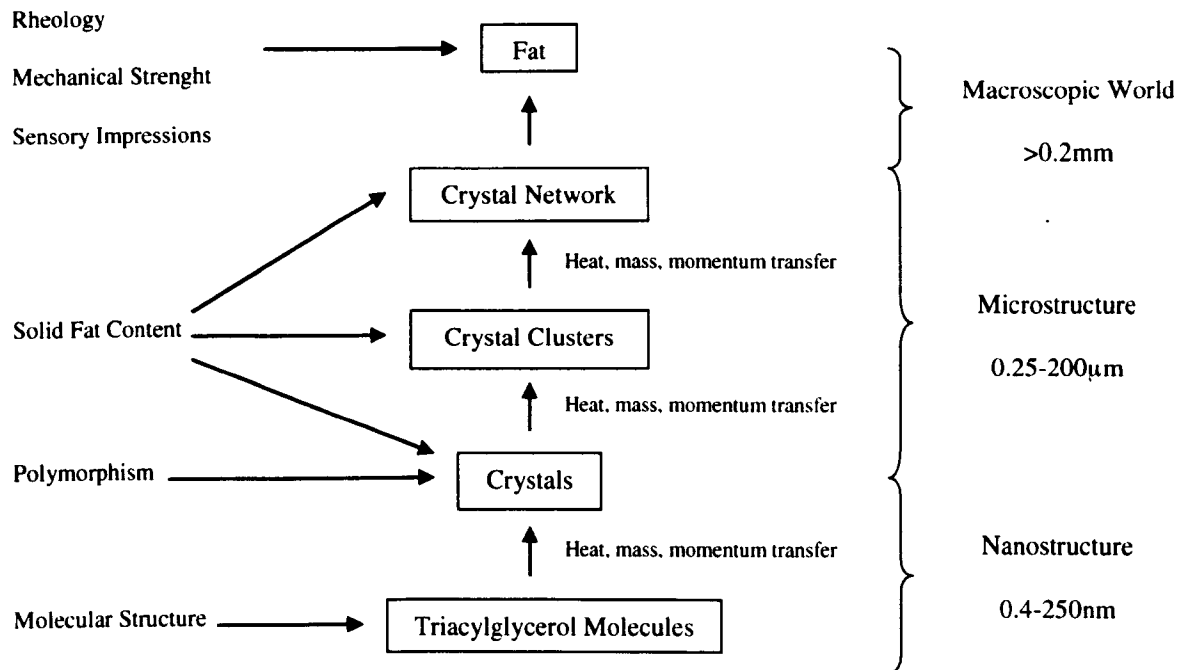


**Figure 2.7 Structural hierarchy of the crystallization process and the formation of the fat crystal network (Narine and Marangoni, 2005).**

McGauley and Marangoni (2002) describe the microstructure of the different cocoa butter polymorphic forms and their relation to the crystallization temperature. Both the  $\alpha$  and  $\gamma$  polymorph, which co-existed, were observed to have similar granular morphologies. The morphology of the  $\beta'$  polymorph depends mainly on the crystallization temperature and to a lesser extent on the formation pathway. When the  $\beta'$  polymorph was formed through a solid-state transition from the  $\alpha$  polymorph, a granular morphology was obtained, which showed evidence of the initial formation of clusters of spherulites at high crystallization temperatures. However, direct crystallization from the melt resulted in  $\beta'$  polymorphs with varying microstructures depending on the crystallization temperature, e.g. a granular morphology at 20 °C and needle-like crystallites ( $\sim 25 \mu\text{m}$ ) at 24 °C. In a similar experiment, Brunello et al. (2003) did not see changes in microstructure during storage at 5°C, assuming that this was the reason for the constant rheological parameters. At higher storage temperatures (20 °C), changes in mechanical properties were observed as a result of the polymorphic ( $\beta'$  to  $\beta$ ) transition, which was accompanied by an increase in solid fat content (SFC) and resulted in a number of different microstructures, e.g. a feather-like morphology. It was concluded that not only SFC but also the network structure, e.g. polymorphism, had a significant influence on the mechanical properties of the fat crystal network.

The microstructure of cocoa butter and fat crystal networks in general, is not influenced by the depth within the sample at which the measurement is taken, i.e. it is not affected by changes in scale or size. As discussed by Narine and Marangoni (2005), this form of symmetry is called self-similarity. Fat crystal networks are statically self-similar, which has been described by Awad and Marangoni (2006) as “*polycrystalline particles arranged in a fractal fashion within*

*clusters, which themselves pack in a Euclidean (homogeneous) nonfractal fashion*". Based on the fractal nature of fats the fractal dimension,  $D$ , a mathematical indicator of structure, can be determined and used as a measure to quantify the microstructure of a system. Crystallization kinetics, on the other hand, can be quantified by the induction time,  $\tau$ , and the Avrami exponent,  $n$  (McGauley and Marangoni, 2002). Toro-Vazquez et al. (2004) identified two different crystal growth mechanisms of the TAGs of cocoa butter, defined by  $n$ , in relation to the crystallization of the  $\beta'$  polymorph as a phase range with different melting temperatures. If  $T_{cr} > 19.0^{\circ}\text{C}$  a tri-dimensional ( $n \approx 4$ ) or spherulitic crystal growth mechanism was observed, whereas at  $T_{cr} < 19.0^{\circ}\text{C}$  a bi-dimensional ( $n \approx 4$ ) or disk-like mechanism was followed. McGauley and Marangoni (2002) established a weak but significant correlation ( $p = 0.0126$ ) between the induction time and the Avrami exponent. A strong correlation ( $p < 0.001$ ) was observed between the Avrami exponent and the fractal dimension, two parameters which both describe microstructural events. A hypothesis was proposed that, under certain conditions, the Avrami exponent and the fractal dimension can predict the mechanical strength or hardness of a network.

### 2.1.3.3 Chocolate crystallization

Processing conditions and ingredients added to cocoa butter during the chocolate manufacturing process significantly affect the crystallization of chocolate. Tempering is the specific processing step required to generate a small amount of stable fat crystal nuclei, which act as seed crystals during further chocolate manufacturing, promoting the formation of stable Form V crystals. An in-depth discussion of the tempering process is given in section 2.1.4.1. In general, temperature, time and shear are three parameters known to affect the tempering process. Stapley et al. (1999) compared tempered and untempered chocolate, and found that the crystal growth rate is lower in tempered chocolate, possibly as a result of changes in cooling rate. A high cooling rate promotes the formation of more unstable polymorphs, whilst at lower cooling rates more time is available for the formation of stable (higher) polymorphs. Similarly, Baichoo et al. (2006) showed that at low cooling rates the growth of stable (Form V) polymorphs in tempered chocolate is favoured over the nucleation and growth of unstable polymorphs. In the case of rapidly cooled chocolate, low-melting polymorphs are formed initially, but melt on heating and re-crystallize in high-melting polymorphs. The commercial tempering process used during chocolate manufacturing consists of a well-controlled temperature program, whereby the chocolate mass is subsequently heated, cooled and re-heated, as can be observed in Figure 2.11, section 2.1.4.1. When re-heating chocolate the temperature is important, as this will affect the number and possibly the size of seed crystals remaining (Stapley et al., 1999). A too high re-heating temperature will melt out the seed crystals, consequently reducing the crystallization rate.

According to Stapley et al. (1999) a longer induction time does not have a significant effect, e.g. the number of seed crystals will not increase with an increase in nucleation time. A strong correlation exists between crystallization temperature and induction time, where a lower degree of super-cooling (higher temperature) significantly increases the induction time. A low induction time, i.e. fast crystallization, is obtained at low hold temperatures (13°C), and is characterized by the formation of low melting polymorphs (Dhonsi and Stapley, 2006). The induction time at higher temperatures is much longer, and favours the formation of the more stable higher melting polymorphs. The main method to reduce the induction time at higher crystallization temperatures is by applying shear during the cooling and holding stages of the tempering process. It appears, however, that a critical shear rate for each temper time below which seed crystals are not formed can be found (Stapley et al., 1999). Simultaneously, a maximum shear rate prevails for application during tempering, because of the production of heat as a result of the applied shear the risk of melting out the recently formed seed crystals exists (Beckett, 2001). The action of shear on cocoa butter and chocolate crystallization has frequently been discussed in literature, and it is generally accepted that shear reduces the induction time, probably by affecting the orientation of fat crystals, consequently accelerating the interpolymorphic transformations from Form III to Form V (Dhonsi & Stapley, 2006).

The three-dimensional network formed within chocolate is a result of the crystallization, i.e. nucleation and crystal growth, of cocoa butter TAGs. As described by Rousseau and Sonwai (2008), the presence of solid particles, e.g. cocoa solids, sugar crystals and milk powder, dispersed in the continuous fat phase will affect the crystallization process and subsequently the fat crystal nuclei spatial distribution. By acting as a foreign surface or catalytic impurity, the solid particles will induce heterogeneous nucleation, accelerating growth processes. Norberg (2006) mentions an increase in nucleation rate as a result of the presence of solid particles. Additionally, these surfaces are expected to reduce the free energy of nucleation, as a result of which a lower degree of supercooling will be required compared to cocoa butter crystallization. However, the solidification process as a result of the crystallization of the fat phase and the viscosity of the chocolate seem to be closely related (Sato & Koyano, 2001). Chocolate can be described as a pseudoplastic, which means that a force, e.g. shear, needs to be applied to the chocolate sample to initiate flow, and that with increasing force the chocolate will become thinner, as described by the Casson equation (Beckett, 2008):

$$\sqrt{\tau} = \sqrt{\tau_{CA}} + \sqrt{\eta_{CA}\sqrt{\dot{\gamma}}}, \quad [2-8]$$

where  $\tau$  is defined as the yield stress,  $\tau_{CA}$  is the Casson yield stress,  $\eta_{CA}$  is the Casson viscosity and  $\dot{\gamma}$  is the shear rate. The yield stress is the amount of energy or the force required to initiate flow, whereas the Casson or plastic viscosity is the amount of energy required to keep flowing. The viscosity of chocolate is affected by recipe, fat content, emulsifier type and content, moisture content, particle size distribution of the solids distributed in the continuous fat phase,

conching time, temper, thixotropy and vibration (Beckett, 1999b). During the crystallization of chocolate, the liquid fat content decreases as a result of the formation of seed crystals, consequently increasing the particle size distribution and increasing the chocolate viscosity. With the increase in viscosity, heat transfer through the chocolate mass is reduced, causing difficulties in creating a uniform temperature control and homogeneous crystallization (Sato & Koyano, 2001). Additionally, the increased frictional heat generated by the increased shear rate required by the highly viscous chocolate, will affect the crystallization process. Temperature differences within the chocolate mass will be responsible for the generation of different crystal polymorphs, which in turn affect the organoleptical and physical properties of the chocolate product. Overall it can be concluded that both viscosity and crystallization are critical factors that need to be controlled in order to ensure the quality of the finished product. The main problem is that it is not always clear what the effect of certain ingredients and/or processing steps on the crystallization of the fat phase is, due to the change in viscosity. For example, addition of an emulsifier to liquid chocolate will influence the flow properties, causing difficulties assessing the effect of the surfactant on the crystallization process (Schantz et al, 2005).

Addition of sugar crystals to cocoa butter has been observed to greatly reduce the induction time required for the formation of seed crystals (Dhonsi and Stapley, 2006). It is hypothesized that this is a result of the sugar crystals acting as heterogeneous nucleation sites, which promote the formation of lower melting polymorphs. Further addition of lecithin to this sugar / cocoa butter mixture resulted in a slight increase in induction time. This may be caused by the combined effect of lecithin reducing the action of sugar as a nucleation site by coating the sugar particles, and a reduction in the shear rate within the fat phase by enhancing the slip between the fat and sugar crystals. According to Norberg (2006) it is a well known fact that lecithin reduces the crystallization rate of fat, and that as a consequence the lecithin concentration needs to be controlled. Schantz et al. (2005) compared dark and whole milk chocolate samples and the effect of surfactant addition on the crystallization, after eliminating shear flow as a factor by applying surfactant specific rotation speeds to approach the torque profile of a lecithin based sample. Their results showed limited differences between dark and whole milk chocolate, and between lecithin and ammoniumphosphatide (YN). Polyglycerol polyricinoleate (PGPR), on the other hand, significantly reduced the induction time, showing a faster seed-forming and shorter total crystallization time compared to the other two surfactants. Loisel et al. (1998b) noticed a significant modification of the overall rheological behaviour after addition of surfactants, e.g. lecithins and PGPR, and as a consequence they had to modify the experimental conditions making direct comparison with dark chocolate impossible. However, as the addition of surfactants did not induce a faster crystallization of the monounsaturated TAGs of cocoa butter, the comment was made that surfactant addition delayed crystallization. Other emulsifiers have shown varying influences on cocoa butter and/or chocolate crystallization.



Addition of the diacylglycerol 1,3-dipalmitin to palm oil resulted in a higher melting point, whereas addition of 1,2-dipalmitin lowered the melting point. Similarly, sorbitan tristearate negatively influenced the crystallization rate, but sorbitan monoesters and monoacylglycerols improved the crystallization rate of systems where cocoa butter replacers and/or substitutes were used (Norberg, 2006). Lawler and Dimick (2002) summarized the effect of surfactants on a cocoa butter system as stabilizing the metastable polymorphs, and consequently delaying the polymorphic transition to Form V.

Fat additives are known to affect the crystallization behaviour of cocoa butter, and in particular the crystallization rate. Lawler and Dimick (2002) hypothesized that crystal growth is enhanced if the chain length of the crystal seed is similar to that of cocoa butter, and that this effect is more important than thermodynamic stability and crystal structure. Incorporation of milk fat in a chocolate recipe is known to decrease crystallization temperatures at which the various crystal polymorphs are formed as a result of the inhibitory effect of milk fat on the cocoa butter crystallization (Liang and Hartel, 2004). In mixtures of cocoa butter and milk fat, the rate of cocoa butter crystallization was slowed down (Beckett, 1999b).

Norberg (2006) summarized the effect of minor components, e.g. fat additives, emulsifiers and solid particles, on the crystallization of cocoa butter and chocolate systems, saying that these minor components play a crucial role in the crystallization process, but the mechanisms through which they act are often not fully understood. One of the reasons for this is that the levels of inclusion of most of these components are low and interactions take place between the individual components.

#### 2.1.3.3.1 Chocolate microstructure

The aim of discussing the microstructure of chocolate is to link its molecular composition with the macroscopic and functional properties of the final product (Rousseau, 2007). Microstructure determines the mechanical and sensorial attributes of a food product, and in this way is an important parameter of the quality of a chocolate product as it is perceived by the consumer. According to Afoakwa et al. (2009), microstructure can be regarded as a fundamental variable which affects transport phenomenon and physical characteristics of a food matrix.

Ingredients used in the chocolate manufacturing process have been discussed in section 2.1.2. Cocoa butter constitutes a major part of the chocolate recipe. Commercial chocolate manufacturing, as discussed in section 2.1.4, aims to mix all the ingredients together, under controlled conditions, to ensure the development of the correct flavour and texture.

A complex combination of processes results in the formation of chocolate, which is defined by Walstra (1996) and Aguilera et al. (2004) as “a dispersion of cocoa solids (particles) and sugar crystals in a continuous fat phase, consisting of fat crystals and liquid fat (proportions depending on temperature)”, i.e. chocolate is a colloidal system. The microstructure of chocolate is largely determined by the size of the fat crystals and solid particles, which lie in the range of 10 – 120  $\mu\text{m}$ , and strongly affect the sensory properties of the chocolate, e.g. taste and flavour (Fryer and Pinschower, 2000). As mentioned by Aguilera et al. (2004), it is important that the dispersed particulate is relatively small, e.g. in the size range of < 20 to 30  $\mu\text{m}$ , to ensure that the mouthfeel is not gritty. Overall it can be concluded that the understanding of the microstructure of chocolate is important with respect to product design, quality preservation and shelf-life prolongation (Rousseau, 2007).

Chocolate microstructure evolves throughout the manufacturing process, as well as on storage. The initial microstructure obtained within the liquid chocolate mass during the mixing, refining and conching stages, is partly determined by the interactions between the different ingredients. A schematic representation of the microstructure of a dark chocolate sample showing the interactions between the solid cocoa and sugar particles and the continuous fat phase is shown in Figure 2.8. Within a milk chocolate product an extra dimension is present with the incorporation of (solid) milk particles.

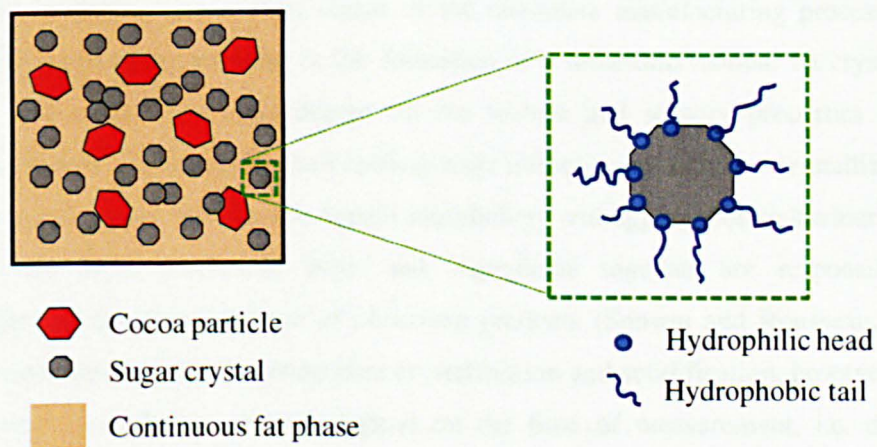


**Figure 2.8 Schematic representation of the microstructure of liquid dark chocolate obtained after conching and the stabilizing effect of a surface active agent, e.g. lecithin (adapted from Beckett, 2008) (not at scale).**

By using confocal laser scanning microscopy (CLSM), Rousseau (2007) was able to assess the internal structure of crystallized milk chocolate and the particle size *in-situ*. Two different fluorescent stains, Nile Red (hydrophobic) and Rhodamine B (hydrophilic), were mixed in with the melted milk chocolate and the mixture was re-crystallized. Nile Red stained the background, consequently corresponding to the continuous (hydrophobic) fat phase, whereas Rhodamine B stains were only observed as small light spots, referring to the either lecithin-coated sugar crystals or perhaps cocoa powder particles. Fat crystals could not be located within the sample

matrix, as solid fats do not fluoresce or interact with hydrophobic stains. Similar chocolate microstructures have been described by other authors (Beckett, 2001; Götz et al., 2005). Due to the fact that the sugar particles are hydrophilic and lipophobic they tend to attract water but repel fat, i.e. in a liquid chocolate system strong interactions are observed between the sugar particles, and simultaneous weak interactions can be observed between the solid sugar particles and the continuous fat (cocoa butter) phase. The lower polarity of solid cocoa particles, in comparison to that of the sugar particles, causes the cocoa butter molecules to stick preferentially to the solid cocoa particle surfaces (Götz et al., 2005). Eventually, the weak interactions or repulsion between the sugar particles and the cocoa butter will lead to destabilization of the colloidal system through phase separation. In order to prevent the system against instability, a surface-active agent, often in the form of lecithin, is added. As a result of its amphiphilic character, lecithin is able to bind with its lipophobic head to the solid sugar particles, while it keeps its lipophilic tail dispersed in the continuous fat phase, as is visualized in Figure 2.8. In this way, the lecithin coats the solid sugar surface and forms a boundary layer between the sugar and the fat, consequently enhancing the flow properties (Beckett, 2008). According to Rousseau and Sonwai (2008) this heterogeneously distributed particulate network, obtained during the chocolate refining and tempering stages, contributes significantly to the morphology and crystallization pathway of the cocoa butter.

During the tempering and cooling stages of the chocolate manufacturing process, the cocoa butter partly crystallizes resulting in the formation of a three-dimensional fat crystal network, which is responsible to a large degree for the texture and sensory properties of the final chocolate product. The tempering and cooling stage influence not only the crystallization rate of the cocoa butter phase, but also the crystal morphology and aggregation behaviour of the solid particles. All these processing steps and ingredients together are responsible for the development of the microstructure of chocolate products (Sonwai and Rousseau, 2008). The exact microstructure of the chocolate after crystallization and solidification, however, is still not exactly understood. In part it will depend on the time of measurement, i.e. directly after processing or after several weeks or months of storage.

Loisel et al. (1997) used Mercury porosimetry to study the microstructure of dark chocolate, based on the hypothesis that chocolate has a porous matrix through which fat or oil migration takes place, which is responsible for the occurrence of fat bloom on the surface. Initial results in a chocolate sample with 31.9% cocoa butter showed only limited penetration of the chocolate matrix by mercury, indicating that the chocolate pores were either closed or completely (or partly) filled with the liquid fraction of cocoa butter. Lowering the cocoa butter content resulted in an increase in apparent porosity. It was also observed that the amount of empty spaces depends on the condition of the chocolate, e.g. well-tempered or over-tempered. With regards to the microstructure they hypothesized that the lecithin coated sugar and cocoa particle surfaces

act as nucleation sites, and this progressive crystal growth leads, via semi-solid intermediates, to a solid-like structure in which the majority of the cocoa butter is crystallized. Driven by the solid fat content, empty spaces occur between crystals during the crystallization process. It was observed that the amount of empty cavities or air filled pores was higher at the surface of the sample than in the bulk. Aguilera et al. (2004) also assumed the existence of a porous structure in chocolate, summarizing its structural composition as a dense bed of solid particles (approximately >60% by volume) with interparticle spaces filled with cocoa butter, and the overall dimensions of the particulate systems in the order of 1 to 10  $\mu\text{m}$ . Considering the particulate nature of chocolate, they debated whether fat migrates through its pores due to diffusion or capillary flow. Based on the microstructure of chocolate, kinetic data in combination with the Lucas-Washburn equation for capillary rise and the temperature dependence of the liquid fat fraction of the chocolate system, they assumed that liquid cocoa butter migrates under capillary forces through interparticle passages and connected pores existing between the groups of fat-coated solid particles. Using atomic force microscopy (AFM), Rousseau (2007) identified the surface structure of a well-tempered milk chocolate surface, showing a complex fine-grained spotty topography. Within this irregular texture, shallow pores with a depth of 2–2.5  $\mu\text{m}$  are observed confirming the porous structure of (milk) chocolate. Afoakwa et al. (2009) investigated the effect of particle size and fat and lecithin content on the microstructure of dark chocolate. Both microstructural and mechanical properties of dark chocolate were observed to be controlled by particle size distribution and ingredient content. Low fat (25%) samples showed extensive particle-particle interactions, which seemed to result in flocculation and agglomeration of the sugar crystal network. Higher fat samples, on the other hand, showed a less dense sugar crystalline network with reduced particle-particle interactions. This resulted in the formation of more open structures with empty or void spaces between the crystals which were filled with liquid fat.

Based on the above discussion the proposed microstructure within this research for a solidified (dark) chocolate sample is shown in Figure 2.9. The schematic representation depicts the particulate nature of chocolate. A crystal network is formed by the fat crystals, in which lecithin-coated sugar and cocoa particles are “locked”. Interparticle pores or crevices are present within the chocolate matrix, and are filled with liquid/solid fat at different ratios, depending on the temperature. In the case of milk chocolate, additional solid milk (powder) particles are present dispersed in the continuous fat phase.



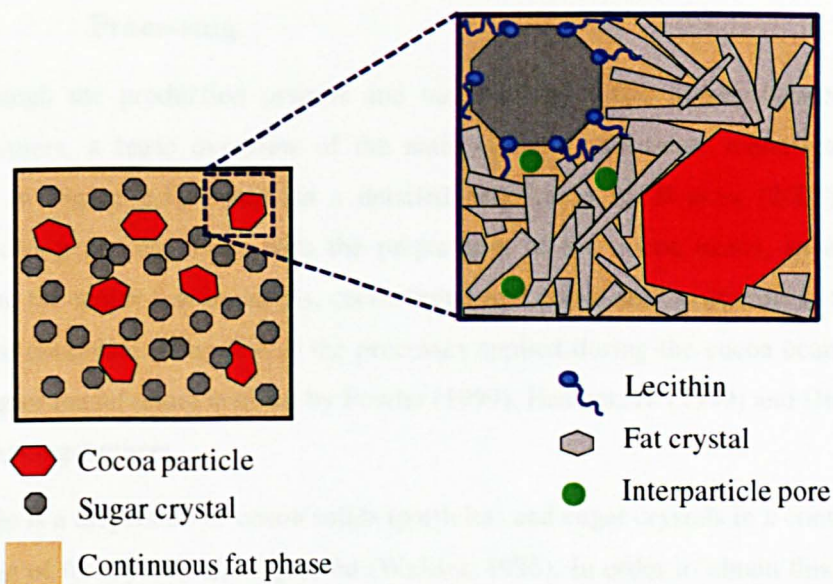


**Figure 2.9 Schematic representation of the microstructure of a crystallized and solidified dark chocolate sample (not at scale).**

Temperature fluctuations and/or liquid fat migration from a filling during storage may result in changes in viscosity (fluidity) and/or re-crystallization. It can be concluded that the dispersed particulates in combination with the changes observed during post-processing influence the micro-structural development and fat crystal growth upon storage (Rousseau and Sonwai, 2008). According to Kinta and Hatta (2007), different areas of a bloomed dark chocolate sample do not differ in their composition, i.e. fat content and triacylglycerol composition, and they assume that fat separation is not responsible for the differences observed in colour. Instead, the roughness of the lighter coloured sample was observed to show an increased number of convexities and concavities affecting the light reflection. Sonwai and Rousseau (2008) followed the micro-structural evolution of a milk chocolate sample during 1 year of isothermal storage. All freshly tempered and cooled chocolates had a smooth surface and were more finely textured than a freshly tempered cocoa butter surface. During storage, conical features appeared on the chocolate sample surfaces. The rate of appearance of these cones depended on sample composition. With time the surface of the cones roughened and small crystals started to grow. A mechanism was proposed for the cone formation and solidification, based on the presence of microscopic pores or holes on the surface of the chocolate through which liquid triacylglycerols could migrate onto the surface. Contraction of the chocolate network, observed if cocoa butter crystallizes in Form V, and the consequent micro-scale reorganization pushes the liquid fat surrounding the dispersed particulate from within the matrix onto the surface where it appears as small cones. As contraction continues during the onset of the Form V to Form VI transition, enhanced cone formation is promoted.

### 2.1.4 Processing

Even though the production process and methodology differ hugely between products and manufacturers, a basic overview of the main (general) chocolate manufacturing process is outlined in Figure 2.10 based on a detailed description by Beckett (2008). The chocolate manufacturing process starts with the preparation of the cocoa beans, an essential element delivering the major raw materials, cocoa butter and cocoa solids, as well as the characteristic flavour of chocolate. A review of the processes applied during the cocoa bean preparation and cocoa liquor manufacture is given by Fowler (1999), Heemskerk (1999) and Dimick and Hoskin (1999), amongst others.

Chocolate is a dispersion of cocoa solids (particles) and sugar crystals in a continuous fat phase, consisting of fat crystals and liquid fat (Walstra, 1996). In order to obtain this colloidal system and to develop the characteristic organoleptic properties of chocolate, it is essential that the main ingredients, sugar, cocoa butter and cocoa liquor, follow the appropriate processing steps. Chocolate refining is a grinding or milling process, which aims at reducing the particle size of the dispersed phase of the chocolate. The solid particles, cocoa liquor, sugar and milk components, are mixed with a limited amount of cocoa butter to form a uniform paste. This paste is passed through roller refiners, to break up large particles and coat the newly formed particle surfaces with fat. For the particles to move past each other and the final chocolate product to flow, with a smooth texture and melt in the mouth, it is essential that the solid particles are coated with a thin film of fat. Mean particle size is an important parameter for the amount of cocoa butter or fat required to coat all particle surfaces. Overall, it can be concluded that the particle size distribution is strongly correlated with the finished product quality, and is particularly sensitive with respect to flow properties and sensory perception (Ziegler and Hogg, 1999). According to Beckett (2008), the target particle size is  $< 30 \mu\text{m}$ , to ensure that there are no large particles giving the chocolate an undesirable (gritty) mouthfeel.

After leaving the roller refiners, the powdery paste or mixture enters the conching phase, aimed first of all at turning the powdery mass into a free flowing liquid. Cocoa butter or other fats are added to ensure that all particle surfaces are coated with a thin layer of fat, allowing them to move past each other, consequently reducing the viscosity of the mixture. For the cocoa butter to be liquid, the conche needs to be heated, allowing the cocoa butter to melt and coat the particle surfaces. The increase in temperature is also required for the removal of moisture, whose presence is detrimental for the chocolate viscosity (Beckett, 1999a). To obtain the optimum viscosity, at the last stage of the conching process surfactants and more cocoa butter are mixed in. Secondly, the conching process is essential for the finalisation of the flavour and taste of the final chocolate product, mainly through removal of undesirable acidic flavours. The exact mechanism responsible for the modification in flavour is not understood, but seems to be a combination of both chemical changes, like the loss of short-chain volatile fatty acids and the

decrease in volatiles and phenols, and physical changes, where the bitterness of the cocoa solids and the sweetness of the sugar particles is masked by the coating of cocoa butter (Dimick and Hoskin, 1999).

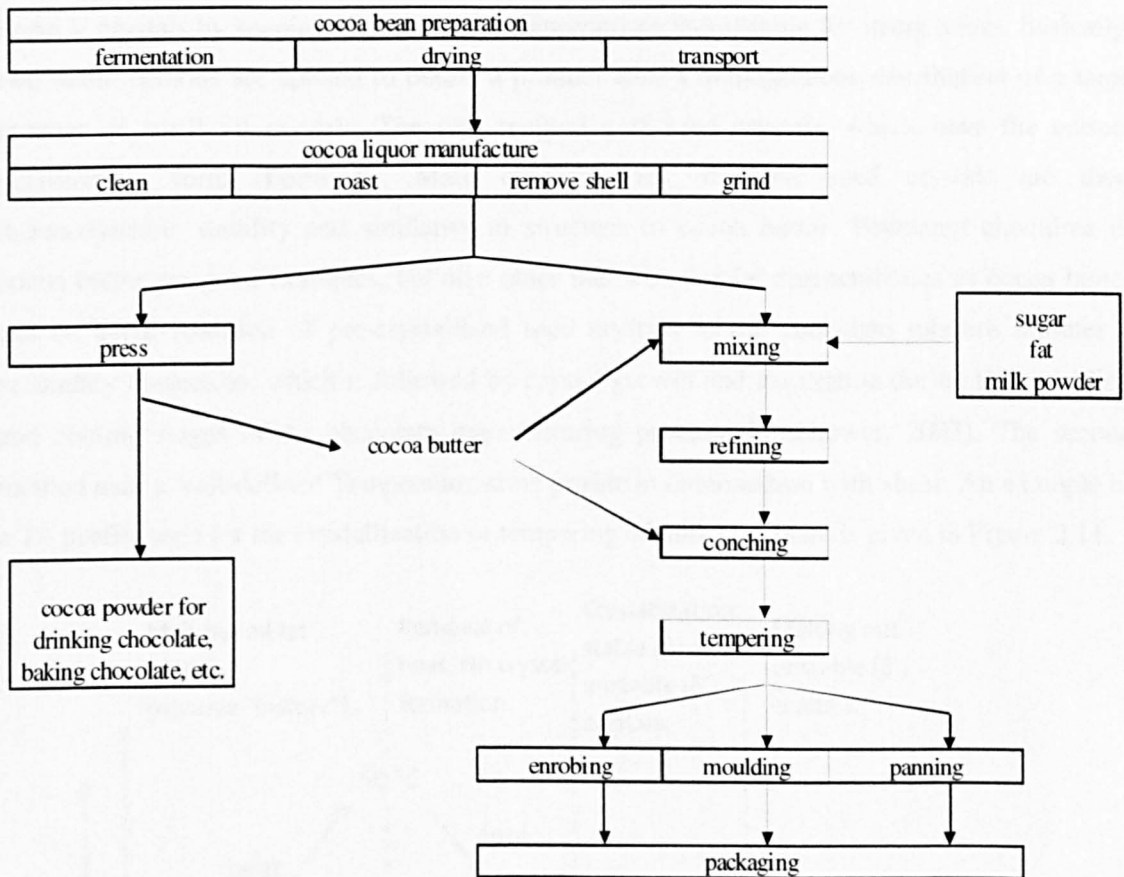


**Figure 2.10 Schematic diagram of the chocolate manufacturing process (adapted from Beckett, 2008).**

Once the mixture has been passed through the refining and conching processes, it can be called chocolate. All ingredients have been mixed, and the chocolate has the correct flow properties, allowing it to be pumped into storage tanks ready for further processing. To be able to sell the chocolate to the consumers, it needs to be solidified. The final processing steps, tempering and moulding, are essential for the creation of a solid chocolate bar with the characteristic snap on breaking, gloss and melting behaviour required by the customer.

#### 2.1.4.1 Tempering or pre-crystallization

The crystal form that is critical for the physical and sensorial properties of the chocolate is Form V. This polymorphic form is obtained during the tempering stage of the chocolate manufacturing process, basically by cooling the conched chocolate mixture from 45 °C to approximately 30 °C, depending on the type of chocolate, i.e. milk or dark chocolate. The aim of the tempering process is the development of a sufficient number of cocoa butter seed crystals and nuclei. These seed crystals are used during the nucleation stage of the crystallization



process, and they encourage the formation of stable Form V crystals in the bulk fat phase (Talbot, 1999a).

As described by Beckett (2001), it is possible to generate a small number of relatively large Form V crystals by keeping chocolate at the appropriate temperature for many hours. Basically, two main methods are applied to obtain a product with a homogeneous distribution of a large number of small fat crystals. The first method uses seed crystals, which have the correct polymorphic form (Form V). Main characteristics of these seed crystals are their thermodynamic stability and similarity in structure to cocoa butter. Powdered chocolate or cocoa butter are good examples, but also other fats with similar characteristics as cocoa butter can be used. Addition of pre-crystallised seed crystals to the chocolate mixture initiates a secondary nucleation, which is followed by crystal growth and maturation during the moulding and cooling stages of the chocolate manufacturing process (Pinschower, 2003). The second method uses a well-defined Temperature-time profile in combination with shear. An example of a T-t profile used for the crystallization or tempering of milk chocolate is given in Figure 2.11.

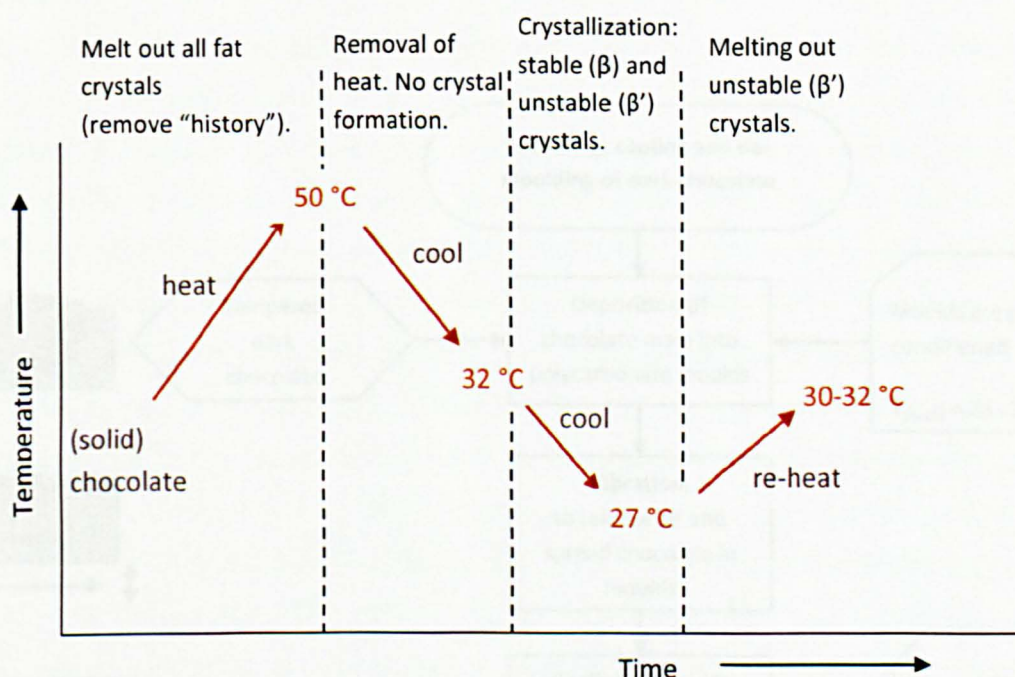


**Figure 2.11** Time-temperature profile for milk chocolate (Talbot, 1999a; Afoakwa et al., 2007).

Shear is applied during the whole cycle to accelerate the cocoa butter crystallisation, although the shear rate should be controlled to avoid the production of heat, and consequent melting out of the formed crystals (Beckett, 2001). The first stage of the tempering process consists of the heating of the chocolate, to melt out all fat crystals and in this way remove the “crystal history” of the chocolate sample. Once the product is completely liquid, it is cooled to ~ 27 °C. Agitation of the mixture during the cooling stage ensures the removal of heat and furthermore initiates the formation of crystal nuclei. From the melting points of the different polymorphs (see Table 2.4) it can be observed that both stable and unstable crystal nuclei are formed, i.e. Forms (III), IV, V



and VI. The third and final stage of the tempering process reheats the chocolate to a temperature of 30–32 °C, melting out unstable polymorphs and leaving only stable Form V (or  $\beta$ ) crystals (Rousseau, 2007). The appropriate tempering regime or T-t profile to be used depends on the chocolate recipe, type of tempering equipment and the final application (Afoakwa et al., 2007).

#### 2.1.4.2 Moulding, cooling and demoulding

In general, two characteristic methods for producing confectionery sweets are in use, 1) through enrobing or 2) by using a moulding technique. Enrobing refers to chocolate products where the liquid chocolate is poured over a sweet or nutty centre, whereas moulded chocolate is obtained by pouring the liquid tempered chocolate in a mould in order to set before removing the mould. A more in-depth description of the enrobing and moulding process and equipment used is given by Nelson (1999). This section will focus purely on the moulding of chocolate, and the aspects related to the moulding step, such as cooling and demoulding. The formation of chocolate shells or filled (moulded) chocolate is also not considered in this discussion.

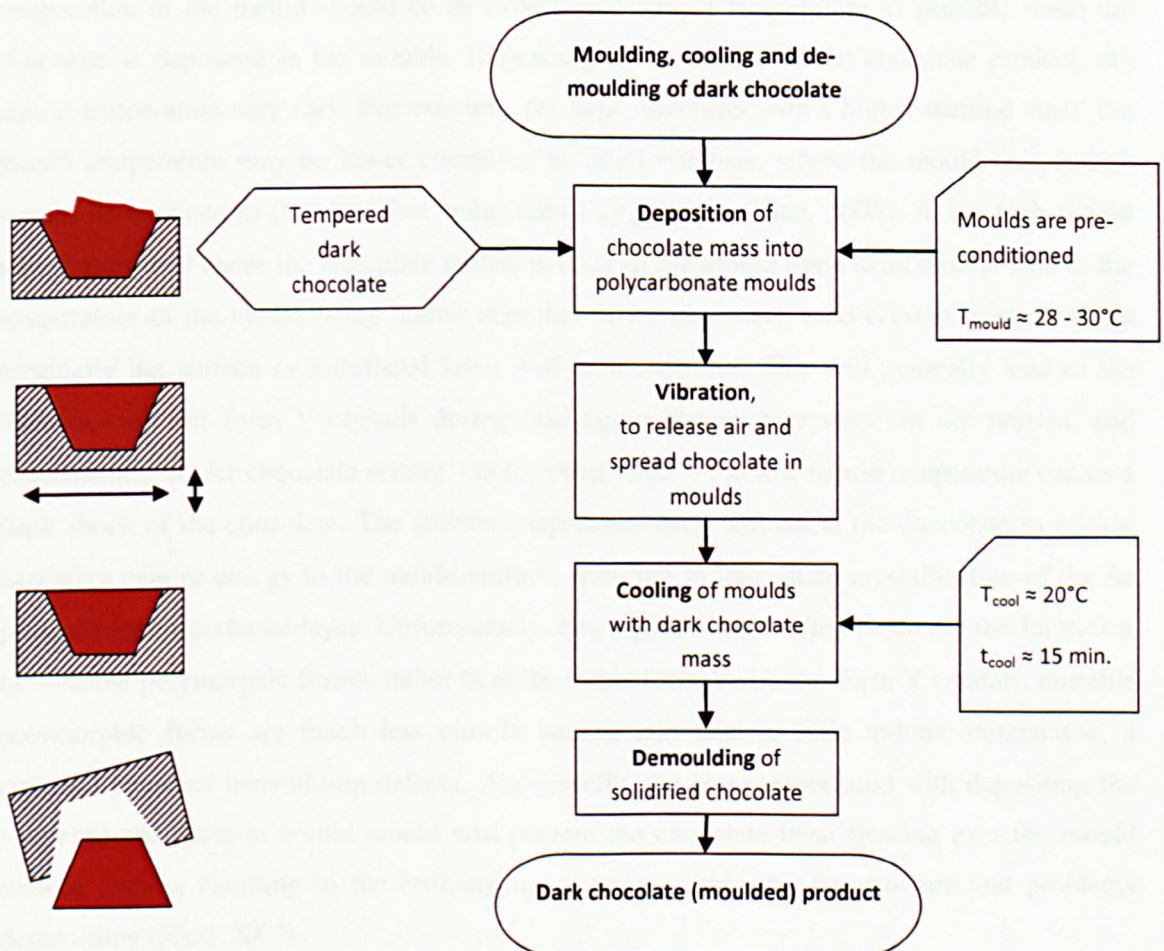


Figure 2.12 Chocolate moulding, cooling and demoulding.

Moulding is one of the final stages of the chocolate manufacturing process, as can be observed from Figure 2.10. The aim of the moulding process is the solidification of the bulk of the fat phase of the tempered chocolate mass with the correct crystallization, as this will lead to contraction of the chocolate and easy removal of the solidified chocolate from the mould. A more detailed description of the moulding process, with the different stages and processing conditions is given in Figure 2.12.

#### 2.1.4.2.1 Chocolate moulding

Tempered dark chocolate with a temperature of 30–32 °C, depending on the composition, is deposited in pre-heated or pre-conditioned polycarbonate moulds. Pre-conditioning takes place at a temperature of 28–30 °C, in an environment with controlled RH. An ideal manufacturing environment should have 35–40 % RH in order to prevent the chocolate from taking up moisture (Beckett, 2001). The use of a well-conditioned mould is predominantly important for obtaining the correct shine or gloss on the chocolate surface (Nice, 2005).

The tempered chocolate is sensitive to large temperature variations and as a result the temperature of the mould should be as close to the temper temperature as possible when the chocolate is deposited in the moulds. Depending on the nature of the chocolate product, the mould temperature may vary. For example, for large quantities with a higher thermal mass, the mould temperature may be lower compared to small volumes, where the mould temperature should be as close to the chocolate temperature as possible (Nice, 2005). A too high mould temperature will cause the chocolate tablets to stick to the mould upon demoulding. Due to the temperature of the mould being higher than that of the chocolate, seed crystals present within especially the surface or interfacial layer will be melted out. This will generally lead to the formation of less form V crystals during cooling, as the seed crystals are not present, and consequently hinder chocolate setting. On the other hand, a too low mould temperature causes a flash shock of the chocolate. The sudden temperature drop will cause the chocolate to release excessive heat or energy to the mould surface, resulting in immediate crystallization of the fat present in the interfacial layer. Unfortunately, this crystallization often results in the formation of unstable polymorphic forms, rather than the stable form V. Unlike form V crystals, unstable polymorphic forms are much less closely packed and lead to little volume contraction, a common cause of demoulding defects. Additionally, the shock associated with depositing the tempered chocolate in a cold mould will prevent the chocolate from flowing over the mould surface evenly, resulting in the building up of stress within the fat structure and problems demoulding (Nice, 2005).

It is important for both the moulding and cooling stage to prevent respectively the presence of moisture on the mould surface and the formation of condensate on the chocolate surface, as moisture is known to have a detrimental effect on chocolate by inducing sugar bloom amongst others. A general recommendation is to keep the cooling temperature above the dew point to prevent moisture condensation (Beckett, 2008).

#### 2.1.4.2.2 Chocolate cooling

Following the moulding stage, the filled moulds are vibrated using a combination of low frequency and high amplitude. This step is necessary to remove excess chocolate and air bubbles present within the tempered mass, and ensure the mould surface is fully wet by the chocolate. Subsequently, the vibrated moulds are transported into cooling tunnels to start the cooling stage. Depending on chocolate recipe, volume, manufacturer and equipment capabilities, different cooling conditions will be used. In general, cooling tunnels are used which can be divided into different sections, enabling the use of temperature profiles (Cruickshank, 2005). The first section uses gentle cooling conditions (12–15 °C), to quickly set the chocolate (Padley, 1997). Whilst the chocolate matrix is still liquid, cocoa butter might migrate to the surface, resulting in the presence of fat bloom on the surface of the chocolate bar. Section 2 applies an air flow with a lower temperature, on average approximately 7–10 °C, resulting in the largest amount of latent heat being removed. The 3rd and final section applies again a relatively gentle cooling, to limit the temperature difference between the chocolate sample and the air in the packaging area, effectively heating the chocolate product to a temperature above the dew point of the packaging area (Cruickshank, 2005). A cold chocolate surface may otherwise result in the condensation of water vapour, causing the formation of blemishes and/or sugar bloom. On average, it takes 40 minutes for a chocolate sample to set, if a cooler with a constant air flow and a temperature of 10–15 °C is used. The goal of the use of a cold air flow is to remove both specific and latent heat from the liquid chocolate sample, so that a solid product can be formed for easy handling during packaging.

On average, a temperature decrease of 10 °C is required during the cooling stage. Assuming the specific heat of chocolate to be about  $1.6 \text{ J g}^{-1} \text{ }^{\circ}\text{C}^{-1}$ , and the latent heat to be  $45 \text{ J g}^{-1}$  (Beckett, 2008), a total of 60 J needs to be removed to cool and solidify each gram of chocolate. The time required for cooling and solidification depends on the rate of heat transfer from the chocolate product to the air, which in turn depends on the temperature and flow rate of the cooling air. Due to the low rate of heat conduction through chocolate, large quantities will require longer cooling times to allow heat from the centre of the chocolate mass to be conducted to the surface, where it can be removed by the cooling air (Cruickshank, 2005). As described by Nelson (1999), the cooling process should not be too short in order to prevent poor chocolate quality. At a low air temperature, an increased risk of sugar bloom and a dull finish on the chocolate

surface exists, due to moisture condensation on the chocolate surface. A low air temperature may also affect the crystallization of the cocoa butter into the correct polymorphic form, consequently decreasing the volume-reduction or contraction desired for easy demoulding (Beckett, 2008). A relatively low cooling temperature or short cooling time will promote the formation of a larger number of polymorphs with a lower melting point, resulting in a chocolate with a lower viscosity (softer) at room temperature and less contraction during solidification (Tewkesbury et al., 2000).

Tewkesbury et al. (2000) studied the temperature distribution in chocolate moulds during cooling. Their results showed that a complex array of crystallization processes occurs simultaneously and results in solidification of chocolate. However, the different polymorphic forms present within the finished product are formed through different cooling paths, which could be identified as a result of the consequent reduction in cooling rate resulting from the evolution of latent heat.

#### 2.1.4.2.3 Chocolate demoulding

Basically, demoulding is the removal of the solidified chocolate bars from the mould after they leave the cooling tunnel. In an optimal process, the demoulding stage is only a minor part of the whole chocolate manufacturing process, with good quality chocolate products without defects leaving the moulds easily and cleanly, so that they can be returned to the start of the moulding line. In general, a low mechanical force in the form of a hammer or a twisting movement is applied to the mould, to aid in the demoulding (Cruickshank, 2005).

The efficiency of the chocolate demoulding process depends on the degree of contraction obtained during the cooling stage. Contraction of chocolate is a consequence of the phase transition from liquid to solid chocolate during the solidification process. However, no or limited contraction is observed when untempered or partially tempered chocolate is used. Nelson (1999) visualized the observed cooling and expansion of untempered chocolate with time, as can be seen in Figure 2.13. A lower crystallization temperature and slower crystallization rate are obtained for untempered compared to tempered chocolate. Most interesting, however, is the relatively large expansion observed during the initial stage of the cooling process. Only after prolonged intense cooling minimal contraction of untempered chocolate takes place.

Chocolate demoulding can be improved not only by using the correct temper, but also through mould design. Harbecke (2005) gives guidelines regarding the angles and mould shapes that should be used. The use of engravings and a low degree of surface texture is recommended, as the mould surface area is increased, consequently enhancing cooling. At the same time, the largest contraction is observed when spherical shapes or even circumferences are used, allowing

an even contraction. The effect of storage and cleaning of moulds on the demoulding efficiency is very well known from practical experience. Small defects on the mould surface have been observed to significantly increase the amount of chocolate residues sticking to the mould surface. Similarly, cleaning of moulds has been shown to negatively affect demoulding properties. This is expected to be due to the removal of a thin film of fat present on the mould surface after demoulding which enhances subsequent moulding and demoulding processes (Harbecke, 2005).

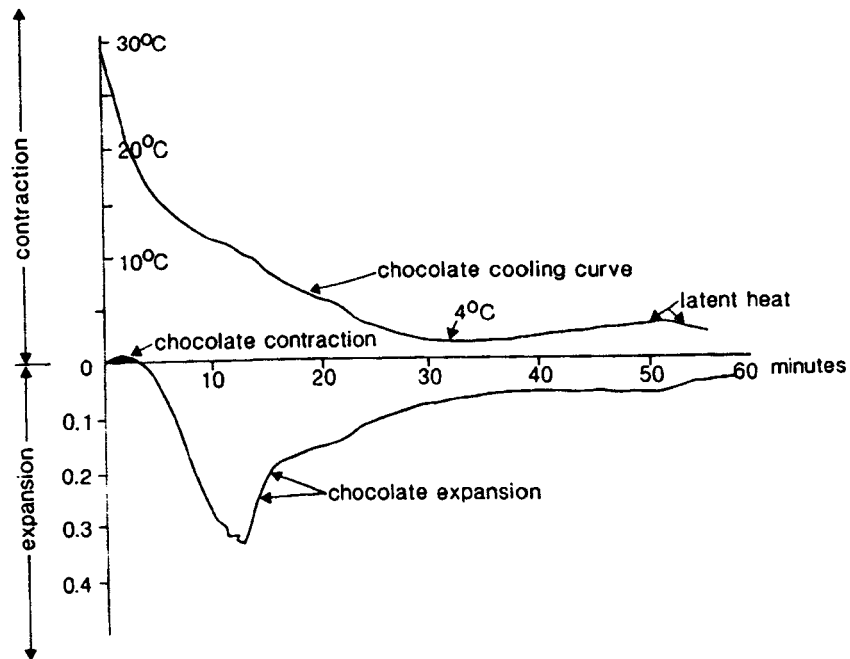


**Figure 2.13** Cooling and expansion curves of untempered chocolate (Nelson, 1999).

Pinschower (2003) studied the direct measurement of the contraction of chocolate during solidification. Initial experiments within this part of the study identified the direction at which cooling was applied to the chocolate as an important parameter regarding the direction of shrinkage, as a result of the applied cooling, as is schematically shown in Figure 2.14. If cooling is applied from the bottom, the chocolate surface shows contraction towards the source of the cooling, i.e. inwards towards the mould, resulting in a tight fitted chocolate product and difficulties demoulding. If cooling is applied from the top, on the other hand, this contraction of the chocolate surface is not observed and it is assumed that it is easier for the chocolate to contract away from the mould. However, surface interactions might affect the degree of contraction, and the adhesion between chocolate and material surface. A strong attachment of chocolate to a cooled metal surface was observed, which seemed to be stronger than the attachment of chocolate to an aluminium mould surface. The effect of cooling direction is further expected to be less distinct at smaller temperature differences, and in mechanically weaker materials, e.g. untempered versus tempered chocolate.



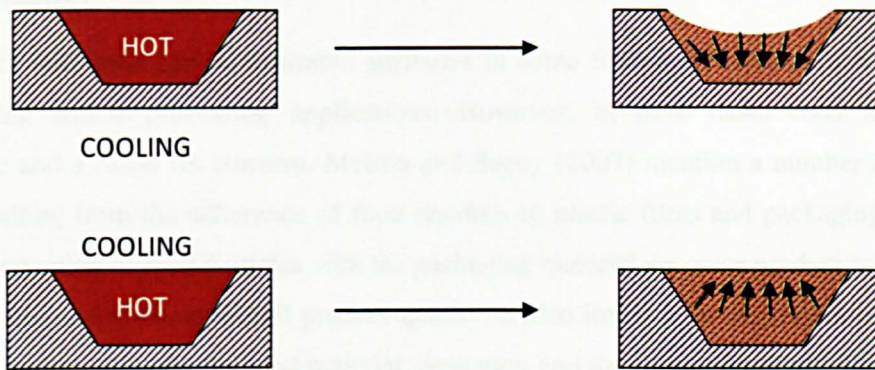


**Figure 2.14 Suspected direction of shrinkage depending on the cooling direction (Pinschower, 2003).**

Volumetric expansion,  $\beta$ , of materials generally occurs upon heating, and results in a decrease in material density. The coefficient of thermal expansion is a physical property used to quantify the degree of expansion with temperature. Volumetric expansion is defined by equation [2-9]:

$$V_1 = V_0(1 + \beta\Delta T), \quad [2-9]$$

where  $V_1$  refers to the volume at a temperature  $T_1$  and  $V_0$  to the volume at the reference temperature  $T_0$ . As the mass of the material does not change with the change in temperature, equation [2-9] can be written as:

$$\frac{1}{\rho_1} = \frac{1}{\rho_0}(1 + \beta\Delta T), \quad [2-10]$$

where  $\rho_1$  refers to the density at a temperature  $T_1$  and  $\rho_0$  to the density at the reference temperature  $T_0$ . A similar equation applies to the volumetric contraction, which is basically a negative expansion.

In order to gain more understanding of the contraction of chocolate, Pinschower (2003) compared the contraction of chocolate samples with varying levels of temper and determined the effect of cooling procedure and processing history, in an effort to relate the observed effects to the volumetric expansion. Chocolate samples with the same level of temper, showed very different contraction behaviours. Further investigation showed that the viscosity of the chocolate sample at the time of deposition in the mould has a significant effect on the degree of contraction, with a high viscosity showing a relatively low contraction. Similar to the observations made by Nelson (1999), Pinschower (2003) concluded that the volume change of untempered chocolate occurs much slower compared to tempered chocolate. Depending on the degree of temper, the contraction takes place at different stages of the cooling process. Finally, the coefficient of expansion,  $\beta$ , was used to differentiate between tempered and untempered chocolate, but only at low cooling rates. At these low cooling rates, the maximum contraction values decreased with increasing temper.

## 2.2 ADHESION

Adhesion or stickiness can be desirable attributes in some food applications, such as specific food coating and/or processing applications. However, in most cases food adhesion is undesirable and a cause for concern. Meiron and Saguy (2007) mention a number of negative effects resulting from the adherence of food residues to plastic films and packaging. Not only does the interaction of food particles with the packaging material decrease product acceptability, increase waste and a lower overall product quality, it also impacts on the risk of migration of packaging compounds into the food material, oxidation and the formation of off-flavours. Chen (2007) describes a similar negative or undesirable effect of the adhesion of food components to packaging on the formation of visual defects of surface texture and consumer rejection of the food product. Another area where adhesion of food particles is undesirable and often unavoidable is in food processing facilities (Bobe et al., 2007), because it leads to fouling of production lines, lower product yields, and increased economic costs (Adhikari et al, 2001; Michalski et al., 1997). In this research particular attention is paid to the application of chocolate manufacturing, where adhesion and sticking of chocolate to the mould surface is a substantial ongoing problem, leading to poor product appearance, production losses (normally those products are considered out of quality standards and rejected), and increased processing costs in equipment cleaning.

### 2.2.1 Adhesion versus stickiness

Adhesion is an important physical phenomenon commonly observed in many food-related situations. With respect to the sensory evaluation of food products, the terms stickiness and adhesion are often used interchangeably (Adhikari et al., 2001). Even though both these terms describe well understood phenomena, their meanings can vary somewhat depending on the context. For example, in relation to oral sensory perception, the term stickiness was defined by Jowitt (1974) as *“possessing the textural property manifested by a tendency to adhere to contacting surfaces, especially the palate, teeth, and tongue during mastication.”* This definition does not refer to stickiness of non-oral surfaces, which is commonly encountered in the manufacturing and transportation of foods. More general descriptions of stickiness are given by Hosoney and Smewing (1999) *“the force of adhesion that results when two surfaces are contacted with each other”* and Bhandari and Howes (2005) *“stickiness is the force of adhesion or cohesion of two similar or dissimilar surfaces. It is influenced by the adhesive balance between contacting surfaces.”* These last two definitions of stickiness use the force of adhesion as an important descriptor of stickiness. A definition of adhesion is given by Kilcast and Roberts (1998) stating that *“adhesion is broadly defined as the sticking together of two materials with or without an intermediate layer. Surface energetic and wetting have been found*



to be of greatest general importance.” Adhesion is commonly referred to as “the physical phenomenon by which two materials ‘stick’ together” (Michalski et al., 1998b).

From the definitions given it can be observed that the concepts of stickiness and adhesion are very closely related and often focus on the same principle. Within this research, stickiness and adhesion are regarded as two different concepts. Adhesion is part of the stickiness definition or theory, but it is not equal to stickiness. Stickiness can be defined as the result of the combined action of the force of adhesion and the force of cohesion, subsequently originating of viscoelastic and adhesive properties of food products. Stickiness is often associated with the sensory properties of food products and is consequently perceived in the palate, teeth, and tongue when food is being masticated or on non-oral surfaces such as fingers and equipment surfaces (Adhikari et al., 2001). Adhesion on the other hand is rather regarded as a theory, model concept or mechanism. The general consensus is that the term adhesion refers to the attractive interaction between two surfaces upon close contact, and in particular the energy that is required to separate these surfaces.

### 2.2.2 Cohesion and adhesion

According to Hosoney and Smewing (1999) the force of adhesion, obtained when two surfaces are in close contact, consists of an adhesive force and a cohesive force. A food material is perceived as being sticky when the adhesive force is high and the cohesive force is low. Bhandari and Howes (2005) described adhesion as a physical phenomenon, where the bond between two surfaces was regarded to be either interfacial (adhesive) or inter-phase (cohesive). Inter-phase bonding is defined as the bonding between two same species, and describes the strength of the attractive force between molecules in solutions or solids.

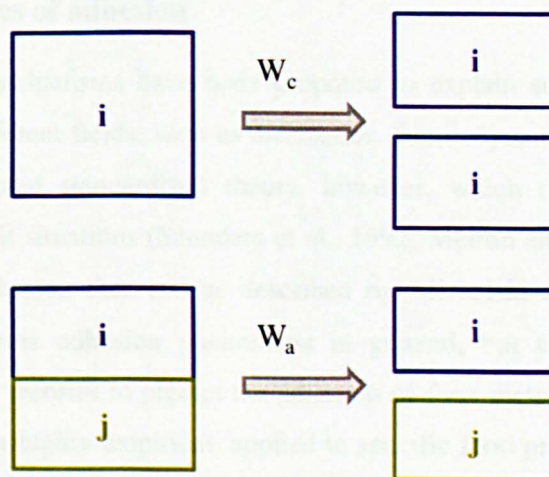


**Figure 2.15** Diagram illustrating the concepts of work of cohesion  $W_c$  and work of adhesion  $W_a$  (McGuire, 2005).

More often used are the terms work of cohesion and work of adhesion, which result from the thermodynamic ‘cohesion’ and ‘adhesion’ process, as illustrated in Figure 2.15.

Cohesion is the (intermolecular) attraction between similar phases. Based on this definition, the work of cohesion  $W_c$  can be defined as the reversible work per unit area required to separate or “create” two surfaces of a bulk material  $i$ :

$$\begin{aligned} W_c &= 2\gamma_i & [2-11] \\ &= \Delta G_c, \end{aligned}$$

where  $G$  represents the free energy per unit area, and  $\gamma$  represents the free energy per unit area as well as the force per unit length. The subscripts  $i$  and  $j$  refer to the phases  $i$  and  $j$ , respectively, whilst  $ij$  refers to the interface. The concepts of surface tension,  $\gamma$ , and surface free energy,  $G$ , will be discussed in more detail in section 2.3.2.

Adhesion is the (molecular) attraction between two different phases. Based on this definition, the work of adhesion can be defined as the reversible work required to separate unit area of interface  $ij$  between two dissimilar phases,  $i$  and  $j$  (McGuire, 2005; Good, 1992):

$$\begin{aligned} W_a &= \gamma_i + \gamma_j - \gamma_{ij} & [2-12] \\ &= \Delta G_a. \end{aligned}$$

As discussed by Myers (1999), the applicability of the thermodynamic work of adhesion and/or cohesion is based on the use of a defined model system which takes molecular interactions, such as van der Waals, dipolar and electrostatic forces, into consideration, but not mechanical and/or chemical interactions. This means that bulk physical properties, for instance, are not taken into consideration, even though these often play a major role in practical adhesion.

### 2.2.3 Theories of adhesion

Various theories and mechanisms have been proposed to explain surface adhesion from the point of view of the different fields, such as mechanics, thermodynamics and chemistry. There is no universally accepted standardized theory, however, which describes or predicts the adhesion behaviour in all situations (Saunders et al., 1992; Meiron and Saguy, 2007). Another disadvantage of the adhesion theories, as described by Michalski et al. (1999), is that the different theories “address adhesion phenomena in general, but only a few studies have attempted to apply such theories to predict the adhesion of food materials to solids. Studies on this subject often remain highly empirical, applied to specific food product and only a few are concerned with fatty products or emulsions.”

The 6 main theories of adhesion are discussed in more detail below (Adhikari et al., 2001; Kinloch, 1980; Comyn, 1997; Michalski et al, 1997):

1. Mechanical interlocking

This is the oldest of the adhesive theories, and is commonly observed to affect flow properties of food products and adhesion on equipment and packaging surfaces.

Mechanical interlocking happens when molecules make a physical bond with other molecules, and in this process they form a closed bond in which other molecules or particles are locked. Rugosity or surface topography is a key parameter by increasing the surface area and number of hooking sites available. Due to the rugosity of a solid surface, a liquid can be locked into irregularities when it spreads over the surface.

2. Wetting and thermodynamic adsorption

The degree of wetting determines whether a liquid will spread on a solid surface. In this process the liquid will form a thin film or layer on top of the solid surface or will retract as a single drop or multiple drops. Wetting of a solid surface by a liquid occurs when the surface energy of the solid is greater than that of the liquid. In order to lower the surface energy of a system, low energy materials (liquids) will adsorb strongly to high energy surfaces (solids). The concept of thermodynamic adsorption is based on the equations of Young (forces equation) and Dupré (energy equation), which will be discussed in more detail in section 2.3.2 (equation [2-30] and [2-32]).

3. Intermolecular and electrostatic forces

The main intermolecular force is the van der Waals force, while the electrostatic forces are a result of opposing charges between particles. Together, these two forces are primarily responsible for the cohesion between particles and the adhesion between surfaces if there are no material bridges present. Van der Waals forces are only effective in close proximity, i.e. by the molecules in the interfacial layer. Although they are relatively weak if compared to other forces, they are capable of forming strong adhesive joints. The close contact of two materials at the interface means that intermolecular or van der Waals forces will always play a role. The DLVO or Derjaguin, Landay, Verwey, and Overbeek theory takes into account the long-range electrostatic and electrodynamic interactions, and is related to the formation of an electrical double layer at the interface. In food systems this approach is often used to explain the adhesion between proteins or micro-organisms and particularly stainless steel surfaces.

4. Diffusion

Within the food industry, diffusion phenomena are often not a concern in relation to adhesion. Diffusion of polymer chains depends largely on the temperature, as the chains need to be mobile, and is mainly observed at close contact between compatible polymers, such as during solvent-welding of thermoplastics.

5. Chemical bonding

The main requirement for chemical bonding is the formation of covalent, ionic or hydrogen bonds across the interface. Chemical bonding in the food industry is commonly observed upon storage only, as a sufficient contact time is required for the reaction to take place. The adhesion of milk protein on glass surfaces is assumed to be an example of chemical bonding.

6. Weak boundary layers

A contaminant present at the clean surface of a solid material which is capable of forming strong adhesive bonds under normal circumstances will create a cohesively weak layer. If the cohesion is weak at the interfacial area between a solid substrate and an adhesive, fracture will take place in this interfacial area rather than an adhesive failure at the interface between the two adhering materials.

The most widely used adhesion theories in industry are mechanical interlocking and wetting and thermodynamic adsorption (Michalski et al., 1997). Similarly, according to Kinloch (1980), the most generally accepted theory is the adsorption theory, which “proposes that, provided sufficiently intimate intermolecular contact is achieved at the interface, the materials will adhere because of the surface forces acting between the atoms in the two surfaces; the most common such forces are van der Waals forces and are referred to as secondary bonds. In addition, chemisorptions may well occur and thus ionic, covalent and metallic bonds may operate across the interface; these types of bonds are referred to as primary bonds”. From this definition of the adsorption theory it can be observed that it is actually a combination of different mechanisms of adhesion: wetting and thermodynamic adsorption, interparticle attraction and chemical adhesion. Additionally, the involvement of several mechanisms simultaneously requires the determination of several different controlling parameters linked to these individual mechanisms, such as surface free energy (thermodynamics), morphology (mechanics) and heterogeneity (interparticle attraction) (Meiron and Saguy, 2007). Liu et al. (2006a and b) investigated the adhesion of fouling deposits, consisting of organic and mineral components, to thermal processing equipment surfaces. They defined a number of principal components, which are responsible for the adhesion between surface and foulant. These include van der Waals forces, electrostatic forces, hydrogen bonding and hydrophobic bonding, in combination with contact area effects. Overall, fouling deposits were assumed to result from the adhesion of components to the surface and cohesion between elements of the material.

Solid and liquid bridges are part of the interparticle attraction mechanism proposed by Adhikari et al. (2001). In this research there is a particular interest in the formation of solid and possibly liquid bridges with respect to the adhesion between a chocolate system and a solid mould surface. Based on the particulate crystal network of chocolate and the presence of pores, as discussed in section 2.1.3.3.1, the formation of liquid bridges seems a possibility. However, as



these liquid bridges are formed within the chocolate system, rather than at the chocolate –mould interface, they are not assumed to participate in the adhesion mechanism. Solid bridges can be formed through several different mechanisms: sintering, melting, crystallization, dissolution and drying. An example of the formation of solid bridges is when a molecule crystallizes and forms solid bridges (crystals) at the point of contact (crystallization). Through the solid bridges several molecules are connected, resulting in the formation of aggregates. With respect to chocolate the possible formation of solid bridges at the chocolate–mould interface should be considered. Contaminants present at the interface may assist in the formation of solid bridges, as well as the possible crystallization of fat molecules present at the interface.

### 2.2.4 Molecular adhesion

A comparison of the range of action of the different adhesion forces in order to distinguish between molecular, electrostatic, gravitational and liquid bridge adhesion was conducted by Kendall (2001).

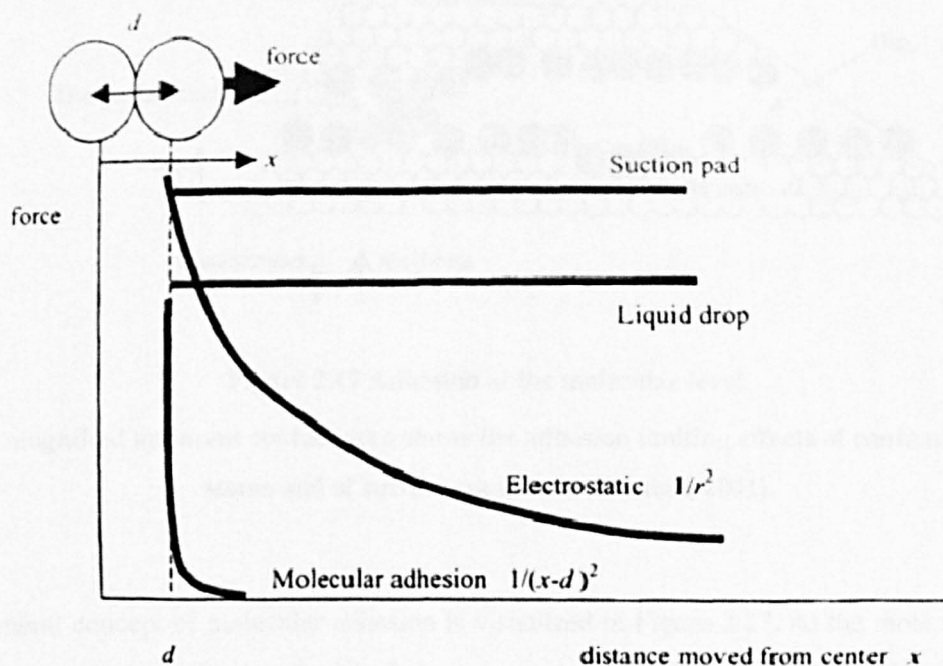


**Figure 2.16 Schematic overview of different types of adhesion forces that exist at various distances when two spheres are pulled apart (Kendall, 2001).**

The schematic overview in Figure 2.16 shows a plot of the force against the distance moved from centre for the example of two spheres that are being pulled apart. Attractive suction (atmospheric pressure) forces and liquid bridge adhesion forces are constant, therefore requiring a high amount of energy to pull the two spheres apart. The energy required to separate the two spheres is represented by the area under the curve. Electrostatic adhesion requires less energy,

but can be regarded as long range. A similar curve as that obtained for the electrostatic adhesion is obtained for Newton's gravitation force, although this latter force is much smaller. Last example in Figure 2.16 is that of molecular adhesion, which is only observed at a very short distance of separation. As the area under the curve is small, the energy required to pull two spheres apart that are adhering due to molecular adhesion is almost negligible. The definition given by Kendall (2001) for molecular adhesion is "*the force experienced when bodies make contact at the molecular level, with gaps near molecular dimensions.*" Even though the forces determined within this research are not at the molecular level, general understanding of the concept of molecular adhesion may increase overall understanding of (macro) adhesion.

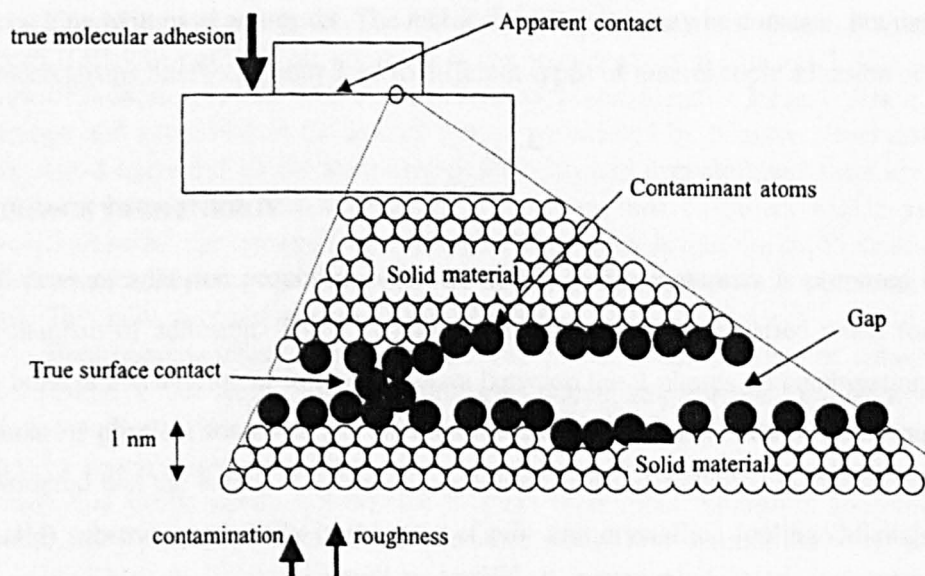


**Figure 2.17 Adhesion at the molecular level.**

**The magnified apparent contact area shows the adhesion limiting effects of contaminating atoms and of surface roughness (Kendall, 2001).**

The general concept of molecular adhesion is visualized in Figure 2.17. At the molecular level the atomic structures of two materials that are in contact at the macroscopic level do not show contact at all. Contaminating foreign materials such as oxygen and water molecules are adsorbed onto the solid surfaces, and subsequently prevent the solid materials from true atomic contact. Secondly, rugosity of the solid materials introduces gaps between the solid surfaces, consequently reducing the surface interactions further. Overall it can be concluded that the adhesion observed at macroscopic level and that observed at molecular level do not always agree well, as a result of which the three laws of molecular adhesion have been developed, which are believed to be universal (Kendall, 2001):

- **1<sup>st</sup> law of molecular adhesion:**

All atoms and molecules adhere with considerable force, causing two solid materials to jump into contact when the separation distance is reduced to nanometers;

- **2<sup>nd</sup> law of molecular adhesion:**

The presence of contaminant “wetting” molecules at the solid material surfaces (or at the interface) reduces adhesion, and can even result in repulsion between two solid materials;

- **3<sup>rd</sup> law of molecular adhesion:**

Molecular adhesion forces act at short range or separation distances (nanometers), which means that various mechanisms such as surface roughness, Brownian motion and cracking, will have an impact. The molecular adhesion may be constant, but the mechanisms interacting may lead to different types of macroscopic adhesion occurring.

## 2.3 SURFACE FREE ENERGY

Of the theories of adhesion proposed in section 2.2.3, thermodynamics is proposed to be the main mechanism of adhesion. The 1<sup>st</sup> condition that needs to be satisfied when forming an adhesive bond is the creation of intimate contact between the 2 phases, in combination with the development of physical forces at the interface (Meiron and Saguy, 2007). Many researchers have considered that the extent of adhesion is predominantly determined by the surface energy of the (solid) substrate, especially in the case of bio- and crystalline fouling (Michalski et al., 1998a, 1998b, 1999; Zhao et al., 2005; Pereni et al., 2006; Rosmaninho and Melo, 2006). Bhandari and Howes (2005) reviewed the stickiness properties of foods during drying, and concluded that surface energy of the materials with which the food is in contact is a critical factor in relation to the adhesion observed. According to them, many authors, however, do not take the solid surface energy into account when investigating the adhesion of food to processing equipment surfaces.

### 2.3.1 Thermodynamics

Thermodynamics is the science that studies the principles of energy transformation in macroscopic systems, describing the reaction of a system to changes in its surroundings (Erbil, 2006). In general, there are three components of thermodynamic equilibriums:

- **Mechanical**: implying that there are no unbalanced forces;
- **Thermal**: implying that there are no temperature gradients;
- **Chemical**: implying that there are no chemical reactions and no net transport of components occurs.

Thermodynamics describes the equilibrium or, if there is no equilibrium, the direction in which a change takes place. However, it does not give information about the rate of a reaction or change (Walstra, 2003). The 1<sup>st</sup> law of thermodynamics states the law of conservation of energy, i.e. *the increase in the internal energy of a system is equal to the amount of energy added to the system by heating, minus the amount lost in the form of work done by the system on its surroundings*:

$$dU = dQ - dW, \quad [2-13]$$

where  $U$  represents the internal energy of the system,  $Q$  the heat added to the system and  $W$  the work done on the system. The 2<sup>nd</sup> law of thermodynamics is described by the Kelvin Planck statement, concerning the direction of natural processes, and states that *the total entropy of any thermodynamically isolated system tends to increase over time, approaching a maximum value*:

$$\frac{dS}{dt} \geq 0, \quad [2-14]$$

where  $S$  represents the entropy of the system.

Application of the 1<sup>st</sup> law of thermodynamics to the boundary layer or interface between two phases shows that interfacial free energy is required for a stable boundary. In order to extend or enlarge the boundary, work needs to be done by the system. If no work was required, any random force would result in the mixing of the two phases (McGuire, 2005).

Thermodynamic potentials are parameters that are used when describing thermodynamic systems and which have the dimensions of energy. The four most common thermodynamic potentials are (Atkins, 1994; Walstra, 2003):

- **Internal energy:** the total energy of a system;

$$U,$$

- **Helmholtz free energy:** the maximum amount of work a system can do at a constant temperature (isothermal changes);

$$F \equiv U - TS, \quad [2-15]$$

- **Enthalpy:** the available thermal energy at constant pressure;

$$H \equiv U + pV, \quad [2-16]$$

- **Gibbs free energy:** the maximum amount of work a system can do at a constant pressure (isobaric changes);

$$G \equiv H - TS = U + pV - TS, \quad [2-17]$$

where  $U$  represents the internal energy,  $T$  the system temperature,  $S$  the entropy,  $p$  the pressure and  $V$  the volume. The term *free* in Gibbs and Helmholtz free energy refers to the portion of internal energy that is free to perform work ( $U-TS$ ). Thermodynamic equilibrium is not obtained directly within a system. Each system evolves from its initial state to the equilibrium

or final state. Thermodynamic potentials measure the energy change during this system's evolution. In that respect, the Helmholtz and Gibbs free energy are measures of the amount of energy that is available for work. Specific for Helmholtz is that a constant temperature and volume are required, whereas Gibbs requires a constant temperature and pressure. Gibbs free energy is most applicable in general situations. In a system with constant pressure, equilibrium is obtained at the lowest Gibbs free energy (Walstra, 2003).

The relations described in equations [2-15] to [2-17] apply to homogeneous closed systems, which mean that there is no exchange of matter between the systems and their surroundings. Energy, on the other hand, may be exchanged. For open systems, which can exchange both energy and matter with their surroundings, the internal energy is a function of  $S$ ,  $V$  and the composition of the system (Erbil, 2006). The result is the fundamental thermodynamic equation for an open system:

$$dU = TdS - PdV + \sum_i \mu_i dn_i, \quad [2-18]$$

where  $\mu_i$  refers to the chemical potential of component  $i$ , and  $n_i$  to the number of moles of component  $i$ . Thermodynamics states that systems tend to minimize their total free energy. Two important mechanisms which are used to minimize the interfacial free energy of a system are minimizing the interfacial area and adsorption of a substance at an interface, respectively (McGuire, 2005).

### 2.3.1.1 Gibbs dividing plane

An interface with respect to the Gibbs dividing plane refers to a macroscopic fluid-fluid interface, which has a relatively large area compared to molecular interfaces, and is thermodynamically defined and a function of state (Lyklema, 2000). Solid-liquid interfaces and their interfacial tensions cannot be measured experimentally, as this requires extending a solid surface reversibly without stretching or cleaving. In contrast to molecular interfaces, the solid-liquid or solid-solid interface is thermodynamically defined by the Gibbs and/or Helmholtz energies of stretching and cleaving. Only flat macroscopic fluid-fluid, one- or two-component systems are considered here. Assuming a two-phase system, whereby the two phases,  $\alpha$  and  $\beta$ , are divided by a flat interface. Both phases are thermodynamically defined and a function of state. The Gibbs convention describes the interface between the two phases as an infinitely thin boundary layer, the Gibbs dividing plane (Norde, 2003). The ideal volume of the Gibbs dividing plane is 0, as a result of which it is also called the ideal interface. Other models exist which consider an extended interfacial region, for example the model of Guggenheim (Butt et al., 2003). Both the model of Gibbs and that of Guggenheim are visualized in Figure 2.18. Focussing on the Gibbs dividing plane, the question is where exactly the ideal interface or dividing plane is located. Assuming a pure liquid in equilibrium with its vapour, it has been



observed that the composition, density, structure, electrical potential, etc., of the liquid deviates depending on the distance from the bulk. Close to the vapour phase, the deviations are larger than close to the bulk of one of the phases. However, it is impossible to define exactly where the water phase ends and where the vapour phase starts. According to Gibbs, the excess internal energy is totally located in the dividing plane, whereas the individual phases keep their bulk properties until the plane (Lyklema, 1991). The interfacial excess is equal to 0 in the middle of the interfacial region or dividing plane. Going back to the example of a pure liquid in contact with its vapour, the deficit of a component in the liquid phase equals the excess of that same component in the vapour phase, creating a net interfacial excess of the respective component equal to 0. At the same time, the Gibbs dividing plane is believed to contain the interfacial excesses of all other components of a particular system (Norde, 2003).

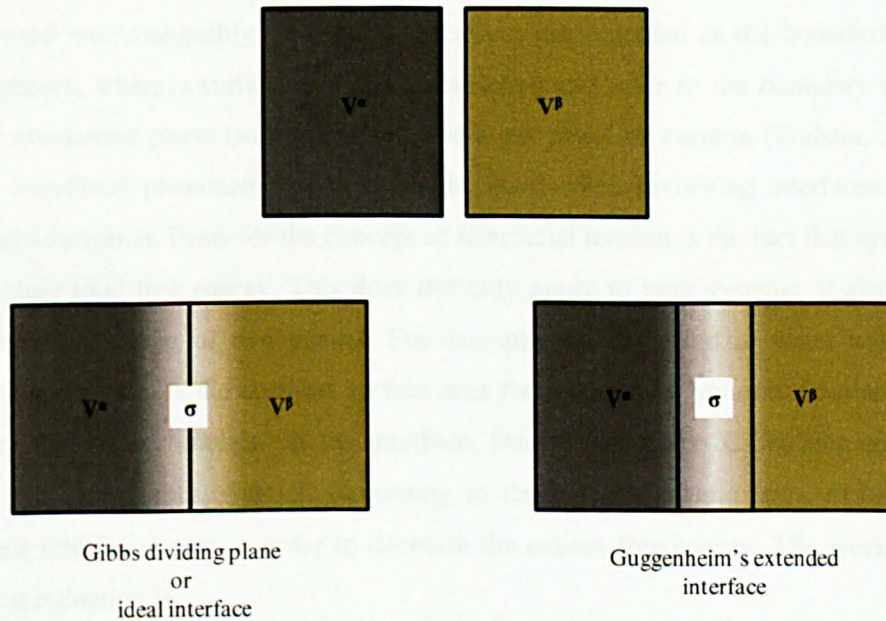


**Figure 2.18 Representation of an interface,  $\sigma$ , according to Gibbs (left), consisting of two phases,  $\alpha$  and  $\beta$  separated by thin boundary layer, and according to Guggenheim (right), where an extended interphase with a volume is present (Butt et al., 2003).**

The interfacial excess or surface concentration,  $\Gamma_i$ , can be defined as the surface concentration and is obtained by dividing the number of molecules of a substance at the interface,  $N_i^{\sigma}$ , by the interfacial area,  $A$  (Butt et al., 2003):

$$\Gamma_i = \frac{N_i^{\sigma}}{A} \quad [2-19]$$

As described by Walstra (2003), the adsorption of solutes at the interface lowers the free energy of the system. Gibbs thereby assumed that in an equilibrium situation the chemical potential of the adsorbate is the same in the solution and at the surface, and that the plane dividing the two phases is infinitely thin.



This leads to the formulation of the Gibbs adsorption equation:

$$d\Pi = -d\gamma = RT\Gamma d \ln a, \quad [2-20]$$

where  $\gamma$  is the surface tension,  $a$  the thermodynamic activity of the adsorbate in the solution and  $\Pi$  the surface pressure. According to Lyklema (1991), the Gibbs adsorption equation can be regarded as the surface equivalent of the Gibbs-Duhem relation, equation [2-18]. If the surface excess is positive, this means that adsorption takes place at the interface. Equation [2-20] then implies that the surface tension,  $\gamma$ , decreases, as a result of this adsorption (Atkins, 1994).

### 2.3.1.2 Thermodynamics of interfaces

When discussing interfaces and surfaces, it is important to define these concepts, although they are often used interchangeably. In general, interfaces are regarded as the boundaries between different phases, whereas surfaces are more restrictive and refer to the boundary or interface between a condensed phase (solid or liquid) and a gas phase or vacuum (Walstra, 2003). Two important interfacial phenomena need to be discussed when reviewing interfaces: interfacial tension and adsorption. Basis for the concept of interfacial tension is the fact that systems try to minimize their total free energy. This does not only apply to pure systems, it also applies to fluid systems consisting of two phases. For example, oil dispersed in water will assume a spherical shape as this is the smallest surface area for a particular volume. Free energy of the two phases will be accumulated at the interface. Due to the excess Gibbs free energy at the interface, they commonly contract. According to the thermodynamic laws, systems tend to reduce their interfacial area in order to decrease the excess free energy. The work used for a surface area reduction is:

$$dW = \gamma dA. \quad [2-21]$$

The thermodynamic interpretation of the interfacial tension is expressed by equations [2-22] and [2-23], which describe the change (increase) in Helmholtz or Gibbs free energy of a system when the area of that particular interface is increased reversibly, respectively. This increase in interfacial area  $dA$  is infinitesimal, and takes place at constant temperature and composition, as well as constant volume (Helmholtz) or constant pressure (Gibbs) (Lyklema, 2000):

$$\gamma = \left( \frac{\partial F}{\partial A} \right)_{V,T,n}, \quad [2-22]$$

$$\gamma = \left( \frac{\partial G}{\partial A} \right)_{p,T,n}, \quad [2-23]$$

where  $\gamma$  refers to the interfacial tension and  $n$  is an abbreviation for the set of amounts  $n_1, n_2, \dots$ , that define the composition of the system.

### 2.3.1.3 Adsorption at the solid surface

The Gibbs adsorption equation and dividing plane apply primarily to liquid–fluid interfaces. According to Lyklema (1995) the driving force for adsorption of gases on solid surfaces are the attractive forces, such as London–van der Waals, between the gas molecules and the solid surface. Assuming that the Gibbs dividing plane in a flat solid–gas system coincides with the physical boundary between gas and solid surface, and that the interfacial or surface excesses are reduced to the corresponding analytical surface concentrations, the Gibbs adsorption equation for a mixture of gases can be written as:

$$d\gamma = -S_a^{\sigma}dT - \sum_i \Gamma_i d\mu_i . \quad [2-24]$$

When a vapour adsorbs onto a solid surface it forms a contaminated solid surface where the adsorbed layer of vapour molecules on the solid surface is in equilibrium with the vapour of the liquid at equilibrium pressure,  $\Pi_e$ . This relation is described by the Young equation, which will be discussed in more detail in section 2.3.2.

$$\gamma_l \cos \theta = \gamma_{sv} - \gamma_{sl} . \quad [2-25]$$

The subscripts l, sv and sl refer to the liquid, solid–vapour and solid–liquid interfaces, respectively. Comparison of the non-contaminated or clean surface and the contaminated surface shows that:

$$\gamma_{sv} = \gamma_s - \Pi_e , \quad [2-26]$$

where the equilibrium pressure is:  $\Pi_e = -\Delta F$ . The increase in Helmholtz free energy,  $\Delta F$ , results from the transformation of the clean solid surface by adsorption of the water vapour (Schrader, 2003).

Adsorption / desorption at a gas–solid interface, as shown in Figure 2.19, results in the formulation of an equation for the surface concentration or interface excess at the solid–gas interface:

$$\Gamma = -\left(\frac{p}{RT}\right)d\gamma/dp . \quad [2-27]$$

where  $p$  is the gas pressure. Similar as for a solvent / solute system, the surface free energy of the solid decreases when gas or vapour molecules adsorb on its surface, although in this case an increase in vapour pressure is observed, resulting in a positive  $\Gamma$ . When the vapour molecules prefer the bulk gas phase, a negative  $\Gamma$  is obtained. However, if there is any adsorption of vapour molecules on the solid surface, than these molecules will be responsible for an increase in solid surface free energy compared to that of a clean or “un-adsorbed” solid surface (Schrader, 2003).

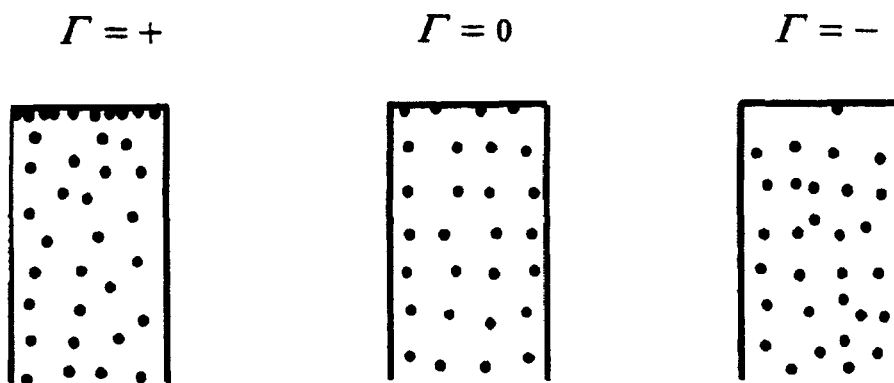


**Figure 2.19 Visualization of the principle of Gibbs adsorption for a solid-gas system (Schrader, 2003).**

Using the principle of the Gibbs adsorption theory and the dividing plane, Chattoraj (2001) discusses the adsorption of solute at solid-water interfaces, in addition to the previously discussed adsorption at air-water interfaces. It is based on the fact that surface active solutes accumulate at the interface, something that can easily be determined experimentally. For the adsorption of a surfactant at a solid-liquid interface equation [2-28] describes the surface excess:

$$\Gamma_2^1 = \Delta n_2 - \Delta n_1 \frac{x_2}{x_1}. \quad [2-28]$$

Isotherms obtained for the adsorption of SDS at alumina-water interfaces have shown that  $\Gamma_2^1$  is positive, resulting in the excess adsorption of solvent,  $\Gamma_1^2$ , to be negative.

### 2.3.2 Solid surface free energy

As mentioned previously, solid surface free energy is not a straight forward concept. In contrast to liquids, where the surface molecules are mobile, the surface molecules of solids can only vibrate around their mean position. Once a new solid surface is formed, that solid surface cannot reduce its surface area and thus not the excess internal energy. The result is the formation of a non-equilibrium surface structure. However, the inward pull responsible for the surface tension of liquids is also present on the solid surface molecules. The cohesion between the surface molecules is similar to that in liquids, but due to the very low mobility of solid surface molecules the surface area reduction is limited and it takes longer for the molecules close to the surface to gain an equilibrium distribution and orientation (Walstra, 2003). Both the concept of liquid surface tension and solid surface tension can be defined by the same equation, whereby the surface tension of any condensed material,  $\gamma_i$ , is defined as minus half the free energy of (non-covalent) cohesion,  $\Delta G_{ii}^{\text{coh}}$  (van Oss, 2006).

$$\gamma_i \equiv -\frac{1}{2} \Delta G_{ii}^{\text{coh}}. \quad [2-29]$$

No experimental method or technique is available to measure the solid surface tension or solid surface free energy directly. A couple of theoretical estimations exist for the surface free energy of solids, which are semi-empirical methods used only for solids which have specific atomic or molecular interactions. Unfortunately these cannot be applied to the materials used in this research. However, several indirect experimental methods have been developed for the determination of the surface free energy of solids. In general, these empirical approaches determine the surface tension of a solid,  $\gamma_s$ , by estimating the surface tension of the solid–liquid interface,  $\gamma_{sl}$ , which is in turn based on the use of two measurable quantities, the contact angle of a liquid drop on a solid surface,  $\theta$ , and the liquid–vapour interfacial tension,  $\gamma_{lv}$ . Several empirical approaches or theories have been applied in this research which interprets the surface free energy in terms of the intermolecular interaction forces at the interface. They are discussed in more detail in section 3.3.1.3.

The basis for these approaches lies in the equations of Young and Dupré (Balkenende et al., 1998). First of all the equation of Young, which is a thermodynamic definition of the contact angle,  $\theta$ . Young's equation describes the relation between three phases in equilibrium at the three-phase contact line, and relates the surface and interfacial tensions of the solid and the liquid to the contact angle (Karbowski et al., 2006):

$$\gamma_{lv} \cos \theta = \gamma_{sv} - \gamma_{sl} , \quad [2-30]$$

where  $\gamma_{lv}$ ,  $\gamma_{sv}$  and  $\gamma_{sl}$  are the surface tensions (or free energy per unit area) of the liquid–vapour, solid–vapour and solid–liquid interfaces, respectively.

The solid–vapour interfacial tension is dissimilar to the solid surface tension, but adsorption of vapour molecules by the solid surface will reduce the solid surface tension,  $\gamma_s$ , to the solid–vapour interfacial tension,  $\gamma_{sv}$  (Bateup, 1981). The relationship between solid surface tension and solid–vapour interfacial tension is given by the spreading or equilibrium film pressure,  $\pi_e$ :

$$\pi_e = \gamma_s - \gamma_{sv} . \quad [2-31]$$

From this equation it can be observed that the spreading pressure represents the reduction of solid surface tension due to vapour adsorption (Garbassi et al., 1994). In order to obtain the real work of adhesion, the spreading pressure should be added to the Young's equation. However, it is often assumed that the adsorption at the solid–vapour or liquid–vapour interface is negligible, implying that  $\gamma_{sv} = \gamma_s$  and  $\gamma_{lv} = \gamma_l$  (Balkenende et al., 1998). Especially for solids with low surface energy,  $\pi_e$  is often regarded as negligible. The spreading pressure is only significant for high energy surfaces, as there is a large degree of adsorption at the surface. Within this research,  $\pi_e$  is assumed negligible.

Secondly, the equation of Dupré, which describes the thermodynamic, reversible work of adhesion:

$$W_{sl}^a = \gamma_{sv} + \gamma_{lv} - \gamma_{sl} . \quad [2-32]$$

The thermodynamic, reversible work of adhesion,  $W_a$ , or the negative of the free energy of adhesion  $-\Delta G_a$  can be interpreted as the work required to separate a unit area of solid–liquid interface between two different materials (Comyn, 1997) to leave a “clean” solid surface and a liquid surface, both in equilibrium with the vapour phase (Karbowski et al., 2006). According to Lee (1993) it corresponds to the negative of the Gibbs (or Helmholtz) free energy change per unit area of interface,  $-\Delta G^a$ , whereby it is assumed that a hypothetical interaction takes place between two phases across a plane boundary without a change in area.

Combining equation [2-30] and [2-32] yields the Young-Dupré adhesion model:

$$W_{sl}^a = \gamma_{lv}(\cos \theta + 1) . \quad [2-33]$$

This model is based on measurable quantities, i.e. the liquid surface tension,  $\gamma_{lv}$  and the contact angle,  $\theta$ , in order to determine the reversible work of adhesion for solid–liquid interactions. In this research, the contact angle refers to the angle that chocolate makes with the solid surface, the mould, and the liquid–vapour surface tension refers to the chocolate–vapour surface tension.

### 2.3.2.1 Surface tension

Surface tension,  $\gamma$ , and surface free energy,  $\Delta G$ , are strictly speaking not the same thing (van Oss, 2006), As can be observed from equation [2-34] where  $\Delta G_1^{coh}$  is the thermodynamic free energy or work of cohesion of material 1, whilst  $\gamma_1$  is the surface tension of this same material:

$$\Delta G_{11}^{coh} = -2\gamma_1 . \quad [2-34]$$

The surface tension can be regarded as a physical parameter, which represents both the free energy per unit area and the force per unit length (Good, 1992). According to Fowkes (1964), the surface tension in a liquid surface resides primarily in the surface monolayer. To ensure, however, that the part of the surface tension which is present in the bulk liquid adjacent to the surface or interfacial monolayer is also taken into account, the term surface or interfacial region is used. Attractive short-range forces between molecules located in the bulk liquid have been observed to experience on average a uniform force field. Molecules located at the surface or at for example a liquid–air interface experience a non-uniform force field with a net inward pull (Shaw, 1992). The attractive forces acting between molecules within the surface region of a liquid are responsible for a net attraction into the bulk of the liquid in a direction normal to the surface (Fowkes, 1964). Summarizing, the surface tension of a liquid results from an imbalance of molecular forces in the surface region of the liquid, as is visualized in Figure 2.20.

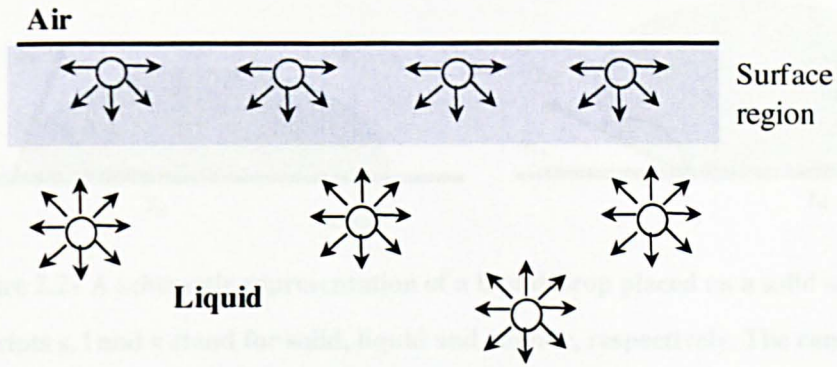


**Figure 2.20 Attractive forces between molecules at the surface region and in the bulk of a liquid which are responsible for the surface tension (Shaw, 1992).**

As described by equations [2-22] and [2-23], the cutting of a bulk liquid results in the formation of a new surface. A consequence of this is that the molecules in the surface need to rearrange themselves, subsequently decreasing molecular interactions until equilibrium is reached. At equilibrium, there is a decreased interaction of the molecules at the new surface (McGuire, 2005). The removal of molecular interactions means that the molecules at the surface have an excess of interfacial energy, compared to the molecules in the bulk liquid, e.g. an increase in the excess surface free energy of the molecules along the new surface is obtained. The excess energy in the surface region is responsible for a force acting towards the bulk of the liquid. As a result of the molecules at the surface showing an increased tendency to minimize their surface area, the excess energy of the whole system is decreased. Surface tension is defined as the force that is responsible for the minimization of the surface area of liquid matter in order to reduce the surface excess energy.

### 2.3.2.2 Contact angle

The interactions between a liquid and a solid–vapour interface can be characterised by the contact angle,  $\theta$ , which is the angle that a liquid drop makes when placed on a solid surface, as is visualized in Figure 2.21. Characteristic for the three-phase system is the orientation of the liquid–vapour interface with respect to the solid surface (McGuire, 2005). Contact angle measurement is regarded as the most accurate method describing the interaction energy of the solid–liquid interface at the minimum equilibrium distance,  $\ell_0$ , (van Oss, 2006). Molecular adhesion forces are not present at distances above  $\ell_0$ , so no interaction is observed. If the distance between a liquid drop and a solid substrate is below  $\ell_0$ , interaction is observed for example by a liquid drop jumping onto the solid substrate and spreading out over its surface (Kendall, 2001). Kwok and Neumann (1999) described the measured contact angle as the result of three interfacial tensions in mechanical equilibrium. At this equilibrium state, the liquid drop exhibits a finite contact angle towards the solid (Fox and Zisman, 1950).



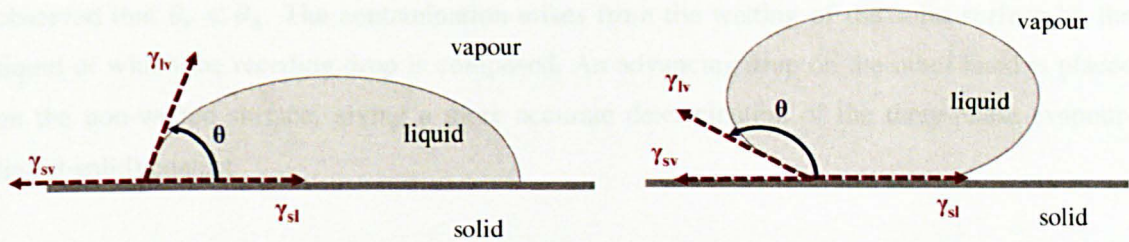


**Figure 2.21** A schematic representation of a liquid drop placed on a solid surface.

The subscripts s, l and v stand for solid, liquid and vapour, respectively. The contact angle,  $\theta$ , is measured through the drop, at the tangent to the drop, starting at the triple point solid–liquid–vapour (adapted from Lyklema, 2000; Neumann and Good, 1979).

The concept of contact angle was first defined by Young in 1805, when he described the three phase equilibrium. Young defined the contact angle in terms of the vectorial sum (vector with magnitude and direction), which resulted in Young's equation of interfacial equilibrium as represented by equation [2-30] (Good, 1992; Kwok and Neumann, 1999). The different interfaces aim to reduce the interfacial area and consequently minimize the overall interfacial energy of the system. The underlying hypothesis for the Young equation states that solid surfaces should be homogeneous and smooth. According to Good (1979), Young's equation can be completed by adding the following term:

$$\text{If } \gamma_{sv} - \gamma_{sl} > \gamma_{lv}, \text{ then } \cos \theta = 1.$$

According to van Oss (2006), the sessile drop is a force balance, which determines macroscopic-scale interaction energies. Within this balance, the cosine of the contact angle results from a combination of the energy of cohesion of the liquid,  $\gamma_l^{\text{tot}}$ , and the energy of adhesion between the liquid and the solid,  $\Delta G_{sl}$ . This force balance is shown schematically in Figure 2.22. Within this balance the equilibrium spreading pressure,  $\pi_e$ , is neglected and it is assumed that  $\gamma_l > \gamma_s$ . It can be observed from the force balance that finite or non-zero contact angles can be obtained only if  $\gamma_l^{\text{tot}} > \Delta G_{sl}$  and gravity is neglected. A small contact angle indicates strong adhesion, high molecular attractions, whereas a large angle shows small or limited adhesion, low molecular attractions (Kendall, 2001).

It can be deduced from Young's equation [2-30] that one contact angle should be obtained from the vectorial sum of the three interfacial tensions. However, experimentally it is observed that a range of contact angles is obtained when a drop of liquid is placed on a solid surface. Within this range of contact angles, a maximum value or advancing contact angle,  $\theta_a$ , and a minimum value or receding contact angle,  $\theta_r$ , can be observed (Garbassi et al., 1994; Kwok and Neumann, 1999). The words receding and advancing are based on the measurement of these two angles, which will be discussed in section 3.3.1.2. According to van Oss (2006) both the Young and Young-Dupré equations are only valid for advancing contact angles. Receding or retreating contact angles are measured on a contaminated surface, as a result of which it is commonly



observed that  $\theta_r < \theta_a$ . The contamination arises from the wetting of the solid surface by the liquid of which the receding drop is composed. An advancing drop on the other hand is placed on the non-wetted surface, giving a more accurate determination of the three-phase (vapour-liquid-solid) contact.

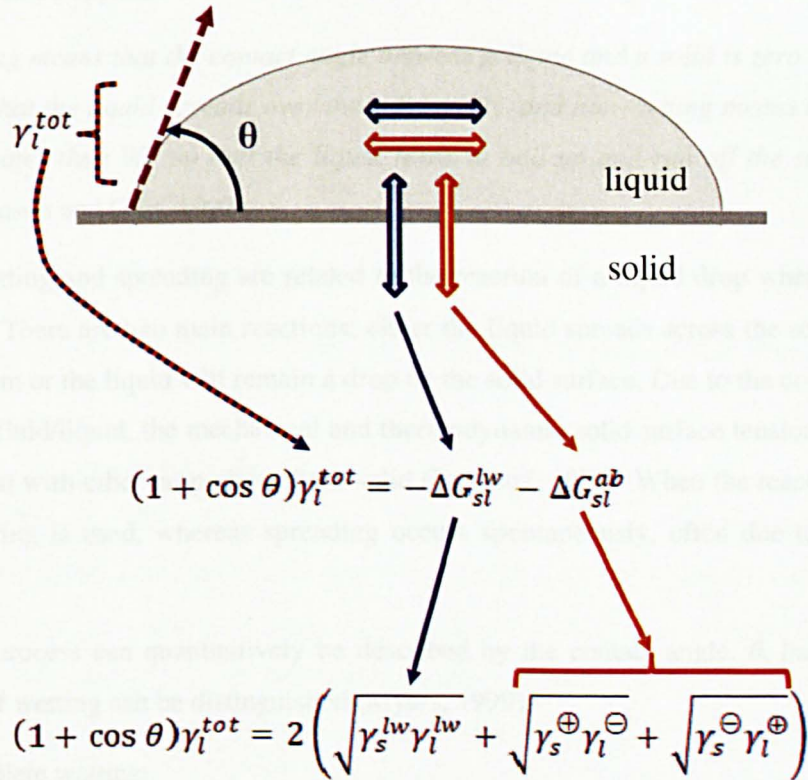


Figure 2.22 The contact angle as a force balance, where  $\cos \theta$  results from the equilibrium between the energy of cohesion within the liquid and the energy of adhesion between the liquid and solid surface.

Correlating this to the Young-Dupré equation it is shown that the left hand side of the equation refers to the energy of cohesion, whilst the right hand side refers to the energy of adhesion. Within the latter a second division can be made between the contribution of apolar ( $\leftrightarrow$ ) or Lifshitz-van der Waals interactions and polar ( $\leftrightarrow$ ) or Lewis acid-base interactions (van Oss, 2006).

#### 2.3.2.2.1 Wetting or spreading

Different definitions exist of what is intended by the word “wetting”. These definitions are mainly based on the field or sector where it is applied. In certain cases wetting can also be considered to be an umbrella term ‘describing all phenomena involving contacts between three phases, of which at least two are fluid’ (Lyklema, 2000). In general, the following description or definition can be applied:

*Wetting means that the contact angle between a liquid and a solid is zero or so close to zero that the liquid spreads over the solid easily, and non-wetting means that the angle is greater than 90° so that the liquid tends to ball up and run off the surface easily’ (Adamson and Gast, 1997).*

The terms wetting and spreading are related to the reaction of a liquid drop when placed on a solid surface. There are two main reactions; either the liquid spreads across the solid surface to form a thin film or the liquid will remain a drop on the solid surface. Due to the contact between a solid and a fluid/liquid, the mechanical and thermodynamic solid surface tension will change, in combination with other properties of the solid (Rusanov, 1996). When the reaction is forced, the term wetting is used, whereas spreading occurs spontaneously, often due to liquid–solid interactions.

The wetting process can quantitatively be described by the contact angle,  $\theta$ , based on which three stages of wetting can be distinguished (Myers, 1999):

- Complete wetting

The liquid will spread on the flat solid surface and form a thin uniform film,  $\theta = 0^\circ$ .  
Important is the long range character of the molecular interactions;

- Partial wetting

The liquid will spread on the solid surface to some degree, but it will not form a uniform film, approximately  $0^\circ < \theta < 90^\circ$ ;

- Non-wetting

The liquid will not or only minimally spread on the solid surface,  $\theta > 90^\circ$ .

#### 2.3.2.2.2 Thermodynamics of wetting

Another way of describing the wetting process is by using thermodynamics, which results in the formation of three types of wetting: *spreading (A)*, *adhesion (B)* and *immersion (C)* wetting. These three types of wetting and the work involved are shown schematically in Figure 2.23 (Lyklema, 2000; Myers, 1999; Shaw, 1992; Bateup, 1981).



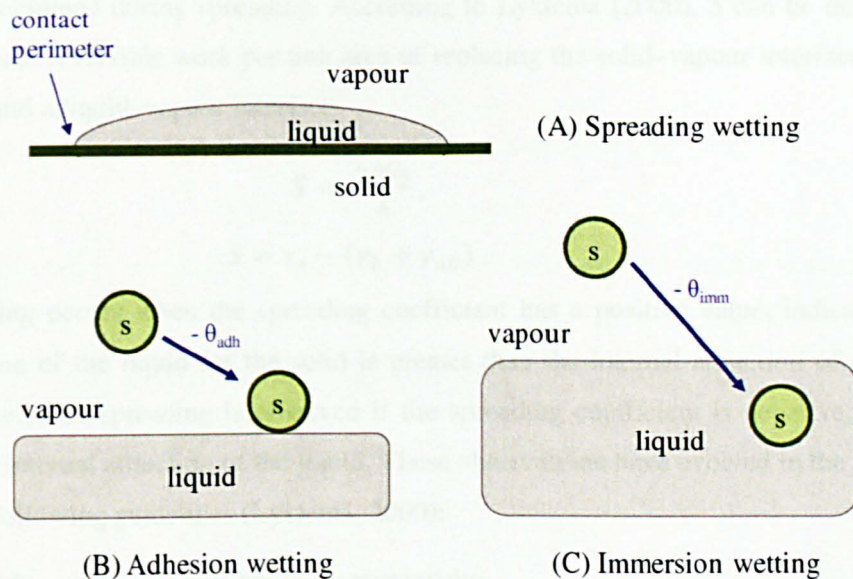


Figure 2.23 Three kinds of wetting, thermodynamically defined (Lyklema, 2000).

### A. Spreading wetting or spreading

Harkins (1941) and Harkins and Feldman (1922) were among the first to describe the different situations that might occur upon contact between a liquid and a solid:

- *All liquids spread on a pure surface*: a theory developed by Lord Rayleigh, based on the principle that all substances attract each other;
- *A liquid (b) will not spread on another liquid (a) if:  $\gamma_a > \gamma_b + \gamma_{ab}$* :  
A theory based on the Neumann triangle of forces, where the surface tension of each respective liquid will pull the liquid away from the other liquid;
- *Liquids whose molecules are polar or contain polar groups, spread on water*: a theory developed by Langmuir, who stated: ‘the only substances which spread are those whose molecules contain both hydrophilic and hydrophobic parts’;
- *A liquid will spread if its work of cohesion is less than its work of adhesion*:  
a theory developed by Harkins and Feldman, whereby the tendency of a liquid to spread is described by its spreading coefficient,  $S$ :  $S = W_a - W_c$ .

The Harkins and Feldman theory is developed from the thermodynamics of surfaces, and is therefore theoretically the most justified theory. According to Harkins and Feldman (1922), spreading wetting or spreading is characterized by the spontaneous wetting of the solid surface by the liquid. The initial situation consists of a solid and a liquid being in contact with each other. Spreading results in the displacement of an area of solid–vapour interface by equivalent areas of solid–liquid and liquid–vapour interfaces.

The thermodynamic spreading coefficient,  $S$ , describes the relationship between the surface free energies that are involved in the spreading process. It gives the free energy decrease

that is obtained during spreading. According to Lyklema (2000),  $S$  can be defined as 'the isothermal reversible work per unit area of replacing the solid–vapour interface by a solid–liquid and a liquid–vapour interface:

$$S = \frac{-\Delta G_s}{A}, \quad [2-35]$$

$$S = \gamma_a - (\gamma_b + \gamma_{ab}).$$

Spreading occurs when the spreading coefficient has a positive value, indicating that the attraction of the liquid for the solid is greater than the internal attraction of a liquid; and oppositely, no spreading is observed if the spreading coefficient is negative, indicating a greater internal attraction of the liquid. These observations have evolved in the development of the following guidelines (Lyklema, 2000):

$S > 0$  spreading will occur spontaneously;

$S = 0$  system is at equilibrium;

$S < 0$  droplets retract their perimeter, leading to partial wetting.

### B. Adhesion wetting

The concept of adhesion wetting is based on the adhesion of a liquid to the solid surface once the two phases make contact. Initially, both the solid and the liquid are in contact with a vapour. Adhesion occurs once the solid is brought into contact with the liquid phase. The adhesion wetting process consists of the displacement of an area of solid–vapour interface by an equal area of solid–liquid interface. Compared to the spreading wetting process, the area of liquid–vapour interface is decreased.

The Young-Dupré adhesion model, described in equation [2-33] is used to mathematically describe the adhesion wetting process. Officially, the equilibrium spreading pressure,  $\pi_c$ , which represents the reduction of solid surface tension due to vapour adsorption (Garbassi et al., 1994), should be added to the Young-Dupré equation. However,  $\pi_c$  has been observed to be negligible for low surface energy solids. As  $\pi_c \approx 0$  for low energy surfaces, the work of adhesion is shown by equation [2-33], the Young-Dupré equation (Hiemenz, 1986).

### C. Immersion wetting

The concept of immersion wetting is based on the complete immersion of the solid in the liquid phase. Initially, both the solid and the liquid are in contact with a vapour phase, similar to the initial situation for the adhesion wetting process. Immersion occurs when the solid is brought into contact with the liquid and is completely wet by the liquid. The immersion wetting process consists of the displacement of the complete unit area of solid–vapour interface by a similar unit area of solid–liquid interface. There is not a change in the area of the liquid–vapour interface during the immersion wetting process.

The free energy change obtained during the immersion wetting process is:



$$W_{imm} = \frac{-\Delta G_i}{A}, \quad [2-36]$$

$$= \gamma_{sv} - \gamma_{sl}.$$

Relating this to the Young-Dupré equation for adhesion wetting [2-33]:

$$W_{imm} = \gamma_{lv} \cos \theta. \quad [2-37]$$

The following conditions or guidelines have been applied to the immersion wetting process:

$\gamma_{sv} > \gamma_{sl}$  then  $\theta < 90^\circ$  and immersion wetting occurs spontaneously;

$\gamma_{sv} < \gamma_{sl}$  then  $\theta > 90^\circ$  and work must be done for immersion to occur.

Within this research, it is assumed that spreading and adhesion wetting will be the most important processes. Spreading wetting applies to the chocolate moulding process, in which liquid chocolate is deposited into the moulds and displaces vapour that is in contact with the mould surface. Important with respect to the vapour displacement are the cohesive intermolecular interactions between the chocolate molecules and the adhesive interactions between the chocolate and mould surface. Knowledge of the spreading coefficient would increase understanding of the process of chocolate moulding. Adhesion wetting, on the other hand, applies to both the chocolate moulding and demoulding process, especially once the liquid chocolate spreads in the moulds and the subsequent removal of the chocolate from the mould.

## 2.4 THERMODYNAMICS VS PRACTICAL ADHESION

Various theories and mechanisms have been proposed in literature to explain surface adhesion and have been discussed in section 2.2.3, i.e. mechanical interlocking, wetting and thermodynamical adsorption, electrostatic adhesion, diffusion, chemical adhesion, and weak boundary layers (Michalski et al., 1997; Comyn, 1997). Of these theories, the concept of thermodynamically driven surface adhesion is probably the most relevant for food applications. Understanding of the mechanisms involved in the phenomena of wetting and spreading, such as solid–liquid interactions, is believed to enhance development of new surfaces and interfaces through artificial modifications, and subsequently improved manufacturing facilities (Karbowski et al., 2006).

Fouling is defined as “the accumulation of unwanted deposits on the surfaces of heat exchangers”, and results in a reduced efficiency of the equipment due to resistance to heat transfer (Bott, 1995). The deposits can be crystalline, particulate or biological material, or the result of a chemical reaction, and are caused by the combined effect of adhesion of species to (thermal) equipment surfaces and cohesion between elements of the material. General factors

believed to be responsible for the adhesion are van der Waals forces, electrostatic forces, hydrogen bonding and hydrophobic binding, as well as contact area effects (Liu et al., 2006a). Many researchers have considered that the extent of adhesion is predominantly determined by the surface energy of the substrate, especially in the case of bio- and crystalline fouling. Michalski et al. (1998a) investigated the relationship between the thermodynamic work of adhesion and the weight of fatty food remaining on packaging material after drainage flow. Their results showed that pure chemical reference materials, in this case vaseline oil, cannot be used to predict the adhesion behaviour of food materials, in particular olive, sunflower and soybean oil. Thermodynamic adhesion, however, was shown to be important in the interactions between oil materials and packaging or equipment surfaces. Especially the use of liquid surface tension and contact angle determinations was recommended for a 'simple and reliable estimation of food-to-solid adhesion. Another study with food emulsions showed a similar result (Michalski et al., 1999). The amount of emulsion that adhered to solid surfaces increased with solid surface energy. More importantly, a minimal or critical solid surface tension was observed for each emulsion, which indicated the starting point for the formation of deposits.

Well known within the field of biofouling is the Baier curve, representing the relation between solid surface free energy and relative bacterial adhesion, see Figure 2.24. Characteristic for this relation is the optimum value or minimum of the surface free energy for which bacterial adhesion is minimal, which lies in the range of 20–30 mN m<sup>-1</sup> (Zhao, 2004). A similar correlation has also been observed for the adhesion of milk protein at surfaces with varying surface energy, where the optimum value of the surface energy falls in the range 30–35 mN m<sup>-1</sup>. Using this information several attempts have focussed on the reduction of fouling using coated polytetrafluoroethylene (PTFE) surfaces, which are known to have low surface energy and non-stick properties (Zhao et al., 2005). Tsibouklis et al. (1999) investigated two particular classes of compounds, silicones and acrylates, in relation to bacterial adhesion, based on suggestions that a flexible linear backbone was required for the coating polymer, as this would enhance the attachment of side-chains with low intermolecular interactions. However, contact angle measurements indicated that the more flexible siloxane coatings exhibited higher surface energy values, but both types of coatings were capable of inhibiting bacterial adhesion. Research by Zhao et al. (2004b) has shown that the Lifshitz–van der Waals component of the surface free energy plays a determining role in the resistance to bio-fouling. Saikhwan et al. (2006) observed a similar dependence on the non-polar / dispersive / Lifshitz–van der Waals component of the surface energy.

Liu et al. (2006b) used the concept of the Baier curve to develop a model which can predict the fouling resistant value at which the foulant adhesion force is reduced and the fouling deposit can be removed more easily, i.e. it assumes that a minimum adhesion energy between deposit and surface exists:

$$\sqrt{\gamma_{surface}^{LW}} = \frac{1}{2} \left( \sqrt{\gamma_{foulant}^{LW}} + \sqrt{\gamma_{fluid}^{LW}} \right). \quad [2-38]$$

Experimental results using baked and unbaked tomato paste showed that the experimentally determined minimum is in the region predicted by the theory, and that the effect of surface energy decreases with increasing deposit thickness.

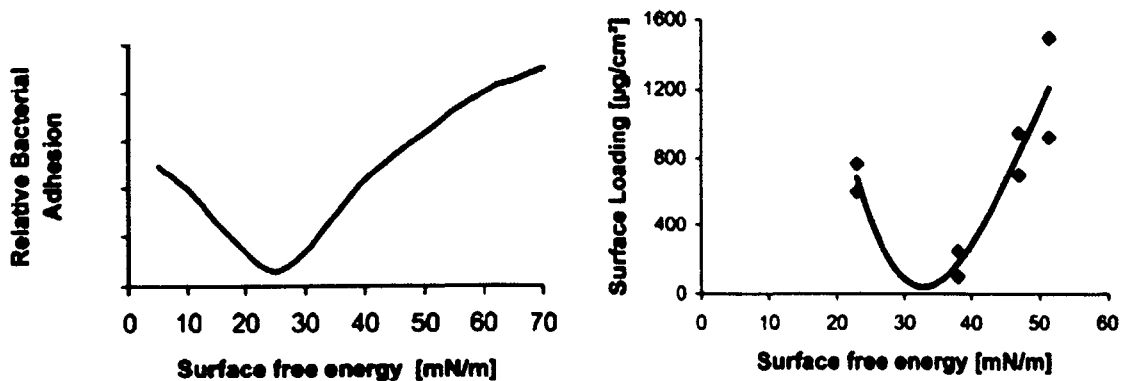


**Figure 2.24** Effect of solid surface free energy on bacterial adhesion, Baier curve (left), and on protein adhesion (right), respectively (Zhao, 2004).

Another area where modified surfaces are applied to reduce the adhesion is in the cleaning of food contact surfaces. In many food manufacturing plants the adhesion of food particles to equipment surfaces is unavoidable (Bobe et al., 2007). Boulangé-Petermann et al. (2006) investigated the effect of chemical and mechanical surface modifications on the surface energy and cleaning ability of stainless steel. A strong correlation was observed between the cleaning performance and the polar component of the solid surface energy, where hydrophilic surfaces had a much higher oil droplet removal rate. Rosmaninho et al. (2004) and Rosmaninho and Melo (2006) concluded that the electron donor component,  $\gamma^-$ , is the main differentiating parameter for different types of stainless steel, both modified and non-modified. It affected the initial deposition rate of calcium phosphate deposits, which in turn determined the deposit structure and amount of material deposited. Surfaces with a high electron donor component were regarded as being more prone to nucleation resulting in an increased ability to form nucleation sites and subsequently developing more compact deposit structures. Low electron donor component surfaces, on the other hand, showed the opposite behaviour and developed larger deposits with a more loose structure.

## CHAPTER 3

### MATERIALS AND METHODS

#### 3.1 INTRODUCTION

This chapter will discuss the experimental materials and methodologies applied during this research.

#### 3.2 MATERIALS

The materials used in this research are divided into four different categories, according to their physical and chemical characteristics and their particular applications:

- **Chocolate systems**

Food grade non-aerated chocolate systems were used for the chocolate–mould adhesion determination (section 2.2.2). The results obtained by using these chocolate systems are discussed in CHAPTERS 4, 5, 6 and 7.

- **Solid mould materials**

Characteristic mould materials were chosen as solid substrates for surface energy (section 2.2.1) and chocolate–mould adhesion determinations. The results obtained by using these solid mould materials are discussed primarily in CHAPTER 4.

- **Contact angle liquids**

Standardized contact angle liquids were applied in contact angle and surface tension experiments as part of the surface energy determination. The results obtained by using these contact angle liquids are discussed in CHAPTER 4.

- **Thin film coating systems**

Food grade coatings composed of a selection of biopolymers and fatty acids were used to modify a standard polycarbonate mould surface, and subsequently used for the chocolate–mould adhesion determination. The results obtained by using these thin film coating systems are discussed in CHAPTER 7.

##### 3.2.1 Chocolate systems

General issues relating to chocolate composition and production were discussed in CHAPTER 2. The chocolate systems used are cocoa butter, dark chocolate and milk chocolate, and their approximate composition is summarized in Table 3.1.

**Table 3.1 Composition (%) of chocolate systems.**

	<b>Cocoa butter</b>	<b>Dark chocolate</b>	<b>Milk chocolate</b>
Cocoa solids	100	52	29
Sugar		47.5	51.5
Milk solids			20
Other components, e.g. lecithin and vanillin		0.5	0.5

The use of aerated chocolate in surface energy and adhesion measurements is hindered due to mechanical constraints. Melting and other preparative techniques are required to be applied to the chocolate samples prior to the application of the various experimental methodologies. However, in the case of aerated chocolate these techniques will normally result in a modification of the characteristic microstructure and physical properties of the aerated sample. As a result the decision was taken to concentrate on the use of “normal”, i.e. non-aerated, chocolate for the validation of the experimental methodologies applied in the research, as well as gaining fundamental understanding.

### 3.2.1.1 *Cocoa butter*

Deodorized cocoa butter (100% cocoa solids, ADM Cocoa, Koog aan de Zaan) was obtained from Nestlé PTC, York. The type of cocoa butter used was so called *press cocoa butter*, which is obtained by means of mechanical pressing of cleaned and ground cocoa nibs and subsequently only filtered / centrifuged and degummed and/or deodorized, and is the highest grade commonly used as a standard within the chocolate manufacturing industry (De Zaan, 2006). Analytical characteristics have been summarized in Table 3.2.

As discussed in section 2.1.2.1, cocoa butter is a unique fat, based on its chemical composition. It consists of 1,3-dipalmito-2-olein, 1-palmito-3-stearo-2-olein, and 1,3-distearo-2-olein in an almost constant ratio of 22 : 46 : 31 (% peak area) (Belitz et al., 2004). As cocoa butter comprises mainly these three triglycerides it behaves like a pure chemical at phase changes, with a relatively sharp melting point rather than a melting range. This clear melting point is also responsible for the characteristic cooling sensation experienced when cocoa butter melts in the mouth. The chemical composition is also responsible for the resistance of cocoa butter to autoxidation and microbiological deterioration. In solid form, the cocoa butter exhibits an ivory colour, whereas in liquid form a clear, yellowish colour was displayed, without signs of solid particles.



In this research cocoa butter was used as a reference or model system. Its chemical and physical behaviour is comparable with that of a pure or single component system. Furthermore, it is one of the main ingredients of chocolate. By using cocoa butter as a model system and comparing it to dark chocolate, it allows the determination of specific effects and/or interactions caused by the other ingredients present within the chocolate matrix.

**Table 3.2 Specification of pure pressed cocoa butter (De Zaan, 2006).**

<b>Characteristics</b>	<b>Press cocoa butter</b>
Acidity	max. 1.75%
Refractive index $n_D$ (40 °C)	1.456 – 1.458
Slip melting point	30 – 34 °C
Clear melting point	32 – 35 °C
Blue value	max. 0.05
Free fatty acids (as % m/m oleic)	0.5 – 1.75%
Saponification value (mg KOH g/fat)	192 – 197
Peroxide value	max. 4
Iodine value	33 – 40
Unsaponifiable matter (% m/m)	max. 0.35%
Adsorbance after washing with alkali	max. 0.14
Colour (yellow + red)	min. 40 + 1.0 / max 40 + 2.0

### 3.2.1.2 Dark chocolate

Dark chocolate was prepared according to standard (commercial) recipe by mixing sugar, cocoa liquor, cocoa butter, lecithin and vanillin, by Nestlé PTC (York) in order to obtain a final product with 52% cocoa solids. All samples were tempered using commercial methods prior to surface energy and/or adhesion measurements. The temperature profile used was similar to that shown in Figure 2.11, except that the temperatures were slightly adjusted for dark chocolate where necessary. Mycryo<sup>®</sup> cocoa butter powder (Cacao Barry) was used as a seeding or nucleation agent, to ease the tempering process, by inclusion (1% concentration) in the melted chocolate mass at a temperature of 34–35 °C.

Dark chocolate was chosen as the experimental system over milk chocolate, as it is the simplest of all chocolate types consisting mainly of cocoa solids, fat and sugar. Artefacts caused by other ingredients are thus negligible. Comparison of dark chocolate and cocoa butter will allow the determination of the combined effect of cocoa solids and sugar particles.

## 3.2.1.3 Milk chocolate

Tempered milk chocolate (29% cocoa solids, 20% milk solids) was obtained from Nestlé PTC (York) and was prepared according to standard (commercial) recipe. All samples were tempered using commercial methods prior to surface energy and / or adhesion measurements. The temperature profile used was similar to that shown in Figure 2.11.

## 3.2.2 Solid mould materials

Different types of solid mould materials were evaluated from a physical, e.g. thermal and mechanical properties, and chemical, especially surface characteristics, point of view. The final four mould materials chosen for surface energy and chocolate–mould adhesion determination are polycarbonate, stainless steel, poly(tetrafluoroethylene) (PTFE) (Teflon) and quartz glass, and a summary of their most important mechanical and thermal properties is given in Table 3.3.

**Table 3.3 Mechanical and thermal properties of solid mould materials**  
(Brydson, 1999; Wyatt et al., 1998; NVON-commissie, 1998).

		Polycarbonate	Stainless steel	PTFE	Quartz glass
Tensile strength	MPa	65.5	580	21	48
Elongation at break	%	110	55	300	-
Density	kg m <sup>-3</sup>	1200	8060	2150	2200
Specific heat	J kg <sup>-1</sup> K <sup>-1</sup>	1180	503	1172	670
Thermal conductivity	W m <sup>-1</sup> K <sup>-1</sup>	0.19	16.2	0.195	1.4
Mean coefficient of thermal expansion	x10 <sup>-6</sup> °C <sup>-1</sup>	0.65	17.3	99	0.55
Glass transition temperature	°C	~145	N/A	130	1175
Crystal melting point	°C	220-230	N/A	-	N/A
Melting point	°C	300	1400	302-310	1683 <sup>1</sup>

<sup>1</sup> Softening point of quartz glass

Of these solid materials, the first three are known because of their commercial application in confectionery manufacturing. Industrial chocolate moulds are now commonly made from polished polycarbonate, although they were traditionally made from stainless steel. Flexible PTFE and/or silicon rubber moulds have also shown practical advantages, due to their flexibility, non-stick character and low surface energy. Quartz glass was primarily chosen as the reference material, because of its purity and well-known high surface energy surface characteristics.

### 3.2.2.1 Polycarbonate

Polycarbonates are polymers belonging to the group of thermoplastic polymers, which are obtained by condensation polymerization of polyhydroxy compounds with a carbonic acid ( $\text{CO}(\text{OH})_2$ ) derivative, resulting in carbonate interunit linkages ( $-\text{O}-\text{CO}-\text{O}-$ ). In commercial applications the polyfunctional hydroxy compounds most commonly applied are diphenyl compounds and in particular bisphenol A 2,2-bis-(4-hydroxyphenyl)propane (Brydson, 1999). Linear polycarbonates, see Figure 3.1, can be synthesized via four practical routes, but the main technique used within industry is the reaction of phosgene ( $\text{COCl}_2$ ) with dihydroxy compounds in the presence of acid acceptors. An example is the interfacial polycondensation by phosgenation process, where bisphenol A and phosgene react in the presence of methylene chloride-water mixtures (Ebewele, 2000).

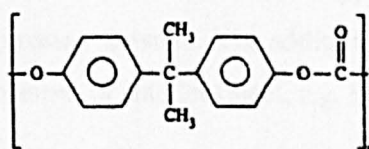


**Figure 3.1 Polycarbonate chemical structure.**

Due to its exceptionally high-impact strength even at low temperatures, low moisture absorption, good heat resistance, good rigidity and electrical properties and light transmission, polycarbonate finds common use in chemical and engineering applications. One of the major disadvantages of polycarbonate is its low chemical and scratch resistance. According to Brydson (1999), the ester groups are relatively easily hydrolysed by many organic solvents, e.g. alkaline solution and amines. Similar destructive observations were reported by Bayer (Bayer MaterialScience, 2004), the producer of Makrolon<sup>®</sup> polycarbonate, who mentions furthermore the migration of low-molecular, aromatic, halogenated, and polar compounds, resulting in dissolution or swelling of the polycarbonate sample.

The polycarbonate samples used during this research were obtained from 2 different suppliers, with Barkston Plastics Ltd. (Leeds) supplying the standard polycarbonate and Agathon GmbH (Bottrop) supplying Bayer Makrolon 2858 polycarbonate samples with different surface

finishes. Both suppliers use similar processing methods, e.g. injection moulding, and the specifications as summarized in Table 3.3 are in good agreement, from which it was concluded that the different samples could be used as interchangeable grades of polycarbonate. The appropriate surface finish of the standard polycarbonate sample was obtained by abrasion using a P600 (3M™, MarineWare, Southampton) wet or dry abrasive paper and an abraded surface plate. Samples supplied by Agathon, the leading producer of chocolate moulds, varied in surface finish and surface texture. Surface finish (gloss and texture) of these samples is a result of the contact with the injection moulding tooling, which has been polished to different levels, depending on the surface finish required for the particular application. For example, the cavities within a chocolate mould which are in direct contact with the chocolate will have a high gloss finish, whereas the rest of the mould surface will be relatively glossy, but less so than the cavities.

### 3.2.2.2 *Stainless steel*

Stainless steel is a low carbon alloy, which contains a minimum of 50% iron and 12% chromium by weight, giving it its characteristic stainless, corrosion resisting properties. The strong oxide-forming elements, such as aluminium, silicon and chromium, confer corrosion and oxidation resistance through the formation of a strong, though, adherent, invisible film which replaces the oxide on the iron surface (Wyatt et al., 1998). Depending on the chromium content and the presence of other elements such as molybdenum, copper, nickel, titanium and nitrogen, stainless steel is more or less corrosion resistant. The addition of other elements also enhances the structure and mechanical properties of stainless steel, e.g. formability and strength.

The stainless steel samples used during this research, type 316, were obtained from Richard Austin Alloys Ltd. (Leeds). Stainless steel type 316 is an austenitic stainless steel type with steel name X5CrMo17-12-2 and steel number 1.4401, and its chemical composition according to the European standard EN 10088-2: 2005 is summarized in Table 3.4. Austenitic stainless steel is most commonly used in dairy and food equipment, chemical and textile plants, and architectural applications.

**Table 3.4 Characteristic chemical composition of type 316 austenitic stainless steel (British Stainless Steel Association, 2007).**

Chemical composition % by mass max.									
C	Si	Mn	P	S	N	Cr	Cu	Mo	Ni
0.07	1.00	2.00	0.045	0.030	0.11	16.5/18.5	-	2.00/2.50	10.0/13.0

Surface finish of the stainless steel samples was obtained by using a P600 (3M™, MarineWare, Southampton) wet or dry abrasive paper and an abraded surface plate.

### 3.2.2.3 Polytetrafluoroethylene (PTFE)

Polytetrafluoroethylene (PTFE) is a high-temperature fluoroplastic, obtained from polymerization of tetrafluoroethylene. The resulting homopolymer is a linear chain of repeating tetrafluoroethylene units, as can be observed from Figure 3.2. In general, fluoropolymers are derived from polyethylenes-polypropylenes by the substitution of fluorine for hydrogen. The resulting C-F bond that is formed is very stable, with high bond strength, especially if compared to C-H or F-O bonds (Wyatt et al., 1998). This bond strength and/or stability, in combination with the particular chain packing, are responsible for the high chemical resistance of PTFE. Teflon<sup>®</sup> is the brand name of PTFE supplied by DuPont and is commonly used as the trademark name for PTFE.

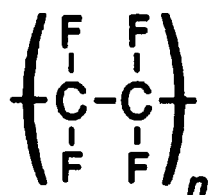


Figure 3.2 PTFE chemical structure.

Due to its high melting point, PTFE cannot be melt processed and other processing techniques like pressing and sintering are required. Furthermore, the lack of polar groups and low surface-free energy of PTFE, cause its surface not to be attractive to adhesives. PTFE therefore finds common use as a non-stick coating in kitchen utensils for example (Comyn, 1997).

The PTFE samples used during this research were obtained from Barkston Plastics Ltd. (Leeds). An appropriate surface finish was obtained by using a fine turn. Flexible PTFE and/or silicon rubber moulds have shown practical advantages in chocolate manufacturing, due to their flexibility and low surface energy. These moulds often consist of a PTFE coating or thin film in combination with an aluminium or stainless steel base. Different degrees of flexibility of PTFE can be obtained through varying processing techniques, e.g. heat sealed, thermoformed, vacuum formed, heat bonded, welded etc. Chemical composition of the PTFE film can furthermore be varied by incorporation of other compounds during the polymerization or derivation process, consequently changing mechanical and thermal properties.

### 3.2.2.4 Quartz glass

Quartz glass (SiO<sub>2</sub>), which is also called fused quartz or fused silica, is obtained by melting pure quartz, forming a clear transparent solid. In the crystalline or amorphous state, quartz glass is extremely resistant to heat shock, has a high corrosion resistance, and can withstand high processing temperatures for relatively long periods of time. Addition of other oxides to the silica

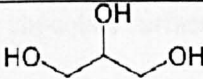
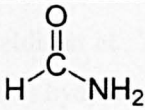
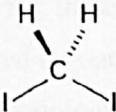
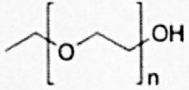
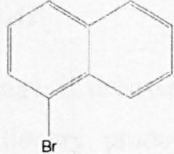
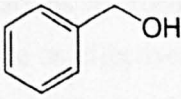
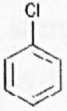


base will result in a reduction of the softening point and an increase in thermal expansion (Wyatt et al., 1998).

The quartz glass sample used during this research was obtained from Scientific Optical (Hastings), and contained an optical finish. Based on its high purity and limited contamination, quartz glass was chosen as a reference material. It is expected that the surface energy will be relatively constant and independent of processing conditions and techniques.

### 3.2.1 Contact angle liquids

**Table 3.5 Characteristics of probe liquids used for surface tension and contact angle determinations (Acros Organics, 2009; Sigma-Aldrich, 2009).**

Liquid	Supplier	Chemical structure	Molecular weight [g mol <sup>-1</sup> ]	Density [g ml <sup>-1</sup> ]	Boiling point [°C]	Melting point [°C]
Deionised water	Millipore	H <sub>2</sub> O	18.02	1.00	0	100
Glycerol	Acros Organics		92.09	1.262	290	18
Formamide	Sigma-Aldrich		45.04	1.132	210	2
Diiodo-methane	Sigma-Aldrich		267.84	3.32	181	5
Poly(ethylene glycol)	Sigma-Aldrich		Characteristics depend on chain length ( <i>n</i> )			
Bromo-naphthalene	Sigma-Aldrich		207.08	1.48	279-281	-2 / -1
Benzyl-alcohol	Sigma-Aldrich		108.14	1.044	205	-16
Chloro-benzene	Sigma-Aldrich		112.56	1.107	132	-46/-45
Hexa-decane	Acros Organics	C <sub>16</sub> H <sub>34</sub>	226.44	0.773	287	18
Decane	Acros Organics	C <sub>10</sub> H <sub>22</sub>	142.29	0.73	174.1	-29.7

Surface energy of solid materials is determined in this research by measuring the contact angle and surface tension of a range of liquids, as described in section 2.3.2. All probe or test liquids used are pure liquids (95-100%), which are commonly mentioned in literature for similar applications. Chemical structures, molecular weight and boiling and melting points are given in Table 3.5. The use of a large range of probe liquids allows the determination of more specific information regarding the surface chemistry or surface composition of the solid surfaces, polycarbonate, stainless steel, PTFE and quartz glass.

### **3.2.2 Thin film coating formulation**

In order to increase the ease of demoulding by reducing the adhesion at the chocolate–mould interface, the surface energy and/or surface chemistry of a polycarbonate mould surface was adjusted using thin film coatings of edible materials. The aim of using edible coatings or films within this research is to change the surface chemistry of the polycarbonate surface and consequently change the interactions taking place at the chocolate–mould interface. By using edible coatings there are two possibilities, the coatings either adhere to the polycarbonate mould surface, or they adhere to the chocolate surface after demoulding.

Edible coatings are generally classified as natural polymers, obtained from animal and vegetable proteins, gums and lipids (Khwaldia et al., 2004). In this research, coatings were prepared using two different types of materials: 1) hydrocolloids (inclusive protein), and 2) lipids or fatty acids. Based on the results obtained for these one component coatings, additional two or three component coatings were prepared by combining a hydrocolloid and a lipid ingredient, and by addition of a plasticizer. The methodology used for the preparation of these thin film coatings is discussed in section 0

#### *3.2.2.1 Hydrocolloids*

The use of hydrocolloid coatings, if necessary in combination with sweeteners or plasticizers, during production of confectionery products is often mentioned in literature. Brake and Fennema (1993) compared various hydrocolloids and their capacities to produce semi-solid edible coatings which should be an effective barrier to lipid migration amongst others. Results obtained indicated that a combination of high methoxyl (HM) pectin, acacia gum, high fructose corn syrup, dextrose, fructose and sucrose was the optimum formulation with respect to lipid barrier and sensory properties, when tested between chocolate and peanut butter. In another experiment, Nelson and Fennema (1991) studied the efficiency of methylcellulose (MC) hydroxypropylmethyl cellulose (HPMC), carboxymethylcellulose (CMC) and carrageenan as barriers against lipid migration. All hydrocolloids tested were effective in retarding migration of moisture and oils. However, when embedded in chocolate products, MC films with a thickness

of 0.0051 mm were readily detected by a sensory panel. Whey protein isolate (WPI) coatings that are plasticized with sucrose have been shown to be highly glossy. Addition of cocoa butter to this mixture further improves consumer acceptance, especially when compared to traditional alcohol based shellac coated chocolates (Lee et al., 2002). Dangaran et al. (2006) further investigated the WPI-sucrose and the effect of crystallization inhibitor inclusion on the coating gloss. They hypothesized that sucrose crystallization is responsible for the loss of gloss of WPI-sucrose coatings upon storage. Their results showed that addition of raffinose as a crystallization inhibitor prevented cracking of coatings and loss of gloss upon storage.

In this research the application of three different hydrocolloid coatings at the chocolate–mould interface were investigated. The hydrocolloids were chosen based on literature observations described previously:

- **High methoxyl pectin**

GENU<sup>®</sup> pectin type 105 G rapid set and GENU<sup>®</sup> pectin type 150 USA-SAG type B rapid set were obtained from CP Kelco (A Huber Company, San Diego, USA). Both pectin types are high ester pectins extracted from citrus peel and standardized by the addition of sucrose. Type 105 G has a degree of esterification of 69.3 %, whereas the degree of esterification of type 150 USA-SAG is 70.2%.

- **Carboxymethylcellulose**

Cekol<sup>®</sup> 30 is a sodium carboxymethylcellulose (NaCMC) or cellulose gum, derived from wood pulp or cotton by introducing carboxymethyl groups on the cellulose backbone. Cekol<sup>®</sup> 30, obtained from CP Kelco BV (Nijmegen, the Netherlands), is refined to a minimum 99.5% purity and has a degree of substitution of 0.72 % and a molecular weight of 120.000 g mol<sup>-1</sup>.

It is known for its good film forming (transparent films) properties.

- **Whey protein isolate**

BiPRO<sup>®</sup> whey protein isolate (WPI) was obtained from Davisco Foods International (Minnesota, USA). It is manufactured from fresh dairy whey that is concentrated and subsequently spray dried, creating a non-denatured, lactose-free protein. The two whey proteins of which WPI is comprised are  $\beta$ -lactoglobulin and  $\alpha$ -lactalbumin.

### 3.2.2.2 Lipids

Where polysaccharide and protein (hydrocolloid) coatings or thin films exhibit good gas barrier and mechanical properties, lipid coatings show the opposite behaviour and exhibit good moisture barrier capacities (Nussinovitch, 2003). Additionally, lipid coatings are often observed to be opaque rather than transparent, relatively inflexible, susceptible to rancidity and may affect sensorical characteristics, displaying a waxy taste. Bilayer, composite or emulsion-based edible films have been developed utilizing the functional characteristics of the different

macromolecules, with the hydrocolloids forming a continuous cohesive network and the lipid fraction providing moisture barrier properties (Quezado Gallo et al., 2000).

Experiments conducted as part of the surface adhesion force determination, see section 4.3.6.1, have shown that a thin lipophilic film or layer is deposited on the mould surface which subsequently reduces the adhesion of chocolate. Based on these observations the use of edible monoglyceride coatings was proposed. The monoglycerides used in this research were chosen based on recommendations from suppliers:

- **Distilled monoglyceride**

Dimodan<sup>®</sup> HP, a distilled monoglyceride prepared from edible, fully hydrogenated palm based oil, is obtained from Danisco A/S (Brabrand, Denmark). It is supplied in the form of beads, with a total monoglyceride content of minimum 90%, with maximum 1% free glycerol and a dropping point of approximately 69 °C. Potential benefits are a reduction of the stickiness of caramels and toffees.

- **Acetic acid ester**

Grindsted<sup>®</sup> Acetem 70-00 P Kosher is an acetic acid ester of monoglycerides made from edible, fully hydrogenated palm based oil, and is obtained from Danisco A/S (Brabrand, Denmark). It is supplied in the form of a plastic wax, with a degree of acetylation of 0.7, a saponification value of approximately 325 and a dropping point of 37 °C. Potential benefits are anti-sticking properties in chewing gum, and the reduction of stickiness of nuts and dried fruits.

- **Cocoa butter**

The cocoa butter used is described in more detail in section 3.2.1.1. It is suggested that the lipophilic film present at the polycarbonate mould surface after demoulding consists of cocoa butter residues, and therefore a cocoa butter coating is used as a type of model system.

- **Lecithin**

Food-grade lecithin was obtained from Degussa / Cargill Incorporated (Minnesota, USA). Its composition is discussed in section 2.1.2.4.1. Lecithin is applied in this coating research because of its surface active properties as a result of which it is capable of lowering the surface tension of a coating solution, subsequently enhancing wettability and adhesion characteristics (Rodriguez et al., 2006).

### 3.2.2.3 *Plasticizers*

Plasticizers such as glycerol, acetylated monoglyceride, polyethylene glycol and sucrose, are additives that are commonly used in coating formulation because of their abilities to reduce the brittleness and enhance flexibility, extensibility and tear resistance of edible coatings. Negative aspect of the addition of plasticizers is a reduction of the structural properties causing increased

permeability to gas and moisture (Greener Donhowe and Fennema, 1994). Plasticizers are believed to decrease intermolecular attractions between polymeric chains, especially adjacent chains, as a result of which flexibility is increased (Rodríguez et al., 2006).

In the present research the inclusion of two plasticizers, sucrose and glycerol (food grade, > 99.5% purity, Acros Organics), was investigated when added to hydrocolloid coatings containing CMC or pectin 105.

### 3.3 METHODS

The methods used in this research are divided into 3 different categories, according to their application. Within these categories, further subdivisions are present:

- **Surface energy determination**

Surface tension of a large range of probe liquids (section 3.2.1) is determined via the Wilhelmy plate, while the contact angle of these probe liquids on different solid substrates (section 3.2.2) is determined via the sessile drop method. Subsequently, solid surface (free) energy can be calculated using a number of different empirical approaches.

- **Chocolate–mould adhesion determination**

The force required to separate a solid mould substrate from a solidified chocolate system (section 3.2.1) is defined as the surface adhesion force, and is determined using the Texture Analyser (TA). An important aspect in relation to the chocolate–mould adhesion is the processing conditions used prior to creating contact between the chocolate and mould surface. A number of additional parameters are measured which quantify the adhesion as well as chocolate quality.

- **Moisture sorption**

Moisture uptake of a polycarbonate surface at predefined conditions is determined using a Cisorp water sorption analyser.

- **Aeration of chocolate**

Aeration of chocolate at controlled air and temperature conditions was conducted at Nestlé PTC (York), using two different techniques: vacuum box and positive batch rig.

- **Coating formulation**

Food grade coatings (section 3.2.2) were prepared using a simple evaporation technique, allowing the formation of thin films on the solid substrates.

- **Surface topology**

Surface topology of solid mould substrates at the micro-scale was visualized using confocal laser scanning microscopy (CLSM).



### 3.3.1 Surface energy determination

The theoretical background to solid surface (free) energy has been discussed in CHAPTER 2, where the Young–Dupré adhesion model (2-33) was used to describe the interactions taking place at the liquid–solid interface. In this equation the only unknowns are the liquid–vapour surface tension,  $\gamma_{lv}$ , and the contact angle,  $\theta$ , two quantities which are relatively easy to determine experimentally in two separate determinations. In this research, surface tension is determined via the Wilhelmy plate method, whereas contact angles are determined via the sessile drop method. Based on the values obtained for these two quantities, the solid surface (free) energy of different solid substrates can be calculated via empirical approaches such as Zisman, Fowkes, Owens and Wendt, van Oss – Chaudhury and Good, Della Volpe and Siboni and the Equation of State approach developed by Kwok and Neumann.

#### 3.3.1.1 Surface tension of liquids

The aim of the surface tension determination is to verify that the probe liquids used have a high purity, consequently showing consistency with surface tension values known from literature. Presence of contaminants within the probe liquids may affect the contact angle determination, and should therefore be avoided.

The surface tension of probe liquids is determined using a Krüss K10 ST digital tensiometer (Krüss), with a platinum Wilhelmy plate. The measurement methodology consists of suspending a thin rectangular plate vertically above liquid L, using a micro-balance. By raising the liquid beaker until the liquid surface touches the hanging plate, the equilibrium within the liquid is disturbed. A thin liquid film is wetting the lower part of the plate upon contact, exerting a small additional force, or additional weight, on the hanging plate (van Oss, 2006), as is shown schematically in Figure 3.3.

The resultant downwards pull is caused by the thin liquid film trying to minimize its surface area, and the force  $F$  applied to resist this surface force exerted by the liquid is measured by the digital tensiometer to which the hanging plate is attached:

$$F = 2\gamma L . \quad [3-1]$$

where  $\gamma$  is the surface tension of the liquid and  $L$  is the plate width. Factor 2 results from the fact that the plate surface is at both faces in contact with the wetting liquid (Kendall, 2001).

Equation [3-1] can be rewritten to include the cosines of the contact angle,  $\theta$ , which the wetting liquid makes with the solid platinum plate. However, as the plate is made of roughened platinum that is optimally wetted, it gives a contact angle of approximately 0 °C. Considering the fact that  $\cos \theta = \cos 0 \approx 1$ , the only parameters that are important for the surface tension are the force acting on the balance,  $F$ , and the wetted length,  $L$ .

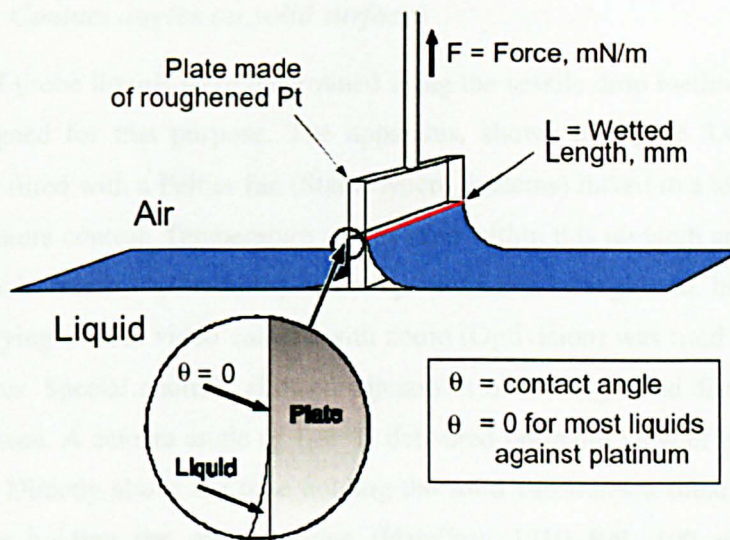


**Figure 3.3 Surface tension determination via the Wilhelmy plate method (KRÜSS GmbH, 2009).**

In order to determine the effect of temperature variations on the surface tension of probe liquids, the thermostat chamber containing the sample vessel is connected to a water bath. Temperature ranges used within this research are 20 – 60 °C similar to the temperature ranges observed during chocolate processing and especially the mould and demoulding stage.

The glass sample vessel is cleaned firstly with a weak detergent solution, followed by acetone and finally rinsed with cold distilled water. A clean paper towel is used to remove chemical residues mechanically. Soft tissues are generally not used, to prevent against small fibres adhering to the glass surface. The Wilhelmy plate is generally cleaned by soaking in a diluted detergent solution, although this step can be missed out for water soluble liquids, followed by extensive rinsing with cold distilled water. In case of organic liquids the soaking step can be replaced by a cleaning treatment using acetone. Before each measurement, the plate is furthermore glowd to red with a Bunsen burner to remove any chemical residues present.

For all measurements an equilibrium step is required after the sample vessel has been placed in the measurement chamber to allow the liquid and the air surrounding the liquid surface to reach equilibrium. Similarly, if elevated temperatures are used an equilibrium step is required to allow the probe liquid to reach the temperature of the sample vessel. The surface tension of each probe liquid is measured 8 times at all temperatures, and the results are averaged to obtain the total surface tension for each individual probe liquid at each temperature.



### 3.3.1.2 Contact angles on solid surfaces

Contact angles of probe liquids were determined using the sessile drop method in an apparatus specifically designed for this purpose. The apparatus, shown in Figure 3.4, consisted of a Perspex chamber fitted with a Peltier fan (Stable Micro Systems) linked to a temperature unit to allow for temperature control. Temperature ranges used within this research are 10 – 40 °C. By using a closed environment, the humidity and temperature can be regulated. Inside the chamber a steel stand carrying a CCD video camera with zoom (Optivision) was used as a base to hold the solid substrates. Special controls allowed adjustment of the angle and distance from which the drop was viewed. A camera angle of 1–2 °C delivered optimum view of the contact line or three phase line. Directly above the base holding the solid substrates a stand was made in the Perspex chamber holding the micro-syringe (Hamilton 1710 RN, 100 µl). This allowed measurement of the dynamic contact angle, by constantly changing the drop volume (and surface boundaries) through successively reducing and enlarging the liquid drop. A light source is placed behind the camera; supplying backlight ensures the creation of a contrast difference between the liquid drop and solid substrate, resulting in a clear drop profile.

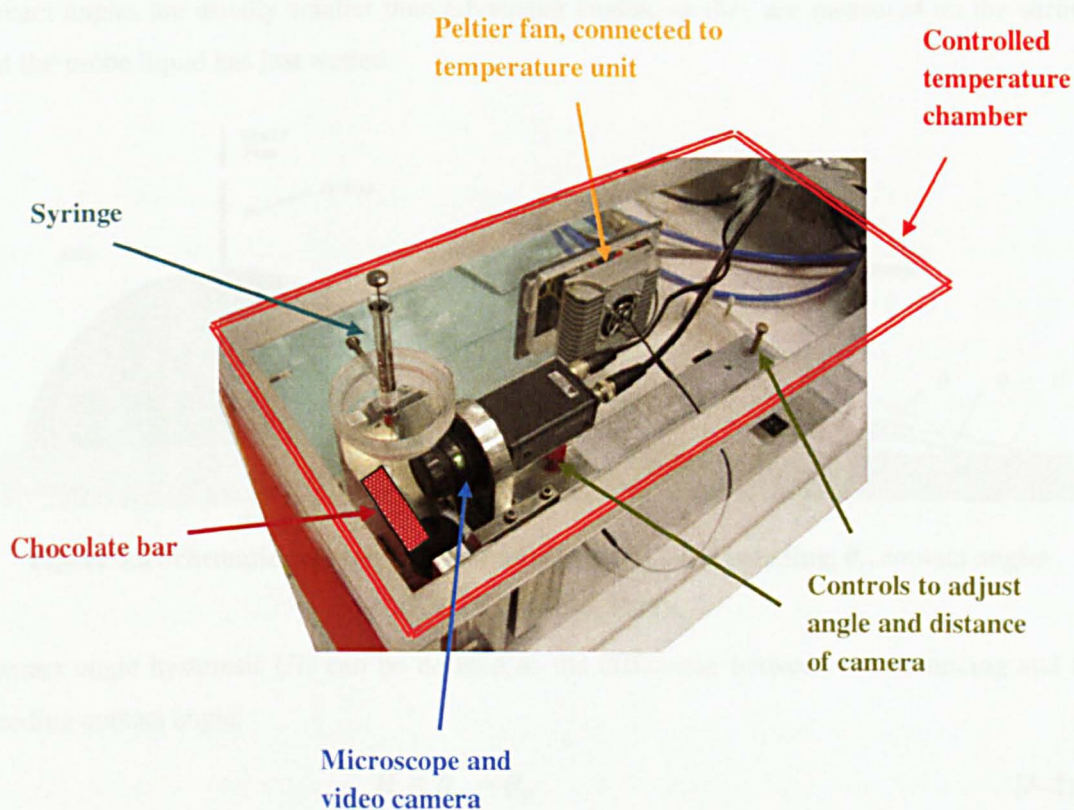


**Figure 3.4** Overview of the contact angle apparatus designed specifically for this research.

Prior to each measurement, the respective solid substrate used is washed to ensure that there are no contamination or chemical residues present from previous measurements. A relatively mild cleaning procedure is used, similar to that used in commercial chocolate manufacturing to clean chocolate moulds. The solid substrate is soaked in a mild detergent solution, rinsed with deionised water (Millipore) and dried using pressurized air, before being placed in desiccators

until use. Similarly, the micro-syringe is cleaned before use. After washing with a diluted detergent solution and several rinses with deionised water, the syringe chamber and needle are extensively washed with the respective probe liquid. An experiment starts with the placement of the respective probe liquid, solid substrate and micro-syringe inside the Perspex measurement chamber at the experimental temperature for 1 hour in order to reach thermal equilibrium and also equilibrium between the vapour and liquid phases. Both solid mould surfaces and chocolate surfaces were used as solid substrates for contact angle measurements. However, due to the physical characteristics of the chocolate system, e.g. low melting point, this substrate was not placed in the measurement chamber for an extensive period of time.

Sessile drops (2–10  $\mu\text{l}$ ) were deposited on the solid substrates using a micro-syringe (Hamilton), and the process was captured by a video camera. Advancing,  $\theta_a$ , and receding,  $\theta_r$ , contact angles were obtained by increasing and decreasing the volume of the drop, respectively, as is shown schematically in Figure 3.5. According to van Oss (2006), the Young–Dupré equation is only valid if the advancing contact angle is used, as this is the angle that a drop makes when it has just ceased advancing, consequently reaching surface areas previously non-wetted. Receding contact angles are usually smaller than advancing angles, as they are measured on the surface that the probe liquid has just wetted.

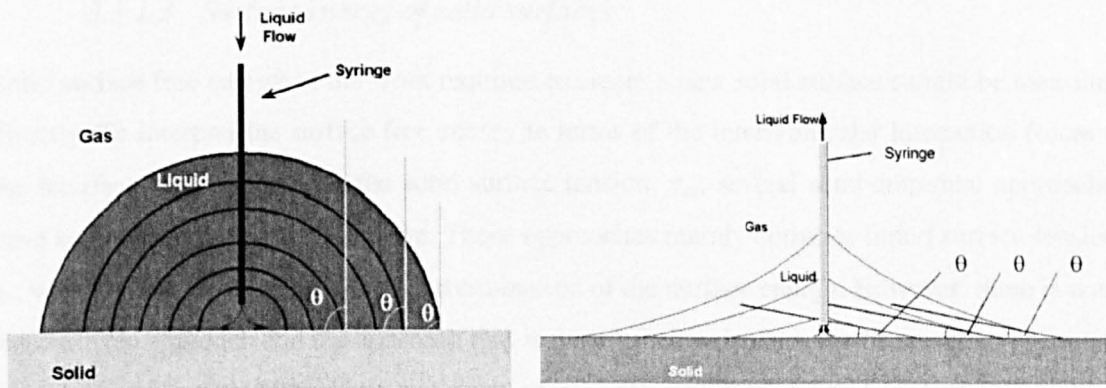


**Figure 3.5** Schematic representation of advancing,  $\theta_a$ , and receding,  $\theta_r$ , contact angles (KRÚSS GmbH, 2009).

Contact angle hysteresis ( $H$ ) can be defined as the difference between the advancing and the receding contact angle:

$$H \equiv \theta_a - \theta_r . \quad [3-2]$$

On average, hysteresis is caused because the system (solid surface) is not ideal, the solid surface does not consist of the required smoothness, rigidity or homogeneity. In the case of polar solids, hysteresis is often caused by reorientation of molecules in the solid surface, with the liquid phase being the driving force. For example, if the liquid phase is water, then the polar parts of the solid material tend to come to the surface. Another possible cause for hysteresis is the transport of molecules from the liquid across the solid surface, due to surface diffusion, evaporation or adsorption onto the solid material (Good, 1992). In general, typical deviations

from ideality can be summarized as: surface roughness, macroscopic homogeneity (chemically and physically), microscopic heterogeneity (surface energy bands), reorientation of molecules, or diffusion, evaporation or adsorption of molecules. Contamination and surface roughness are classified as two of the most important causes for hysteresis. With respect to surface roughness, it is advised to use surfaces with radii of roughness significantly smaller than 1  $\mu\text{m}$  (van Oss, 2006). Kendall (2001) compared adhesive hysteresis for example between a rubber and a glass surface with contact angle hysteresis. According to his observations he concluded that the solid nature of the materials is not responsible for hysteresis, but rather intrinsic properties of the interface.

Contact angles were determined from digital images using the DropSnake program, which is based on a cubic B-spline snake (active contours), similar to the polynomial-fitting approach. A piecewise-polynomial function is used in combination with an image energy function, for the detection of the drop contour profile. An optimization algorithm is then used to determine the contact angle (Stalder et al., 2006). The averages of the left and right contact angle of five different drops placed on two different clean surfaces were used to determine the reported surface energy values.

### 3.3.1.3 *Surface energy of solid surfaces*

Solid surface free energy or the work required to create a new solid surface cannot be measured directly. To interpret the surface free energy in terms of the intermolecular interaction forces at the interface, and to calculate the solid surface tension,  $\gamma_{sv}$ , several semi-empirical approaches have been developed in the literature. These approaches mainly correlate liquid surface tension,  $\gamma_{lv}$ , with the contact angle,  $\theta$ , for the determination of the surface energy. However, there is not a standardized approach and the approach that is most suitable depends on the specific application for which it is used. The oldest and most practicable and easy method is Zisman's 'critical surface tension' theory, which uses a direct estimation of  $\gamma_{sv}$ . Due to the unreliability of this theory, new and different models have been formulated. In general, all approaches fall within one of two classes:

1. Surface Tension Component (STC) theory: based on the solid/vapour and liquid/vapour interfacial tensions and specific intermolecular interactions, called the components of the surface energy:
  - Fowkes, Owens and Wendt, Owens – Wendt and Kaelble, Wu, van Oss – Chaudhury and Good, and more recently Della Volpe and Siboni;
2. Equation of State (EOS) approach: based on an equation of state relation, which in turn is based on thermodynamics:  $\gamma_{sl} = f(\gamma_{lv}, \gamma_{sv})$ 
  - Berthelot, Antonow, Good and Girifalco, and several developments by Kwok and Neumann.



Within this research five of the most widely used approaches for the determination of  $\gamma_{sv}$  have been considered, and are discussed in more detail below.

### 3.3.1.3.1 Zisman critical surface tension approach

Fox and Zisman (1950, 1952a, 1952b) introduced the concept of the critical surface tension,  $\gamma_c$ , as a measure of the ‘wettability’ of solid surfaces. Their approach is based on a plot of the cosine of the contact angle versus the surface tension of the test liquids, a Zisman plot, see Figure 3.6. All data points are approximately on a straight line and a range of “critical” surface tensions can be observed above which no liquid wets the solid surface, and below which all studied liquids spread (Fox and Zisman, 1950). Linear regression of the data determines  $\gamma_{lv}$  at the value of  $\cos \theta = 1$  (i.e.  $\theta = 0$ ), which is defined as the critical surface tension of wetting,  $\gamma_c$ . Liquids with a surface tension below  $\gamma_c$  are expected to spread easily on the respective solid surface.

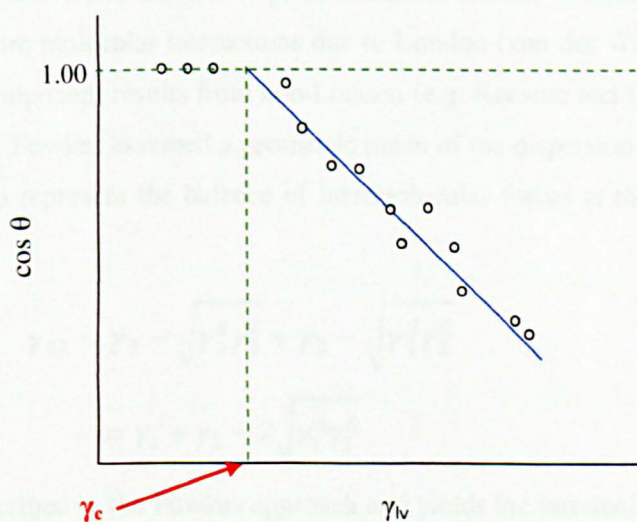


**Figure 3.6 Critical surface tension according to Zisman.**

For a first approximation this is a very easy and useful method. However, the applicability or reliability of this method depends on the number of liquids used and is questioned by several authors. If extrapolation over a significant region is required to determine the intercept with the line  $\cos \theta = 1$ , considerable errors may be introduced (Neumann et al., 1974). Dann (1970) showed that the value obtained for the critical contact angle of a particular solid surface depends on the types of test liquids used. And finally, in Zisman’s theory polar liquids cannot be used for the determination of the solid surface components (Sharma and Rao, 2002). Or, as stated by van Oss (2006), Zisman’s approach is valid only for completely apolar liquids. The measurements done with polar liquids will deviate on the Zisman plot from linearity.

## 3.3.1.3.2 Fowkes surface tension component approach

Fowkes (1964) was the first to postulate the solid surface free energy to be composed of a sum of different surface tension components. These components are the result of the attractive forces existing between the solid surface layer and the liquid phase due to different intermolecular forces at the surface. In Fowkes approach the components are regarded as independent additive terms, and his equation describes the contribution of the different forces to the free energy:

$$\gamma = \gamma^d + \gamma^p + \gamma^h + \gamma^i + \gamma^{ab} , \quad [3-3]$$

where  $\gamma$  is the total surface tension and the superscripts d, p, h, i and ab refer to the dispersive, dipole-dipole, hydrogen bonding, induced dipole and acid–base interactions of the surface tension components, respectively. Equation [3-3] can be rearranged into:

$$\gamma = \gamma^d + \gamma^n , \quad [3-4]$$

where the superscripts d and n refer to the dispersive and non-dispersive (or polar) surface tension component, respectively. Basically, equation [3-4] assumes that the total surface tension is the sum of the dispersive and the non-dispersive surface tension components. The dispersive component results from molecular interactions due to London (van der Waals) forces, whereas the non-dispersive component results from non-London (e.g. Keesom and Debye) forces (Kwok and Neumann, 1999). Fowkes assumed a geometric mean of the dispersion force components of the surface tension to represent the balance of intermolecular forces at the interface (Fowkes, 1964).

$$\begin{aligned} \gamma_{12} &= \gamma_1 - \sqrt{\gamma_1^d \gamma_2^d} + \gamma_2 - \sqrt{\gamma_1^d \gamma_2^d} \\ &= \gamma_1 + \gamma_2 - 2\sqrt{\gamma_1^d \gamma_2^d} . \end{aligned} \quad [3-5]$$

Equation [3-5] is described as the Fowkes approach and yields the interfacial energy, the sum of the tensions in two interfacial layers, 1 and 2. Combining this geometric mean with the Young equation for a solid–liquid interface yields (Kloubek, 1992):

$$\gamma_{lv}(1 + \cos \theta) = 2\sqrt{\gamma_s^d \gamma_l^d} , \quad [3-6]$$

where the superscripts d refers to the dispersive surface tension component, while the subscripts s and l refer to the solid and the liquid, respectively. Consequently, the contact angle of only one liquid is required for the calculation of the dispersion force component of the solid surface energy,  $\gamma_s^d$  (Sharma and Rao, 2002).

As the theoretical viewpoint of the Fowkes approach is not physically real, several adjustments have been proposed. The approach, however, is still often used for the determination of the dispersion component of the total surface energy.



## 3.3.1.3.3 Owens and Wendt geometric mean approach

Owens and Wendt (1969) further extended Fowkes' concept of surface tension components, by dividing the total surface energy into two components, a dispersion force component and a hydrogen bonding or polar component, the latter consists of both hydrogen bonding and dipole–dipole interactions. Approximately at the same time as Owens and Wendt, Kaelble also published an equation dividing the total surface energy in terms of dispersion and polar forces. This approach is therefore often referred to as either Owens–Wendt theory or as Owens–Wendt–Kaelble theory (Kwok and Neumann, 1999). Extending Fowkes equation [3-5] with a hydrogen bonding (h) or polar (p) surface tension component results in:

$$\gamma_{12} = \gamma_1 + \gamma_2 - 2\sqrt{\gamma_1^d \gamma_2^d} - 2\sqrt{\gamma_1^p \gamma_2^p} \quad [3-7]$$

Combining this equation with the Young equation for a solid–liquid interface yields:

$$\gamma_{lv}(1 + \cos \theta) = 2\sqrt{\gamma_s^d \gamma_l^d} + 2\sqrt{\gamma_s^p \gamma_l^p} \quad [3-8]$$

In this approach, the contact angles of at least two liquids with known surface tension components (e.g. water and diiodomethane) are required in order to calculate the surface tension of the solid surface and its components. From a practical point of view the total surface energy and its dispersive and hydrogen or polar components can be determined by plotting

$\frac{\gamma_{lv}(1+\cos\theta)}{2\sqrt{\gamma_l^d}}$  against  $\sqrt{\frac{\gamma_l^p}{\gamma_l^d}}$ . The linear Owens and Wendt relationship thus obtained, as

visualized in Figure 3.7, gives a straight line with slope  $\sqrt{\gamma_s^p}$  and y-intercept  $\sqrt{\gamma_s^d}$ .

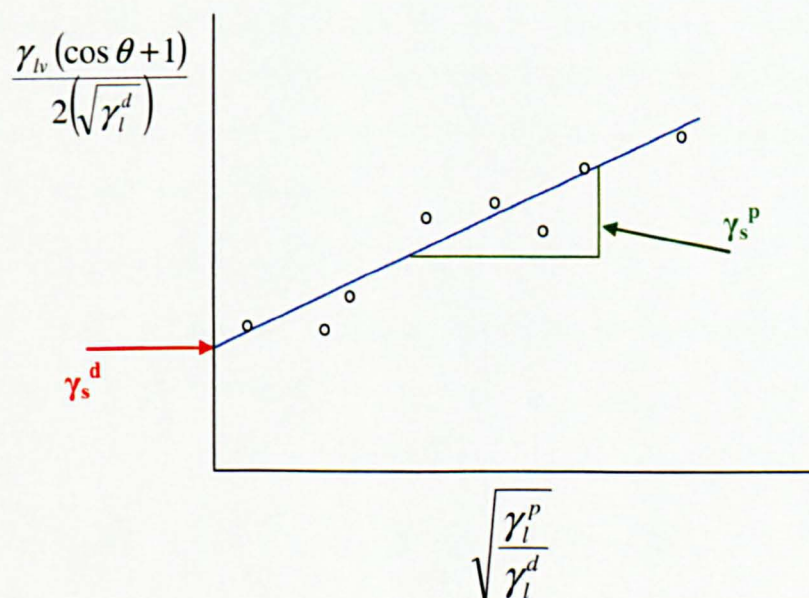


Figure 3.7 Linear Owens and Wendt relationship.

Similar to Kaelble, Wu proposed the division of the total surface energy in a polar and a dispersion component, using a harmonic mean to combine the two components of the surface energy. This approach also requires the contact angles of at least two liquids with known surface tension components. Although deviation has been observed in the results obtained using either a geometric or harmonic mean, the two approaches seem compatible (Sharma and Rao, 2002).

#### 3.3.1.3.4 Van Oss, Chaudhury and Good approach

This is also known as the *Lifshitz–van der Waals / acid–base* approach. The basis of this approach is again the Fowkes methodology, except that the interactions taking place at the interface are separated into long range Lifshitz–van der Waals (LW) interactions and short range hydrogen bonding (SR) interactions (van Oss et al., 1986, 1988a, 1988b; van Oss and Good, 1989). The Lifshitz–van der Waals (LW) interactions include all the electrodynamic contributions: the dispersion (London) force, the orientation (Keesom) force, and the induction (Debye) force:

$$\gamma^{LW} = \gamma^{Keesom} + \gamma^{Debye} + \gamma^{London} \quad [3-9]$$

The Lifshitz–van der Waals interactions between a solid and a liquid can be calculated using the Good–Girifalco–Fowkes combining rule (van Oss et al., 1988b):

$$\gamma_{sl}^{LW} = \gamma_s^{LW} + \gamma_l^{LW} - 2\sqrt{\gamma_s^{LW}\gamma_l^{LW}}. \quad [3-10]$$

The short range polar or hydrogen bonding (SR) interactions can be classified as Lewis acid–base interactions, including the electron acceptor,  $\gamma^+$ , and the electron donor,  $\gamma^-$ , interactions. Problem with defining these acid–base interactions is their asymmetry, and the fact that the electron acceptors at the solid surface will interact with the electron donors at the liquid surface. Anyway, according to van Oss et al. (1988b) the Lewis acid–base interactions between a solid and a liquid can be expressed as:

$$\gamma_{sl}^{AB} = 2\left(\sqrt{\gamma_s^+\gamma_s^-} + \sqrt{\gamma_l^+\gamma_l^-} - \sqrt{\gamma_s^+\gamma_l^-} - \sqrt{\gamma_s^-\gamma_l^+}\right). \quad [3-11]$$

The total free energy and the total interfacial tension of the interfacial interactions of a solid–liquid system can now be defined as:

$$\gamma_{sl}^{TOT} = \gamma_{sl}^{LW} + \gamma_{sl}^{AB} \quad [3-12]$$

$$\gamma_{sl}^{TOT} = \left(\sqrt{\gamma_s^{LW}} - \sqrt{\gamma_l^{LW}}\right)^2 + 2\left(\sqrt{\gamma_s^+} - \sqrt{\gamma_l^+}\right)\left(\sqrt{\gamma_s^-} - \sqrt{\gamma_l^-}\right). \quad [3-13]$$

Combining this equation with the Young equation for a solid–liquid interface yields:

$$\gamma_{lv}(1 + \cos \theta) = 2 \left( \sqrt{\gamma_s^{LW} \gamma_l^{LW}} + \sqrt{\gamma_s^+ \gamma_l^-} + \sqrt{\gamma_s^- \gamma_l^+} \right). \quad [3-14]$$

Due to the presence of three unknown parameters in equation [3-14], the contact angles of at least three liquids (two polar and one apolar) with known surface tension components are required to calculate the surface tension of the solid material and its components (Kwok and Neumann, 1999; Sharma and Rao, 2002). In this research, equation [3-14] is solved using SurfTen4.3, a software program developed in MathPad by Della Volpe and Siboni for the calculation of acid–base solid surface free energy components (Della Volpe and Siboni, 2004).

### 3.3.1.3.5 Della Volpe and Siboni modified acid–base approach

Della Volpe et al. (2004) and Siboni et al. (2004) compared the surface tension component (STC) theory developed by Fowkes and van Oss, with the equation of state (EQS) approach developed by Neumann and co-workers. Even though the theoretical background for these two semi empirical models is very different, they proved that the practical results obtained are fairly similar. Furthermore, a new model was developed, using the van Oss theory as a basis. Instead of the van Oss scale, giving values of acid–base components of liquids proposed by van Oss, Chaudury and Good, a new scale was developed, called the Della Volpe and Siboni scale. The authors made this change, due to the unreliability of the methods used by van Oss, Chaudury and Good. The Della Volpe and Siboni scale calculates the surface tension (acid–base) components using the best-fit to an over determined nonlinear set of equations. Basically, the Della Volpe and Siboni approach calculates the surface energy of a solid surface based on equation [3-14], using the alternative Della Volpe and Siboni scale rather than the original van Oss, Chaudhury and Good scale. A so called Singular Value Decomposition (SVD) procedure forms the basis of the software program (SurfTen4.3). Using three different probe liquids, the van Oss, Chaudhury, Good or acid–base approach delivers a linear set of three equations, with the three unknowns relative to the solid. These equations can be written in the form of a matrix ( $Ax=b$ ), which can be solved using a linear method calculation (Least Squares procedure) for the determined and overdetermined cases (Della Volpe et al., 2004).



## 3.3.1.3.6 Equation of state (EQS) approach

An equation of state is a thermodynamic relationship, which on its own cannot be used for the determination of the solid surface tension:

$$\gamma_{sl} = f(\gamma_{lv}, \gamma_{sv}) . \quad [3-15]$$

Berthelot's combining rule, which is based on molecular interactions between like pairs, and is related to the London theory of dispersion forces, is often used as the starting point for the formulation of an Equation of State:

$$C_6^{ij} = \sqrt{C_6^{ii} C_6^{jj}} , \quad [3-16]$$

where  $C_6^{ij}$  refers to the dispersion coefficient, and  $C_6^{ii}$  and  $C_6^{jj}$  to the pair of molecules of species  $i$  and  $j$ , respectively. Various researchers adopted Berthelot's combining rule as the basis for their work, e.g. the methods of Good and Girifalco, Li and Neumann, Kwok and Neumann (Neumann et al., 1974; Li and Neumann, 1990, 1992a, 1992b). They further used the thermodynamical Gibbs-Duhem relations for the three different interfaces, solid-liquid, liquid-vapour and solid-vapour. From these relations it was observed that the different surface or interfacial tensions each are functions of the temperature,  $T$ , and the chemical potential of the liquid components,  $\mu_2$ .

Kwok and Neumann developed the third formulation or proposal of an equation of state for the solid surface energy, which is again based on a modified Berthelot's combining rule.

$$\varepsilon_{ij} = \left(1 - \kappa_1 (\varepsilon_{ii} - \varepsilon_{jj})^2\right) \sqrt{\varepsilon_{ii} \varepsilon_{jj}} , \quad [3-17]$$

where  $\kappa_1$  is an empirical constant. The term  $(1 - \kappa_1 (\varepsilon_{ii} - \varepsilon_{jj})^2)$  is the modifying factor, which is a decreasing function of the different  $(\varepsilon_{ii} - \varepsilon_{jj})$  and equals unity when  $(\varepsilon_{ii} = \varepsilon_{jj})$ . Kwok and Neumann (1999, 2000a, 2000b) further modified the equation of state specifically for applications to solid-liquid free energy determination.

$$\gamma_{sl} = \gamma_{lv} + \gamma_{sv} - 2\sqrt{\gamma_{lv}\gamma_{sv}(1 - \beta_1(\gamma_{lv} - \gamma_{sv})^2)} . \quad [3-18]$$

They used an empirical constant,  $\beta$ , which was obtained by fitting their equation of state to a set of contact angle data from polymeric solids. Combining this modified equation of state with Young's equation leads to the 3<sup>rd</sup> formulation of the equation of state:

$$\gamma_{lv}(1 + \cos \theta) = 2\sqrt{\gamma_{sv}\gamma_{lv}(1 - \beta_1(\gamma_{sv}\gamma_{lv})^2)} . \quad [3-19]$$

where  $\beta_1 = 0.0001057 \text{ (m / mN)}^2$ . The advantage of this method is that only one liquid is required in order to calculate the surface free energy. However, this approach determines only the total surface free energy with no consideration of the components.

The thermodynamic foundations of several of the previously discussed semi empirical approaches are questioned. Based on these objections, different researchers favour either the equation of state approach or the surface tension components approach. Nevertheless, there is not one approach that is generally accepted. The most used and probably most accessible approach is Zisman's theory, whereas the Lifshitz–van der Waals / acid–base approach and the third formulation of the Equation of State are probably good alternatives for estimating the solid surface tension. In this research, the estimations of the solid surface energy obtained via the different approaches will be compared to determine which approach is most appropriate for the determination of surface energy of solid mould materials in relation to the adhesion of chocolate.

### *3.3.1.4 Work of Adhesion*

Similar to the definition by Kilcast and Roberts (1998), the thermodynamic work of adhesion emphasizes the interactions between two materials or surfaces. The Young–Dupré adhesion model, see equation [2–33], can be used to determine the work of adhesion,  $W_a$ . In this equation there are only two unknowns, the liquid–vapour surface tension,  $\gamma_{lv}$ , and the contact angle,  $\theta$ , two quantities which are relatively easy to determine experimentally. With respect to the present research, the contact angle,  $\theta$ , refers to the angle that chocolate makes with the solid surface, the mould, and the liquid–vapour surface tension,  $\gamma_{lv}$ , refers to the chocolate–vapour surface tension.

Due to the viscoelastic nature and the relatively high melting point of chocolate, it is not practicable to measure the contact angle of chocolate on different mould surfaces under ambient conditions. Therefore, in order to obtain some indication of the interactions involved and the degree of wetting, cocoa butter was used as a model replacement system to represent chocolate in the application of the Young–Dupré adhesion model. Using the Wilhelmy plate method the surface tension of liquid cocoa butter (~ 30 °C) was determined, whereas the sessile drop method was used to assess the contact angle of cocoa butter on different mould surfaces.

### *3.3.1.5 Wetting Envelope*

The wetting envelope is a graphical method that is used to give a representative overview of the wettability of solids, based on the polar and dispersive solid surface free energy components. Based on the wetting envelope diagram a prediction can be made as to whether a particular liquid, with known surface tension components, will wet a specific solid surface completely. Referring back to the relation between work of adhesion and cohesion, as described in section 2.2.2, complete wetting of a solid surface will occur when the work of adhesion between the solid surface and a liquid is greater than the work of cohesion within the liquid. As the

difference between the work of adhesion and the work of cohesion is defined as the spreading coefficient,  $S$ , a solid surface will be completely wet if  $S > 0$ . From the equation of Dupré [2-32] it can be observed that  $S = 0$  if  $\theta = 0$ .

A wetting curve is obtained by reversing the empirical surface energy approaches (see section 3.3.1.3), which have previously been used to calculate the dispersive and polar components of the solid surface energy. Assuming that the cosine of the contact angle of a liquid drop on the solid that is being examined is 1, the reversed empirical approaches can be used to calculate the polar and dispersive fractions of the liquid. The wetting diagram is then obtained by plotting the polar component against the dispersive component of a liquid that satisfies the requirement  $\cos \theta = 1$ , as is shown in Figure 3.8. A solid surface will be wet by a liquid whose polar and dispersive components lie within the area enclosed by the wetting envelope.

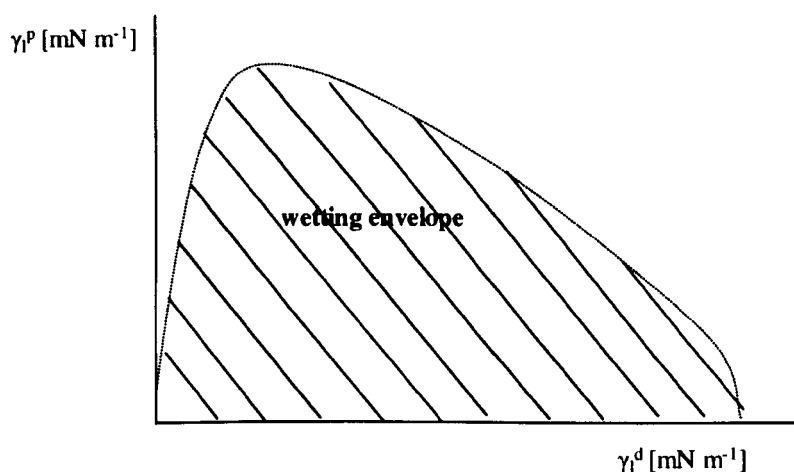


Figure 3.8 Wetting envelope diagram.

### 3.3.2 Chocolate–mould adhesion determination

The theoretical background and mechanisms of adhesion have been discussed in CHAPTER 2. In this research, chocolate–mould adhesion is determined via an experimental approach based on the measurement of the force required to pull a mould surface off a solidified chocolate surface. This approach simulates the chocolate demoulding process, and analyses the balance between the cohesive forces of the chocolate system and the adhesive forces between chocolate and mould material (Bhandari and Howes, 2005). The results obtained via this experimental or practical approach will be compared to the results obtained for the thermodynamic work of adhesion of mould materials, based on the interactions between probe liquids and solid mould surfaces.

Various mechanisms and instrumental measurements of adhesion of food materials to contact surfaces are discussed by Adhikari et al. (2001) and Hosoney and Smewing (1999). There is no standardized technique that can be used for all food systems, and the technique most appropriate for a certain food system depends on food composition, processing and/or measurement conditions. Michalski et al. (1998, 1999) discuss the adhesion of food emulsions and edible oils to various contact surfaces, and relate the mass of food residues adhering to these surfaces after contact to the solid surface energy of the respective contact surfaces. Food emulsions and/or edible oils are placed on the top of a tilted solid surface and allowed to flow down. The weight of the food sample or residues adhering to the solid surface after flow has stopped is measured and is used as an indication of the global adhesion amount resulting from adhesion and cohesion strengths. A different technique is applied when determining the relation between biofouling and solid surface energy. Zhao et al. (2005) counted the number of bacteria adhering to a solid surface after treatment and forming visible colonies. At the same time, for the measurement of crystalline fouling deposits, they weighed the amount of  $\text{CaSO}_4$  deposit formed on a heated solid surface. Rosmaninho and Melo (2006) used a similar technique, whereby they placed a simulated milk ultrafiltrate solution in a thermostatted vessel of a rotating disk apparatus. Upon heating calcium phosphate precipitate in the bulk and adhered to the heated surfaces. After weighing the amount of precipitate that adhered, they repeated the experiment replacing the milk solution with distilled water to simulate a cleaning process, giving them the total amount of deposit detached from the surface. Oláh and Vancso (2005) discuss a number of destructive, e.g. tensile, peel and shear experiments, and non-destructive, e.g. atomic force microscopy (AFM) and surface forces apparatus (SFA), techniques. The SFA is one of the first instruments which successfully applied a direct measurement technique to determine the forces acting on a surface. Main principle of this technique is the measurement of contact forces, separation and contact areas between two surfaces, and is based on the Johnson-Kendall-Roberts (JKR) theory of contact mechanics.

In the case of confectionery or high-sugar products, Kilcast and Roberts (1998) recommend the use of tests based on probe separation or on flat plate separation. A probe separation test simulates the oral or tactile processes taking place when a confectionery product is consumed, while a flat plate separation test rather simulates the adhesion of confectionery products to packaging materials or equipment surfaces used during manufacturing. In this research, a flat plate separation type test was used to determine the experimental adhesion force. Due to the physical characteristics of chocolate, the use of other instrumental measurements to determine the adhesion between the chocolate and the mould surface was limited. Main complication was the fact that contact between mould surface and chocolate needed to be created at a temperature where the chocolate was liquid, whereas the adhesion needed to be measured at a temperature where the chocolate was solidified.

### 3.3.2.1 Probe geometry development

Three different probe geometries were developed, based on the adhesive forces involved in the commercial chocolate demoulding process, as discussed in section 2.1.4.2.3. The three probe geometries, called slide off, pull off and combined, respectively, and their correlation with the chocolate demoulding process are shown in Figure 3.9. A pull off force is obtained by using a flat plate placed directly on top of the chocolate surface, creating a force which is working perpendicular to the chocolate surface. A slide off force, on the other hand, is obtained by using a cylindrical probe placed inside the chocolate sample, consequently creating a force that takes friction into account. Compared to the pull off force which measures the surface adhesion, the slide off force rather measures the bulk adhesion. A combined force, finally, is obtained by using a cone type probe which represents a combination of the pull off and the slide off force.

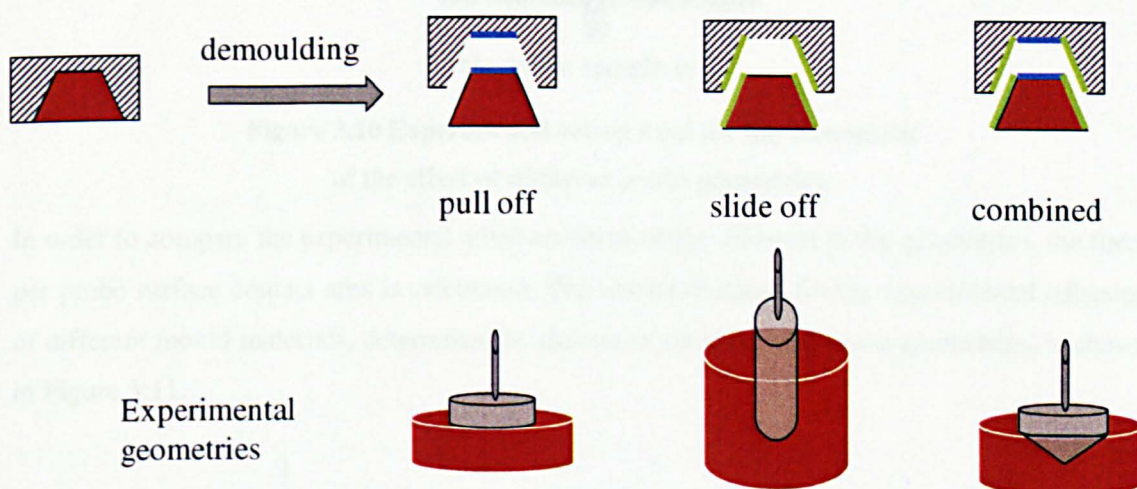


**Figure 3.9** Probe geometries developed specifically for the experimental adhesion force determination, based on the forces involved in the commercial chocolate demoulding process.

A preliminary study was conducted to assess the applicability of the previously defined probe geometries to determine the experimental adhesion force. Central within the experimental set-up for this preliminary study is the TA-XTplus Texture Analyser (Stable Micro Systems), which is used to measure the force required to separate the experimental probe from the chocolate system. Figure 3.10 shows the central set-up used during this preliminary study.

Contact between a liquid chocolate system and the probe is made at room temperature, and the whole set-up is left to solidify for 1 hour. A sample cell holder keeps the chocolate sample cell in place. After the chocolate has solidified, the probe is pulled upwards at a constant speed and the force required to separate the probe from the chocolate surface is determined from the peak force obtained during the separation process. The set-up described here is only used for the preliminary study investigating the use of different probe geometries, whilst the final probe geometry and set-up used to determine the surface adhesion force are described in more detail in sections 3.3.2.2 and 3.3.2.4.



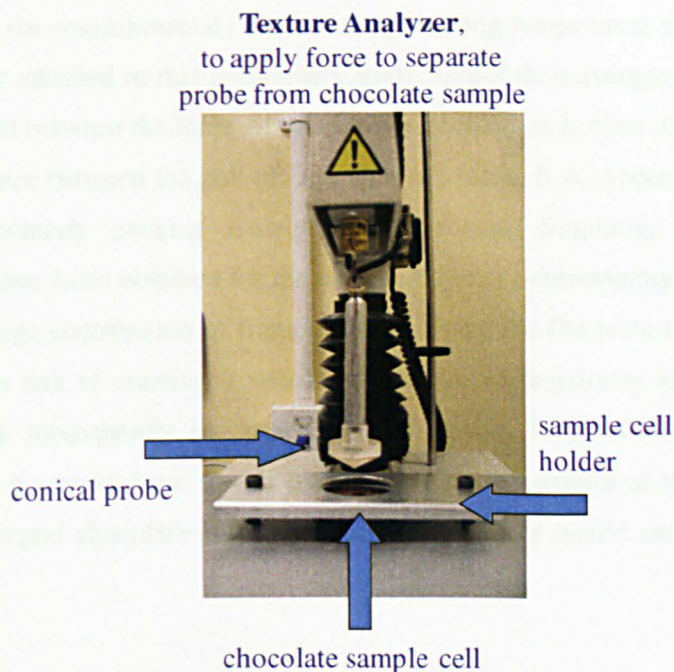


**Figure 3.10** Experimental set-up used for the assessment of the effect of different probe geometries.

In order to compare the experimental adhesion force of the different probe geometries, the force per probe surface contact area is calculated. The results obtained for the experimental adhesion of different mould materials, determined by the use of three defined probe geometries, is shown in Figure 3.11.

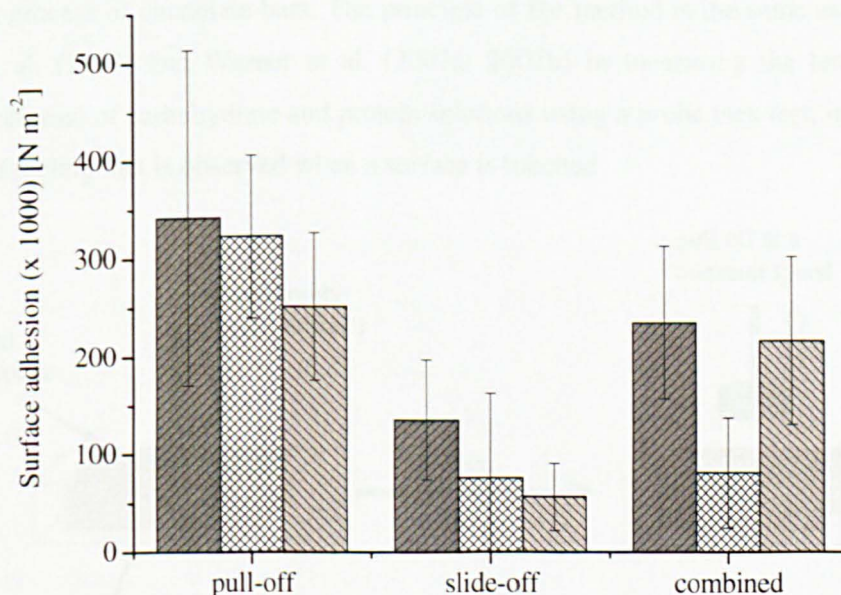


**Figure 3.11** Experimental surface adhesion as affected by probe geometry.

Three different probe materials are evaluated: polycarbonate (▨), stainless steel (▩) and PTFE (▧).

Error bar is representative of the standard deviation,  $n = 6$ .



Due to the fact that the environmental conditions, e.g. cooling temperature and relative humidity of the air, are not controlled in this preliminary study, larger than average errors are obtained. But the overall trend between the three different probe geometries is clear. On average there is a factor three difference between the pull off and slide off force. It is expected that this is due to the cylindrical geometry evoking mainly friction forces. Similarly, the relatively low experimental adhesion force obtained for the conical geometry determining the combined force is a result of the large contribution of friction forces. Using the flat plate to determine pull off forces, there was a risk of creating a vacuum which would negatively affect the chocolate–mould contact and subsequently the experimental adhesion force. The experiments in this preliminary study, however, have shown that there is not a vacuum at the chocolate–mould interface, and the liquid chocolate is fully wetting the probe or mould surface, creating direct contact.

### 3.3.2.2 Experimental adhesion force

Experimental determination of chocolate adhesion to the mould surface was performed on the TA-XTplus Texture Analyser (Stable Micro Systems), and was based on a flat plate separation technique, using a fixture and set-up specifically developed for this work. The surface adhesion force (or stickiness) was measured by pulling the flat probe off a solid chocolate sample, as shown schematically in Figure 3.12, imitating the forces involved in the commercial demoulding process of chocolate bars. The principle of the method is the same as that used by Adhikari et al. (2007) and Werner et al. (2007a; 2007b) in measuring the tensile strength (surface stickiness) of carbohydrate and protein solutions using a probe tack test, mimicking the stickiness or feeling that is observed when a surface is touched.

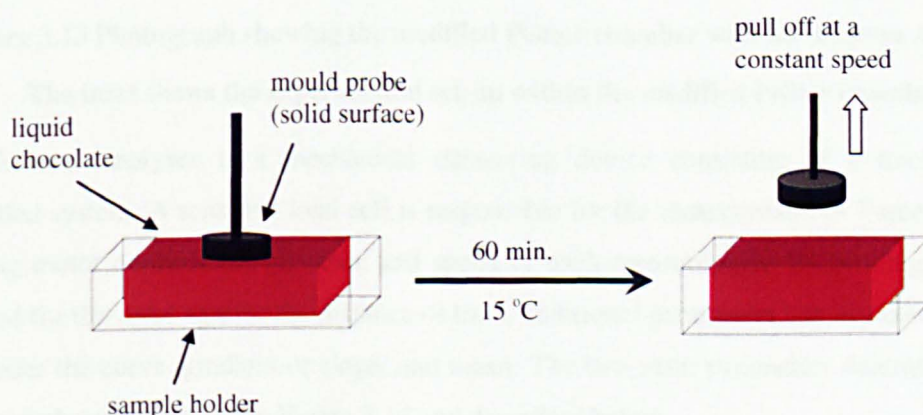


**Figure 3.12 Schematic representation of the procedure and conditions of the surface adhesion measurements.**

All adhesion tests were carried out in a modified Peltier chamber (Stable Micro Systems), see Figure 3.13, under a controlled environment of temperature and relative humidity, which will be discussed in more detail in section 3.3.2.4. A flat probe was brought into contact with the liquid



chocolate sample. The contact or chocolate–mould interface is created at a temperature of around 30 °C, depending on the type of chocolate used. Prior to contact, both chocolate and mould probe were thermally equilibrated in the controlled environment for 30 minutes. Once the interface had been created, the temperature was adjusted to 15 °C and the sample was left without disturbance for 60 minutes, ensuring complete solidification. The flat probe, attached to the Texture Analyser, was then pulled off the chocolate sample using the tension test mode, at a constant speed of 0.001 m sec<sup>-1</sup> over a distance of 5 mm. The chocolate container was held firmly in its original position with the help of a titanium covering plate screwed to the base of the Texture Analyser. In the centre of the covering plate is an opening to allow free movement of the probe. After each surface adhesion determination additional measurements are taken to assess the hardness of the chocolate samples, the gloss of both chocolate and mould surfaces, the surface chemistry of the mould surface and the residue weight. These parameters are discussed in more detail in section 3.3.2.5.

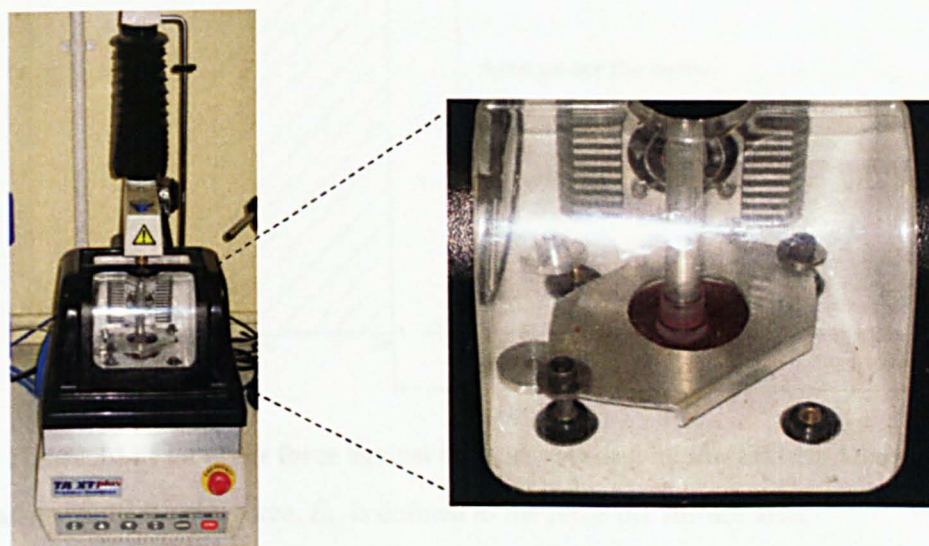


**Figure 3.13** Photograph showing the modified Peltier chamber with the Texture Analyser.

**The inset shows the experimental set-up within the modified Peltier chamber.**

The Texture Analyser is a mechanical measuring device consisting of a microprocessor controlled system. A sensitive load cell is responsible for the measurement of Force, whereas a stepping motor controls the Distance and speed of each measurement. By plotting the results obtained for the force against the distance or time, additional parameters can be determined, e.g. area under the curve, gradient or slope, and mean. The two main parameters determined within this research are visualized in Figure 3.14 and described below:

- *Maximum positive peak*

In a force-time or force-distance plot, the y-axis is searched until the largest positive value is found. This value is regarded as the maximum peak force.



- *Area under the curve*

The sum of all the y axis data values between  $t_0$  (start of experiment) and  $t_1$  (Force = y = 0) are divided by the number of points, multiplied by the sum of the x axis value differences. This value can also be regarded as the work of adhesion.

As can be observed from Figure 3.14, the force does not start at zero. At the time of the chocolate–mould interface creation, the liquid chocolate exerts a suction force on the solid mould surface, slightly pulling the probe surface into the chocolate system subsequently applying pressure on the load cell of the Texture Analyser. The slight negative force obtained after separation, is expected to be due to the contraction of the chocolate system away from the probe surface, consequently resulting in a negative force.

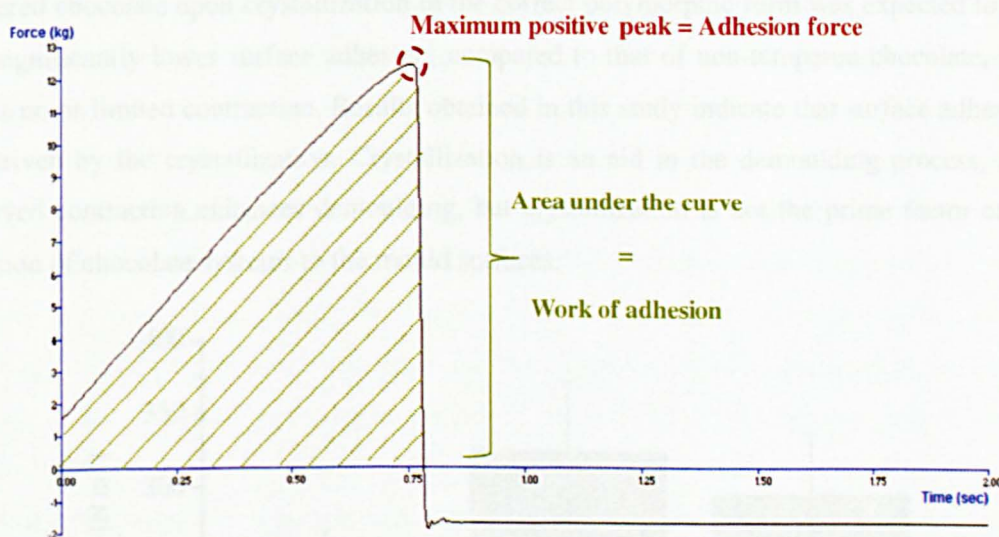


**Figure 3.14** Plot of the force against time, as obtained by the Texture Analyser.

The experimental adhesion force,  $E_a$ , is defined as the force per surface area,

$$E_a = \frac{\text{adhesion force}}{\text{surface area}}, \quad [3-20]$$

where the adhesion force is the peak separation force or maximum positive peak measured by the probe pulling test and the surface area is the contacting area between the probe and the chocolate. The measurement of the adhesion force of two different polycarbonate mould probes was repeated four times. As the results obtained for these measurements showed low standard deviations (< 10%), the procedure was accepted as generally valid. Subsequent measurements were repeated four times for each surface.

### 3.3.2.3 Chocolate crystallization

A small investigation was conducted to assess the effect of chocolate crystallization. Three chocolate samples, one tempered, one non-tempered and one bloomed were compared to determine if the presence of different cocoa butter polymorphs and subsequently crystal networks impacts on the surface adhesion force. The results presented in Figure 3.15 do not show significant differences in surface adhesion for the chocolate systems tested. Non-tempered and bloom give very similar surface adhesion values, which was expected due to the crystallization state of these samples. Bloom is known to arise on surfaces of over- and/or under-tempered chocolate and of course non-tempered chocolate. More surprising is the limited difference between the tempered and non-tempered chocolate systems. The contraction of tempered chocolate upon crystallization in the correct polymorphic form was expected to result in a significantly lower surface adhesion, compared to that of non-tempered chocolate, which shows no or limited contraction. Results obtained in this study indicate that surface adhesion is not driven by the crystallization. Crystallization is an aid in the demoulding process, as the observed contraction enhances demoulding, but crystallization is not the prime factor causing adhesion of chocolate systems to the mould surfaces.

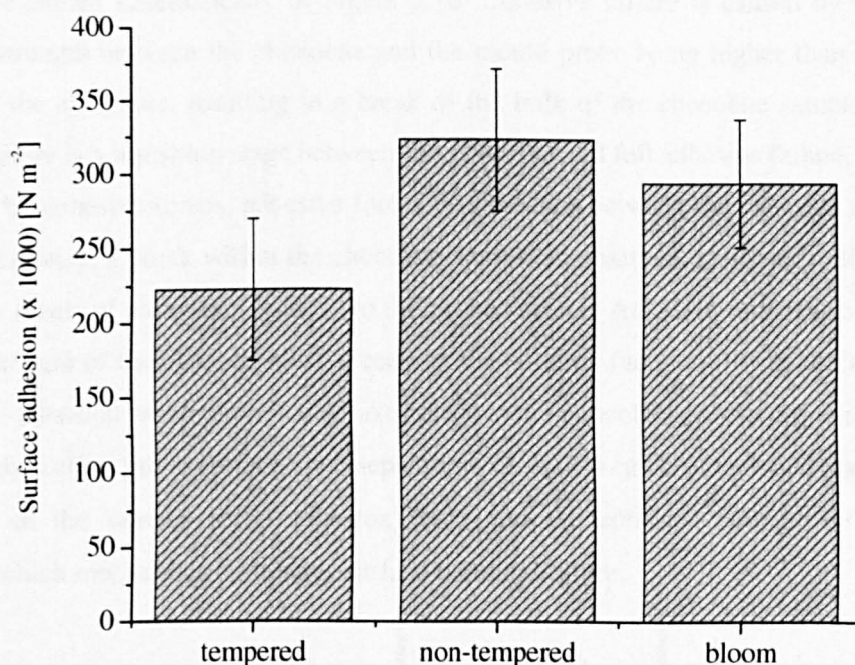


**Figure 3.15** Surface adhesion as affected by the level of chocolate crystallization.

**Error bar is representative of the standard deviation, n = 5.**

Although the advice is to use tempered chocolate, the results obtained by using non-tempered or bloomed chocolate are not significantly different. In this research tempered chocolate is used for all surface adhesion determinations, wherever possible. Correct crystallization, however, is not deemed essential and minor temperature variations in the chocolate system during the preparation stage of the chocolate-mould adhesion determination are therefore neglected.



### 3.3.2.4 Cohesive–adhesive failure

The set-up used in this research to assess chocolate adhesion basically consists of a chocolate sample placed in between two surfaces, the glass sample cell and the (mould) probe surface. Stickiness is thereby a result of the force required to separate the probe surface from the chocolate system, and is assumed to be dependent on the work required for this separation (Dunnwind et al., 2004). Upon separation of the probe surface, the interactions between the chocolate and the respective probe surface will determine whether the chocolate will adhere to the probe or to the glass sample surface. Kilcast and Roberts (1998) defined two different failure mechanisms, adhesive and cohesive failure respectively. Adhesive failure is obtained when the cohesive strength of the food sample is higher than the adhesive strength of the packaging material for example, resulting in a clean failure of the bond between two materials. Cohesive failure is the opposite; the cohesive strength of the food sample is lower than the adhesive strength of the packaging material, resulting in the adhesion of food residues to the packaging material (Hoseney and Smewing, 1999). Werner et al. (2007a) and Adhikari et al. (2003) explained the failure of surface bonding via one of three different mechanisms, adding a cohesive-adhesive failure component. The three different failure mechanisms defined for this research are shown schematically in Figure 3.16. Cohesive failure is caused by the adhesive (bonding) strength between the chocolate and the mould probe being higher than the cohesive strength of the chocolate, resulting in a break of the bulk of the chocolate sample. Cohesive–adhesive failure is a transition stage between full cohesive and full adhesive failure, and is either dominated by cohesive forces, adhesive forces or a balance between the cohesive and adhesive forces. Either way, a break within the chocolate sample is observed, resulting in the adherence of different levels of chocolate residues to the probe surface. Adhesive failure is caused by the cohesive strength of the chocolate just exceeding the bonding (adhesive) strength, resulting in a state of non-adhesion where no bonding takes place at the chocolate–mould probe interface, and consequently a clean probe surface upon separation. Overall it can be concluded that the relative magnitude of the sample–probe adhesion force and the cohesion strength of the sample determine which mechanism dominates surface bonding failure.

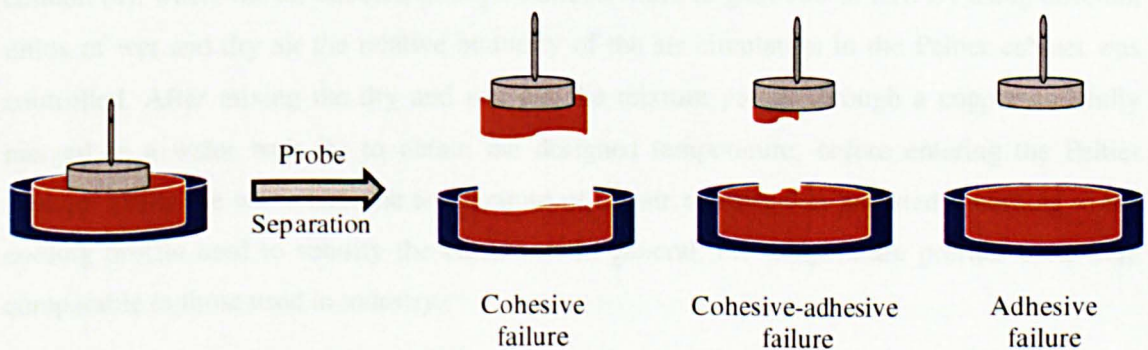


**Figure 3.16 Schematic representation of the three different failure mechanisms specified in this research, i.e. cohesive, cohesive–adhesive and adhesive failure.**

In the case of solid and semi-solid materials, e.g. gels, chewing gums, dough, both cohesive and adhesive failure are observed as a result of the balance between the interfacial bonding and the internal mechanical strength. In viscous or viscoelastic fluid foods, on the other hand, cohesive failure is observed to be the dominant mechanism (Chen et al., 2008).

Within this research the failure mechanism is determined by visual observation of both the chocolate and mould probe surfaces after the surface adhesion determination, to determine macroscopic failure. Additionally, the weight of the probe after each separation is measured, to assess if there is any microscopic failure and to compare the degree of failure obtained.

### *3.3.2.5 Chocolate processing conditions*

In order to study the effect of different processing conditions on the surface adhesion force the experimental set-up outlined in Figure 3.17 was developed. Not only did this set-up enable the controlled variation of a number of processing conditions, such as cooling temperature, probe or mould surface temperature, contact time and relative humidity, it also allowed the crystallization process of the cocoa butter to be more controlled.

The central point within the developed application is the sealed Peltier cabinet (9) (dimensions: 145 mm (W) × 130 mm (D) × 105 mm (H)), shown in Figure 3.13, which is temperature controlled to enable the adjustment of the experimental cabinet temperature between 0 and 50 °C. A ventilator (8) situated at the back of the Peltier cabinet is connected to a Peltier cooling / heating unit (7), and in combination with the relative small size of the chamber the temperature can be adjusted quickly from 32-33°C, at which temperature the chocolate–mould interface is created, to 15-20°C, the cooling temperature. Unfortunately it is not possible to adjust the cooling rate.

The relative humidity of the air in the Peltier cabinet is controlled via a separate configuration, also shown in Figure 3.17, whereby the supplied air (1) is pressurized (2) to decrease the pressure to approximately 2 Bar, before passing through a dry (~ 0 %RH) (3 and 5) and/or wet column (4), where the air bubbled through distilled water to gain 100 % RH. By using different ratios of wet and dry air the relative humidity of the air circulation in the Peltier cabinet was controlled. After mixing the dry and wet air, the mixture passes through a copper coil fully merged in a water bath (6) to obtain the designed temperature, before entering the Peltier cabinet. Using the water bath the temperature of the air mixture was adjusted according to the cooling profile used to solidify the chocolate. In general, the temperature profiles used were comparable to those used in industry.



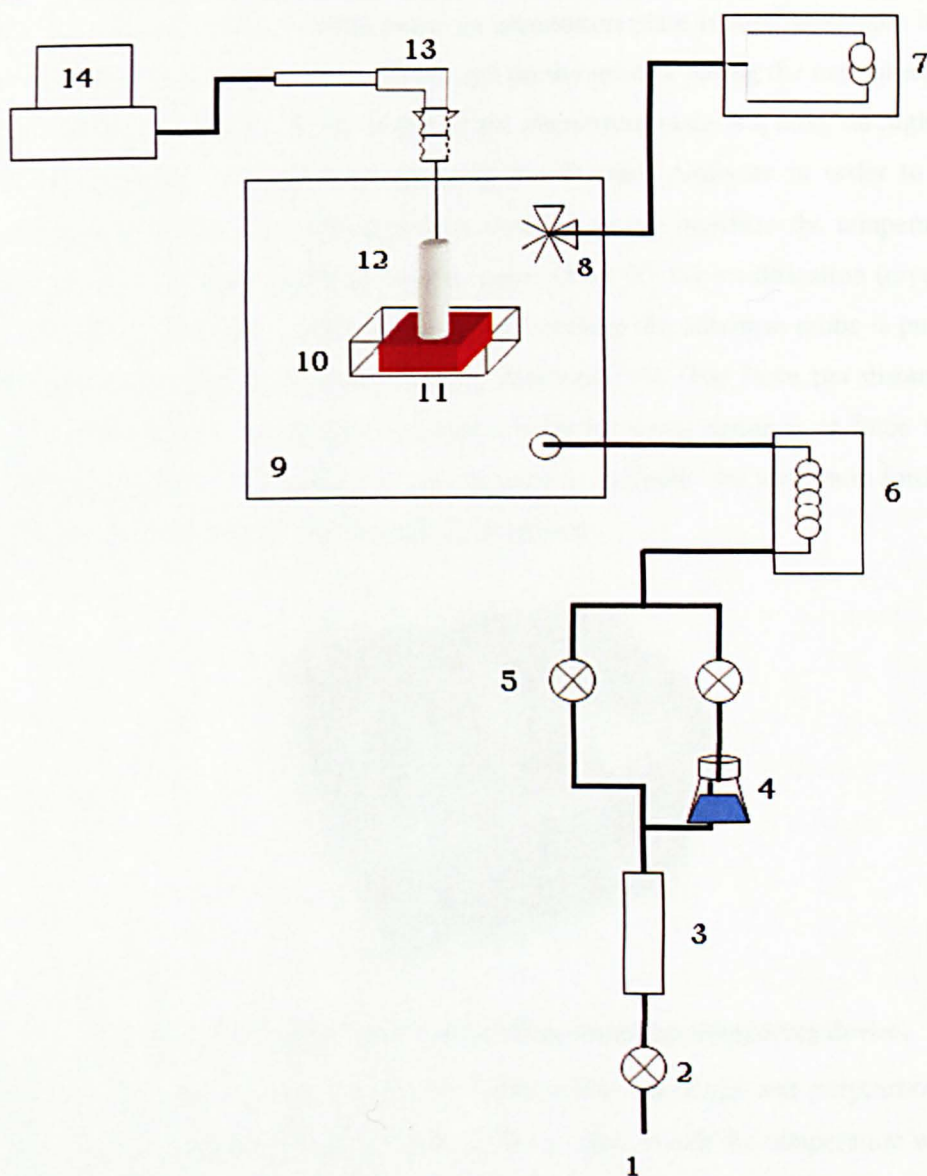


**Figure 3.17** Experimental set-up developed to measure the effect of processing conditions on the surface adhesion force.

The numbers refer to the air supply (1), pressure valve (2), dry column (3), water column (4), valve (5), water bath (6), cooling/heating unit (7), ventilator (8), Peltier chamber (9), sample holder (10), chocolate sample cell (11), adhesion probe (12), texture analyser (TA)(13), computer (14), respectively.

Tempered chocolate is melted using a scraped surface heat exchanger type tempering device (Revolution 2, ChocoVision), shown in Figure 3.18, which allowed the melting temperature to be controlled to ensure that the crystallization of the cocoa butter in the correct polymorphic form was not affected. The melted chocolate sample (32–33 °C) was poured into a glass Petri dish or chocolate sample cell (11), which was subsequently placed in the pre-conditioned (33–34 °C) Peltier cabinet. A glass sample cell was chosen because of its high surface energy, to which it was expected that the chocolate would prefer to ‘stick’. If the surface energy of the sample cell surface is too low, the complete solidified chocolate sample might be pulled out,

resulting in a cohesive failure. Furthermore, an aluminium plate is used as sample holder (10), to keep the chocolate sample and the sample cell on the ground during the experimental surface adhesion force determination. In the centre of the aluminium plate is a hole, through which the adhesion force probes (12) are lowered using the Texture Analyser in order to create the chocolate–mould interface. Immediately after creation of the interface the temperature of the Peltier cabinet and the water bath (air) are decreased to 15 °C, for solidification (crystallization) of the chocolate to take place. After 60 minutes of cooling the adhesion probe is pulled off the solidified chocolate surface using the Texture Analyser (13). The force per distance and per second are recorded on a computer (14), and the force versus distance or force versus time profile that is obtained, see Figure 3.14, can be used to calculate the maximum force and work of adhesion (area under the curve) for each measurement.



**Figure 3.18 Revolution 2 (ChocoVision) chocolate tempering device.**

As described in section 3.3.2.2, the contact between the chocolate and polycarbonate surface was created at a temperature of approximately 30 °C, after which the temperature was normally adjusted to 15 °C using a standardized temperature profile. In order to vary the cooling temperature, the temperature of the cabinet was decreased after the chocolate–mould interface creation to 20, 15, 10, 5 or 0 °C, respectively. For variations in mould temperature the thermal equilibration step of chocolate and mould probe of 30 minutes was omitted. The respective mould surface temperatures of -20, 0, 10, 20, 30 and 50 °C were obtained by cooling the polycarbonate mould probe in a fridge or freezer or heating in an oven for 30 minutes, respectively. Contact time refers to the time that the chocolate–mould interface was in place, i.e. from the moment of contact/interface creation, until the time of probe separation controlled by the Texture Analyser (13). During this research the evolution of surface adhesion with contact time was followed from 0 to 450 minutes.

### 3.3.2.6 *Chocolate and mould parameters*

The temperature and relative humidity in the Peltier cabinet were recorded at the time of creation of the chocolate–mould interface and just before determining the experimental adhesion force to control the experimental conditions. Additionally, a set of parameters related to the physical and chemical properties of the chocolate and/or mould surface were analysed as part of the surface adhesion experiments to increase understanding of the interactions taking place at the chocolate–mould interface and their relation to the adhesion or stickiness of chocolate to mould materials:

#### Hardness:

The solidified chocolate samples were analyzed for hardness by a method described by Liang and Hartel (2004), using the Texture Analyser (TA-XTplus, Stable Micro Systems). A 2-mm cylindrical stainless steel probe was used to penetrate the solidified chocolate sample at a constant speed of 0.1 mm/s to a depth of 5 mm. The maximum force ( $N$ ) obtained during this penetration was taken as a measure of the hardness. Hardness measurements were done in duplicate, at two different positions on the surface. First of all, the hardness was measured at the chocolate–mould interface, after the probe or mould surface was removed, as is shown in Figure 3.19C. Occasionally this measurement could not be employed, as a result of a cohesive-adhesive failure. Secondly, the hardness was measured at the chocolate–air interface, i.e. the chocolate surface area that has been in contact with air during the whole experiment. Furthermore, based on the force against distance (or time) profile recorded by the Texture Analyser during the penetration test, both the surface and the bulk hardness can be determined. An example can be seen in Figure 3.19A, where there is an initial sharp increase in the force (hardness), and after a maximum has been reached the force stabilizes and does not change during the rest of the test. The maximum peak force obtained within the first 5 seconds is defined as the hardness of the surface (1), whereas the maximum force obtained after approximately 20 seconds is defined as the hardness of the bulk (2). At this stage the cylindrical probe has travelled into the chocolate sample for > 4 mm. In Figure 3.19B a sudden drop in hardness (3) is observed after the initial maximum peak force has been reached. This is expected to be due to either the presence of an air bubble directly under the surface layer (< 0.5 mm), or the formation of a ‘skin’ layer on the chocolate surface during solidification. This skin layer can be a result of differences in crystallization at the surface and in the bulk, variations in temperature caused by heterogeneous heat transfer, adsorption of moisture at the surface affecting the viscosity of the surface layer or maybe the presence of a pore within the particulate network. Either way, the initial maximum force is used as the surface hardness, whereas the plateau force is used as the bulk hardness.



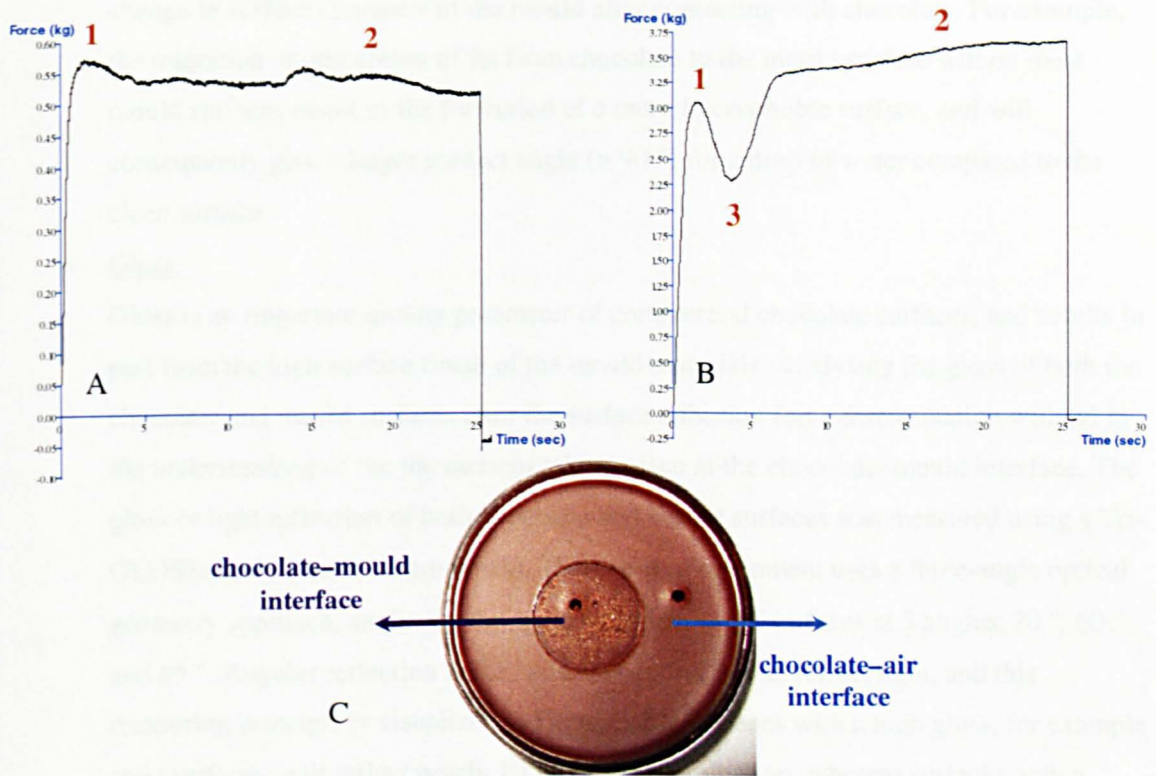


**Figure 3.19** Force against time profile obtained for a surface penetration (5 mm depth) test of chocolate at both the chocolate–mould and chocolate–air surfaces.

The numbers refer to the hardness of the surface (1), and of the bulk (2), respectively.

Number 3 indicates the presence of a defect, causing a temporary decrease in the hardness force measured.

- Chocolate residue weight:

As mentioned in section 3.3.2.4, the weight of the experimental mould probes is rated after each surface adhesion force determination to assess the failure mechanism. The chocolate residue weight or the left-over residues at the probe surface, expressed as the amount of chocolate per unit surface area ( $\text{mg m}^{-2}$ ), refers to the amount of chocolate left on the mould surface after separation tests. A macroscopic failure will normally be visible by eye, due to the combined effect of relatively large residues and the dark colour of the chocolate. Microscopic failure, on the other hand, may not be observed by visual inspection and can more easily be determined by weight changes.

- Contact angle:

Changes in surface chemistry of the mould surface layer are assessed by measuring the contact angle of water on the probe surface after the separation tests. The sessile drop method, described in section 3.3.1.2, was used for this purpose using only distilled water as the reference liquid. Within this research the difference in contact angle between a clean probe surface and the fouled probe surface is defined as  $\Delta\text{Contact angle}$ , and is based on 10 measurements on the clean surface, whilst the measurements on the fouled surface were done in duplicate. The aim of this test was to establish the



change in surface character of the mould after contacting with chocolate. For example, the migration or adsorption of fat from chocolate to the mould surface will on most mould surfaces result in the formation of a more hydrophobic surface, and will consequently give a larger contact angle ( $> 90^\circ$ ) for a drop of water compared to the clean surface.

- Gloss:

Gloss is an important quality parameter of commercial chocolate surfaces, and results in part from the high surface finish of the mould materials. Analysing the gloss of both the chocolate and mould surfaces after the surface adhesion force determination will aid in the understanding of the interactions taking place at the chocolate–mould interface. The gloss or light reflection of both chocolate and mould surfaces was measured using a Tri-GLOSSmaster (Sheen Instruments). This piece of equipment uses a three-angle optical geometry approach, analysing the specular reflection of surfaces at 3 angles,  $20^\circ$ ,  $60^\circ$  and  $85^\circ$ . Angular reflection is the capacity of a surface to reflect light, and this measuring principle is visualized in Figure 3.20. Surfaces with a high gloss, for example steel surfaces, will reflect nearly 100% of the illumination, whereas surfaces with a lower gloss and/or a higher surface roughness, for example plastics, will absorb and/or scatter part of the illumination, as a result of which the reflectance is lower due to part of the reflection not reaching the detector.

Within this research the aim of the gloss measurements was to determine the possible deposition of (fat) residues on the mould surface, as well as changes in chocolate gloss. The value obtained for the gloss at an angle of  $60^\circ$ , which is the universal measurement angle that is often used specifically for medium or semi-gloss surfaces, is used for the determination of the surface gloss.

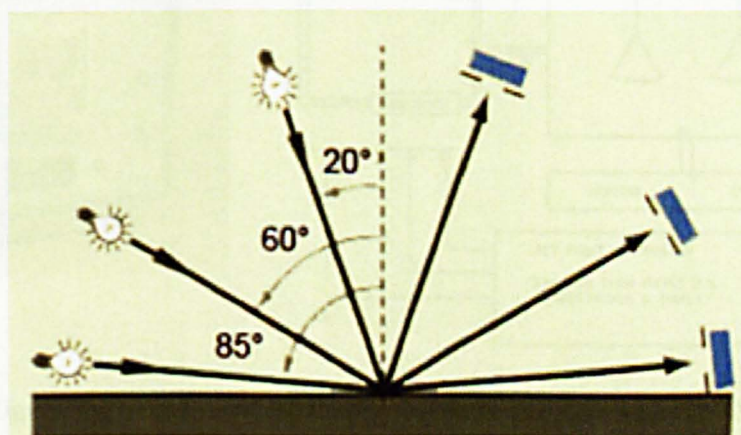


**Figure 3.20** Visualization of the measurement principle of the Tri-GLOSSmaster by determining the angular reflection at three angles (Sheen Instruments, 2003).



### 3.3.3 Moisture sorption

Adsorption is a phenomenon observed at the surface of a solid or liquid, whereby a monomolecular layer of adsorbate is formed by the adsorption of molecules from a nearby fluid phase on the respective solid or liquid surface (Walstra, 2003). An isotherm describes for a specific temperature the relation between the amounts adsorbed per unit surface area at equilibrium and the activity of the adsorbate. Moisture adsorption to the polycarbonate mould surface at varying relative humidities (RHs) was determined using a Cisorp water sorption analyser (CI Electronics Ltd.). The operating principle of the Cisorp, visualized in Figure 3.21, can be defined as a gravimetric method at an ambient pressure. Basically, it consists of three separate chambers: a weighing chamber, a balance chamber and a humidifier. The humidifier is responsible for the temperature conditioning and for supplying a wet air flow, by passing dry gas (nitrogen or air) at reduced pressure through a cavity filled with distilled water. Both the wet and the dry flow are brought up to the temperature of the weighing chamber, after which they are mixed and the mixed air flow is fed to the weighing chamber. A calibrated humidity probe present in the weighing chamber is used to monitor the RH. Two microbalances are placed in the balance chamber, with a thin rod, to which a sample holder is connected, being suspended into the weighing chamber. Counterweights, located in the balance chamber, are used to mechanically balance the weighing arm. A microprocessor is responsible for the conversion of the forces required to hold the balance arms horizontal into weight readings (Mangel, 2007).

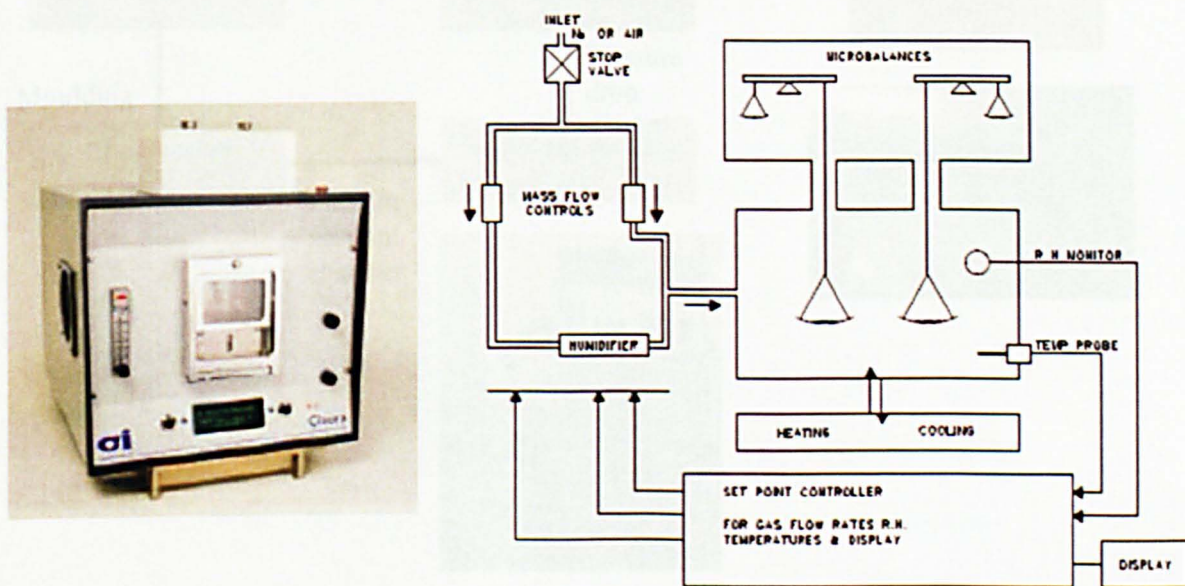


**Figure 3.21** Operating principle of the Cisorp moisture sorption analyser (Mangel, 2007).

In order to determine the moisture sorption by a polycarbonate surface during the mould conditioning stage, a polycarbonate mould piece was placed in the Cisorp weighing chamber for 30 minutes at a specific RH and a temperature of 30 °C, whilst the change in weight per minute was recorded. The moisture uptake by the polycarbonate mould surface was calculated as a percentage compared to the moisture uptake responsible for saturation, e.g. 100%,



$$\text{Moisture uptake } [\%] = \frac{m_{RH}}{m_{sat}} \times 100 . \quad [3-21]$$

where  $m_{RH}$  is the amount of moisture uptake after 30 minutes at a specific RH, and  $m_{sat}$  is the amount of moisture uptake required to reach saturation. By plotting the moisture uptake against the RH at 30 °C, an isotherm for the adsorption of moisture by the polycarbonate surface can be obtained.

### 3.3.4 Aeration of chocolate

In this research two different techniques are used to introduce bubbles into a chocolate system:

#### 1. Vacuum box

The principle of this method is based on de-sorption of gas that is either present within the tempered chocolate system naturally or injected into the system, e.g. CO<sub>2</sub>. De-sorption of the gas is obtained by applying a vacuum, triggering a pressure drop. As the gas solubility increases with pressure, a pressure drop causes the gas to be released from the continuous fat phase (Beckett, 2008). An overview of the principle of bubble inclusion under vacuum is shown in Figure 3.22.

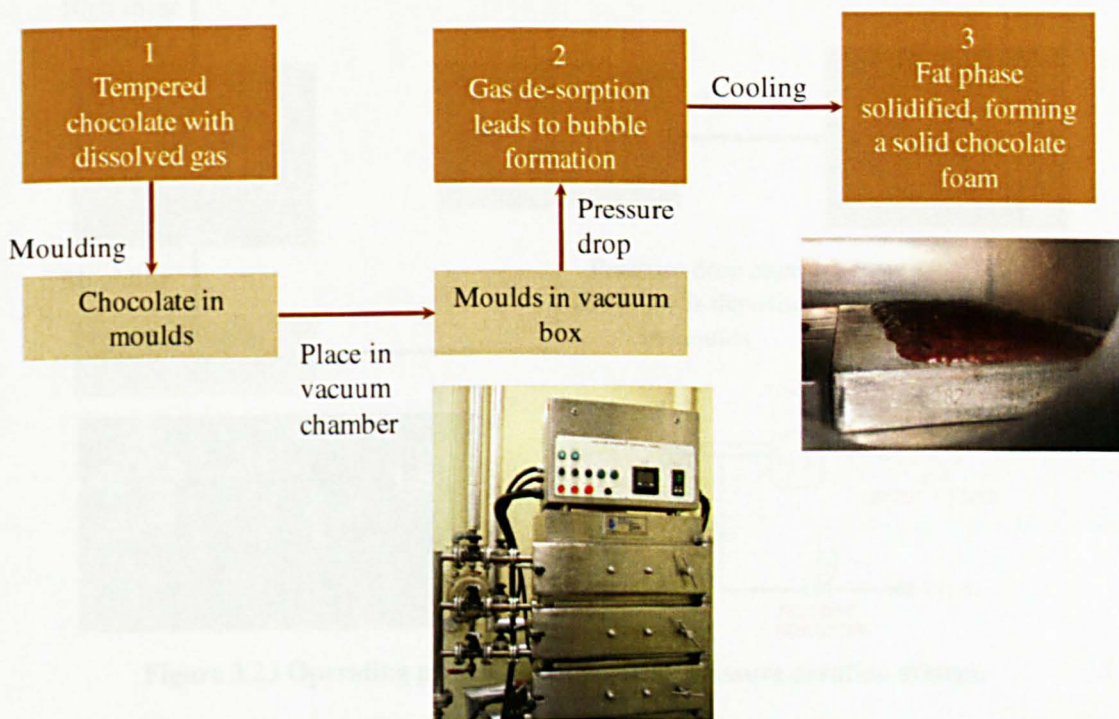


Figure 3.22 Operating principle of the vacuum box.

Tempered chocolate (~ 32 °C) is deposited in polycarbonate moulds, which are subsequently placed in a vacuum box (Euro-Vent Ltd.). After sealing the stainless steel enclosure containing the chocolate moulds a vacuum (ranging from 0.04 to 0.1 bar) is applied to the chamber. Using the manual vacuum-setting valve the pressure applied can be adjusted. The chamber operates at a temperature of approximately 10 °C, which



ensures the immediate solidification of the cocoa butter or fat phase. This solidification of the fat network is responsible for the trapping of the gas released from the fat phase when applying a vacuum. Once the complete chocolate system has been solidified the vacuum is released and the chocolate moulds can be removed from the vacuum box.

## 2. Positive pressure batch rig

The principle of this method is based on de-sorption of gas that is injected within the tempered chocolate system under application of a positive pressure. This positive pressure ensures the dissolution of the gas into the continuous fat phase of the chocolate system, creating a chocolate–gas liquid that will flow. Once the mixture leaves the system, the pressure drops to atmospheric pressure, resulting in the expansion of the dissolved gas.

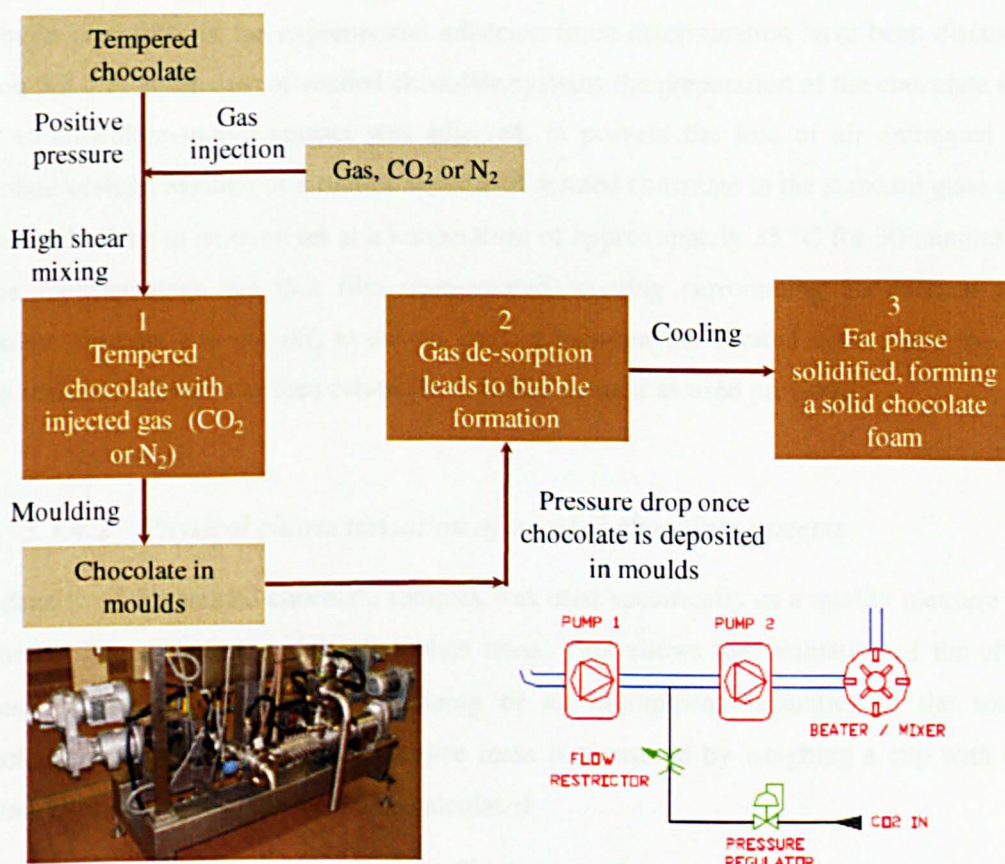


Figure 3.23 Operating principle of a positive pressure aeration system.

Typical examples of the use of positive pressure are Novac, Mondomix and the Sollich aero-temperer. An overview of the principle of bubble inclusion using a positive pressure is shown in Figure 3.23. A positive pressure is applied to a batch tank containing the tempered chocolate (~ 32 °C). From the tank the chocolate is pumped towards the beater / mixer, via two pumps. In between these two pumps pressure regulated gas, e.g. CO<sub>2</sub> or N<sub>2</sub> is injected into the chocolate system. The amount of gas that is injected will depend on the chocolate volume. A high shear mixing action by the



stator and rotor arrangement in the mixing head is responsible for mechanically dispersing the gas phase in the liquid chocolate mass. The mixture is subsequently deposited in pre-conditioned chocolate moulds, and as a result of the pressure dropping to atmospheric pressure upon discharge of the mixture, the dissolved gas desorbs to form bubbles. A final cooling phase is required to solidify the system and form a stable, solid chocolate foam.

Within this research different aerated chocolate systems were prepared to assess the relation between chocolate aeration and mould surface adhesion. Main aim was the preparation of systems with significantly different air bubble sizes.

#### 3.3.4.1 *Experimental adhesion force of aerated chocolate systems*

The main principles of the experimental adhesion force determination have been discussed in section 3.3.2.2. In the case of aerated chocolate systems the preparation of the chocolate sample prior to chocolate–mould contact was adjusted, to prevent the loss of air entrapped in the chocolate system. Melting of a routine volume of aerated chocolate in the standard glass sample holder took place in an oven set at a temperature of approximately 35 °C for 30 minutes. Prior to the melting stage the thin film (non-aerated) coating surrounding commercial aerated chocolate systems was cut off, to ensure contact between the aerated system and the mould probe surface. Contact was then created in a similar manner as used previously.

#### 3.3.4.2 *Physical characterisation of aerated chocolate systems*

The density of the aerated chocolate samples was used specifically as a quality measure and to determine the gas hold-up of the chocolate mass. This allows the evaluation of the effect of processing parameters on the gas holding or air entrapment capacities of the solidified chocolate. Density of the aerated chocolate mass is measured by weighing a cup with known volume, from which the density can be calculated:

$$\rho_{aero} = \frac{m_{aero}}{V} . \quad [3-22]$$

where  $m$  is the mass of the aerated chocolate present within a cup with a volume,  $V$ , of 30 ml. This simple technique enables a quick determination of the density during aeration experiments.

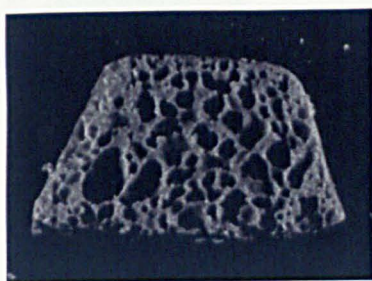
Gas hold-up is subsequently calculated by comparing the density of the aerated chocolate,  $\rho_{aero}$ , with the density of the same non-aerated or gas-free chocolate system,  $\rho_{std}$ :

$$\epsilon = \left( 1 - \frac{\rho_{aero}}{\rho_{std}} \right) \times 100 , \quad [3-23]$$

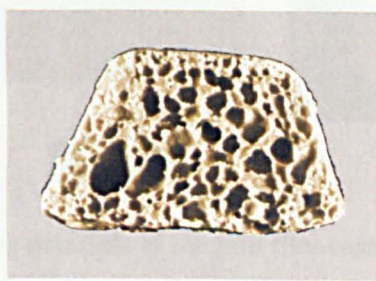
where  $\epsilon$  represents the gas hold-up value.

### 3.3.4.3 Structural characterisation of aerated chocolate systems

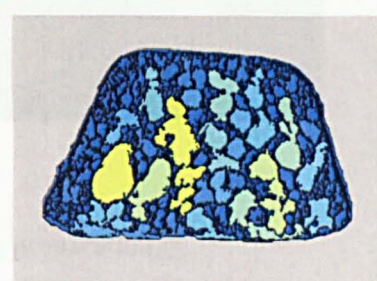
A non-invasive and non-destructive technique previously used for structural analysis of aerated chocolate is X-ray tomography (Haedelt, 2005). The generation of heat during measurements, however, was observed to negatively affect the structural characterisation. As a result, a new technique was tested at Nestlé PTC (York) using a C-Cell Imaging System manufactured by Calibre Control International in partnership with Campden & Chorleywood Food Research Association (CCFRA) who developed the system. The measurement principle of the C-Cell is based on the latest image analysis technology, using high definition imaging and controlled illumination. As the system operates under standardized conditions, there is no risk of affecting the crystallization and solidification of chocolate. Using the C-Cell equipment slices of aerated chocolate are examined and a number of objective parameters are defined: cells/mm<sup>2</sup>, number of cells, area of cells (%), cell diameter (mm) and non-uniformity. Graphical visualizations are prepared that show the structural characterisation, see Figure 3.24. This approach will allow the qualification and quantification of the internal microstructure of aerated chocolate systems.



**Raw Image:**  
image of the sample as collected by the high resolution optics.



**Brightness Correction Image:**  
the raw image is corrected for brightness variations, allowing textural features to be assessed.



**Cell Image:**  
Different cell sizes are coloured differently. Lighter shades indicate larger cell sizes, whereas red represents a hole.

**Figure 3.24 Images obtained for the structural characterisation of aerated chocolate using C-Cell.**



### 3.3.5 Thin film coating preparation

As described by Nussinovitch (2003), the addition of hydrocolloids or high-molecular weight molecules to a solvent results in the formation of highly viscous suspensions, solutions or gels with low dry substance content.

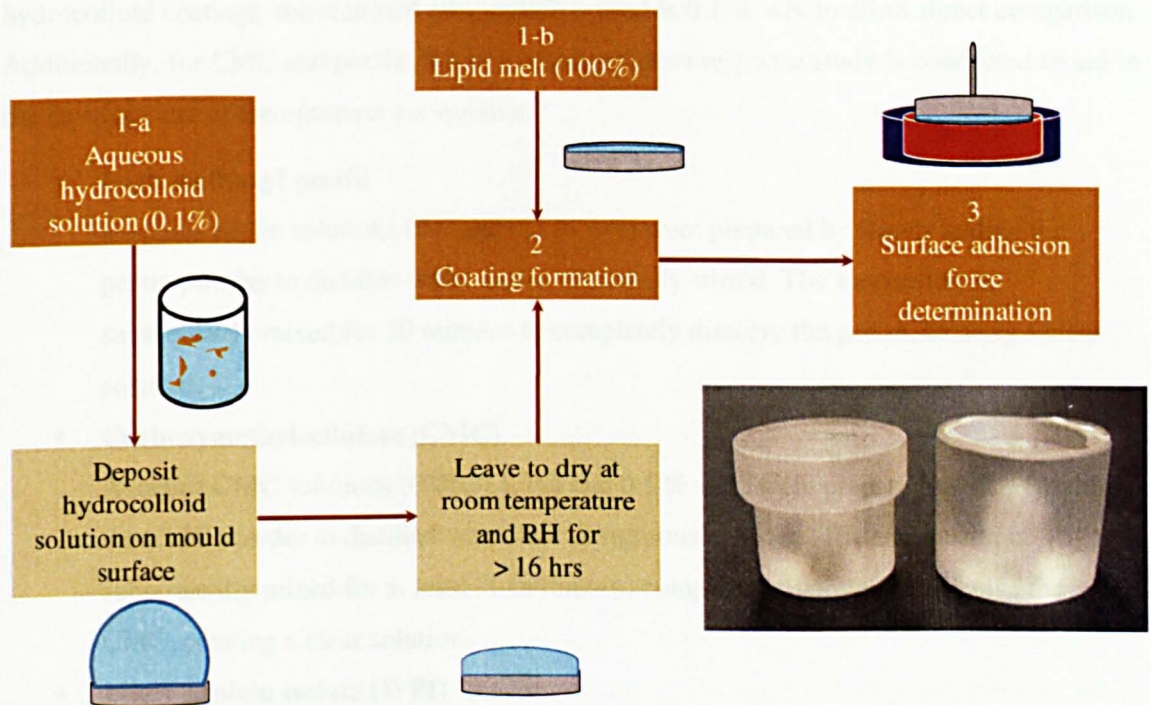


**Figure 3.25 Operating principle of the thin film coating preparation.**

Thin layers or films are obtained by drying the hydrocolloid solutions, aimed at decreasing the water content. Furthermore, the drying process may enhance the adhesion between the coating film and the coated object, bringing the two into maximal contact. Removal of the moisture at the surface layer of aqueous coating solutions, in combination with the sedimentation of hydrocolloid particles, results in the formation of a thin, dry film layer.

The general methodology followed to prepare and subsequent apply thin film coatings is shown in Figure 3.25. There are three main steps: 1) the formation of an aqueous hydrocolloid solution, which will be discussed in more detail in section 0 ; 2) the formation of a thin film coating by evaporating the moisture from the aqueous solution whilst in contact with a polycarbonate mould surface; and 3) surface adhesion force determination using the operating principle described in section 3.3.2.2, except that the polycarbonate mould surface is coated with a thin hydrocolloid film.

### 3.3.5.1 Hydrocolloid coatings

Hydrocolloid coatings are prepared according to the general operating principle described in Figure 3.25, with particular focus on pathway 1-a. The method of preparation of the aqueous hydrocolloid solutions, however, varies depending on the type of hydrocolloid used. For all hydrocolloid coatings, the standard concentration used is 0.1 % w/v to allow direct comparison. Additionally, for CMC and pectin 105 in particular a dose response study is conducted to aid in the development of the optimum formulation.

- **High methoxyl pectin**

Aqueous pectin solutions (0.1 and 0.5 % w/v) were prepared by slowly adding the pectin powder to distilled water that is vigorously stirred. The suspension is subsequently mixed for 30 minutes to completely dissolve the pectin, creating a clear solution.

- **Carboxymethylcellulose (CMC)**

Aqueous CMC solutions (0.01, 0.1, 0.2 and 0.5 % w/v) were prepared by slowly adding the CMC powder to distilled water that is vigorously stirred. The suspension is subsequently mixed for at least 30 minutes to completely hydrate and dissolve the CMC, creating a clear solution.

- **Whey protein isolate (WPI)**

An aqueous WPI solution (0.1%) was prepared by adding the WPI powder to distilled water that is vigorously stirred. The suspension is subsequently mixed for 30 minutes to completely dissolve the WPI, creating a clear yellowish solution. A small study was conducted to investigate the effect of protein denaturation on the film forming capabilities of WPI by heating the solution, but no significant differences in thin film coating were obtained.

The prepared solutions are deposited on the polycarbonate mould surfaces using a pipette and left to dry over night at room temperature to remove the moisture and create a thin film.



### 3.3.5.2 Lipid coatings

Lipid coatings are prepared in a slightly different way compared to the hydrocolloids coatings, although they are also prepared according to the general operating principle described in Figure 3.25, with particular focus on pathway 1-b. The method of preparation, however, varies depending on the type of lipid or fatty acid blend used. For all lipid coatings, the standard concentration used is 100% (no dilution) to allow direct comparison. Additionally, for Grindsted<sup>®</sup> Acetem, a dose response study is conducted to aid in the development of the optimum formulation. All three lipids or fatty acid blends contain emulsifying properties, but because of physical properties only the acetic acid ester is used at different concentrations.

- **Distilled monoglyceride**

Distilled monoglyceride coatings were prepared by carefully heating the Dimodan<sup>®</sup> HP beads to above their dropping point (~ 69 °C), to create a liquid solution. The polycarbonate mould surface was subsequently dipped in the liquid distilled monoglyceride solution (100%) and left to solidify (set / cool) at room temperature.

- **Acetic acid ester**

Acetic acid ester coatings were prepared by carefully heating the Grindsted<sup>®</sup> Acetem wax to above its dropping point (~ 37 °C), to create a liquid solution. The polycarbonate mould surface was subsequently dipped in the liquid distilled monoglyceride solution (100%) and left to solidify (set / cool) at room temperature. For the dose response study, aqueous acetic acid ester solutions (0.1 and 1.0% w/v) were prepared by adding the Grindsted<sup>®</sup> Acetem wax to distilled water that is stirred. The suspension is subsequently heated to above the dropping point of Grindsted<sup>®</sup> Acetem (~ 37 °C) to melt the wax and create a clear solution.

- **Cocoa butter**

Cocoa butter coatings were prepared by carefully heating the cocoa butter to above its melting point, to create a liquid solution. The polycarbonate mould surface was subsequently dipped in the liquid cocoa butter solution (100%) and left to solidify (set / cool) at room temperature (max. 20 °C).

- **Lecithin**

An aqueous lecithin solution (1.0% w/v) was prepared by slowly adding the lecithin powder to distilled water that is stirred. The suspension is subsequently slightly heated to dissolve all the lecithin and create a clear solution.

### *3.3.5.3 Plasticizer and multicomponent coatings*

Plasticizer coatings are prepared in a similar way as used for the hydrocolloid coatings. Aqueous coating solutions are prepared by adding a hydrocolloid (0.1% w/v) and a plasticizer (0.1 or 1.0% w/v) to distilled water under continuous stirring. The hydrocolloids used are pectin 105 and CMC.

Multicomponent coatings consist of a hydrocolloid (0.1% w/v CMC), with a lipid component (0.1 and 1.0% w/v acetic acid ester) and a plasticizer (0.1 and 1.0% w/v sucrose). Aqueous solutions are prepared by adding all three components to distilled water under continuous stirring. In order to dissolve the lipid wax the solution is heated slightly.

### **3.3.6 Solid surface topology**

Confocal Laser Scanning Microscopy (CLSM) is used in reflection imaging mode to determine the surface topology of solid mould surfaces. Surface roughness is known to negatively affect contact angle measurements, and contact angle hysteresis can be used to assess the homogeneity of surfaces from a macroscopic point of view. CLSM can be used in addition to this to assess the surface roughness at a microscopic level, i.e. the surface microstructure. By using reflection imaging, the intensity of the reflected light will be analysed. It is assumed that surface roughness negatively affects the reflection intensity, which can therefore be used as a measure of surface topology. A 30/70 RT filter is used to allow the 488 laser line to return to the detector, in combination with a PMT collection window which allows 488 nm light in.

## **CHAPTER 4**

# **SURFACE ENERGY INVESTIGATION OF CHOCOLATE ADHESION TO SOLID MOULD MATERIALS**

### **4.1 INTRODUCTION**

Within the chocolate manufacturing industry, the adhesion and sticking of chocolate to the mould surface is a substantial ongoing problem, leading to poor product appearance, production losses (normally those products are considered out of quality standards and rejected), and increased processing costs partly due to superior equipment cleaning. The extent of adhesion is assumed to be dependant of the adhesive force between the chocolate and the mould surface, and the cohesive force of the chocolate only. Understanding of the interactions taking place at the chocolate–mould interface can be gained by investigating the surface energy of the different (solid) surfaces involved. Solid surface energy (or surface tension) is regarded as a characteristic parameter of both surface and interfacial processes, such as adsorption, wetting or adhesion (Karbowski et al., 2006). This part of the research specifically applies the principles of thermodynamic adhesion and surface energy to the case of chocolate adhesion, with the aim of establishing relationships between the thermodynamic work of adhesion and the observed extent of adhesion of chocolate to mould materials.

### **4.2 MATERIALS AND METHODS**

The equipment and methodologies used to determine the surface tension, contact angle and experimental chocolate–mould surface adhesion force, as well as empirical approaches used to calculate the solid surface energy, have been discussed in CHAPTER 3. This section will describe specific materials and methodologies that have been used to investigate the surface characteristics of a number of solid surfaces, both mould and chocolate materials.

#### **4.2.1 Materials**

The solid mould materials used in this research were chosen because of their link with commercial chocolate manufacturing, as discussed in section 3.2.2, except for quartz glass which was chosen as the reference material because of its well-known high surface energy. Prior to use in surface energy or adhesion force determinations, the solid surfaces were cleaned with detergent (Springdown High Active) containing 5% ionic surfactant and 5–15% non-ionic surfactant, followed by distilled water (Millipore) and acetone (AR grade), where applicable, and dried using compressed air.

In addition to the probe liquids mentioned in Table 3.5, two additional liquids were included especially for the surface energy determination of chocolate surfaces: 1,3-propanediol ( $\text{CH}_2(\text{CH}_2\text{OH})_2$ ) and n-octane ( $\text{CH}_3(\text{CH}_2)_6\text{CH}_3$ ). The use of 1,3-propanediol (Sigma Aldrich) was based on work done by Galet et al. (2004), who used different mixtures of water and 2-propanol to determine the surface free energy of cocoa powder. n-Octane (Fisher Scientific) was chosen as a liquid with a low surface tension.

Dark chocolate (52% cocoa solids) was used as the standard system for the investigation of the relationship between solid surface energy and chocolate–mould adhesion. Deodorized cocoa butter (100% cocoa solids) and palm olein, supplied by Nestlé PTC (York) were used as model or reference systems. For surface tension measurements, the standard dark chocolate (52% cocoa solids) system is compared to a milk chocolate (Nestlé commercial recipe, 29% cocoa solids) and a dark chocolate (Côte D'Or, 70% cocoa solids) system. For solid surface energy measurements of solid chocolate bars, four commercial chocolate products from Nestlé are used: Heaven Dark truffle (minimum 43% cocoa solids), Heaven Milk truffle (minimum 30% cocoa solids and 18% milk solids), After Eight (52% cocoa solids) and AERO (aerated milk chocolate, minimum 25% cocoa solids and 14% milk solids).

#### 4.2.2 Methods

The surface tension of the probe liquids as well as the chocolate systems was determined using the Wilhelmy plate. Especially for the chocolate systems the use of the Du Noüy ring is discouraged as this will not give the actual surface tension force. Chocolate systems were carefully melted in an oven at 40 °C prior to surface tension measurements. In all cases the average of 10 measurements was taken as the liquid surface tension.

Contact angles of probe liquids on mould and chocolate surfaces were determined using the sessile drop method in an apparatus specifically designed for this purpose. With respect to solid chocolate surfaces particular attention was paid to the temperature and the time of the measurement. All chocolate experiments were conducted at temperatures below the melting point of chocolate (< 30 °C), and the equilibrium stage was omitted to prevent the chocolate from interacting with the solvents. Contact angles were taken within seconds after the drop was deposited on the surface, and no receding contact angles were measured. In all cases the average of the left and right contact angle of 5 different drops placed on two different clean or new surfaces was taken as the contact angle and used to determine the reported solid surface energy values.



## 4.3 RESULTS

### 4.3.1 Surface tension

As described in section 3.3.1.1, the liquid surface tension was measured using a Krüss K10 ST digital tensiometer, with a platinum Wilhelmy plate. Using this technique, the surface tension of a set of probe liquids and chocolate systems was determined, as well as the temperature dependence of the probe liquids in the temperature range of 20 – 60 °C.

#### 4.3.1.1 Surface tension components

The Wilhelmy plate method is used to determine the total surface tension of liquids,  $\gamma_l$ . However, in order to increase understanding of the surface chemistry of the solid materials the liquid surface tension components are used, as is shown in section 3.3.1.3 by the empirical approaches of Fowkes, Owens and Wendt, and van Oss, Chaudhury and Good. These approaches assume that different intermolecular forces, such as polar and dispersive, or short range and long range forces are responsible for the interactions between a liquid and a solid surface. In order to calculate the total surface energy and its components according to the methods mentioned previously, knowledge of the liquid surface tension components is required. The dispersive or apolar or Lifshitz–van der Waals,  $\gamma^{lw}$ , and the polar or Lewis acid–base,  $\gamma^{ab}$ , components of the liquid surface tension can be determined experimentally.

**Table 4.1 Experimental and literature surface tension data.**  
Error is representative of the standard deviation, n = 12.  
(Good, 1992; van Oss, 2006; Della Volpe, 2004; Lyklema, 2000).

Liquid	Experimental	Literature				
	Total surface tension $\gamma_l^{tot}$	Total surface tension $\gamma_l^{tot}$	Dispersive component $\gamma_l^{lw}$	Polar component $\gamma_l^{ab}$	Electron acceptor $\gamma_l^+$	Electron donor $\gamma_l^-$
	[mN m <sup>-1</sup> ]	[mN m <sup>-1</sup> ]	[mN m <sup>-1</sup> ]	[mN m <sup>-1</sup> ]	[mN m <sup>-1</sup> ]	[mN m <sup>-1</sup> ]
Deionised water	72.79 ± 0.45	72.8	21.8	51.0	25.5	25.5
Glycerol	65.02 ± 0.14	64.0	34.0	30.0	3.9	57.4
Formamide	59.18 ± 0.3	58.0	39.0	19.0	2.3	39.6
Diiodomethane	50.85 ± 0.58	50.8	50.8	≈ 0	≈ 0.01	≈ 0
Poly(ethylene glycol)	45.19 ± 1.04	48.0	29.0	19.0	3.0	30.1
$\alpha$ -Bromonaphthalene	43.61 ± 0.72	44.4	44.4	≈ 0	≈ 0	≈ 0
Benzylalcohol	39.71 ± 0.54	39.0	30.3	8.7		
Chlorobenzene	33.41 ± 0.22	33.6	32.1	1.5		
Hexadecane	27.34 ± 0.52	27.5	27.5	27.5	0.0	0.0
Decane	23.79 ± 0.22	23.8	23.8	0.0	0.0	0.0
1,3-Propanediol	48.74 ± 0.15	46.5				
n-Octane	21.80 ± 0.06	21.6	21.6	0.0	0.0	0.0

One technique measures the contact angle of a liquid with known total surface tension on a purely apolar solid surface such as polyethylene or polypropylene, to determine the dispersive surface tension component of the respective liquid (van Oss, 2006). Based on the assumption that the liquid surface tension is known, the polar surface tension component can then be derived from:

$$\gamma_l = \gamma_l^{lw} + \gamma_l^{ab} . \quad [4-1]$$

The total liquid surface tensions of the probe liquids determined in this research using the Wilhelmy plate method are shown in Table 4.1. In the 2<sup>nd</sup> column the experimental values are shown, whereas the 3<sup>rd</sup> column refers to total liquid surface tension data from literature (Good, 1992; van Oss, 2006; Della Volpe, 2004). Comparison of these two columns indicates that the surface tensions measured agreed within  $\pm 1.2 \text{ mN m}^{-1}$  of the values found in literature. Therefore, surface tension components of the probe liquids are taken as the literature values, as shown in columns 4, 5, 6 and 7 in Table 4.1. Empty cells indicate that no literature data were available for that specific liquid.

#### 4.3.1.2 Surface tension of chocolate systems

Measurement of the liquid surface tension of chocolate was conducted at a temperature of 50 °C. At this temperature all crystallization history is melted out and the chocolate has a viscosity that is sufficient for the wetting of the Wilhelmy plate in order to determine the liquid surface tension. Figure 4.1 presents the surface tension of a number of chocolate samples with different cocoa solids content. For all samples the equilibrium force is taken as the liquid surface tension. Upon initial contact, the force with which the chocolate is pulling on the Wilhelmy plate is relatively high ( $\approx 47 \text{ mN m}^{-1}$ ). However, within seconds the force drops and stays constant (not shown here). It is assumed that this effect can be ascribed to the presence of a surfactant (lecithin) within the chocolate system. Surfactants present in a liquid are known to affect the liquid surface tension (Walstra, 2003). For aqueous solutions, a low concentration of surfactant can significantly reduce the surface tension. Non-aqueous solutions require a higher concentration to obtain a similar reduction. In most cases surfactants alter the liquid surface tension negatively, reducing the overall surface tension. The mechanism of action of surfactants is based upon their ability to adsorb in the surface layer or onto different materials, due to their chemical structure and amphiphilic character (Erbil 2006; Lyklema, 2000). An example of a food system where the migration of surface-active agents to the surface was responsible for a decrease in surface tension in time is milk (Michalski and Briard, 2003). In the present research the presence of the surfactant lecithin in chocolate systems is believed to be responsible for the drop in surface tension observed for all chocolate systems after the initial contact. Cocoa butter may contain residues of surface active agents but their presence is not detected during surface tension measurements, where the force pulling on the Wilhelmy plate is constant from the

moment that contact is made. Upon cooling of the chocolate system in time, a slight increase in surface tension is observed, which is believed to result from the solidification of the chocolate. With time the viscosity of the chocolate especially on the surface decreases until after sufficient time a solidified chocolate sample will be obtained. The presence of a heated water mantle surrounding the sample holder will prevent the bulk chocolate from setting and solidifying. However, it cannot prevent the surface of the chocolate system against a decrease in temperature and subsequently viscosity.

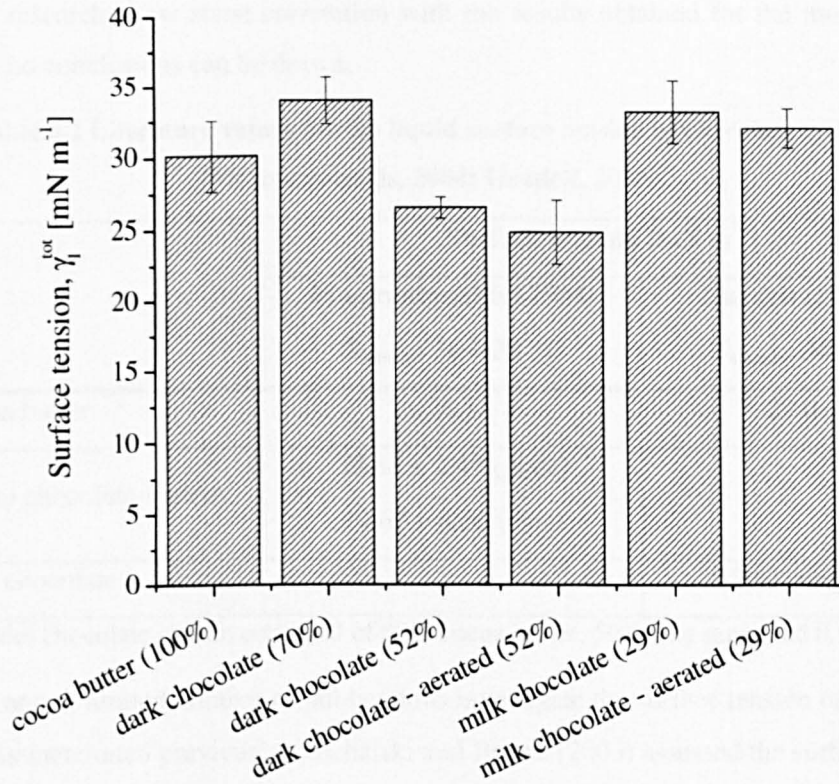


**Figure 4.1** Surface tension as affected by total cocoa solids content.

**Error bar is representative of the standard deviation, n = 12.**

Comparison of the different chocolate systems shows a significant difference between cocoa butter and standard dark chocolate (52% cocoa solids) and between the standard dark chocolate and milk chocolate (29% cocoa solids) systems. Aeration, furthermore, does not significantly alter the liquid surface tension. The question is raised though to what extent the Wilhelmy plate actually measures the surface tension of the liquid chocolate foam. A defined interface between two phases does not exist using the plate method in combination with foam. Combined with the fact that both the plate and ring method assess the static surface tension, it is assumed that the surface tension obtained for the aerated chocolate is actually the surface tension of the chocolate rather than that of the foam. Foam properties can be assessed by dynamic surface tension techniques, which measure for example the maximum bubble pressure and conclude whether it is easy to create foams from a liquid solution or not. The addition of lecithin to chocolate systems is believed to be responsible primarily for the difference in surface tension between

cocoa butter and standard dark chocolate. Further addition of milk proteins may explain the increase in surface tension observed for milk chocolate systems.

Review of literature indicates that only on two previous occasions the surface tension of chocolate was assessed. These results are summarized in Table 4.2. The results obtained by Haedelt are regarded as less accurate, based on the temperature that was used (30 °C) and the technique (Du Noüy ring). With high viscosity samples such as chocolate it takes time to reach an equilibrium situation, which cannot be measured by the ring method. The results obtained in the present research show some correlation with the results obtained for the model chocolate system, but no conclusions can be drawn.

**Table 4.2 Literature values for the liquid surface tension of chocolate systems (Mastrantonakis, 2004; Haedelt, 2005).**

	Surface tension [ $\text{mN m}^{-1}$ ]	
	Mastrantonakis (2004) $T_{\text{sample}}: 36 - 38 \text{ }^{\circ}\text{C}$	Haedelt (2005) $T_{\text{sample}}: 30 \text{ }^{\circ}\text{C}$
Cocoa butter	26.1	29.0
Model chocolate system <sup>1</sup>	29.88 ± 2.49 (plate) 29.62 ± 0.56 (ring)	
Milk chocolate		39.3 (ring)

<sup>1</sup> The model chocolate system consisted of 50% cocoa butter, 50% fine sugar and 0.5% lecithin.

In general, only a limited number of publications investigate the surface tension of non-aqueous mixtures. As mentioned previously, Michalski and Briard (2003) assessed the surface tension of milk. They observed a decrease in surface tension with increasing milk fat content, up until a certain level after which the effect was negligible. This raises the question to what extent the cocoa butter level is responsible for the surface tension of chocolate. The different chocolate systems assessed in this research indicate that there might be an effect of the cocoa butter content on the liquid surface tension, although the trend is not clear and no conclusions can be drawn. Allen et al. (1999) devised a method to predict the surface tension of biodiesel fuels, based on the fatty acid composition. They found that the surface tension of a mixture is based on a weighted mass-average of the pure components of that mixture. In other words, the components with a higher surface tension have more influence at the surface of the mixture, forcing the components with a lower surface tension away from the surface. Overall, the liquid surface tension values observed in literature for vegetable oils and fatty acids show strong agreement with the surface tension values obtained in this research for the different chocolate systems (26 – 33  $\text{mN m}^{-1}$ ), as can be observed from Table 4.3. Cocoa butter consists for 95% of the fatty acids palmitic ( $\text{C}_{16:0}$ ) (P), stearic ( $\text{C}_{18:0}$ ) (St) and oleic ( $\text{C}_{18:1}$ ) (O), whereas soybean and cottonseed oil are vegetable fats that can be used as cocoa butter equivalents.



**Table 4.3 Literature values for the liquid surface tension of fatty acids and vegetable oils (Allen et al., 1999, Chumpitaz et al., 1999).**

	Surface tension [ $\text{mN m}^{-1}$ ]						
	Cocoa butter	Coconut oil	Soybean oil	Cottonseed oil	Palmitic acid ( $\text{C}_{16:0}$ )	Stearic acid ( $\text{C}_{18:0}$ )	Oleic acid ( $\text{C}_{18:1}$ )
Measured	30.11	26.11	28.2		28.40 28.20	29.0	22.80 31.90
Predicted		26.82	28.93	28.76	28.47	28.89	28.88

Based on this agreement it is hypothesized that the surface tension of chocolate depends on cocoa butter and its fatty acid composition. As cocoa butter is a natural product its fatty acid composition will differ depending on cocoa bean origin and processing techniques. According to Talbot (1999) especially the StOS/StOO ratio, which is the ratio of a TAG consisting of stearic-oleic-stearic acid over a TAG consisting of stearic-oleic-oleic acid, will vary depending on origin. Amongst the chocolate systems analysed within this research cocoa butters from various origins may have been used, which may explain the variability in surface tension, i.e. the variability between dark chocolate with 52% cocoa solids and 70% cocoa solids (different manufacturers), and that between dark chocolate and milk chocolate.

#### 4.3.1.3 Relation between surface tension and temperature

The chocolate moulding process consists of the deposition of liquid chocolate into pre-conditioned moulds. In the subsequent cooling stage, the mould and chocolate are cooled to a temperature of approximately 15-20 °C. On deposition, the liquid tempered chocolate has a temperature of on average 30 °C, and the mould is pre-heated to within a few degrees of that temperature (Beckett, 2008). In order to assess the impact of the mould surface energy on the adhesion of chocolate it is important to know the relation between temperature and mould surface energy within the temperature range over which the chocolate is in contact with the mould, i.e. 20 – 40 °C. As solid surface energy is calculated using the liquid surface tension and contact angle, the impact of temperature on these parameters needs to be determined. Figure 4.2 shows the surface tension of the probe liquids in the temperature range 20 – 60 °C. For all liquids the surface tension declines linearly with increasing temperature, with a value of on average  $\leq 1 \text{ mN m}^{-1}$  per 10 °C. Due to this linearity the surface tension outside this temperature range can be estimated by extrapolation.

The linear relation observed between surface tension and temperature is well known in literature. Due to the increased temperature, the molecular interactions become weaker and the surface tension decreases. However, when the temperature reaches the critical temperature,  $T_c$ , the surface tension vanishes altogether:  $\gamma = 0$ . This effect is due to the restraining force on the surface molecules which disappears, whereas the vapour pressure increases (Erbil, 2006). Padday (1969) describes the relation between surface tension and temperature with Le Chatelier's principle. By increasing the surface area of a liquid adiabatically, work is performed on the system. As a result, the temperature drops and the surface tension increases, preventing further expansion. Furthermore, the thermodynamic dependence of surface tension on temperature is shown in equations [2-15] and [2-17]. With increasing temperature, the entropy,  $S$ , increases and the surface free energy decreases.

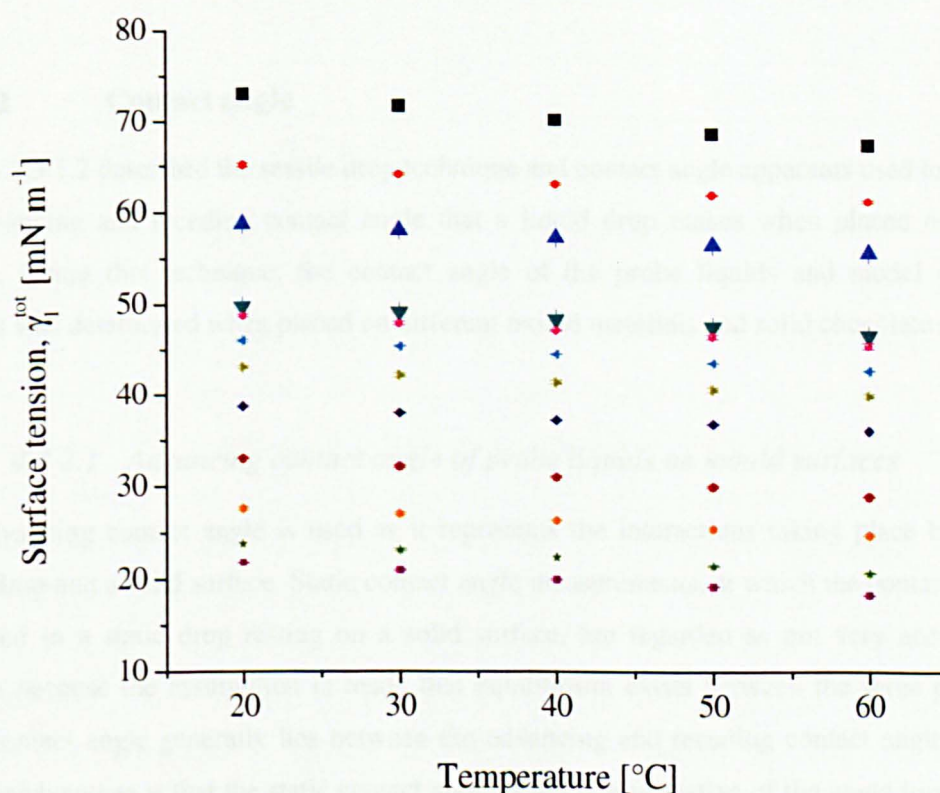


Figure 4.2 Surface tension as a function of temperature.

The symbols refer to the different liquids used: water (■), glycerol (●), formamide (▲), diiodomethane (▼), poly(ethyleneglycol), (◄) bromonaphthalene (►), benzylalcohol (◆), chlorobenzene (◆), hexadecane (●), decane (★), 1,3-propanediol (●) and octane (■).

Several empirical equations have been developed to relate the surface tension and the temperature, e.g. Eötvös and Guggenheim–Katayama. However, these approaches use critical properties and molar volume and are only applicable for the prediction of the surface tension of pure liquids. The linear correlations obtained experimentally for the probe liquids will be used to calculate the surface tension at different temperatures, and these values will be used for the surface free energy determinations at various temperatures. An interesting observation was

made by Zhao et al. (2004a) who noticed a decrease in total surface free energy and dispersive surface free energy of different materials with increasing surface temperature, while the acid–base surface free energy component increased with increasing temperature.

The temperature dependence of the chocolate surface tension was assessed in a similar way as that used for the probe liquids. However, the results obtained (not shown here) showed no significant differences in liquid surface tension for dark chocolate systems between 30 and 70 °C. This is primarily a result of the large error obtained at both 30 and 70 °C, which is assumed to be a result of differences in total solids content. At higher temperatures all crystals are melted out, and the total solids content is reduced. The overall trend shows a decrease in chocolate surface tension with increasing temperature, indicating that less energy is required to stretch the chocolate surface at higher temperature.

### 4.3.2 Contact angle

Section 3.3.1.2 described the sessile drop technique and contact angle apparatus used to measure the advancing and receding contact angle that a liquid drop makes when placed on a solid surface. Using this technique, the contact angle of the probe liquids and model chocolate systems was determined when placed on different mould materials and solid chocolate surfaces.

#### 4.3.2.1 *Advancing contact angle of probe liquids on mould surfaces*

The advancing contact angle is used as it represents the interactions taking place between a liquid drop and a solid surface. Static contact angle measurements, at which the contact angle is measured in a static drop resting on a solid surface, are regarded as not very accurate and reliable because the assumption is made that equilibrium exists between the three phases. A static contact angle generally lies between the advancing and receding contact angle, and the main disadvantage is that the static contact angle is not representative of the angle formed upon initial contact with a fresh, clean surface (Erbil, 2006). Advancing contact angles on the other hand are taken when the three phase contact line is changing, and therefore take into consideration the interactions at the interface. Table 4.4 gives an overview of the values obtained for the advancing contact angles,  $\theta_{adv}$ , of the probe liquids when placed on the different solid mould surfaces. Empty cells indicate that it was impossible for these specific probe liquids and mould materials to be used in combination. From the results obtained it can be observed that the probe liquids used give significantly different contact angles depending on the solid surface that is used. The general trend for the individual probe liquids is that the highest contact angle is formed when placed on the PTFE surface, whereas the lowest contact angle is obtained on the quartz glass surface. On average, the value obtained for the contact angle decreases with decreasing polarity of the probe liquid. However, none of the probe liquids show complete



wetting of the solid mould surface. The general conclusion that can be drawn is that the contact angle that a liquid makes depends on the surface chemistry of the solid material and the intermolecular interactions taking place at the solid–liquid interface.

**Table 4.4** The average advancing contact angles,  $\theta_{adv}$ , and standard deviations obtained when placing the individual probe liquids on the four mould materials at room temperature ( $n = 10$ ).

Liquid	Contact angle, $\theta_{adv}$ [°C]			
	PTFE	Polycarbonate	Stainless steel	Quartz glass
Deionised water	130.5 ± 1.1	89.8 ± 1.1	58.9 ± 1.1	38.7 ± 0.3
Formamide	108.4 ± 1.3	62.8 ± 0.9	51.8 ± 1.6	20.9 ± 1.2
Diiodomethane	98.6 ± 1.1	51.9 ± 1.5	44.8 ± 1.9	41.4 ± 0.7
Poly(ethylene glycol)	91.9 ± 1.3	44.7 ± 2.1	41.0 ± 1.9	28.82 ± 1.1
$\alpha$ -Bromonaphthalene			30.9 ± 1.0	
Benzylalcohol	87.8 ± 1.0		35.3 ± 2.1	
Hexadecane	57.4 ± 1.2			
n-Octane	30.6 ± 1.4		14.7 ± 0.9	6.8 ± 0.8

Contact angles obtained in this research cannot be compared with values referred to in literature. Their values are determined by two main parameters, first of all the analytical method in combination with the mathematical method used to determine the contact angle and secondly the level of ideality of the solid surface. Lyklema (2000) collected contact angle data for water and a small number of other familiar liquids with the aim of giving an impression of magnitude and extent of (dis-)agreement between different sources. For example, the advancing contact angle for water on a stainless steel surface varied from 0 to 76 °, whereas for a PTFE surface the range of angles varied from 90 – 130 °. One of the explanations for this level of variability is the different (pre-) treatments of the solid and the liquid. In general, the data obtained in this research for particularly stainless steel and PTFE fall within the range of advancing contact angles published by Lyklema (2000).

Glycerol, chlorobenzene and decane, probe liquids that were initially proposed in Table 3.5, have not been used for contact angle measurements. During a preliminary study it was observed that the viscosity of glycerol did not allow the determination of either advancing or receding contact angles. Chlorobenzene in particular interacted with the solid surfaces in a negative way, and similar observations were made for bromonaphthalene, benzylalcohol, hexadecane and decane on specific mould surfaces. Examples of negative interactions observed are visualized in Figure 4.3. For polycarbonate the chemical resistance is described by Bayer MaterialScience (2004), who mention in particular the destroying power of alkaline solutions, ammonia gas and its solution and amines, the dissolving power of a large number of industrial solvents and the



swelling power of organic compounds such as benzene, acetone and carbon tetrachloride. Particular notification is given to the use of low-molecular, aromatic, halogenated and polar components which migrate into the polycarbonate and cause dissolution and/or swelling of the surface layer, subsequently reducing the mechanical strength. Based on these observations it was decided not to use acetone for the cleaning of the solid surfaces, but rather apply a more gentle cleaning process using detergents and cleaning procedures commonly utilized by commercial chocolate manufacturing companies.

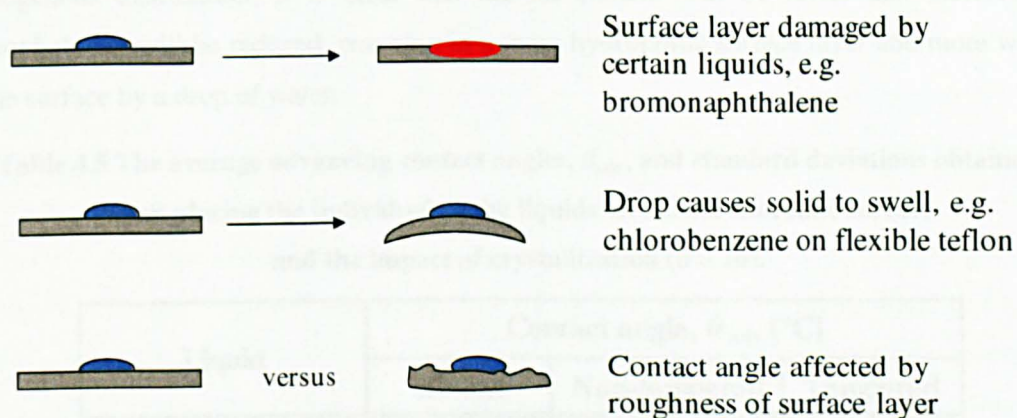


**Figure 4.3 Negative interactions observed between certain probe liquids and solid mould surfaces.**

#### 4.3.2.2 Advancing contact angle of probe liquids on chocolate surfaces

In the same manner as used for the solid mould surfaces, the advancing contact angles of the set of probe liquids on different solid chocolate surfaces are determined. Within the time frame of the measurement no interactions are observed between the chocolate and the probe liquids. However, receding contact angles are not determined, as the chocolate surface layer will dissolve in certain probe liquids. For the advancing contact angle the angle is measured upon contact of the liquid with the “fresh” chocolate surface, and negative interactions between chocolate and probe liquid are assumed to be minimal. Contact angles are determined on both the chocolate–mould interface and the chocolate–air interface.

Three different sets of chocolates and their corresponding advancing contact angles are assessed in this research. Liquid surface tension of chocolate systems can only be determined by melting the chocolate systems, and as a result the impact of crystallization cannot be defined. Advancing contact angles are determined on solid surfaces, and can therefore be used to measure possible differences in surface chemistry between chocolate systems with varying crystallization conditions. Table 4.5 presents the advancing contact angles that are obtained when individual probe liquids are placed on dark chocolate surfaces that are classified by different crystallization conditions, i.e. bloom, non-tempered and tempered. Significant differences are visible especially for the water contact angles, which seem to decrease from the bloomed surface to the non-

tempered and finally the tempered surface. The high value for the bloomed surface (143.7 °) indicates a relatively hydrophobic surface, with limited spreading of the water drop over the bloomed chocolate surface. It is assumed that this is caused by the presence of fat molecules at the surface which are crystallized and responsible for the white appearance of fat bloom (Beckett, 2008). In contrast, the tempered chocolate consists of a homogeneous dispersion of cocoa solids (particles) and sugar crystals in a continuous fat phase consisting of fat crystals and liquid fat (Aguilera et al., 2004). When assuming that the surface layer consists of a similar homogenous distribution, it is clear that the fat content will be lower and therefore the hydrophobicity will be reduced, resulting in a more hydrophilic surface layer and more wetting of the surface by a drop of water.

**Table 4.5 The average advancing contact angles,  $\theta_{adv}$ , and standard deviations obtained when placing the individual probe liquids on a dark chocolate surface and the impact of crystallization (n = 10).**

Liquid	Contact angle, $\theta_{adv}$ [°C]		
	Bloom	Non-tempered	Tempered
Deionised water	143.7 ± 1.3	112.4 ± 1.4	89.0 ± 0.8
Formamide	133.2 ± 0.8	86.6 ± 1.2	82.5 ± 1.7
Diiodomethane	67.1 ± 0.3	72.1 ± 0.8	65.3 ± 1.3
Poly(ethylene glycol)	80.6 ± 1.8	71.9 ± 1.2	77.9 ± 1.1
Benzylalcohol	36.7 ± 0.5	60.7 ± 1.4	55.5 ± 0.8
Hexadecane	29.5 ± 0.2	38.1 ± 1.1	35.7 ± 1.3

Further investigation of the differences between milk and dark chocolate resulted in Table 4.6, which shows the advancing contact angles that are obtained when individual probe liquids are placed on chocolate surfaces that are classified by different ingredient compositions, i.e. dark chocolate (After Eight and Heaven Dark) and milk chocolate (Heaven Milk and AERO).

Both the angles measured on the chocolate–mould interface and on the chocolate–air interface are reported. The differences between these two values are not significant, except for the contact angles of water and formamide on the Heaven milk chocolate surface. Overall it can be concluded that the impact of chocolate composition or ingredients is limited and is not expected to significantly alter the chemistry of the surface layer.



**Table 4.6** The average advancing contact angles,  $\theta_{adv}$ , obtained when placing the individual probe liquids on chocolate surfaces and the impact of ingredients.

Liquid	Contact angle, $\theta_{adv}$ [°C]							
	After eight		Heaven dark		Heaven milk		AERO	
	Mould	Air	Mould	Air	Mould	Air	Mould	Air
Deionised water	105.5	103.9	113.8	108.2	123.4	107.2	111.9	111
Formamide	78.2	83.9	85.7	87.6	97.9	88.4	81.9	83.8
Diiodomethane	71.2	71.7	67.3	69.3	64.6	63.3	62.2	65.7
Poly(ethylene glycol)		77.8		76.0		75.6		79.3
Benzylalcohol		67.3	62.7	63.4	63.8	62.5		66
Hexadecane		41.1		40.4		41.1		43.6

Table 4.7 shows the advancing contact angles that are obtained when individual probe liquids are placed on dark chocolate surfaces that are classified by different cooling regimes, i.e. room temperature (20 °C), refrigerator (4-7 °C) and freezer (-18 °C). Again, both the angles measured on the chocolate–mould interface and on the chocolate–air interface are reported. In contrast to previous results significant differences are observed between the chocolate–mould and the chocolate–air interface for the chocolate systems cooled at room temperature and in a freezer. A general trend cannot be deduced from the results. The presence of water vapour in the air is believed to be responsible for the relatively low water contact angles at the chocolate surfaces cooled at room temperature or in the freezer.

**Table 4.7** The average advancing contact angles,  $\theta_{adv}$ , obtained when placing the individual probe liquids on dark chocolate surfaces and the impact of cooling conditions.

Liquid	Contact angle, $\theta_{adv}$ [°C]						
	Room temperature		Fridge			Freezer	
	Mould	Air	Mould	Air	24h - Mould	Mould	Air
Deionised water	103.6	77.6	97.3	93.0	111.0	116.7	88.8
Formamide	93.6	110.3	85.1	86.4	83.5	115.2	109.9
Diiodomethane	60.7	70.8	62.5	64.1	57.9	59.4	70.1
Poly(ethylene glycol)	65.8		72.3		64.2	71.7	
Benzylalcohol	54.8	58.4	54.9	59.3	45.9	55.7	67.5
Hexadecane	36.7	40	37.7	42.7	32.6	39.3	38.2

### 4.3.2.3 Advancing contact angles of model chocolate systems

The viscoelastic nature and relatively high melting point of chocolate mean that it is not practicable to measure the contact angle of chocolate on different mould surfaces under ambient conditions. Therefore, in order to obtain some indication of the interactions involved and the degree of wetting, cocoa butter and palm olein were used as model chocolate systems. Furthermore, by using one of these two materials as model replacement system to represent chocolate in the application of the Young-Dupré equation, the Work of Adhesion,  $W_a$ , can be calculated. Cocoa butter is a logical choice as a model chocolate system because it is one of the main components of the basic chocolate recipe. Palm olein is chosen as a second reference or model system as its physical and chemical properties are closely related to those of cocoa butter.

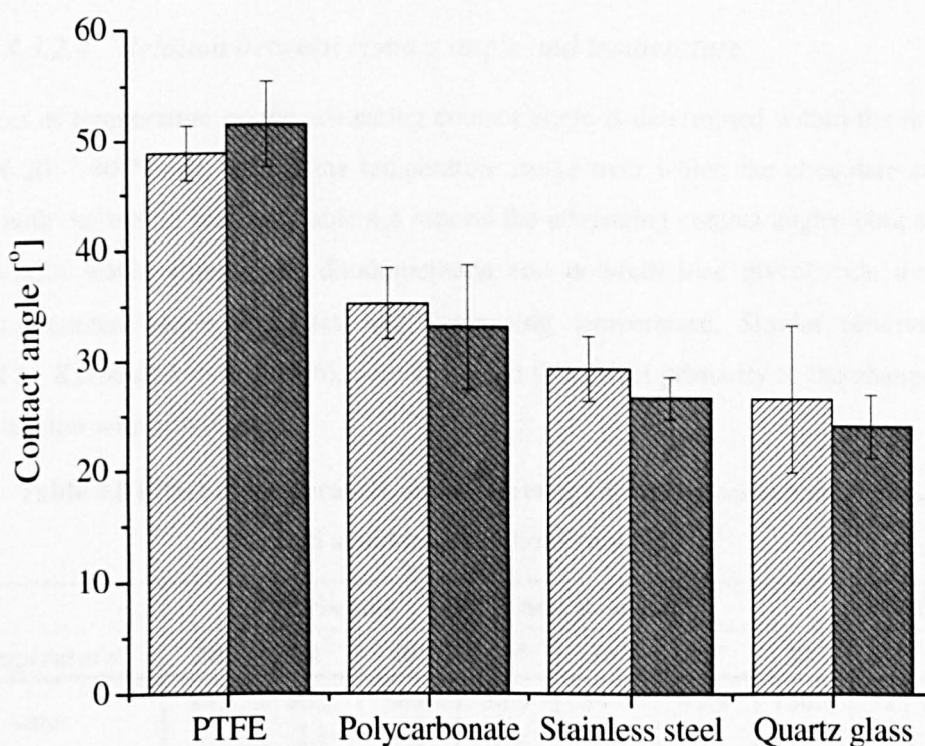


**Figure 4.4** Contact angles of cocoa butter (▨) and palm olein (■), as affected by solid mould surfaces.

**Error bar is representative of the standard deviation, n = 10**

The average advancing contact angles obtained when placing cocoa butter and palm olein on the four mould surfaces are shown in Figure 4.4. No significant differences are present between cocoa butter and palm olein, based on which it is assumed that they can be used interchangeably. As the melting temperature of palm olein lies close to room temperature (20 °C), it cannot be used for experimental surface adhesion force determinations and preference is therefore given to the use of cocoa butter within this research. The results obtained for the cocoa butter contact angle on the different mould surfaces shows the opposite trend observed for the water contact angle with respect to the expected surface chemistry. PTFE has the highest cocoa butter contact angle, indicating a low degree of spreading of the cocoa butter on the PTFE



surface, based on which the assumption is made that PTFE is a relatively hydrophilic surface. From Table 4.4, however, it can be observed that PTFE also gives the highest water contact angle, raising the expectation that PTFE is relatively lipophilic. The results obtained for quartz glass, which has the lowest cocoa butter contact angle, indicate that it is the most lipophilic surface of the four mould materials tested. Again, the water contact angle raises the opposite assumption, that it is the most hydrophilic surface. Fats are normally regarded as hydrophobic components, and it is assumed that the hydrophilic type of behaviour observed for cocoa butter results from the glycerol backbone making up the TAG of cocoa butter. The differences in cocoa butter contact angle between stainless steel and quartz glass appear not to be significant, and the contact angle on polycarbonate is only marginally higher.

#### 4.3.2.4 Relation between contact angle and temperature

The effect of temperature on the advancing contact angle is determined within the temperature range of 20 – 40 °C, as this is the temperature range over which the chocolate comes into contact with the mould surface. Table 4.8 reports the advancing contact angles obtained for the probe liquids water, formamide, diiodomethane and poly(ethylene glycol). On average, the advancing contact angle decreases with increasing temperature. Similar observations are reported by Karbowski et al. (2006), who attributed this effect primarily to the change in liquid surface tension with temperature.

**Table 4.8 Effect of temperature on the average advancing contact angle,  $\theta_{adv}$ , and standard deviations (n = 10).**

Temperature	Polycarbonate			Stainless steel			PTFE		
	20°	30°	40°	20°	30°	40°	20°	30°	40°
water	89.8 1.1	90.2 2.3	88.6 1.8	58.9 1.1	54.4 1.9	49.9 1.4	130.5 1.1	125.9 1.9	122.2 1.6
formamide	62.8 0.9	60.6 0.9	58.1 0.9	51.7 1.6	47.5 1.2	42.7 2.7	108.4 1.3	105.8 0.8	102.7 1.1
diiodomethane	51.9 1.5	45.2 1.8	40.7 1.8	44.8 1.9	41.5 1.7	37.6 1.1	98.6 1.1	95.0 0.8	91.3 1.4
poly(ethylene glycol)	44.7 2.1	45.7 1.2	39.1 1.1	41.0 1.9	34.5 2.5	31.8 0.9	91.9 1.3	89.8 1.4	88.2 1.0

#### 4.3.2.5 Contact angle hysteresis

The dynamic process used in this research to determine the advancing and receding contact angles of a set of probe liquids describes the interactions taking place at the liquid-solid boundary during the respective wetting and de-wetting processes (Karbowski et al., 2006). Contact angle hysteresis, as described in section 3.3.1.2 and equation [3-2], is referred to as the difference between the advancing and the receding contact angle, and is an indication of the quality of the solid surface. An ideal surface would have almost identical advancing and receding contact angles. With increasing surface heterogeneity or surface roughness the value of the contact angle hysteresis,  $H$ , will increase.

Within this research the advancing and receding contact angles are measured for water, formamide and diiodomethane on the four solid mould surfaces. The results obtained for the contact angle hysteresis,  $H$ , are presented in Table 4.9. Although there are slight differences between the three probe liquids the overall trend is clear. It appears that all four materials have relatively high values of contact angle hysteresis, due to probably heterogeneous surface chemistry or surface roughness. The polycarbonate and stainless steel surfaces, which have both been treated with abrasive paper, show similar values for  $H$ . Therefore it is reasonable to believe that their surface roughness is the main cause of their deviation from ideality. Quartz glass, which is used as a reference material, shows the lowest level of contact angle hysteresis.

**Table 4.9 Contact angle hysteresis,  $H$ , of water, diiodomethane and formamide on the four different mould materials.**

	$H_{\text{water}}$	$H_{\text{formamide}}$	$H_{\text{diiodomethane}}$
Polycarbonate	57.4	43.5	41.2
Stainless steel	52.7	42.5	30.3
PTFE (Teflon)	39.9	37.1	37.7
Quartz glass	30.5		10.3

##### 4.3.2.5.1 Surface microstructure

In order to quantify the differences in surface roughness, confocal laser scanning microscopy (CLSM) was applied to analyse the microstructure of the four mould materials used in this research, as is visualized in Figure 4.5 by the  $x/z$ -profiles (top images) and the 3D-structures (bottom images). The surface profile indicates the variation in height of the surfaces studied. Both PTFE and quartz glass show limited roughness at a microscopic scale, with a relatively flat  $x/z$ -profile. An increase in surface roughness can be seen for the polycarbonate and stainless steel surfaces. Comparison of these two surfaces indicates that stainless steel has the highest

surface roughness, with an average height difference between the peaks and valleys of  $\sim 5 \mu\text{m}$ , whereas the difference for polycarbonate is  $\sim 3 \mu\text{m}$ .

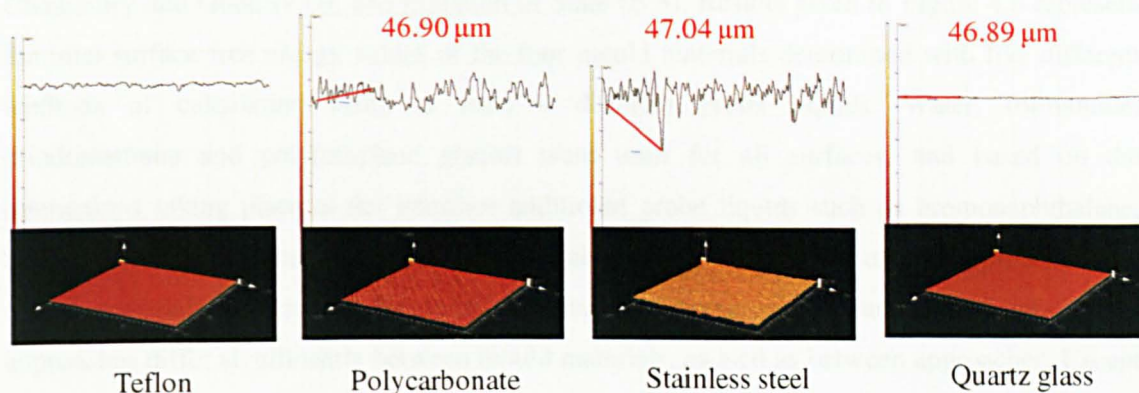


**Figure 4.5** Surface microstructure of the solid mould materials.

The trend described by Table 4.9 for the macroscopic surface roughness shows good agreement with the results obtained for the microscopic surface roughness. Based on these results it is assumed that the quartz glass surface approaches ideality, and can therefore be used as a reference surface. The surface roughness of the other mould materials decreases from stainless steel to polycarbonate and finally to PTFE, which has the lowest surface roughness of these surfaces and approaches ideality from a structural point of view.

### 4.3.3 Surface energy of solid mould materials

The total surface energy of solid mould materials and its components are calculated via the semi-empirical approaches described in section 3.3.1.3, using the experimental data obtained for the surface tension and contact angle described in sections 4.3.1 and 4.3.2, respectively. Depending on the semi-empirical approach adopted in this research, the surface chemistry in terms of the intermolecular interaction forces at the interface of the different solid materials will be discussed in more detail. This approach is applied to both the solid mould and chocolate surfaces. For the mould materials the impact of temperature on the surface energy is determined in the temperature range  $20 - 40 \text{ }^\circ\text{C}$ . Finally, a wetting envelope is developed to link the surface energy of different mould materials with that of chocolate, in order to determine the wetting behaviour of chocolate on the different materials.



#### 4.3.3.1 Semi-empirical approaches

The semi-empirical approaches applied for the determination of the surface energy of the different mould surfaces are: Zisman (Z), Fowkes (F), Owens & Wendt (O W), van Oss – Chaudhury and Good (v O), and Equation of State (E S). Results given in Figure 4.6 represent the total surface free energy values of the four mould materials determined with five different methods of calculation using at least 4 different probe liquids. Water, formamide, diiodomethane and poly(ethylene glycol) were used for all surfaces, and based on the interactions taking place at the interface additional probe liquids such as bromonaphthalene, benzylalcohol, hexadecane or n-octane were also used. Comparison of the approaches and mould materials shows that the calculated surface energy values based on these various approaches differ significantly between mould materials, as well as between approaches. Except for polycarbonate, the critical surface energy values calculated using the Zisman approach lie below the total surface energy values achieved with all other methods. Furthermore, the standard deviation is much higher compared to other approaches. The total surface energy values calculated for polycarbonate and PTFE by the different approaches are in good agreement, but for both stainless steel and quartz glass much more deviation between the values calculated by the different approaches can be observed.

Statistical analysis (one-way ANOVA,  $p < 0.05$ ) is used for the interpretation of Figure 4.6. Boxplots are used to visualize the data, with the box between the lower and upper quartiles representing the middle 50% of the data and the line across the box representing the median. Observations beyond the extent of the whiskers are called outliers and are represented as individual points (circles). Because of the relatively low sample size, a boxplot is the best method for comparison of the approaches and surfaces. Analysis of variance is used to test the null hypothesis,  $H_0$ , that the surface energy means obtained by the different approaches for a particular surface are equal at a confidence level of 95%. It is assumed that the data follow a normal distribution, as a result of which the t-test can be used. The alternative hypothesis,  $H_1$ , is that the means for a particular surface obtained by the different approaches are not equal. As the Levene test of homogeneity of variances is significant ( $p < 0.05$ ), the hypothesis of equality of variances is rejected for all surfaces. The ANOVA or analysis of variance gives a p-value  $< 0.05$  for all surfaces, rejecting the  $H_0$  and accepting the  $H_1$  in all cases, i.e. the mean total surface energy values calculated via the different approaches are statistically not equal. Rejection of the equality of variances means that the Tamhane's test should be used for multiple comparisons of all pairs of mean differences.



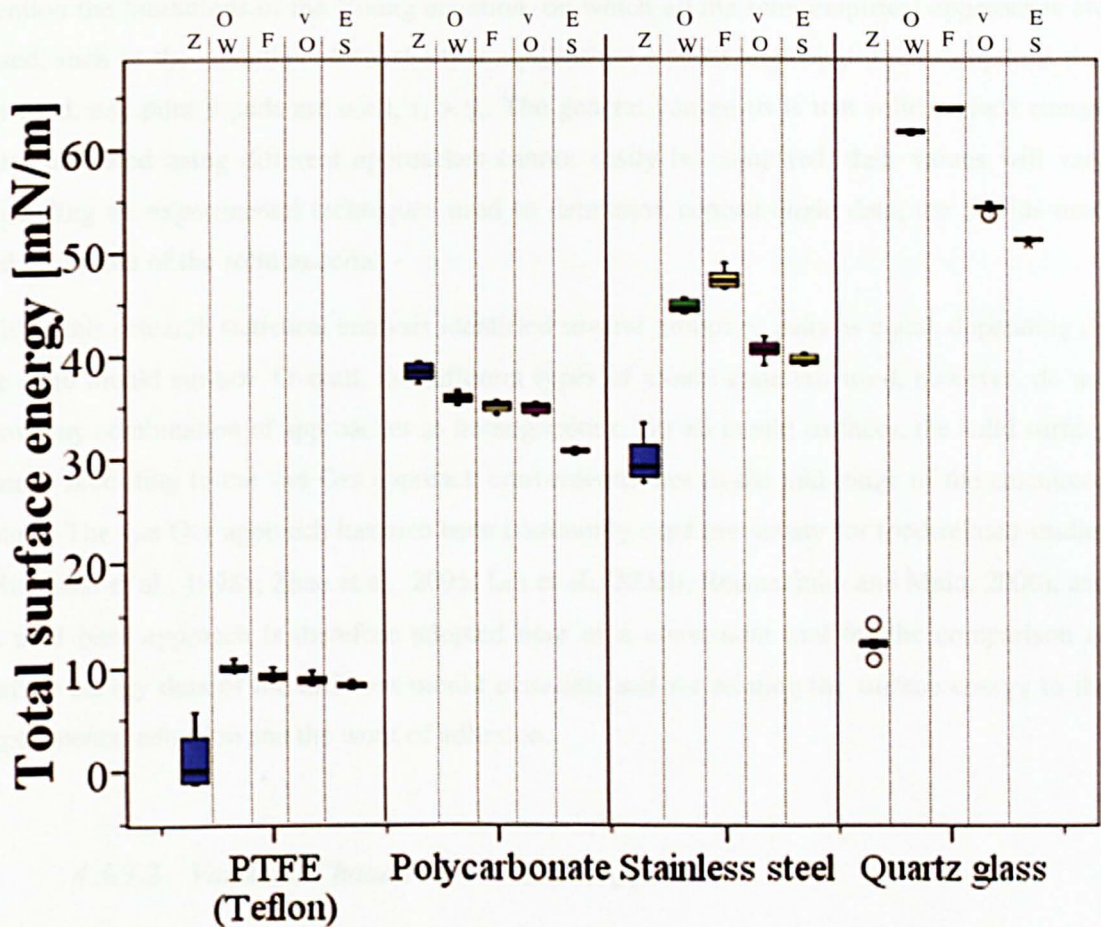


Figure 4.6. The total surface energy of different mould materials calculated using various empirical approaches.

The empirical approaches used where: Zisman (■), Fowkes (■), Owens & Wendt (■), van Oss, Chaudhury & Good (■) and Equation of State (■). Outliers are indicated by ○, and not used in the calculation of the median and distance from the median.

Comparison of the approaches per surface indicates that for the polycarbonate surface the total surface energy values obtained via the Fowkes and the van Oss, Chaudhury and Good approaches are not statistically significant different ( $p = 0.999$ ). For stainless steel the approaches that give statistically similar values for the total surface energy are the approach of van Oss, Chaudhury and Good and the Equation of State ( $p = 0.275$ ). In the case of PTFE, both the approach pair Fowkes – van Oss, Chaudhury and Good, and van Oss, Chaudhury Good – Equation of State, calculate similar values for  $\gamma_s^{\text{tot}}$ . Finally, for quartz glass the mean results obtained via the 5 semi-empirical approaches are all significantly different ( $p = 0.000$ ).

In general, the critical surface energy values obtained by the approach of Zisman fall below the total surface free energy values obtained with the other approaches. Reasoning for this deviation is given by Gindl et al. (2001), who describe that the value obtained by Zisman is an empirical parameter, rather than the total solid surface free energy. They recommend the use of the acid–base or van Oss, Chaudhury and Good approach, as the value calculated for the total solid surface energy via this approach lies close to the mean of all methods. Karbowiak et al. (2006)

mention the limitations of the Young equation, on which all the semi-empirical approaches are based, such as the deviations from the true equilibrium contact angle and the assumptions that are used, e.g. pure liquids are used,  $\gamma_l > \gamma_s$ . The general consensus is that solid surface energy data calculated using different approaches cannot easily be compared, their values will vary depending on experimental techniques used to determine contact angle data, the liquids used and the nature of the solid material.

Within this research statistical analysis identified several groups or pairs as equal, depending on the solid mould surface. Overall, the different types of mould materials used, however, do not show any combination of approaches as homogeneous. For all mould surfaces, the solid surface energy according to the van Oss approach conveniently lies in the mid-range of the calculated values. The van Oss approach has also been commonly used previously for food-related studies (Michalski et al., 1998a; Zhao et al., 2005; Liu et al., 2006b; Rosmaninho and Melo, 2006), and its acid–base approach is therefore adopted here as a convenient tool for the comparison of surface energy data of the different mould materials and for relating the surface energy to the experimental adhesion and the work of adhesion.

#### 4.3.3.2 *Van Oss, Chaudhury and Good approach*

Using the van Oss, Chaudhury and Good or acid–base approach, the surface characteristics of the different mould surfaces are calculated. Figure 4.7 shows the distribution of the total surface energy data in a box plot for the four individual mould surfaces. A general ranking of  $\gamma_s^{\text{tot}}$  can be observed: PTFE < polycarbonate < stainless steel < quartz glass. Statistical analysis (ANOVA - F test,  $p < 0.05$ ) confirmed that all the mould surfaces have significantly different values for  $\gamma_s^{\text{tot}}$ . This trend or ranking, with the lowest value of  $\gamma_s^{\text{tot}}$  for PTFE and the highest for quartz glass, correlates well with trends of literature values (Lewin et al., 2005; Gülec et al, 2006). However, the actual numerical values do deviate, as a result of different empirical approaches used for the surface energy calculation and different experimental conditions. On average, the surface energy of PTFE reported in this research,  $8.9 \text{ mN m}^{-1}$ , is fairly low compared to values reported in literature, which range from  $18.6$  to  $23.9 \text{ mN m}^{-1}$  (Lewin et al., 2005). It can be noticed that the experimental contact angles obtained on the PTFE surface in this research were moderately higher than those observed by Lyklema (2000). It is suspected that the deviation may be caused by the relative inaccuracy of the DropSnake method at high contact angles, leading as a result to a lower total surface energy. An experimental condition that may cause deviations is the cleaning procedure used. General surface energy experiments often use extensive cleaning procedures to ensure a clean surface that is close to ideality. Within this research relatively gentle cleaning procedures are used, similar to commercial chocolate manufacturing practices. Tsibouklis and Nevell (2003) studied ultra-low surface energy polymers, as these are known to exhibit non-stick characteristics. According to them, the value of  $\gamma_s^{\text{tot}}$  of polymeric materials is

primarily defined by the chemical structure of the surface layer, with the following ranking of the constituent groups:  $> \text{CH}_2$  (36)  $> \text{CH}_3$  (30)  $\gg \text{CF}_2$  (23)  $> \text{CF}_3$  (15). Furthermore, with respect to PTFE, they mention the fact that PTFE coatings often possess lower surface energies than their substrates, and that the degree of fluorination is critical. Overall, it can be observed that with minor changes in surface chemistry the surface energy will change. As a result there is not a standard value for the solid surface energy, not even for quartz glass surfaces. Janczuk and Zdziennicka (1994) discuss the surface free energy of quartz and its components based on the use of the van Oss acid–base method and the approach of Fowkes. For  $\gamma_s^{\text{tot}}$  the results varied, depending on the probe liquids used, but the average value reported was  $57.20 \text{ mJ m}^{-2}$ . This is in good agreement with the results obtained in this research ( $54.36 \text{ mN m}^{-1}$ ).

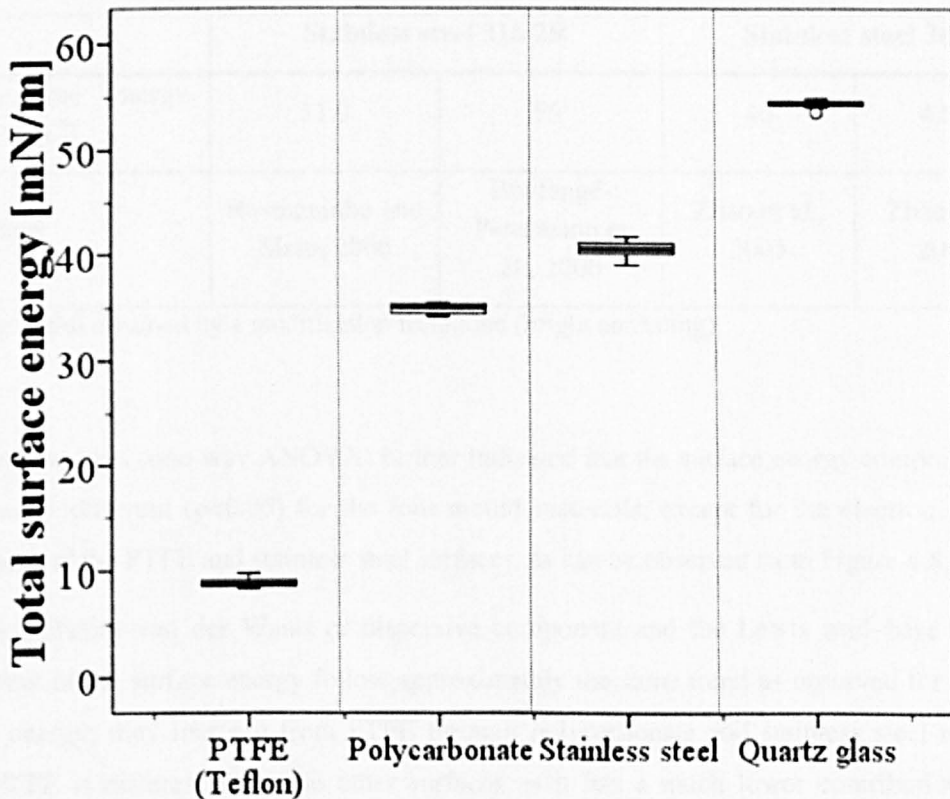


Figure 4.7 Total surface energy,  $\gamma_s^{\text{tot}}$ , of the different mould materials according to the Lifshitz–van der Waals / acid–base or van Oss, Chaudhury and Good approach.

Taking stainless steel as an example, there are various types of stainless steel such as type 304, 316 and 317. Although the composition of the steel may be relatively similar for these different types, the surface layer shows significant differences with respect to surface texture, roughness and chemistry, which subsequently results in varying surface energies. Research by Boulangé-Petermann et al. (2006) investigated different methods used to modify the surface finishing, such as bright annealing, pickling and texturing, and their effect on the surface energy of a stainless steel surface. All these different final surface conditions were observed to behave independently, showing surface energies,  $\gamma_s^{\text{tot}}$ , ranging from 38 to  $58 \text{ mN m}^{-1}$ .



Furthermore, the surface conditions influenced the surface chemistry, as different polar and dispersive components were obtained for the solid surface energy. A comparison of literature data on stainless steel 316 and 304 is given in Table 4.10. From these data it can be observed that stainless steel 316 has on average a solid surface free energy of  $53.5 \text{ mN m}^{-1}$ , whereas stainless steel 304 has a solid surface energy of approximately  $41 \text{ mN m}^{-1}$ . The type of stainless steel used in this research is 316 and, similar to the results obtained for PTFE, the result obtained in this research for the total surface free energy of stainless steel ( $40.57 \text{ mN m}^{-1}$ ) is relatively low compared to those found in literature ( $53.5 \text{ mN m}^{-1}$ ).

**Table 4.10 Surface free energy data of different types of stainless steel found in literature.**

	Stainless steel 316 2R		Stainless steel 304	
Surface free energy, $\gamma_s^{\text{tot}}$ [ $\text{mN m}^{-1}$ ]	51.9	55 <sup>1</sup>	40	42.62
Reference	Rosmaninho and Melo, 2006	Boulangé-Petermann et al., 2006	Zhao et al., 2005	Zhao et al., 2004a

<sup>1</sup> Surface finish obtained by a modification technique (bright annealing).

Statistical analysis (one-way ANOVA) further indicated that the surface energy components are significantly different ( $p < 0.05$ ) for the four mould materials, except for the electron acceptor component of the PTFE and stainless steel surfaces, as can be observed from Figure 4.8.

Both the Lifshitz–van der Waals or dispersive component and the Lewis acid–base or polar component of the surface energy follow approximately the same trend as observed for the total surface energy; they increase from PTFE through polycarbonate and stainless steel to quartz glass. PTFE is different from the other surfaces as it has a much lower contribution of the dispersive component, and for quartz glass the opposite is true as it holds a much higher polar contribution to the surface free energy compared to the other surfaces. The dispersive component can be observed to be the component dominating the total surface energy of PTFE. Although the electron acceptor contribution is statistically only similar for stainless steel and PTFE, there is little variation for the other surfaces. Based on these observations, the assumption is made that the electron donor contribution to the surface free energy is the main differentiating factor amongst the different mould surfaces.



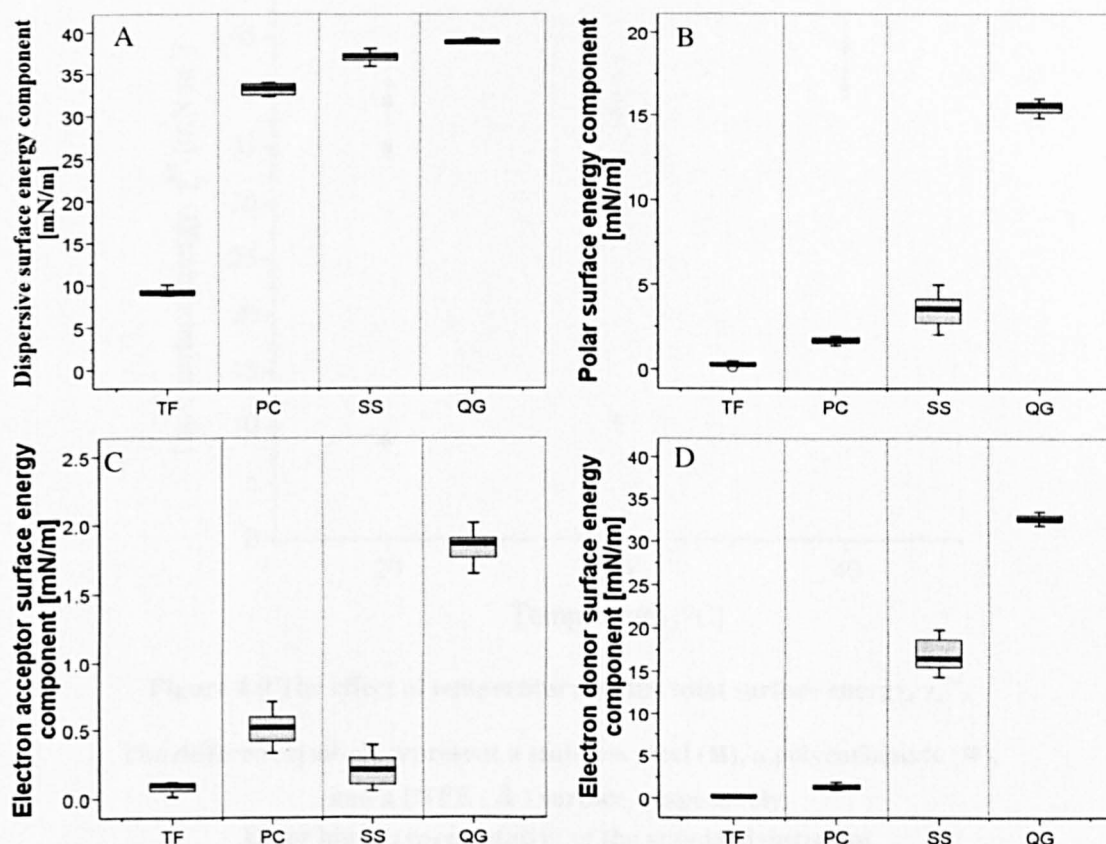


**Figure 4.8** Surface free energy components of the different solid mould surfaces according to the Lifshitz–van der Waals / acid–base method of van Oss, Chaudhury and Good.

The dispersive component (A) represents the Lifshitz–van der Waals,  $\gamma_s^{lw}$ , interactions, whereas the polar component (B) represents the Lewis acid–base,  $\gamma_s^{ab}$ , interactions. The latter can be further subdivided into the electron acceptor (C),  $\gamma_s^+$ , and the electron donor (D),  $\gamma_s^-$ , components of the total surface free energy,  $\gamma_s^{tot}$ .

#### 4.3.3.3 Temperature

The effect of temperature on the surface energy of solid surfaces is determined by using the results obtained for the contact angles and surface tension within the temperature range of 20 – 40 °C. For this calculation the van Oss approach is applied and only the results of water, diiodomethane and formamide are used. The results shown in Figure 4.9 indicate a linear relation between  $\gamma_s^{tot}$  and temperature for all three mould materials within the temperature range investigated. However, the effect of temperature is not statistically significant at all temperatures and for all surfaces. Based on these results it is assumed that within the temperature range used for commercial chocolate manufacturing, limited changes in surface energy are present, and as a result it is proposed to use the data obtained at 20 °C for future references within this research.

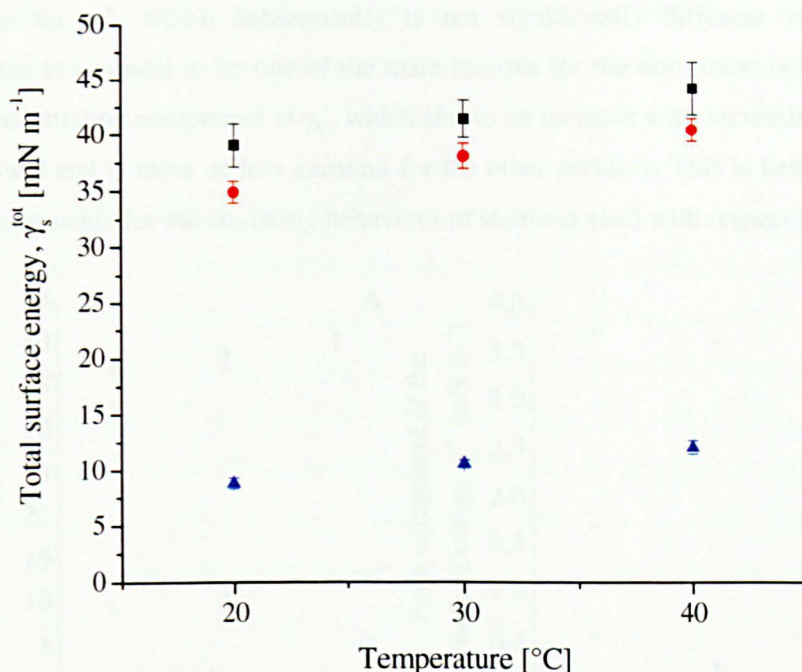


**Figure 4.9** The effect of temperature on the total surface energy,  $\gamma_s^{\text{tot}}$ .

The different symbols represent a stainless steel (■), a polycarbonate (●), and a PTFE (▲) surface, respectively.

Error bar is representative of the standard deviation.

Zhao et al. (2004a) investigated the effect of temperature on the surface free energy of stainless steel 304, titanium, and diamond-like carbon (DLC) and tetrahedral amorphous carbon (ta-C) coatings in the temperature range 20 – 95 °C. Their results showed on average a decrease of  $\gamma_s^{\text{tot}}$  with increasing temperature for all surfaces. For the stainless steel and titanium surface this decrease was, however, not statistically significant in the temperature range 20 – 44 °C. This effect is opposite to the observations made in this research, where an increase in  $\gamma_s^{\text{tot}}$  with increasing temperature was observed. According to Zhao et al. (2004a) the effect observed can be explained by expressing the surface free energy,  $\gamma_s$ , as a function of surface internal energy,  $U_s$ , temperature,  $T$ , and surface entropy,  $S_s$ :

$$\gamma_s = U_s - TS_s . \quad [4-2]$$

An increase in temperature is responsible for an increase in surface entropy, consequently causing the surface energy to decrease with increasing temperature.

Investigation of the effect of temperature on the surface energy components resulted in the formulation of Figure 4.10. Similar to  $\gamma_s^{\text{tot}}$ , the dispersive or Lifshitz–van der Waals component,  $\gamma_s^{\text{lw}}$ , increased with increasing temperature. The effect of temperature on the polar or Lewis acid–base component,  $\gamma_s^{\text{ab}}$ , however, varied depending on the mould material. For stainless steel and PTFE  $\gamma_s^{\text{ab}}$  stays more or less constant, whereas for polycarbonate a decrease with increasing temperature is observed. As  $\gamma_s^{\text{ab}}$  is calculated from the electron acceptor,  $\gamma_s^+$ , and electron donor,  $\gamma_s^-$ , components, respectively, their effect on the trends observed can be determined. A large



error characterizes  $\gamma_s^+$ , which subsequently is not significantly different with increasing temperature, but is assumed to be one of the main reasons for the non linear behaviour of  $\gamma_s^{ab}$ . The main differentiating component is  $\gamma_s^-$ , which shows an increase with increasing temperature for stainless steel and is more or less constant for the other surfaces. This is believed to be the main factor responsible for the deviating behaviour of stainless steel with respect to  $\gamma_s^{ab}$ .

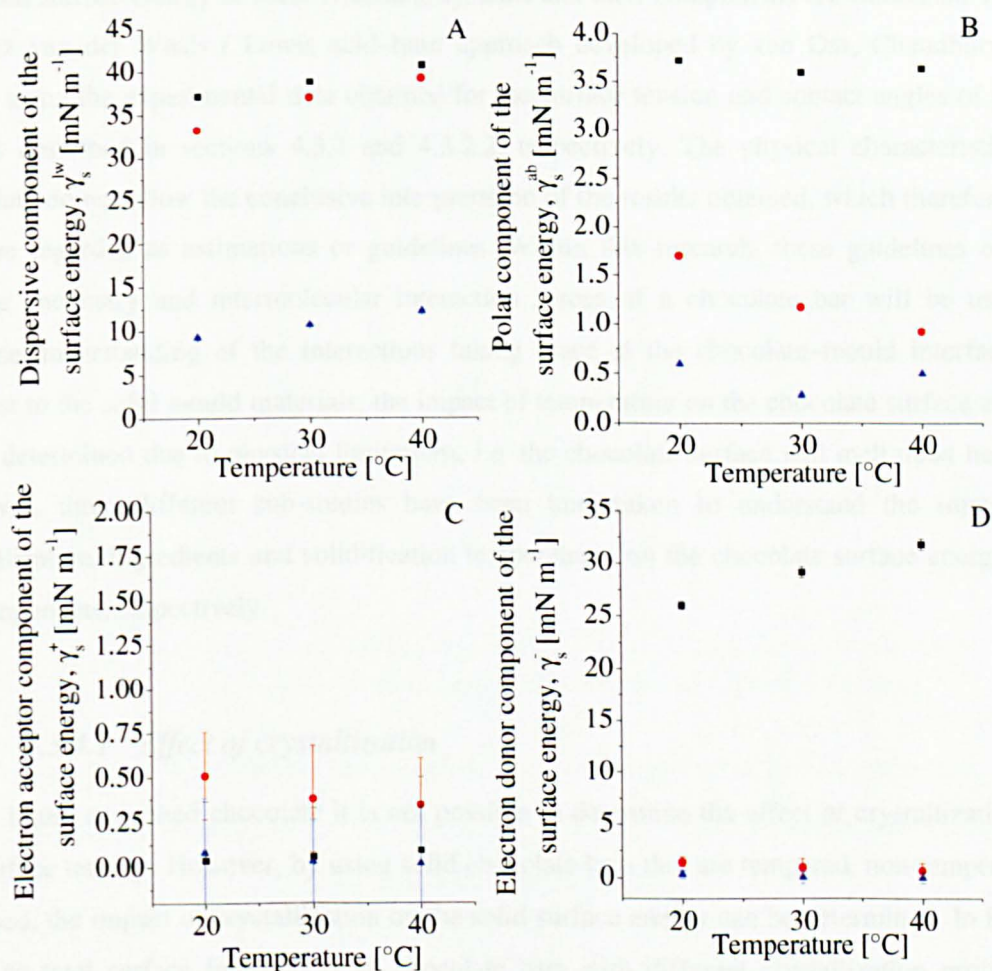


**Figure 4.10** The effect of temperature on the dispersive or Lifshitz–van der Waals component (A), the polar or Lewis acid–base component (B), the electron acceptor component (C) and the electron donor component (D) of the total surface energy.

In all graphs (■) represents a stainless steel surface, (●) a polycarbonate, and (▲) a PTFE surface.

Error bar is representative of the standard deviation.

The work reported by Zhao et al. (2004a) also investigated the effect of temperature on the surface energy components. Results were similar to those observed for  $\gamma_s^{tot}$ , showing a decrease with increasing temperature, except for the acid–base or polar component,  $\gamma_s^{ab}$ , whose behaviour depended on the semi-empirical approach used to calculate the data. For stainless steel and titanium,  $\gamma_s^{ab}$  increased with increasing temperature, which was hypothesized to be a result of the increase of  $\gamma_s^+$  with temperature. However, the main increase of  $\gamma_s^+$  was observed at the

higher temperatures, which are not of concern in this research. In the lower temperature range, between 20 and 40 °C, limited variation in surface energy and its components is observed.

#### 4.3.4 Surface energy of chocolate

The total surface energy of solid chocolate systems and their components are calculated via the Lifshitz–van der Waals / Lewis acid–base approach developed by van Oss, Chaudhury and Good, using the experimental data obtained for the surface tension and contact angles of probe liquids described in sections 4.3.1 and 4.3.2.2, respectively. The physical characteristics of chocolate do not allow the conclusive interpretation of the results obtained, which therefore can only be regarded as estimations or guidelines. Within this research, these guidelines on the surface chemistry and intermolecular interaction forces of a chocolate bar will be used to increase understanding of the interactions taking place at the chocolate–mould interface. In contrast to the solid mould materials, the impact of temperature on the chocolate surface energy is not determined due to physical limitations, i.e. the chocolate surface will melt upon heating. However, three different sub-studies have been undertaken to understand the impact of crystallization, ingredients and solidification temperatures on the chocolate surface energy and its components, respectively.

##### 4.3.4.1 Effect of crystallization

Using liquid or melted chocolate it is not possible to determine the effect of crystallization on the surface tension. However, by using solid chocolate bars that are tempered, non-tempered or bloomed, the impact of crystallization on the solid surface energy can be determined. In Figure 4.11 the total surface free energy of chocolate bars with different crystallization profiles is plotted. The results obtained previously for the surface free energy of polycarbonate using the van Oss approach are included as a reference. Statistical analysis has confirmed that  $\gamma_s^{\text{tot}}$  is not significantly different ( $p < 0.05$ ) for the chocolate bars with varying crystallization characteristics. A significant difference ( $p > 0.05$ ) is observed, on the other hand, between the solid chocolate bars and the polycarbonate mould surface.

The application of the Van Oss method allows the determination of the surface chemistry characteristics of the chocolate bars, as can be seen in Figure 4.12. In contrast to  $\gamma_s^{\text{tot}}$ , significant differences can be observed for the surface energy components as a result of the different crystallization profiles. The general conclusion is that the chocolate surfaces have a primarily dispersive character. The Lewis acid–base or polar component has a large error and non-normal distribution for the bloomed and tempered chocolate surfaces.



This is driven by the electron acceptor component for the bloomed surface and by the electron donor component for the tempered surface. For the other surfaces the electron donor and electron acceptor components are similar and very close to the characteristics of polycarbonate.

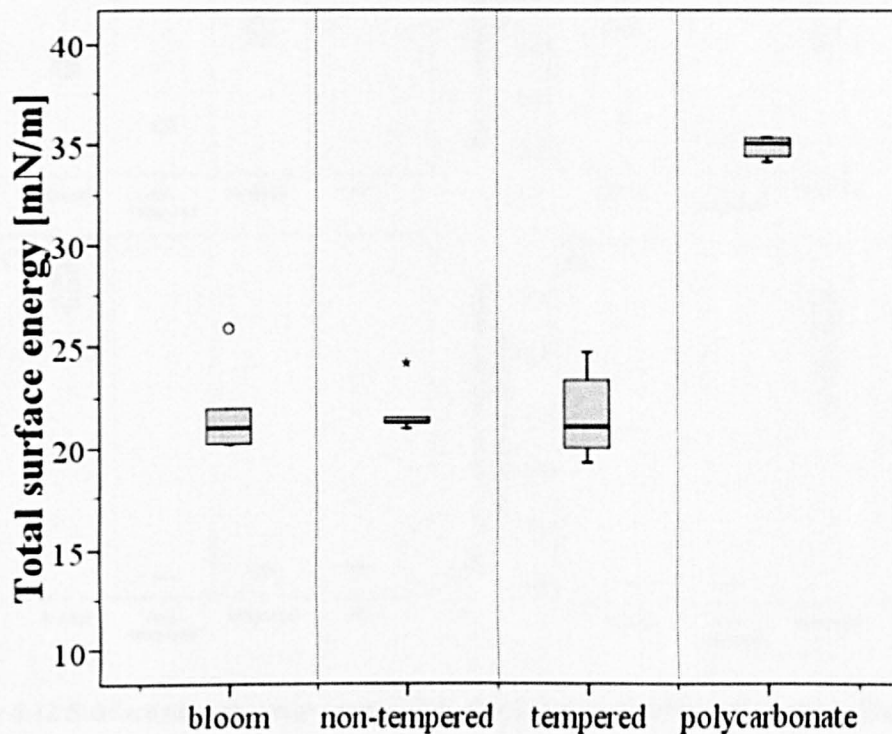
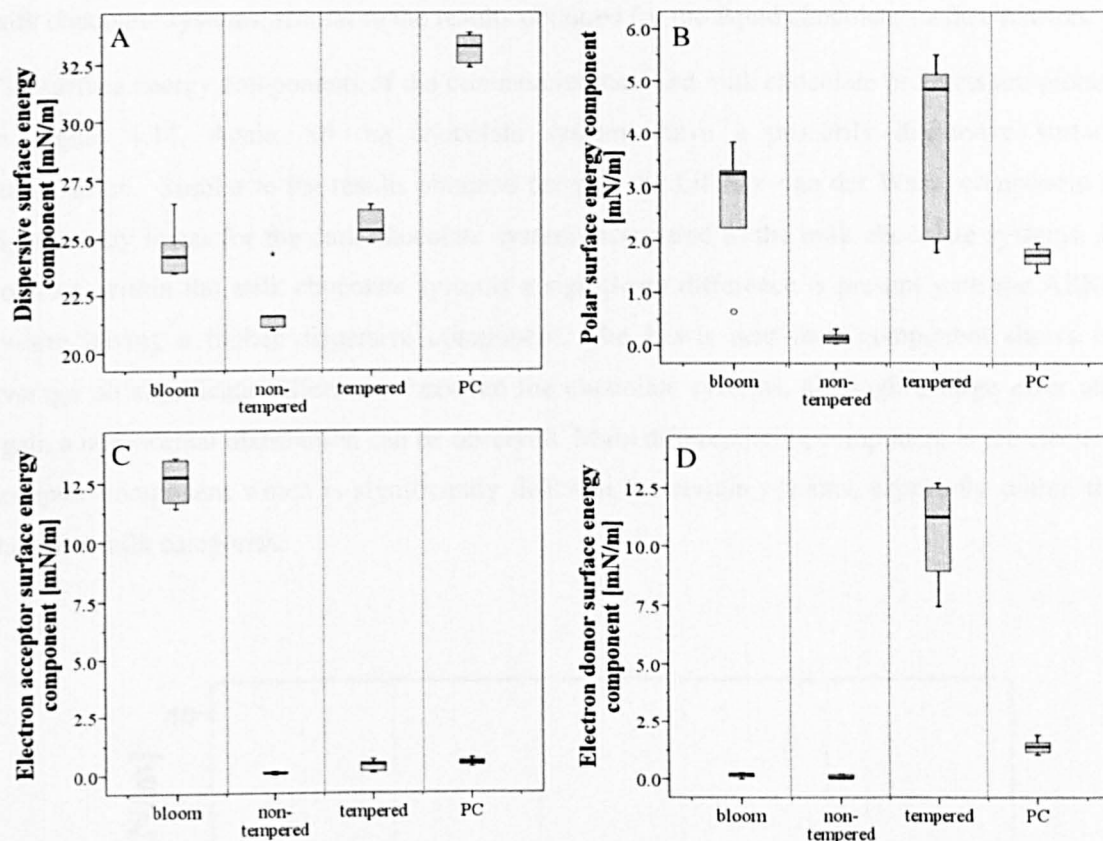


Figure 4.11 Total surface energy of dark chocolate as affected by crystallization.

Outliers are indicated by  $\circ$  or  $*$ , and not used in the calculation of the median and distance from the median.

Bloomed chocolate can only be obtained after solidification and storage, and the experimental adhesion force can therefore not be determined as this requires melting and recrystallization of the chocolate system. Based on the results obtained for  $\gamma_s^{\text{tot}}$ , limited differences in adhesion are expected for the tempered and non-tempered chocolate systems. One of the main questions is to what extent the differences in surface energy components are a result of the presence of different cocoa butter polymorphs. As these are formed upon cooling and in part during storage, it is expected that their effect will be limited for the adhesion force determinations. Contact between the liquid chocolate and mould surface is created at a temperature where a small amount of crystals is present, and the crystals formed upon cooling are assumed not to impact on the interactions at the chocolate–mould interface.



**Figure 4.12** Surface energy components of dark chocolate as affected by crystallization, calculated according to the Lifshitz–van der Waals / acid–base method developed by van Oss, Chaudhury and Good.

The dispersive component (A) represents the Lifshitz–van der Waals,  $\gamma_s^{lw}$ , interactions, whereas the polar component (B) represents the Lewis acid–base,  $\gamma_s^{ab}$ , interactions. The latter can be further subdivided into the electron acceptor (C),  $\gamma_s^+$ , and the electron donor (D),  $\gamma_s^-$ , components of the total surface free energy,  $\gamma_s^{tot}$ .

Outliers are indicated by  $\circ$  or  $*$ , and not used in the calculation of the median and distance from the median.

#### 4.3.4.2 Effect of ingredients

Comparison of the liquid surface tension of chocolate systems with varying total cocoa solids content, as was discussed in section 4.3.1.2, indicated significant differences between dark chocolate (52% cocoa solids) and milk chocolate (29% cocoa solids). In Figure 4.13 the total solid surface free energy of a set of commercial dark and milk chocolate products is presented. The results obtained for the commercial dark chocolate systems are not significantly different ( $p < 0.05$ ), and are in good agreement with the results obtained for the tempered dark chocolate. Similarly, no significant difference ( $p < 0.05$ ) is observed for the milk chocolate systems. However, the dark chocolate systems are significantly different ( $p > 0.05$ ) from the milk

chocolate systems, and show a value for  $\gamma_s^{\text{tot}}$  that lies approximately  $10 \text{ mN m}^{-1}$  below that for milk chocolate systems, similar to the results obtained for the liquid chocolate surface tension.

The surface energy components of the commercial dark and milk chocolate products are plotted in Figure 4.14. Again, all the chocolate systems have a primarily dispersive surface composition. Similar to the results obtained for  $\gamma_s^{\text{tot}}$ , the Lifshitz–van der Waals component is significantly lower for the dark chocolate systems compared to the milk chocolate systems. In contrast, within the milk chocolate systems a significant difference is present with the AERO system having a higher dispersive component. The Lewis acid–base component shows on average no significant differences between the chocolate systems, although a large error and again a non-normal distribution can be observed. Main differentiating component is the electron acceptor component which is significantly different for certain systems, especially within the dark and milk categories.

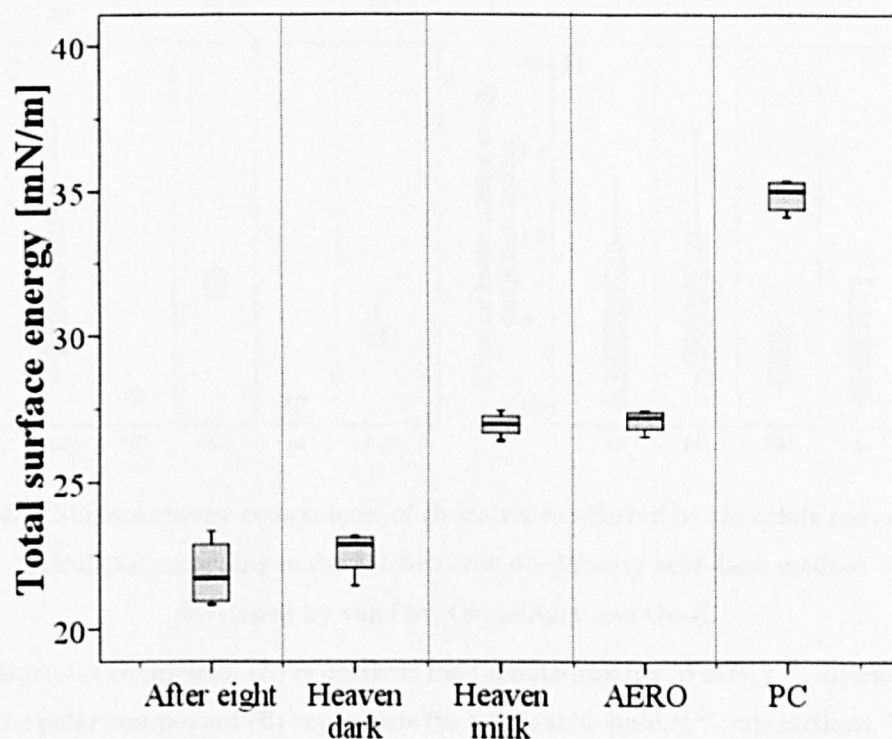


**Figure 4.13 Total surface energy of chocolate as affected by chocolate composition.**

**After Eight (52% cocoa solids) and Heaven Dark (min. 43% cocoa solids) are both dark chocolate systems; Heaven Milk (min. 30% cocoa solids) and AERO (min. 25% cocoa solids) are both milk chocolate systems.**

The main conclusion that can be drawn from the results discussed here is that dark chocolate and milk chocolate systems are significantly different from a surface free energy point of view. Although the surface characteristics or surface chemistry may not be that different, as both

systems show primarily dispersive or Lifshitz–van der Waals interactions,  $\gamma_s^{\text{tot}}$  is significantly different for these systems and this often drives adhesion. To what extent the physical characteristics such as viscosity, hardness or melting point play an important role in the surface chemistry is not known. It is assumed, however, as the contact angle and surface tension data are obtained under constant conditions, that the data calculated for the surface free energy are representative for the systems investigated.

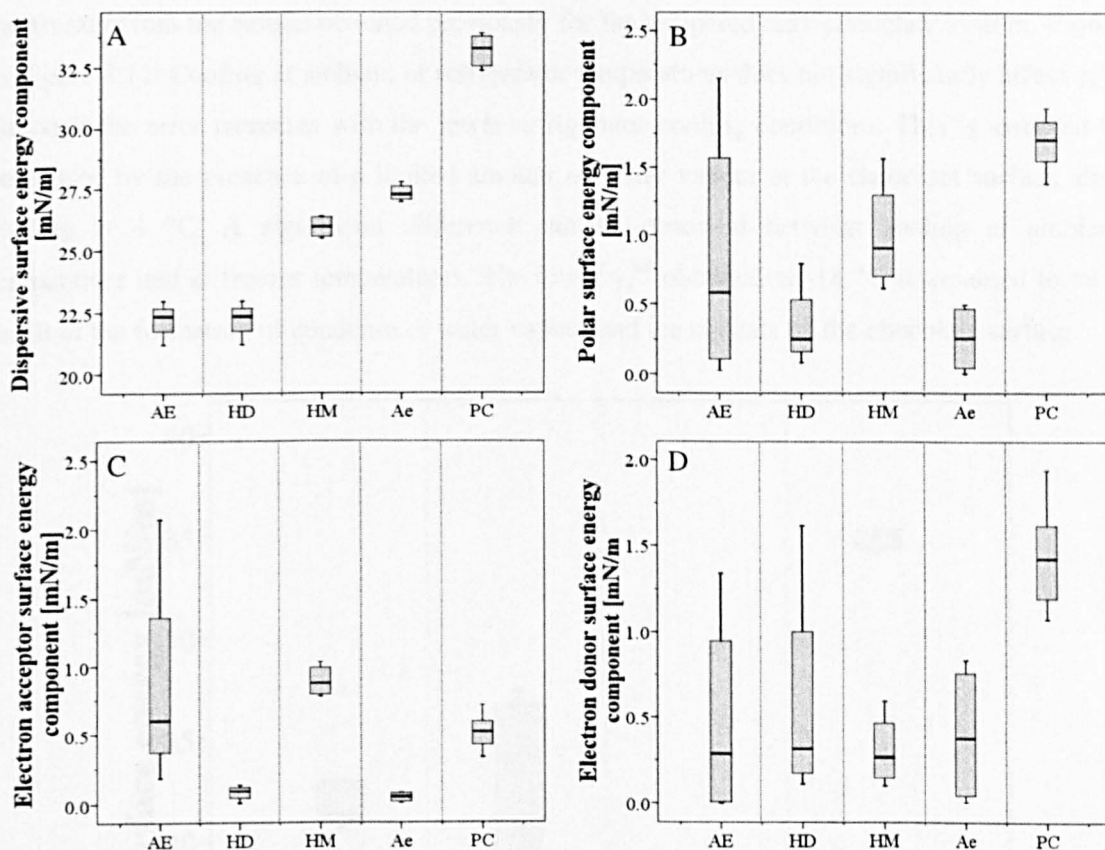


**Figure 4.14** Surface energy components of chocolate as affected by chocolate composition, calculated according to the Lifshitz–van der Waals / acid–base method developed by van Oss, Chaudhury and Good.

The dispersive component (A) represents the Lifshitz–van der Waals,  $\gamma_s^{\text{lw}}$ , interactions, whereas the polar component (B) represents the Lewis acid–base,  $\gamma_s^{\text{ab}}$ , interactions. The latter can be further subdivided into the electron acceptor (C),  $\gamma_s^+$ , and the electron donor (D),  $\gamma_s^-$ , components of the total surface free energy,  $\gamma_s^{\text{tot}}$ . AE refers to After Eight, HD to Heaven Dark, HM to Heaven Milk, Ae to AERO and PC to polycarbonate.



## 4.3.4.3 Effect of cooling temperature

Preliminary research (Hoare, 2007) has suggested that the cooling conditions and especially the cooling temperature impact the surface free energy of chocolate systems. In order to test this hypothesis a tempered dark chocolate system was cooled in three different ways: at ambient or room temperature (20 °C), in a refrigerator (4–7 °C), and in a freezer (-18 °C). The results obtained for  $\gamma_s^{\text{tot}}$  are shown in Figure 4.15, and indicate a clear deviation by the system cooled in the freezer from the results obtained previously for the tempered dark chocolate system, shown in Figure 4.11. Cooling at ambient or refrigerator temperatures does not significantly affect  $\gamma_s^{\text{tot}}$ , although the error increases with the lower refrigerator cooling conditions. This is assumed to be caused by the presence of a limited amount of water vapour at the chocolate surface after cooling at 4 °C. A significant difference can be observed between cooling at ambient temperature and at freezer temperatures. The lower  $\gamma_s^{\text{tot}}$  obtained at -18 °C is assumed to be a result of the formation of condense or water vapour and ice crystals on the chocolate surface.

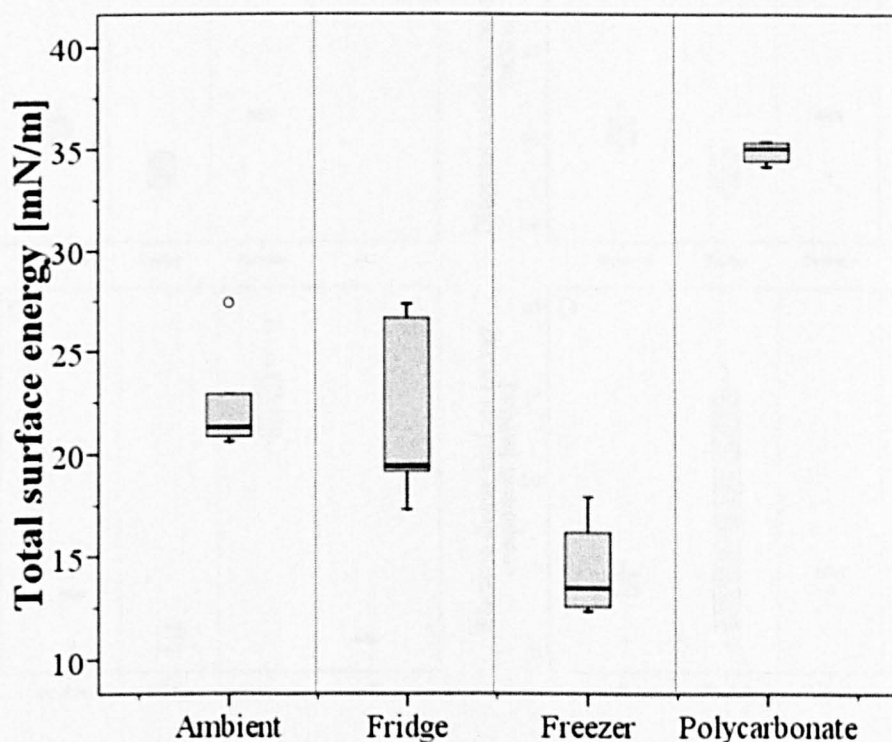


Figure 4.15 Total surface energy of dark chocolate as affected by cooling temperature.

Outliers are indicated by  $\circ$ , and not used in the calculation of the median and distance from the median.

It is expected that the presence of water vapour and/or ice crystals will be visible by an increase in the polar or Lewis acid–base component of the surface energy, when compared to the tempered dark chocolate discussed in section 4.3.4.1. Figure 4.16 shows the surface energy components of a dark chocolate system as a function of cooling temperature. In comparison to the previous results obtained for different chocolate systems in Figure 4.12, the most remarkable result is the relatively high Lewis acid–base or polar component, especially for the chocolate

system cooled in the freezer. The Lifshitz–van der Waals or dispersive component is again the most important with respect to the surface chemistry. Similar to the results obtained for the chocolate systems with varying composition, the electron acceptor is the main differentiating component with significant differences between the three cooling temperatures.

Processing conditions, in particular cooling temperatures, impact the surface free energy and surface chemistry of chocolate systems. Based on these results it is concluded that it is essential to control the temperature upon commercial chocolate manufacturing, to prevent the introduction of an important factor controlling surface characteristics and possibly adhesion.

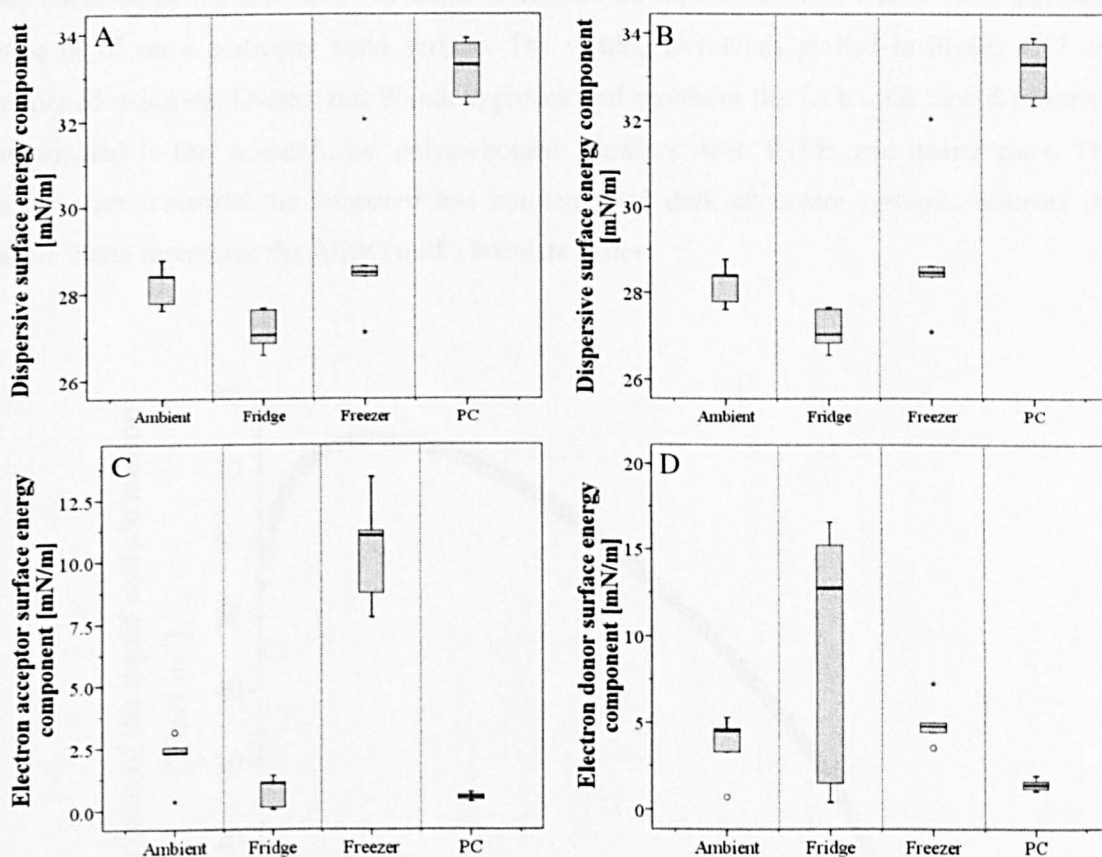


**Figure 4.16** Surface energy components of dark chocolate as affected by cooling temperature, calculated according to the Lifshitz–van der Waals / acid–base method developed by van Oss, Chaudhury and Good.

The dispersive component (A) represents the Lifshitz–van der Waals,  $\gamma_s^{lw}$ , interactions, whereas the polar component (B) represents the Lewis acid–base,  $\gamma_s^{ab}$ , interactions. The latter can be further subdivided into the electron acceptor (C),  $\gamma_s^+$ , and the electron donor (D),  $\gamma_s^-$ , components of the total surface free energy,  $\gamma_s^{tot}$ .

Outliers are indicated by  $\circ$  or  $*$ , and not used in the calculation of the median and the distance from the median.



### 4.3.5 Wetting envelope

A wetting envelope is prepared by plotting the polar and dispersive surface energy components of a liquid for the particular case where the contact angle is  $0^\circ$  ( $\cos \theta = 1$ ), against each other. These data can be calculated using the semi-empirical surface free energy approaches, such as Owens and Wendt, or van Oss, Chaudhury and Good, in reverse. In other words, the previously determined polar and dispersive components of the solid surface free energy are used to calculate the polar and dispersive components of the liquid for which  $\cos \theta = 1$ . In general, plotting the polar component against the dispersive component results in a closed contour which is called the wetting envelope (Janssen et al., 2006). Using the same mechanism, a contour can be developed for other situations, such as a contact angle of  $20^\circ$  or  $80^\circ$ . Within this research, the area enclosed by the contour or envelope represents the liquids that will wet or make a contact angle of  $0^\circ$  on a particular solid surface. The wetting envelopes plotted in Figure 4.17 are calculated using the Owens and Wendt approach and represent the four solid mould materials investigated in this research, i.e. polycarbonate, stainless steel, PTFE, and quartz glass. The purple stars represent the tempered and non-tempered dark chocolate systems, whereas the purple circle represents the AERO milk chocolate system.

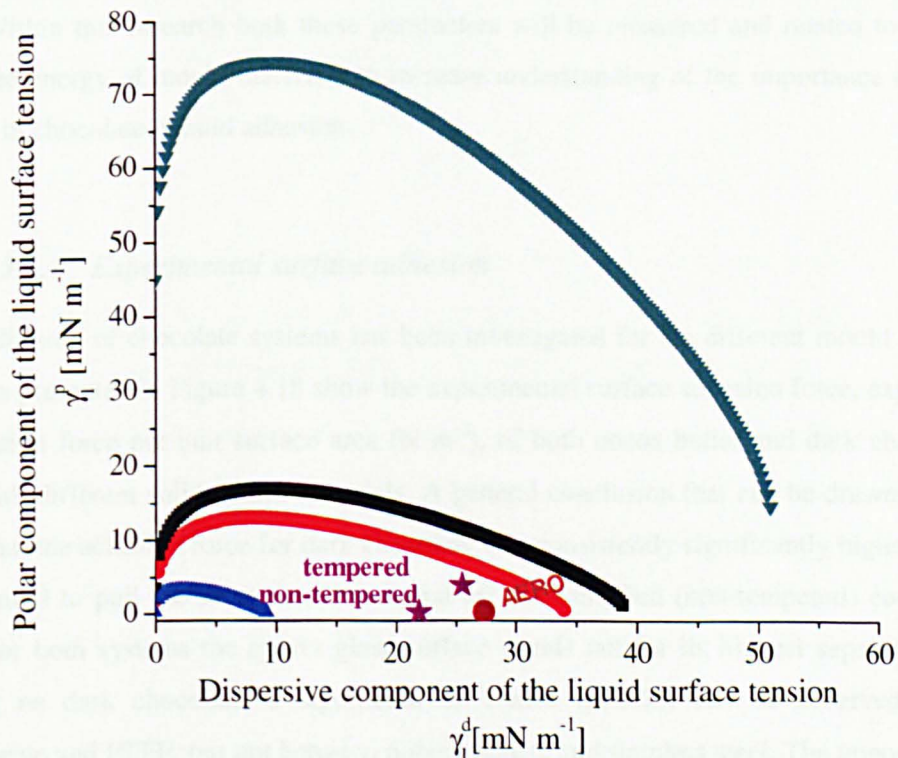


**Figure 4.17** Wetting envelopes with  $0^\circ$  contour for the four solid mould materials based on the Owens and Wendt approach.

In this graph, (■) represents the stainless steel mould surface, (●) the polycarbonate surface, (▲) the PTFE surface, and (▼) the quartz glass surface.

Polar and dispersive components are taken from the solid chocolate surface energy determinations discussed in section 4.3.4. All three liquid chocolate systems lie outside the PTFE envelope, but fall within the wetting envelopes of polycarbonate, stainless steel and quartz glass. This indicates that the respective chocolate systems will not wet the PTFE surface, but they will wet all other solid mould surfaces.

A liquid that wets a solid surface is assumed to have a higher number of interfacial interactions, consequently resulting in a higher adhesion force. Based on the low wettability of the PTFE surface by the different chocolate systems it is expected that this surface will show the lowest adhesion.

### **4.3.6 Adhesion of chocolate to mould surfaces**

Adhesion is quantified by two different parameters, the experimental surface adhesion and the work of adhesion, respectively. Experimental determination of the adhesion of chocolate systems to different mould surfaces was performed on the TA-XTplus Texture Analyser, using a fixture specifically developed for this work, as is described in section 3.3.2. The determination of the work of adhesion is based on the Young-Dupré adhesion model (equation [2-33], described in section 3.3.1.4), which uses the contact angle that an adhesive makes on a solid surface. Within this research both these parameters will be measured and related to the solid surface free energy of mould materials to increase understanding of the importance of surface chemistry in chocolate–mould adhesion.

#### *4.3.6.1 Experimental surface adhesion*

Surface adhesion of chocolate systems has been investigated for the different mould materials. The results presented in Figure 4.18 show the experimental surface adhesion force, expressed as the separation force per unit surface area ( $\text{N m}^{-2}$ ), of both cocoa butter and dark chocolate in contact with different solid mould materials. A general conclusion that can be drawn from this graph is that the adhesion force for dark chocolate was consistently significantly higher than the force required to pull the same mould material off the solidified (non-tempered) cocoa butter system. For both systems the quartz glass surface stands out for its highest separation force. Focussing on dark chocolate, a significant difference ( $p > 0.05$ ) can be observed between polycarbonate and PTFE, but not between polycarbonate and stainless steel. The opposite is true for cocoa butter, where the adhesion force of stainless steel is significantly different from that of polycarbonate and PTFE, but no difference can be observed between the latter. The overall trend observed for both systems is that the adhesion force increases from PTFE through polycarbonate and stainless steel to quartz glass.



Surface roughness of the different mould materials, as discussed in sections 3.3.6 and 5.3.7, shows limited differences in surface roughness between PTFE and quartz glass, with the latter approaching ideality. This trend does not relate well to the results obtained for the experimental surface adhesion force, where a significant difference is observed between these two surfaces. Quartz glass, with the lowest surface roughness, can be seen in Figure 4.18 to have the highest surface adhesion force. This indicates that the surface roughness of different mould materials is not the determining factor with respect to surface adhesion.

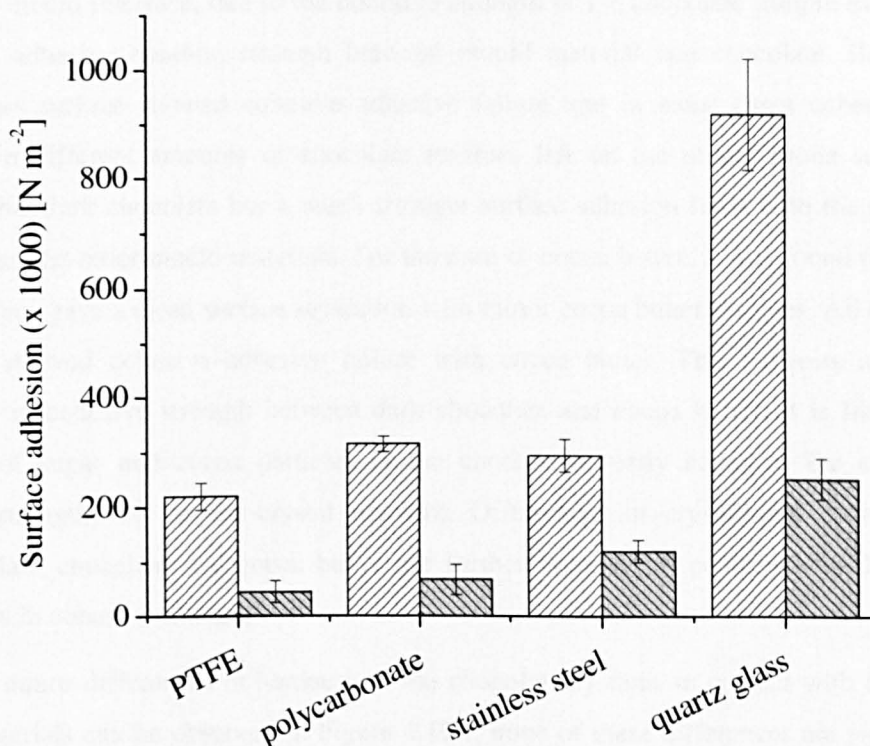


Figure 4.18 Surface adhesion as affected by different solid mould materials.

▨ ) refers to a dark chocolate system, whereas (■) refers to a cocoa butter system.

Error bar is representative of the standard deviation,  $n = 10$ .

Further investigation of the relationship between mould surface and surface adhesion points out the importance of the cohesive forces within the cocoa butter and dark chocolate systems. The amount of residue left-over at the probe surface was rather different amongst the various mould surfaces and between dark chocolate and cocoa butter, as can be seen in Figure 4.19A. Based on these results it is suggested that different failure mechanisms are involved in the surface adhesion process. According to Werner et al. (2007a and 2007b) and Adhikari et al. (2003), the failure of surface bonding is via one of three different mechanisms: cohesive failure, cohesive–adhesive failure, and adhesive failure, as discussed in more detail in section 3.3.2.4. Relative magnitude of the sample–probe adhesion force and the cohesion strength of the sample determine which mechanism dominates surface bonding failure. By examining the probe surfaces after separation, two main types of separation were identified in this part of the research: adhesive failure and cohesive–adhesive failure.

The images shown in Figure 4.20 visualize the concepts of adhesive and cohesive–adhesive failure, with image A representing a clean polycarbonate surface after separation and image C representing a polycarbonate surface with chocolate residues adhering as an example of cohesive–adhesive failure. The transition from adhesive failure to cohesive failure for probes of high surface energy is clearly reflected by the amount of residue left on these probes, as is shown in Figure 4.19A. For the dark chocolate samples a clean separation was observed for the polycarbonate, PTFE and stainless steel surfaces, indicating an adhesive failure at the chocolate–mould interface, due to the cohesive strength of the chocolate sample exceeding the interfacial adhesive bonding strength between mould material and chocolate. However, the quartz glass surface showed cohesive–adhesive failure and in some cases cohesive failure, resulting in different amounts of chocolate residues left on the mould probe surface. This suggests that dark chocolate has a much stronger surface adhesion force with the quartz glass surface than the other mould materials. For the case of cocoa butter, it was found that only the PTFE surface gave a clean surface separation with minor cocoa butter residues. All other mould materials showed cohesive–adhesive failure with cocoa butter. This suggests a significant difference in cohesive strength between dark chocolate and cocoa butter. It is likely that the presence of sugar and cocoa particles in the chocolate greatly enhances the cohesiveness (internal strength) of the fat crystal network. Differences in crystallinity (polymorphism) between dark chocolate and cocoa butter are further assumed to contribute to the observed differences in cohesive strength.

Although minor differences in hardness of the chocolate systems in contact with the different mould materials can be observed in Figure 4.19B, none of these differences are significant. In general, it can be observed that the hardness of cocoa butter is lower than that observed for dark chocolate, but this is only significant ( $p > 0.05$ ) on the quartz glass surface. The general trend is that contact with a stainless steel surface gives a chocolate sample with an increased hardness, whereas a quartz glass surface tends to decrease the hardness of the chocolate sample. A similar trend can be observed for cocoa butter.

In order to evaluate the change in the surface of the mould probe after its contact with chocolate or cocoa butter, the surface contact angle of water and the glossiness of the probes have also been monitored. Figure 4.19C shows the change of surface glossiness, whilst Figure 4.19D shows the change of water contact angle of the four mould probes after their contact with chocolate. Glossiness is a measure of the extent of light reflection by the surface. Its magnitude is affected by parameters like surface roughness and composition. The glossiness of nearly all mould surfaces decreased after contact with the chocolate sample, although this decrease was not significant ( $p < 0.05$ ) for the PTFE surface. Glossiness of the mould surfaces was not measured after contact with cocoa butter due to the visible presence of cocoa butter residues. A decrease in glossiness of the mould surface indicates a change of its surface layer, either an increased roughness or the adsorption of components from the sample which consequently

changes the composition of the surface layer. Stainless steel shows by far the highest reduction in glossiness, which is assumed to be a result of the high initial value obtained for the clean surface. Compared to the other surfaces, the stainless steel surface is very shiny, and is therefore expected to reflect the light most effectively. Polycarbonate and PTFE surfaces are believed to absorb the light better, compared to the stainless steel and quartz glass surfaces. The quartz glass surface is expected to change the direction of the light, but not necessarily reflect the light in the same angle as stainless steel.

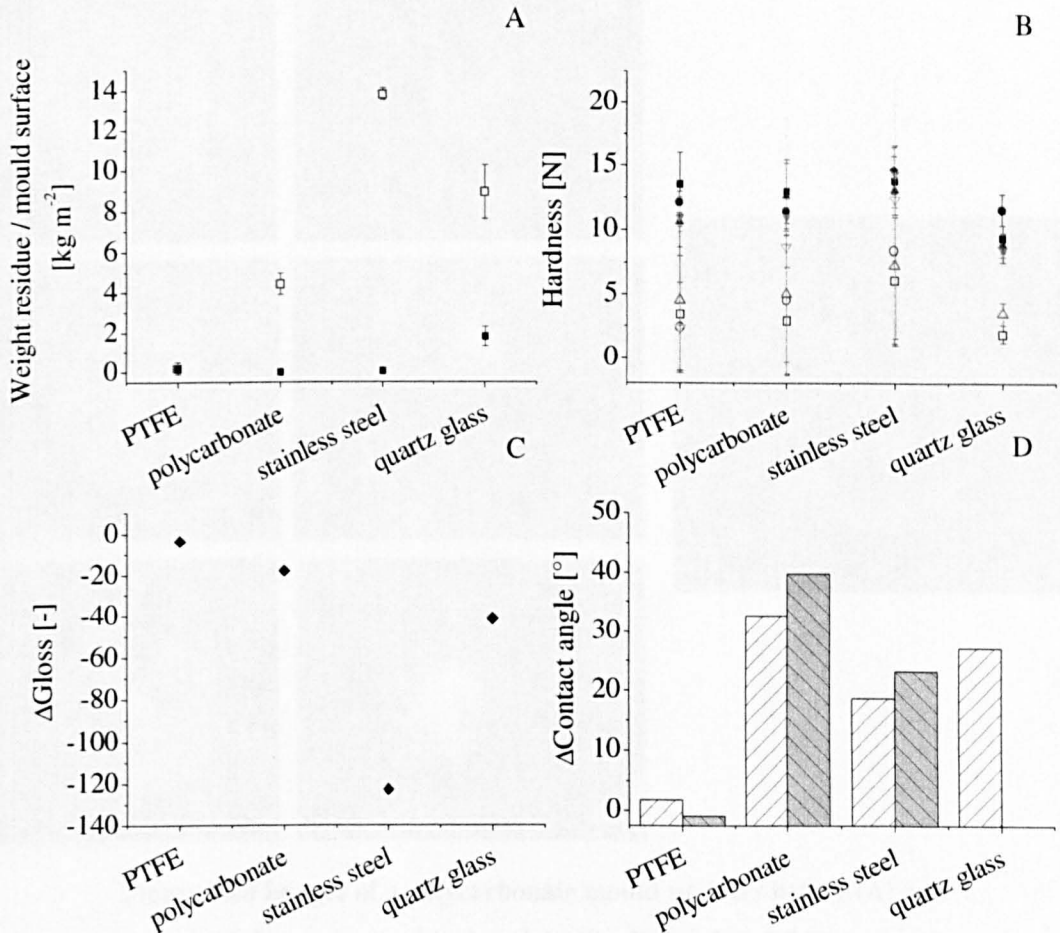


**Figure 4.19** The effect of different mould materials on the amount of residues after probe separation (A), the hardness of the solidified chocolate samples (B), the difference of surface glossiness (C) and the difference of contact angle (D) of the mould surfaces before and after chocolate contact.

In (A) (■) represents the dark chocolate system, whereas (□) represents the cocoa butter system. In (B) (■) and (□) represent the hardness of the bulk at the chocolate–air and cocoa butter–air interface, (●) and (○) the bulk at the chocolate–mould and cocoa butter–mould interface, (▲) and (△) the surface at the chocolate–air and cocoa butter–air interface, and (▼) and (▽) the surface at the chocolate–mould and cocoa butter–mould interface, respectively. In (D) (▨) and (▩) represent the contact angle difference after contact with chocolate and with cocoa butter, respectively.

Error bar is representative of the standard deviation,  $n = 10$ .



In contrast to the surface glossiness, which was lower after chocolate contact, the contact angle of water on the mould surfaces showed a significant increase for most mould materials, indicating an enhanced hydrophobicity of the probe material. The increase in hydrophobicity was lowest for the PTFE surface, which also showed a reduced change in surface glossiness. A contact angle of water on the quartz glass surface after contact with cocoa butter has not been measured due to the large number of cocoa butter residues adhering to the mould surface. In general, contact with cocoa butter or chocolate has the same effect on the mould surface.

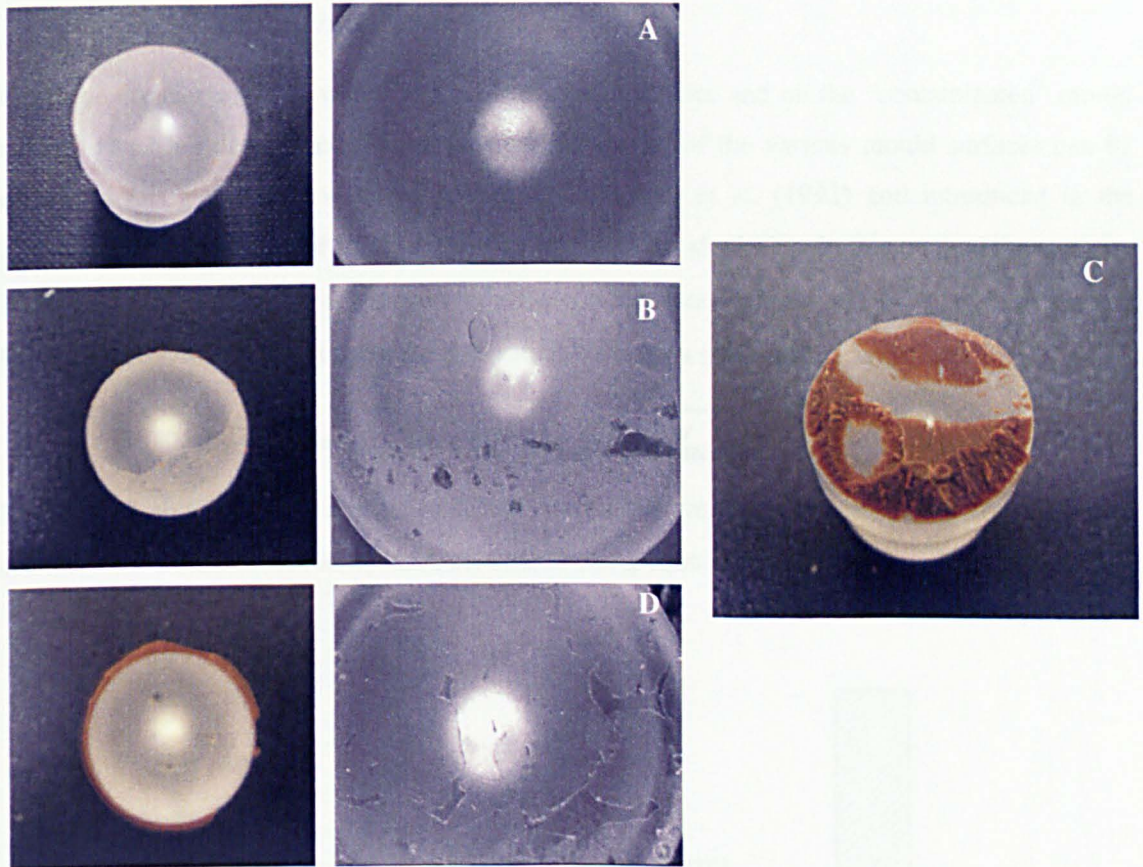


**Figure 4.20** Images of a polycarbonate mould surfaces before (A) and after contact with chocolate (B – D) (scale 1:0.34).

**Images B and D show a clean surface separation with the formation of an apparent thin film of contamination. Image C refers to a cohesive–adhesive failure.**

Results from surface glossiness and contact angle measurements seem to suggest an important fact that, even though these probes have a clean separation with little surface residue, the surface after contact appears to be rather different. This applies particularly to the stainless steel, polycarbonate and PTFE surfaces. In combination with optical examination of these surfaces, as shown by the images in Figure 4.20B and D, it is proposed that a very thin layer of chocolate (fat) deposits onto the probe surface during its contact with chocolate, making the surface more hydrophobic and less glossy. Similar observations were made by Luengo et al. (1997) when they conducted a number of wettability experiments on freshly cleaved mica surfaces after contact with chocolate. The surface area that had been in contact with chocolate was washed



clean with distilled water and dried in an oven, before the contact angle of water was measured at different locations both within the area of chocolate–mica contact and several radial distances away. Results obtained showed contact angles of  $> 60^\circ$  in the chocolate–mica contact area and no spreading, based on which it was concluded that the whole mica surface became hydrophobic during the washing stage. The general conclusion that can be made is that contact with chocolate increases the hydrophobicity of mould surfaces.

#### 4.3.6.2 Surface hydrophilicity

Once the contact angle of water on the clean mould surface and on the “contaminated” mould surface has been determined, the surface hydrophilicity of the various mould surfaces can be estimated using the method developed by Krisdhasima et al. (1992) and introduced in the investigation of adhesion of food systems by Michalski et al. (1999). In this method the quantity  $Wa_{water}^p$  or the polar part of the work of adhesion for water, is regarded as an index of surface hydrophilicity, and is based upon the interaction between a solid surface and water:

$$Wa_{water}^p = \gamma_{water}(\cos \theta + 1) - 2\sqrt{\gamma_{water}^{LW}\gamma_s^{LW}}. \quad [4-3]$$

Figure 4.21 shows the surface hydrophilicity of the different mould materials before and after contact with a dark chocolate system, calculated using equation [4-3].

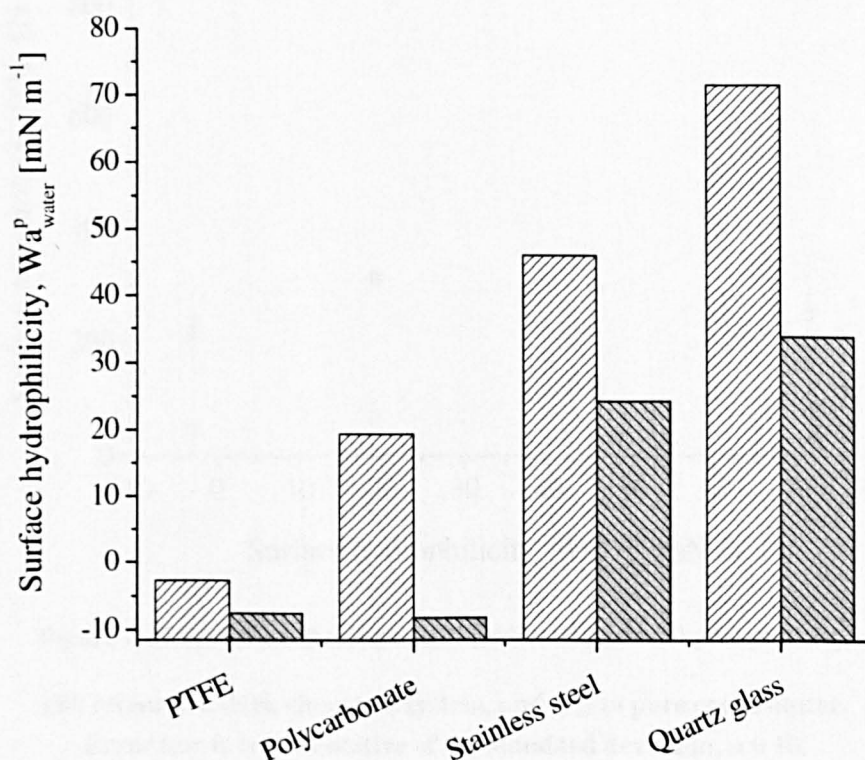


Figure 4.21 Surface hydrophilicity as affected by different mould materials.

(▨) represents the surface hydrophilicity of the clean mould surface, whereas (■) represents the surface hydrophilicity of the “contaminated” mould surface, after contact with chocolate.



The surface hydrophilicity values estimated for the clean mould materials used in this research compare well to those reported by Michalski et al. (1999). More importantly,  $Wa_{water}^p$  appears to differ distinctively between the mould materials, indicating its potential use as another discriminating factor with regards to the measured adhesion force. Quartz glass, one of the most hydrophilic surfaces, has the highest value ( $71.42 \text{ mN m}^{-1}$ ), whereas PTFE, a well-known hydrophobic surface, has even a negative surface hydrophilicity ( $-2.78 \text{ mN m}^{-1}$ ). In order to calculate the surface hydrophilicity of the “contaminated” mould surface, after contact with chocolate, it is assumed that the dispersive or Lifshitz–van der Waals component of the solid mould surface does not change. It can be observed that the hydrophilicity of all surfaces decreases due to the contact with chocolate, again indicating that the surface chemistry of the mould surface is changed possibly by the adsorption of a thin hydrophobic film on the solid mould surface. Compared to the initial value, only a limited change is observed for the PTFE surface. Interestingly, the estimated values of  $Wa_{water}^p$  for PTFE and polycarbonate after contact with chocolate are not significantly different, suggesting that the maximum surface hydrophobicity is reached.

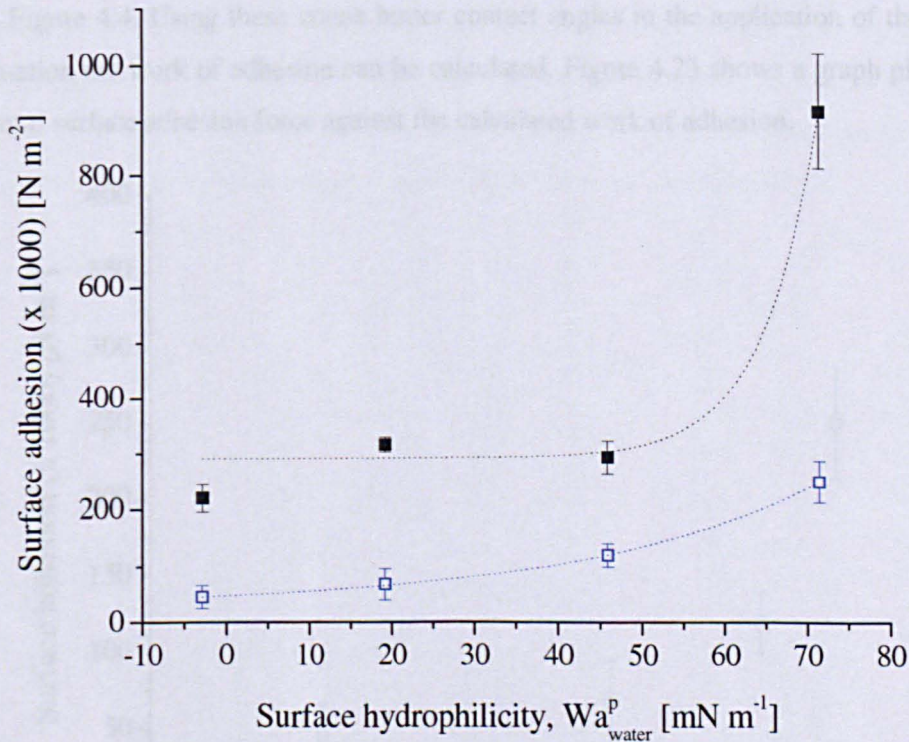


Figure 4.22 Surface adhesion as a function of surface hydrophilicity.

(■) refers to a dark chocolate system, and (□) to pure cocoa butter.

Error bar is representative of the standard deviation,  $n = 10$ .



The surface hydrophilicity can be regarded as a solid surface characteristic, and by plotting the experimentally determined surface adhesion force against the surface hydrophilicity, as shown in Figure 4.22, the different interactions at the chocolate–mould interface can be revealed. The results obtained show an exponential growth of the surface adhesion with increasing surface hydrophilicity for both dark chocolate ( $R^2 = 0.763$ ) and cocoa butter ( $R^2 = 0.999$ ). In other words, a hydrophobic mould surface is expected to give a lower surface adhesion force for both dark chocolate and cocoa butter.

#### 4.3.6.3 Work of adhesion

The Young–Dupré adhesion model (equation [2-33]) uses the contact angle of the adhesive on a solid surface for the determination of the work of adhesion. In this research chocolate would represent the adhesive and the mould material the solid surface. As discussed in section 4.3.2.3, it is not practicable to measure the contact angle of chocolate on different mould surfaces under ambient conditions, and cocoa butter was used as a model replacement system to represent chocolate. The contact angles of cocoa butter on the respective mould materials have been shown in Figure 4.4. Using these cocoa butter contact angles in the application of the Young–Dupré equation the work of adhesion can be calculated. Figure 4.23 shows a graph plotting the experimental surface adhesion force against the calculated work of adhesion.

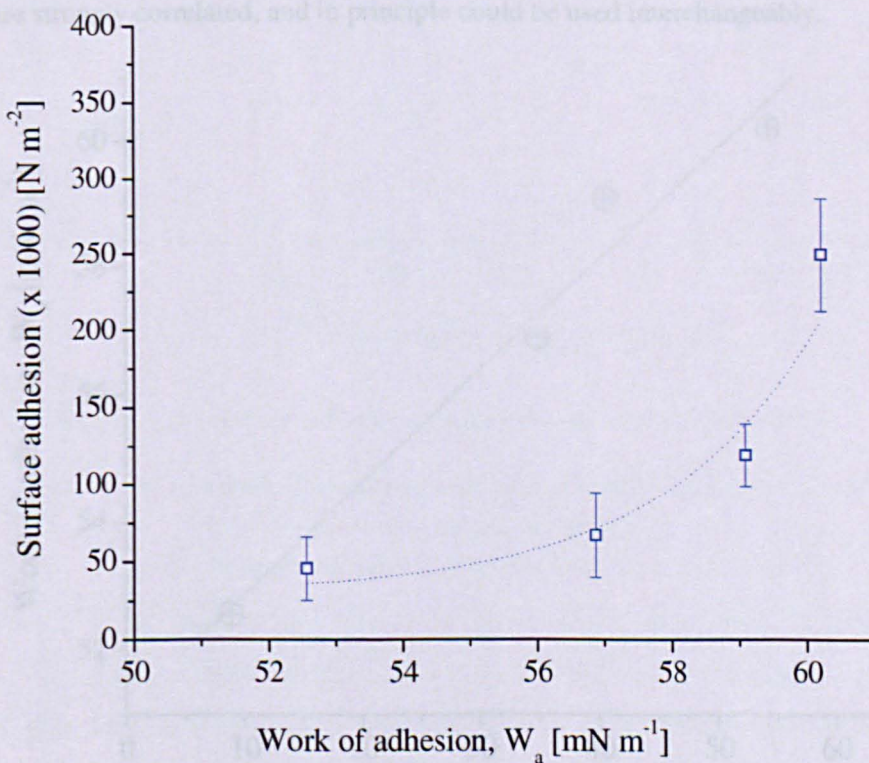


Figure 4.23 Surface adhesion as a function of the work of adhesion.

Error bar is representative of the standard deviation,  $n = 10$ .

The results show an exponential growth relationship ( $R^2 = 0.901$ ) between the experimental surface adhesion force and the calculated work of adhesion, although a comment has to be made about the range observed for the thermodynamic work of adhesion, which varies from 52 to 62  $\text{mN m}^{-1}$ , approximately. Ranking of the four mould materials with respect to the work of adhesion places PTFE at the bottom with the lowest value, followed by polycarbonate, stainless steel and quartz glass, respectively. This is exactly the same ranking as obtained for the total surface free energy, as discussed in section 4.3.3.2. Of course, it should be noted that chocolate and cocoa butter are two different materials, which would be expected to have different values for the work of adhesion. Therefore, the results discussed here can only be treated as a useful approximation to the behaviour expected for chocolate.

### 4.3.7 Comparison of the total surface energy and surface adhesion

The primary principle of this part of the research was to apply the principles of thermodynamic adhesion and surface energy to the case of chocolate adhesion, with the aim of establishing relationships between the thermodynamic work of adhesion and the observed extent of adhesion of chocolate to mould materials. Plotting the thermodynamic work of adhesion,  $W_a$ , against the total surface free energy,  $\gamma_s^{\text{tot}}$ , gives a linear relationship ( $R^2 = 0.969$ ), as can be observed in Figure 4.24. This implies that the total surface free energy and the thermodynamic work of adhesion are strongly correlated, and in principle could be used interchangeably.

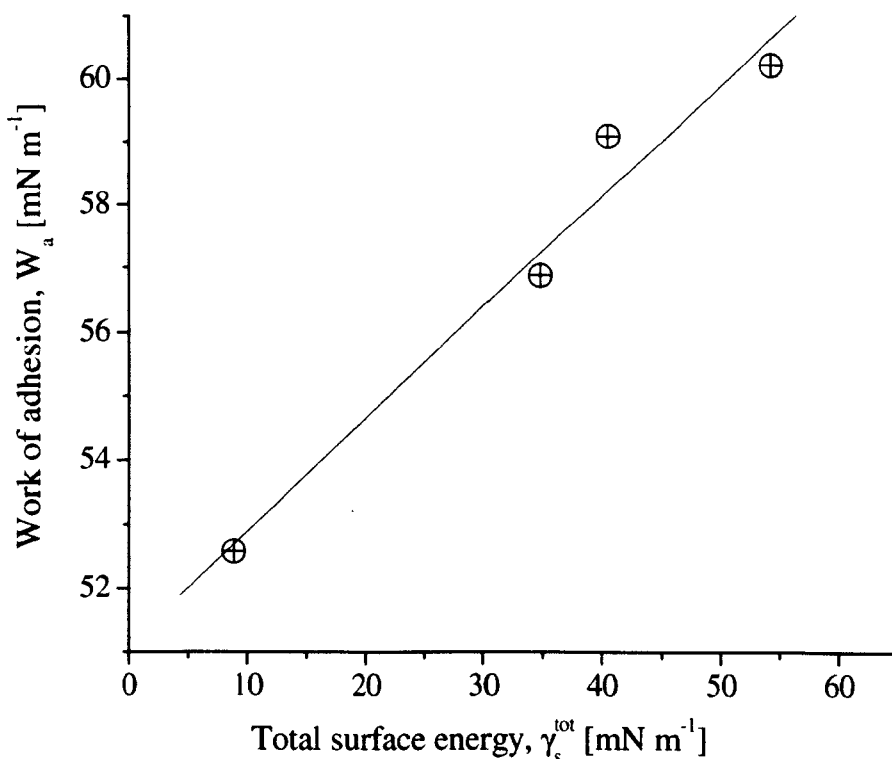
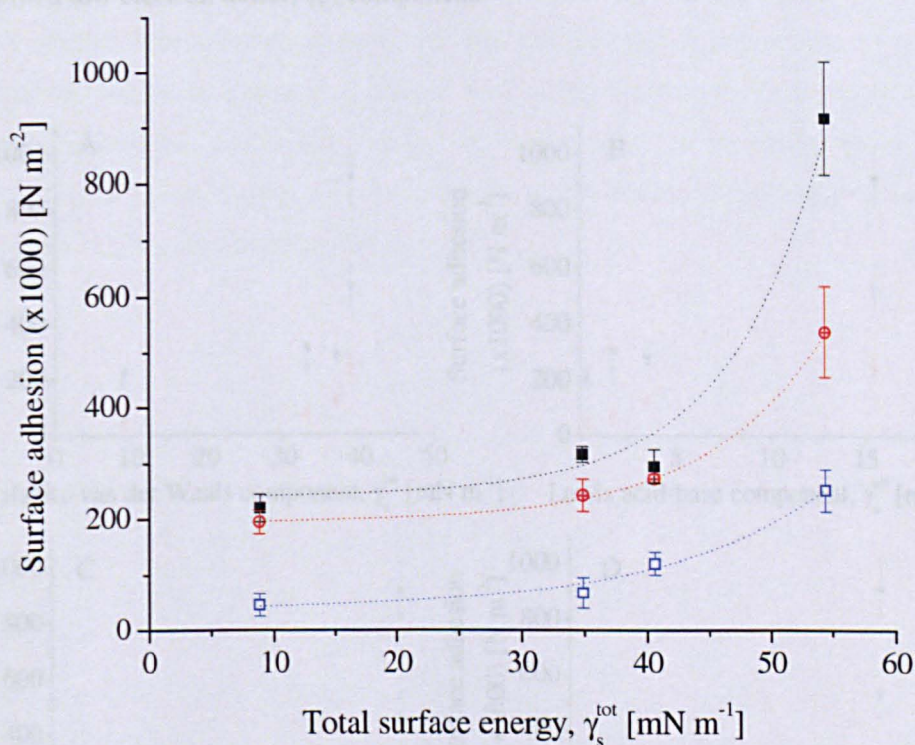


Figure 4.24 Work of adhesion as a function of total surface energy.



Figure 4.25 plots the experimental surface adhesion force against the total surface free energy, from which immediately a non-linear correlation is evident. Exponential growth curves fitted to the data indicate the possible existence of a critical surface energy, below which chocolate has minimal surface adhesion with the mould substrate. For all three systems, cocoa butter, dark chocolate and milk chocolate, the apparent critical surface free energy of the mould substrate is  $\sim 30 \text{ mN m}^{-1}$ . A significant increase in surface energy beyond this value leads to a pronounced increase in surface adhesion. Mars Incorporated (1999) report a similar relation between mould surface energy and the ease of demoulding. They recommend a mould material with a surface energy between  $5$  and  $25 \text{ mJ m}^{-2}$ , which provides sufficient wetting of the mould shape by the respective chocolate system in combination with good demoulding characteristics. In reality, however, such low surface free energy surfaces or materials are not commonly available.



**Figure 4.25** Surface adhesion as a function of total surface energy.

(■) refers to a dark chocolate system, (□) to a milk chocolate system and (⊕) to pure cocoa butter.

Error bar is representative of the standard deviation,  $n = 10$ .

The existence of a minimum surface energy has previously been observed by Michalski et al. (1999), who proposed a critical surface tension ( $\sim 38 \text{ mN m}^{-1}$ ) for the adherence of emulsion residues. Within the area of fouling, the Baier curve is an often used reference when discussing the relationship between surface free energy and relative bacterial adhesion. According to the Baier curve, an optimum exists for the surface free energy at which the bacterial adhesion is minimized. Within literature the optimum range for minimal bacterial adhesion is defined as  $20 - 30 \text{ mN m}^{-1}$  (Zhao et al., 2005; Liu et al., 2006b).



Similar to the biofouling and Baier curve correlation, optimum values have been reported for food based systems, such as the optimum value for milk protein adhesion ( $30 - 35 \text{ mN m}^{-1}$ ) (Zhao et al., 2004a), the minimum  $\text{CaSO}_4$  deposit formation ( $26 - 30 \text{ mN m}^{-1}$ ) (Zhao et al., 2005), the minimum adhesive strength of tomato deposit ( $20 - 25 \text{ mN m}^{-1}$ ) (Liu et al., 2006b), or a model food soil ( $26.5 \text{ mN m}^{-1}$ ) (Saikhwan et al., 2006). Within the area of crystalline fouling, much research focuses on the relation between surface free energy and ease of removal or cleaning of surfaces. Boulangé-Petermann et al. (2006) discussed the presence of a critical polarity, when defining the relationship between the polar component of the surface energy and oil removal. According to Rosmaninho et al. (2007) the solid surface chemistry impacts the fouling behaviour, but the exact mechanism depends on the processing stage. Earlier research by Rosmaninho et al. (2004) showed that calcium phosphate deposit formed faster on solid surfaces with a low electron donor,  $\gamma_s^-$ , component.

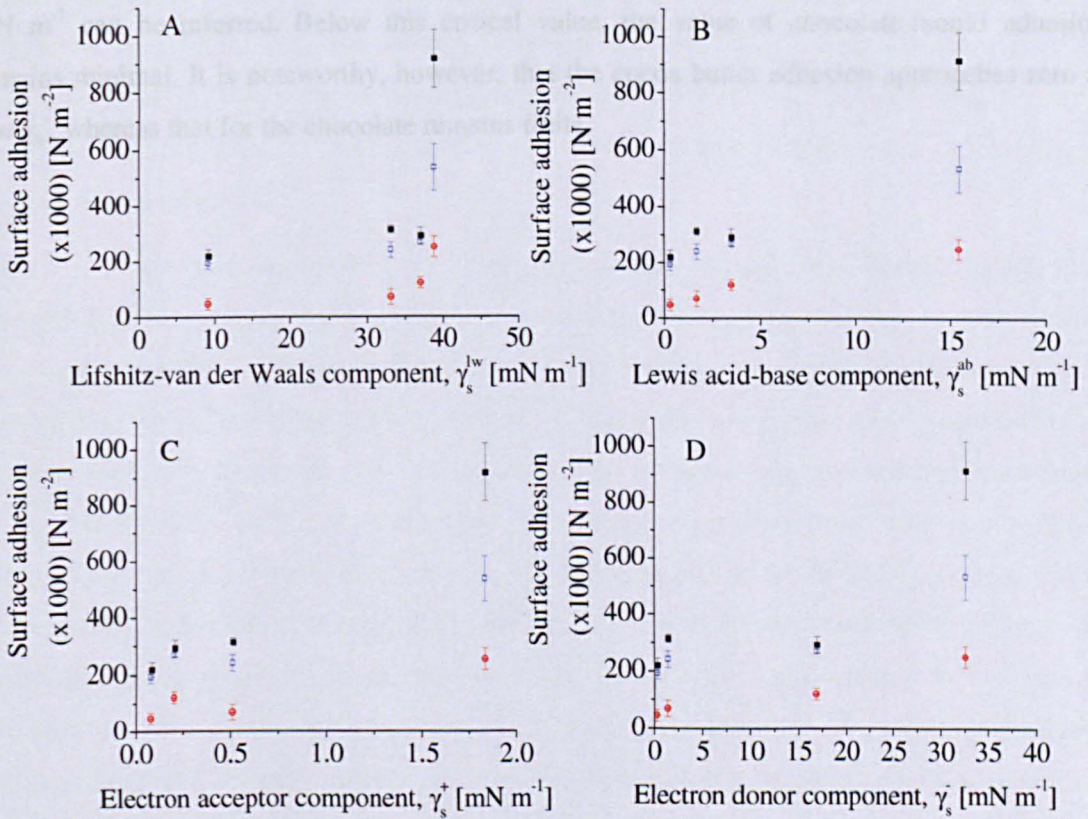


**Figure 4.26** Surface adhesion of different chocolate systems as a function of the surface free energy components, according to the Lifshitz–van der Waals / Lewis acid–base approach.

In all graphs, (■) refers to a dark chocolate system, (□) to a milk chocolate system and (⊕) to pure cocoa butter.

Error bar is representative of the standard deviation.

In Figure 4.26 the surface adhesion force is plotted against the different surface free energy components of the solid mould materials used within this research. Comparison of the different solid surface free energy components indicates a linear relationship between the polar or Lewis acid–base component (B) and the experimental adhesion of both dark chocolate ( $R^2 = 0.97$ ) and cocoa butter ( $R^2 = 0.97$ ). For the dispersive or Lifshitz–van der Waals component (A) a similar (exponential growth) relationship can be observed as was previously obtained for the total surface free energy, except for dark chocolate where a sharp and sudden increase is present from 37 to 38  $\text{mN m}^{-1}$ . As for the other chocolate systems the results obtained are consistent with the trends observed, it is assumed that this particular graph represents the true relationship between the dispersive component and the surface adhesion force. A plot of the electron donor component (D) against the experimental surface adhesion, which can be used as an effective differentiating factor, also shows an obvious positive relationship. Fitting a trend line to the data indicates a similar functional dependence for the electron donor component as previously obtained for the total surface energy. A critical value of the electron donor component of  $\sim 15 \text{ mN m}^{-1}$  can be inferred. Below this critical value, the value of chocolate-mould adhesion remains minimal. It is noteworthy, however, that the cocoa butter adhesion approaches zero at low  $\gamma_s^-$ , whereas that for the chocolate remains finite.

#### 4.4 DISCUSSION

This research has shown that chocolate adhesion to mould materials has a strong correlation with the surface energy of these respective mould substrates. According to Mars Incorporated (1999) a good chocolate demoulding is the result of the cohesive forces within the chocolate overcoming the adhesive forces between the chocolate and the mould, as is observed during standard moulding and demoulding practices in commercial chocolate manufacturing. The cohesive forces of chocolate are believed to increase during crystallization, and a low surface energy mould material is required to enhance the demoulding characteristics of such chocolate systems. Within the current research, the hardness and gloss of the chocolate samples, combined with the surface adhesion data, indicate that the crystallization of the cocoa butter (or the continuous fat phase) is affected by the surface energy of the mould substrates. According to Mullin (2001), heterogeneous nucleation can be induced by the presence of foreign bodies or surfaces. It is expected therefore that the varying surface energies of the mould substrates used in this research are responsible for differences in degrees of nucleation, consequently resulting in different crystal structures. Crystal growth results in structures with a minimum surface area and consequently minimum surface energy, according to the traditional surface energy theories, and so the surface energy of the chocolate–mould interface is likely to play a role in determining the final crystal structure.

Cho et al. (2003) and Rosmaninho and Melo (2006) independently investigated the effect of substrate surface energy on the crystallization behaviour of isotactic polypropylene and calcium phosphate, respectively. They both found that the microstructure of the final crystallized sample depended on the surface energy of the substrate. Rosmaninho and Melo (2006) found that solid substrates with a high electron donor component of the surface energy showed a higher number of nucleation sites, enabling the formation of a more compact structure. Cho et al. (2003) observed different crystalline morphologies, dependent on the substrate surface energy. It was believed that the formation of a purely transcrystalline region (transcrystallites) on high energy substrates was responsible for an increase in interfacial adhesion strength. On low energy substrates, however, both spherulites and a minority of transcrystallites were present, resulting in fracturing at the boundary of these two morphologies. A similar effect of substrate surface energy was also observed by Zhao et al. (2005) when investigating the microstructure of calcium phosphate deposits. Förster and Bohnet (1999; 2000) investigated the relation between interfacial free energy crystal / heat exchanger surface and fouling, and the effect of modifications of the molecular interactions. They indicate that the surface free energy of the heat transfer surface is crucial in relation to the deposition process, and that low energy surfaces can aid in reducing the nucleation rate and adhesive strength between crystals and heat transfer surface.



The observations made by Zhao et al. (2005) seem to have some parallel with the chocolate solidification on mould surfaces observed in this work. One may expect that different surfaces (or surfaces of different surface energy) will lead to different crystal structures, which consequently will affect the microstructure of the chocolate in the surface region. Based on the above results and discussion, it is clear that a material with a high surface energy, i.e. a high electron donor component, should not be used as a mould material. Such a material would be expected to produce a more compact structure of chocolate with strong crystal-crystal interactions in the interface region, which will tend to make demoulding more difficult. Figure 4.27 visualizes this hypothesis about the relation between surface energy and chocolate microstructure development during cooling / solidification. Starting with the liquid chocolate, the microstructure can be described as a dispersion of cocoa solids (particles) and sugar crystals in a continuous fat phase, consisting of fat crystals and liquid fat (Walstra, 1996; Aguilera et al., 2004). After tempering, the liquid chocolate is deposited in the chocolate moulds and cooled to set or solidify the chocolate, before demoulding can take place. The results obtained in this research indicate that the surface free energy of the mould material impacts on the crystallization of the cocoa butter forming the continuous phase in a chocolate system. A low surface energy material such as PTFE promotes the formation of a loose and porous structure as nucleation is limited. Rather than the formation of a large number of nucleation sites, growth of the primary nucleus will take place, forming large crystals with an open structure and a relatively low adhesion force. High surface energy materials such as quartz glass, on the other hand, promote the formation of more packed and dense structures. Nucleation is favoured, resulting in a large number of nucleation sites and relatively small crystals. The increased crystal-crystal and crystal-mould interactions result in both higher cohesive and adhesive forces.

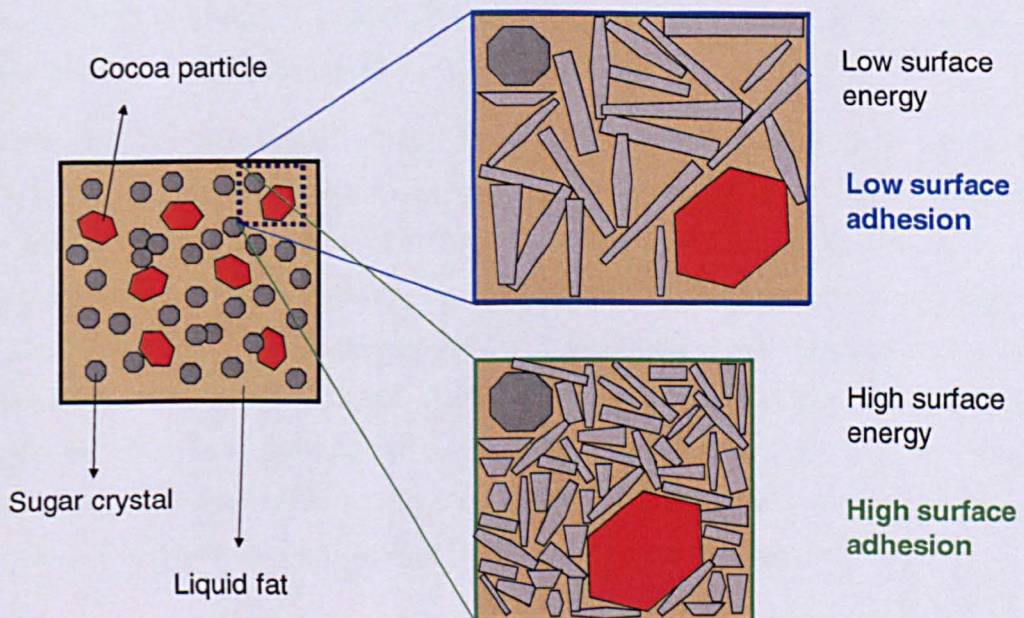


**Figure 4.27 Relation between chocolate microstructure and solid surface free energy, evolution upon cooling.**

## 4.5 CONCLUSIONS

Contact angle, wetting and thermodynamic surface energy data all are in good agreement, indicating that mould material choice is important in relation to chocolate adhesion. Surface energy (thermodynamics) is the major controlling factor for the adhesion between chocolate and mould material and the adhesion at the chocolate–mould interface can be minimized if an appropriate mould material is applied.

The properties of the mould surface have been shown to have significant influences on how chocolate adheres and solidifies during the moulding process. The separation of solidified chocolate from the mould was found to be dominated by two different failure mechanisms, adhesion failure or cohesive failure, depending on the nature of the mould surface. PTFE, polycarbonate, and stainless steel showed clean surface separation of the chocolate, and a mechanism of adhesive failure; but quartz glass, a material of much higher surface energy, showed predominantly cohesive failure with substantial amounts of chocolate residue left on the probe surface. The measured separation forces showed a direct correlation with the surface energy of the mould and the work of adhesion. A high surface energy material is generally unfavourable for easy separation of the mould from the chocolate. A solid material with a surface energy below  $30 \text{ mN m}^{-1}$ , and an electron donor component of  $\sim 15 \text{ mN m}^{-1}$ , is recommended as a suitable mould material for chocolate production.



## CHAPTER 5

### PROCESSING CONDITIONS AND THEIR EFFECT ON CHOCOLATE DEMOULDING.

#### 5.1 INTRODUCTION

A limited number of publications have investigated the relationship between processing conditions and chocolate adhesion. Much of the knowledge concerning chocolate manufacturing is based on experience, and observations made during processing are often not published. The production process and methodology differ hugely between products and between manufacturers, as was already mentioned in CHAPTER 2. A basic overview has been outlined in Figure 2.10, and extensively discussed by Beckett (2008). With respect to the demoulding of chocolate, the basic process techniques and conditions have been discussed in section 2.1.4.2.3. One of the critical parameters controlling the demoulding behaviour of chocolate is the cocoa butter crystallization. The formation of a large number of polymorphs with lower melting points results in a chocolate with a lower viscosity (softer) at room temperature and less contraction during solidification, consequently causing difficulties demoulding (Tewkesbury, 2000). Low cooling temperatures, for example, may cause the cocoa butter to crystallise in a crystal form other than the stable Form V. At the same time, the use of cooling temperatures above the dew point is recommended to prevent moisture condensation (Beckett, 2008). The formation of (moisture) condense on the chocolate surface will induce sugar bloom, which is not necessarily related to the adhesion of chocolate to the mould surface, but does affect the quality of the chocolate. From that point of view, Beckett (2001) advised to keep the equilibrium relative humidity (ERH) at around 35 – 40% during manufacturing, to prevent detrimental effects of moisture on chocolate viscosity and the ease of processing.

Chocolate deposits on a mould surface after demoulding are believed to be caused by an imbalance between the adhesion force (between the chocolate and the mould) and the cohesion force within the chocolate matrix. As discussed in CHAPTER 4 and by Keijbets et al. (2009), the surface energy of mould materials significantly impacts on chocolate–mould interactions. Based on these results, a recommendation was made to use mould materials with a surface energy less than  $30 \text{ mN m}^{-1}$  to improve the ease of chocolate demoulding. Aim of this part of the research was to investigate the effect of processing conditions on the level of adhesion of chocolate to the polycarbonate mould surface during demoulding, in order to enhance the understanding of interactions taking place at the chocolate–mould interface.

## 5.2 MATERIALS AND METHODS

The equipment and methodology of chocolate–mould adhesion determinations have been discussed in CHAPTER 3. This section will describe specific analyses or processing conditions that have been investigated, e.g. mould and cooling temperature, contact time, relative humidity (RH), cleaning methods and mould surface roughness.

### 5.2.1 Materials

Polycarbonate was chosen as the solid mould substrate in this research because of its commercial application as a mould material in chocolate manufacturing. Prior to experimental adhesion force determinations the polycarbonate substrates were cleaned with boiling, distilled water (Millipore) and dried using compressed air.

Dark chocolate (52% cocoa solids) was chosen as the standard system for the investigation of the relationship between processing conditions and chocolate demoulding. In order to determine the effect of different ingredients, the adhesion of the standard system is compared to the adhesion of samples of cocoa butter (100% cocoa solids), milk chocolate (29% cocoa solids) and dark chocolate (70% cocoa solids, Côte D'Or).

### 5.2.2 Methods

The experimental set-up outlined in Figure 3.17 was developed specifically to determine the relationship between process variables and chocolate–mould adhesion. Different cooling temperatures were obtained by adjusting both the temperature of the fan in the Peltier chamber (9) and the temperature of the water bath (6), used to control the air temperature, after contact had been created between the chocolate and the mould surface. Contact time refers to the time that the chocolate–mould interface was in place, i.e. from the moment of interface or contact creation, until the time of probe separation. A contact time of 10 minutes,  $t_{10}$ , means that the experimental adhesion force was determined 10 minutes after the creation of the chocolate–mould interface,  $t_0$ , i.e. the time of formation of contact between the liquid chocolate surface and the mould surface. In order to vary the mould surface temperature, the pre-conditioning or thermal equilibration step was omitted. The temperature of the polycarbonate mould samples was varied by either cooling the mould probe in a refrigerator (4 °C) or freezer (–18 °C) or heating in an oven. Relative humidity of the air used during the pre-conditioning stage was adjusted to the appropriate level by using different ratios of wet and dry air. Table 5.1 describes the specific process conditions used to assess the influence of various process variables in more detail.



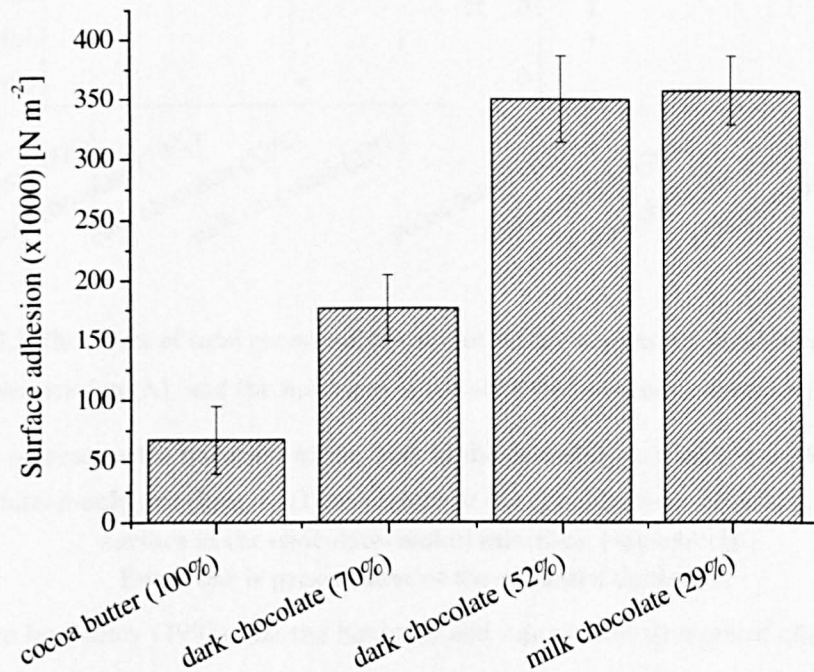
Experiment title	Pre-conditioning or thermal equilibrium stage				Semi-dynamic cooling stage		Comments
	Time [min.]	Mould temperature [°C]	Air flow [l/min.]	Relative humidity air [%RH]	Temperature [°C]	Time [min.]	
Contact time	30	30	10	0	15	0, 10, 30, 40, 60, 90, 150, 180, 250, 450	
Mould surface temperature	-	-20, 0, 10, 20, 30, 50	-	-	15	60	Pre-conditioning stage was omitted to enable the use of appropriate temperature conditions
Cooling temperature	30	30	10	0	0, 5, 10, 15, 20	60	
Relative humidity	30	30	10	0, 5, 10, 17.5, 25, 35, 50, 60, 70, 80, 100	15	60	
Cleaning materials	30	30	10	0	15	60	Cleaning materials used: water, detergent, rinsing agent or no cleaning
Non-cleaning	30	30	10	0	15	60	No cleaning of mould surface for 4 subsequent measurements
Mould surface structure	30	30	10	0	15	60	Roughness values according to supplier: 0, 30, 36, 39, 40, 42
Ingredients	30	30	10	0	15	60	Ingredients used: cocoa butter, dark chocolate (52 and 70% solids), milk chocolate

Table 5.1 Overview of processing conditions used for each individual experiment.

## 5.3 RESULTS

### 5.3.1 Ingredients

Three chocolate systems with varying compositions were compared to cocoa butter with respect to their surface adhesion forces. The results presented in Figure 5.1 show significant differences in surface adhesion of the chocolate systems tested. With decreasing cocoa solids content the surface adhesion force increases, until a maximum is obtained at approximately  $350 \text{ N m}^{-2}$  or 52% cocoa solids. Further decrease of the cocoa solids content to 29% does not increase the surface adhesion, but the comment has to be made that this sample contains 20% milk solids making a total solids content of approximately 49%. Comparison of the two dark chocolate systems and cocoa butter indicates a remarkable effect of cocoa solids content on the surface adhesion. Dark chocolate with 70% cocoa solids is known from experience to have a lower viscosity than a similar system with 52% cocoa solids. In this research the assumption is made that a system with a low viscosity will show superior wetting behaviour, consequently increasing the interfacial interactions and the adhesion. Furthermore, a highly viscous chocolate system may have a higher cohesive strength, which is expected to increase the surface adhesion force. This hypothesis, however, has not been tested.



**Figure 5.1** Surface adhesion as affected by total cocoa solids content.

Error bar is representative of the standard deviation,  $n = 6$ .

Further investigation of the relationship between cocoa solids content and surface adhesion shows that the reduction in total cocoa solids content results in a reduction of the amount of (chocolate) residues present on the mould probe surface after separation and an increase in hardness of the chocolate systems, as can be observed from Figure 5.2. The milk chocolate system, with 29% cocoa solids, deviates, again, from the trend observed for the dark chocolate



systems. In comparison to the dark chocolate system containing 52% cocoa solids, the milk chocolate system is observed to have both a much lower hardness and cohesive or internal chocolate strength, resulting in an increased amount of residues sticking to the mould surface after separation. This is believed to be due to the addition of milk fat, which is known to have a softening effect on cocoa butter and/or chocolate as it is mainly liquid at ambient temperature (Liang and Hartel, 2004; Beckett, 2008). Cohesive strength describes the interactions within the chocolate system, holding everything together. If the cohesive strength is low, this means that there are limited interactions between the components of the system, resulting often in a soft and brittle system that is easily pulled apart. The reduction in total cocoa solids content, mainly obtained through the inclusion of an increased level of sugar, results in an increase in cohesive strength of the system, shown by both the reduction in residues sticking to the mould surface and the increase in hardness.

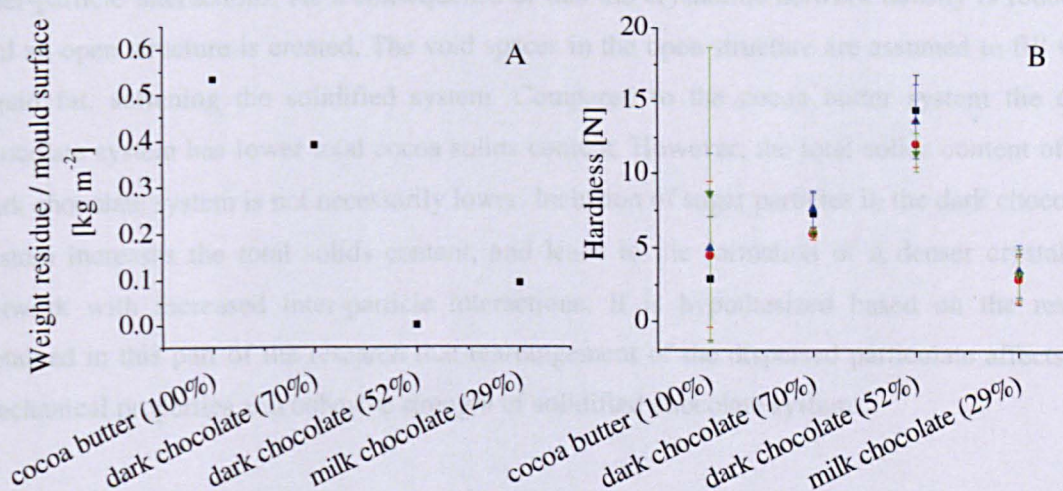


**Figure 5.2** The effect of total cocoa solids content on the amount of residues after probe separation (A), and the hardness of the solidified chocolate samples (B).

In (B) (■) represents the hardness of the bulk at the chocolate–air interface, (●) the bulk at the chocolate–mould interface, (▲) the surface at the chocolate–air interface, and (▼) the surface at the chocolate–mould interface, respectively.

Error bar is presentative of the standard deviation.

It was shown by Padley (1997) that the hardness and mechanical strength of chocolate develop after most of the fat has been crystallized. In other glyceride systems, however, higher or lower degrees of hardness or firmness are associated with higher or lower solid fat contents, respectively. Specifically for chocolate systems he proposed that solid sugar or cocoa particles and fat form random agglomerates during the initial crystallization stage, and that these are linked together by the sintering of fat crystals during the subsequent 2<sup>nd</sup> stage of the crystallization process. Differences in total solids content within the chocolate systems used in this research are believed to be responsible for the formation of a variety of networks which are more open with lower solids content, and which will subsequently show a reduced hardness.



Afoakwa et al. (2009) discuss the effect of particle size distribution and composition on the mechanical properties and microstructure of dark chocolate. A combined effect of fat content and particle size distribution was observed to be responsible for variations in hardness. A similar effect has been discussed by Narine and Marangoni (1999) who describe the dependence of hardness on solid fat content, particle size distribution and particle diameter, although this last was an inverse relationship. The solid fat content of milk chocolate is lower than that of dark chocolate (Liang and Hartel, 2004), and is responsible for the lower hardness of milk chocolate systems. The particle size distribution in part determines the packing ability and inter-particle interactions of the solid particles present within (dark) chocolate systems. This effect is reduced at high fat contents, though, as the fat coats the particle surfaces resulting in a reduction in the inter-particle interactions and the creation of a softer system. In this research it is proposed that the high fat content of the cocoa butter system is responsible for a reduction in the inter-particle interactions. As a consequence of this the crystalline network density is reduced, and an open structure is created. The void spaces in the open structure are assumed to fill with liquid fat, softening the solidified system. Compared to the cocoa butter system the dark chocolate system has lower total cocoa solids content. However, the total solids content of the dark chocolate system is not necessarily lower. Inclusion of sugar particles in the dark chocolate system increases the total solids content, and leads to the formation of a denser crystalline network with increased inter-particle interactions. It is hypothesized based on the results obtained in this part of the research that rearrangement of the dispersed particulate affects the mechanical properties and cohesive strength of solidified chocolate systems.

### 5.3.1.1 Surface tension

The surface tension of the liquid chocolate systems is presented in Figure 5.3. Although there are differences between the systems, it is not possible to observe a clear trend in the relation between cocoa solids content and surface tension. A slight increase in surface tension is obtained for the milk chocolate system compared to the dark chocolate system containing 52% cocoa solids.

The Gibbs' equation [5-1] describes the relationship between the surface tension, concentration and adsorption of a solute (in a dilute solution) (Walstra, 2003). It predicts that the solute gradient at the surface layer compared to the interior is negative, i.e. an increase in solute concentration is expected to increase the surface tension.

$$d(\gamma) = -RT\Gamma d(\ln C) , \quad [5-1]$$

where  $\gamma$  refers to the surface tension,  $\Gamma$  to the amount of solute adsorbed,  $C$  to the concentration of the solute in the (diluted) solution,  $R$  is the gas constant and  $T$  is the absolute temperature. Even though the chocolate systems used in this research are not dilute or pure solutions, the Gibbs' equation can be applied to give an indicative measure.



As the cocoa solids are non-surface active substances which do not have any affinity for the surface, it is expected, as a result of the Gibbs' equation that the surface tension will increase with "solute" concentration. This would explain the results obtained for the 52% and 70% cocoa solids systems, but not for the 100% cocoa solids system. However, the presence of other components such as sugar may be responsible for these differences. The difference between the two dark chocolate systems cannot be fully explained by their composition, but is also thought to be partly due to experimental errors, especially in relation to the viscosity of the chocolate systems. Loss of heat during the measurements in combination with the system viscosity are known to negatively affect the reliability of surface tension measurements using the Wilhelmy plate, and in combination with the non-ideality of the chocolate system this increases the experimental error related to liquid chocolate surface tension measurements.

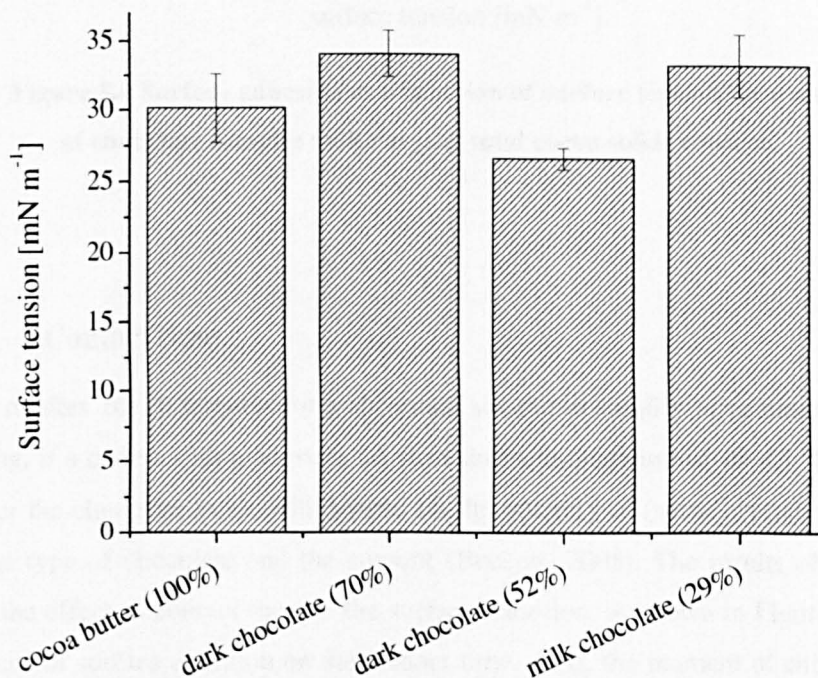


**Figure 5.3** Surface tension as affected by the total cocoa solids content.

**Error bar is representative of the standard deviation, n = 12.**

By plotting the surface tension against the surface adhesion of the chocolate systems, as shown in Figure 5.4, it is clear that there is no correlation between the surface tension of chocolate systems and their surface adhesion. From the limited or non significant differences in surface tension or surface forces between chocolate systems, it is concluded that these are not the main determining factor for surface adhesion.

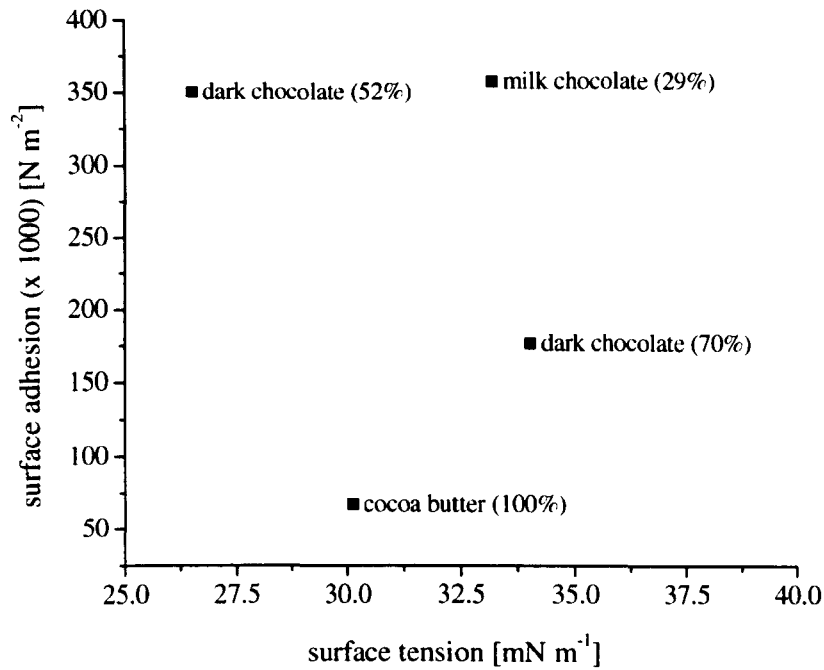


**Figure 5.4** Surface adhesion as a function of surface tension for a set of chocolate samples with varying total cocoa solids content.

### 5.3.2 Contact time

On average, it takes 10–20 minutes for a chocolate sample to solidify in commercial chocolate manufacturing, if a cooler with a constant air flow and a temperature of 10–15 °C is used. The exact time for the chocolate to set will depend on the quantity of (seed) crystals present in the fat phase, the type of chocolate and the amount (Beckett, 2008). The results obtained in this research for the effect of contact time on the surface adhesion, as shown in Figure 5.5, indicate the dependence of surface adhesion on the contact time. At  $t_0$ , the moment of chocolate–mould interface creation, the surface adhesion is minimal. However, as can be seen from the schematic representation in Figure 5.5, the amount of residues on the mould surface at this stage was very high (see Figure 5.6A). Due to the liquid character of the chocolate at  $t_0$ , chocolate is in close contact with the probe (good wetting) and a bridge is formed during separation. With increased time the liquid character of the chocolate declines, as crystallization and solidification processes continue, resulting in a clean separation, i.e. residue weight becomes neglectable, after approximately 60 minutes (see Figure 5.6A). The adhesion force, meanwhile, increases linearly with time until a contact time of 100 minutes, after which the force stays constant (see Figure 5.5).



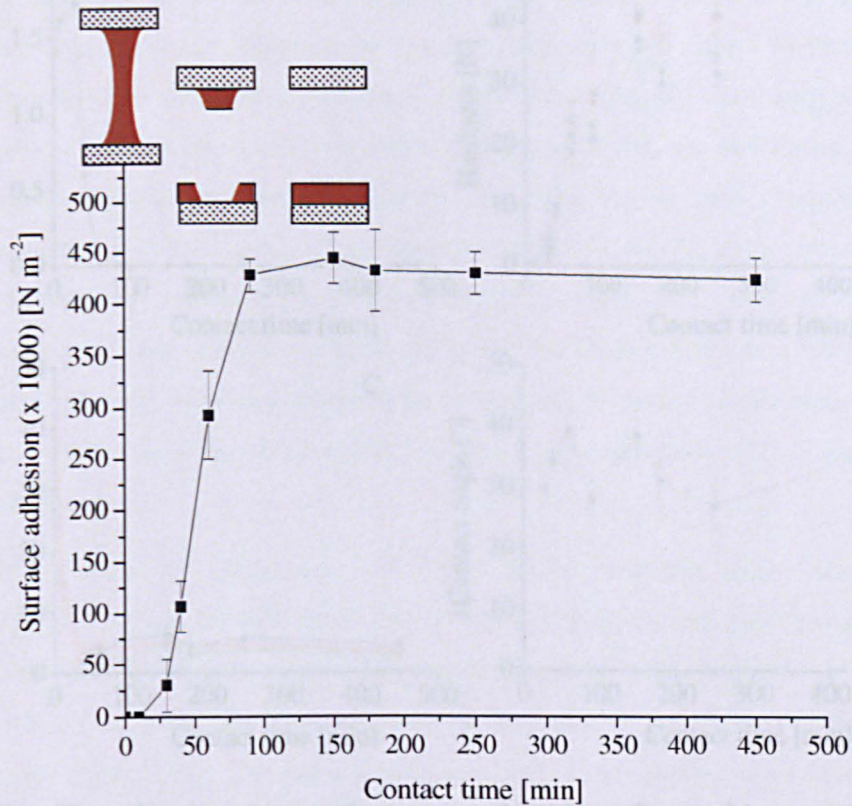


**Figure 5.5** Surface adhesion of dark chocolate as a function of contact time.

Error bar is representative of the standard deviation,  $n = 3$ .

Further investigation of the relationship between contact time and surface adhesion shows no effect of contact time on the surface gloss of both the chocolate and the mould surface and the surface chemistry of the mould material, as determined by the change in contact angle before and after chocolate contact, as can be seen in Figure 5.6C and D. With respect to the amount of (chocolate) residues adhering to the mould probe surface after separation, see Figure 5.6A, an initial increase in residues deposited on the mould surface is clearly visible. After approximately 20 minutes a sharp decline in residue weight is observed, which coincides with an increase in chocolate hardness. The crystallization taking place during cooling is basically a transformation of liquid fat into solid fat crystals. Depending on the stage of crystallization, there are different quantities of solid and liquid fat present, which are responsible for differences in hardness as observed during this part of the research. A low hardness or soft chocolate system simultaneously gives a large amount of residues adhering to the mould surface and a low surface adhesion force. This indicates that the rate of setting or solidification determines the cohesive strength of the chocolate system, which in turn determines the resistance against surface separation. A low cohesive strength shows a low resistance against separation, but with increasing cohesive strength the resistance against separation also increases.



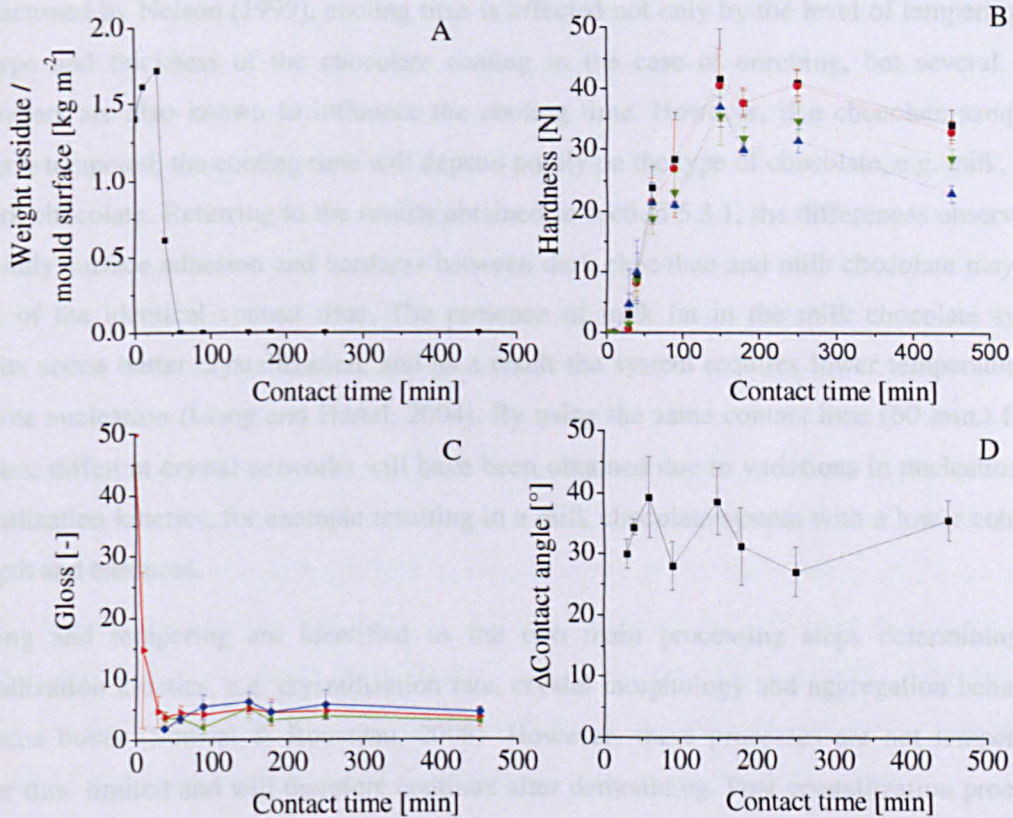


**Figure 5.6** The effect of contact time on the amount of residues after probe separation (A), the hardness of the solidified chocolate samples (B), the difference of surface glossiness (C) and the difference of contact angle (D) of the polycarbonate mould surface before and after chocolate contact.

In (B) (■) represents the hardness of the bulk at the chocolate–air interface, (●) the bulk at the chocolate–mould interface, (▲) the surface at the chocolate–air interface, and (▼) the surface at the chocolate–mould interface, respectively. In (C) (◆) represents the surface glossiness of the mould surface, (◀) the chocolate–mould interface, and (▶) the chocolate–air interface.

Error bar is representative of the standard deviation.

Above results also suggest that, with the applied cooling conditions, a contact time of 60 minutes is required to form a relatively strong crystal network so that the chocolate will have a high enough cohesive strength to withstand the separation force of demoulding. It can be observed that a constant surface adhesion force is observed only after a contact time  $\geq 100$  minutes, even though the recommendation is 60 minutes. This indicates that the crystallization and solidification processes have not been completed after 60 minutes of cooling, but the cohesive strength is larger than the adhesive strength, consequently resulting in a clean separation. It can be concluded that crystallization and solidification are important factors in relation to the adhesion between chocolate and mould surface and the consequent separation force on demoulding.



As discussed by Nelson (1999), cooling time is affected not only by the level of tempering and the type and thickness of the chocolate coating in the case of enrobing, but several other parameters are also known to influence the cooling time. However, if a chocolate sample is properly tempered, the cooling time will depend purely on the type of chocolate, e.g. milk, plain or dark chocolate. Referring to the results obtained in section 5.3.1, the differences observed in especially surface adhesion and hardness between dark chocolate and milk chocolate may be a result of the identical contact time. The presence of milk fat in the milk chocolate system inhibits cocoa butter crystallization, and as a result the system requires lower temperatures to promote nucleation (Liang and Hartel, 2004). By using the same contact time (60 min.) for all samples, different crystal networks will have been obtained due to variations in nucleation and crystallization kinetics, for example resulting in a milk chocolate system with a lower cohesive strength and hardness.

Cooling and tempering are identified as the two main processing steps determining the crystallization kinetics, e.g. crystallization rate, crystal morphology and aggregation behaviour of cocoa butter (Sonwai & Rousseau, 2008). However, these processes are not temperature and/or time limited and will therefore continue after demoulding. Post crystallization processes occurring upon storage vary in timescale from minutes to months. The two main post crystallization mechanisms are sintering, which is the formation of a crystal network due to the formation of solid bridges between crystals, and Ostwald ripening, as a result of polymorphic transformations towards a higher stability and changes in size distribution (Himawan et al., 2006). Examples of polymorphic transformations are discussed in section 2.1.3.2.1 and 2.1.3.3.1, with the transformation of Form V crystals into Form VI crystals upon storage (fat bloom), indicating that crystallization is an ongoing process (Beckett, 2008). The dispersed particulate in chocolate, e.g. milk and cocoa solids, also affects the fat crystal growth of cocoa butter during storage. Rousseau and Sonwai (2008) observed the formation of localized micron-scale amorphous zones within a milk chocolate system directly after demoulding, which was not observed for cocoa butter systems. It is believed that these zones are a result of the contraction force pushing liquid-state triacylglycerols to the surface via surface imperfections. Upon storage, these amorphous zones evolve further into disordered crystal agglomerates. Lonchamp and Hartel (2006) determined the surface composition of chocolate samples that were either under-, over or well-tempered. They suggest that growth of cocoa butter crystals at the surface of over-tempered chocolate is responsible for its dull surface and essentially happens within minutes to hours after solidification. Tscheuschner and Markov (1989) observed significant texture changes of chocolate within the first six weeks of storage, which they described as after-crystallization. The main question that remains is at which time during the chocolate manufacturing process this after-crystallization starts, e.g. during moulding, cooling, demoulding or upon storage.

Within this part of the research it is proposed, based on the observations made, that crystallization during the early stages of the cooling process results in the formation of a limited number of crystals, resulting in a low adhesion force and soft, liquid-like, product. Increasing the contact time during cooling will enable further crystallization, and the formation of an enhanced fat crystal network. The packing arrangement of the dispersed phase in chocolate systems influences the mechanical properties of the solidified chocolate product (Liang and Hartel, 2004). Also, the Form IV polymorph crystallizes in a double chain, whereas the Form V polymorph crystallizes in a triple-chain, enabling closer packing and a denser and harder end product (Afoakwa et al., 2007). The packing arrangement of the crystal network will depend on the cooling temperature, temper of the chocolate and the presence of Form V seeding crystals. These factors, in combination with the amount of liquid cocoa butter present, will determine the porosity of the final chocolate product. The evolution of the chocolate microstructure with contact time is visualized in Figure 5.7. A reduction in the amount of liquid fat present within the chocolate system as a result of crystallization is responsible for the increase in hardness and surface adhesion force observed. Once crystallization is complete reorganization of the crystal network will take place, however this is beyond the scope of this research.

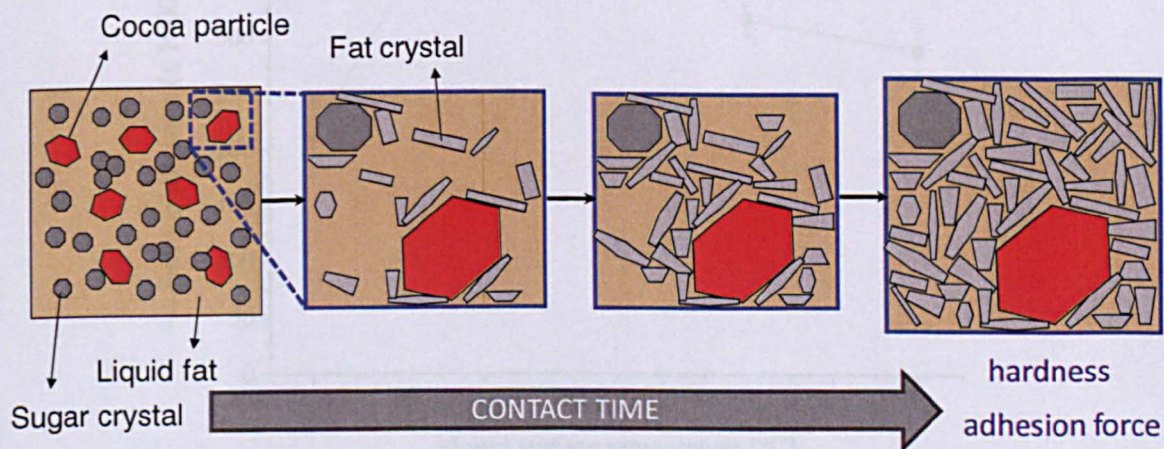


Figure 5.7 Evolution of microstructure with contact time.

### 5.3.3 Mould surface temperature

The manufacturing of chocolate tablets requires the liquid, tempered chocolate ( $\sim 28\text{--}32\text{ }^{\circ}\text{C}$ ) to be deposited into pre-conditioned moulds, which are subsequently passed over a vibrator, to spread the chocolate evenly throughout the mould without air bubble incorporation, as discussed in section 2.1.4.2.1. In Figure 5.8 the surface adhesion of dark chocolate is plotted against the mould surface temperature, to investigate the effect of different mould temperatures at the time of moulding on the final demoulding properties as measured by the surface adhesion force. Significant differences are clearly observable. The surface adhesion force decreases almost linearly with the increase of mould surface temperature, except for a temperature of  $-20\text{ }^{\circ}\text{C}$ ,



where the adhesion force drops to a level significantly lower than that obtained for any of the other temperatures. This reduction in surface adhesion force at  $-20\text{ }^{\circ}\text{C}$  is assumed to be caused by the formation of a hydrophilic layer at the interface between the mould and chocolate surface. With low temperatures, there is an increased risk of moisture vapour condensation and/or ice crystal formation on the mould surface during the pre-conditioning stage, depending on the pre-conditioning temperature. The hydrophilic layer thus formed reduces the interactions between chocolate and mould surface, consequently greatly reducing the experimental surface adhesion force. Crystallization and solidification processes taking place at the interface are expected to be the main reason for the observed decrease in surface adhesion with increasing mould temperature, especially the formation of unstable polymorphs at low mould surface temperatures and the melting out of seed crystals at relatively high mould temperatures. These mechanisms are discussed in more detail in section 2.1.4.2.1

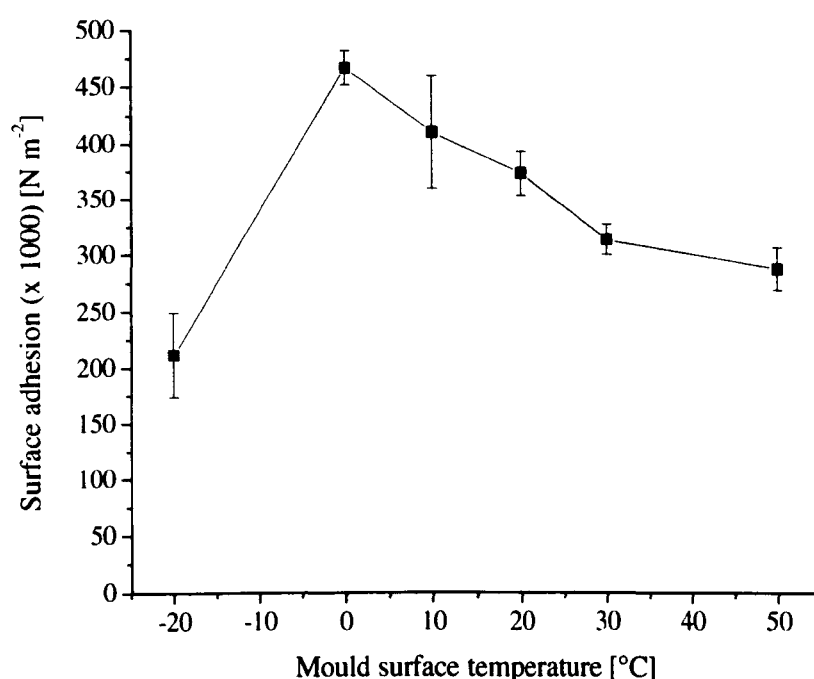


**Figure 5.8 Surface adhesion of dark chocolate as a function of mould surface temperature.**

**Error bar is representative of the standard deviation,  $n = 4$ .**

Further investigation of the relationship between mould surface temperature and surface adhesion shows that at nearly all surface temperatures some degree of cohesive–adhesive failure is obtained, as can be observed by the amount of chocolate residue present on the mould surface after demoulding, shown in Figure 5.9A. If the cohesive strength of the chocolate sample is slightly lower than the interfacial adhesive bond strength between mould material and chocolate, a break within the chocolate sample is observed upon separation, resulting in chocolate residues adhering to the mould surface. This behaviour can be expected, due to the formation of different polymorphic forms at the chocolate–mould interface as a result of the variation in mould surface temperature. A mould temperature of  $50\text{ }^{\circ}\text{C}$  results in the melting out of seed crystals present at the surface, consequently reducing the crystallization and

solidification of the surface layer of the chocolate sample. The amount of chocolate residues adhering to the mould surface at this temperature was large, and is thought to be caused by the fact that there was no extensive crystal network present to give the surface layer of the chocolate the required cohesive strength and hardness. A similar trend as that observed for the surface adhesion was obtained for the hardness of dark chocolate, as is shown in Figure 5.9B. This indicates that solidification might not be complete when mould surface temperatures of  $\geq 30$  °C are used. A significant reduction in hardness and cohesive strength of the chocolate sample, together with an increase in cohesive–adhesive failure and the amount of chocolate residues present on the mould surface, causes a reduction in the surface adhesion force.

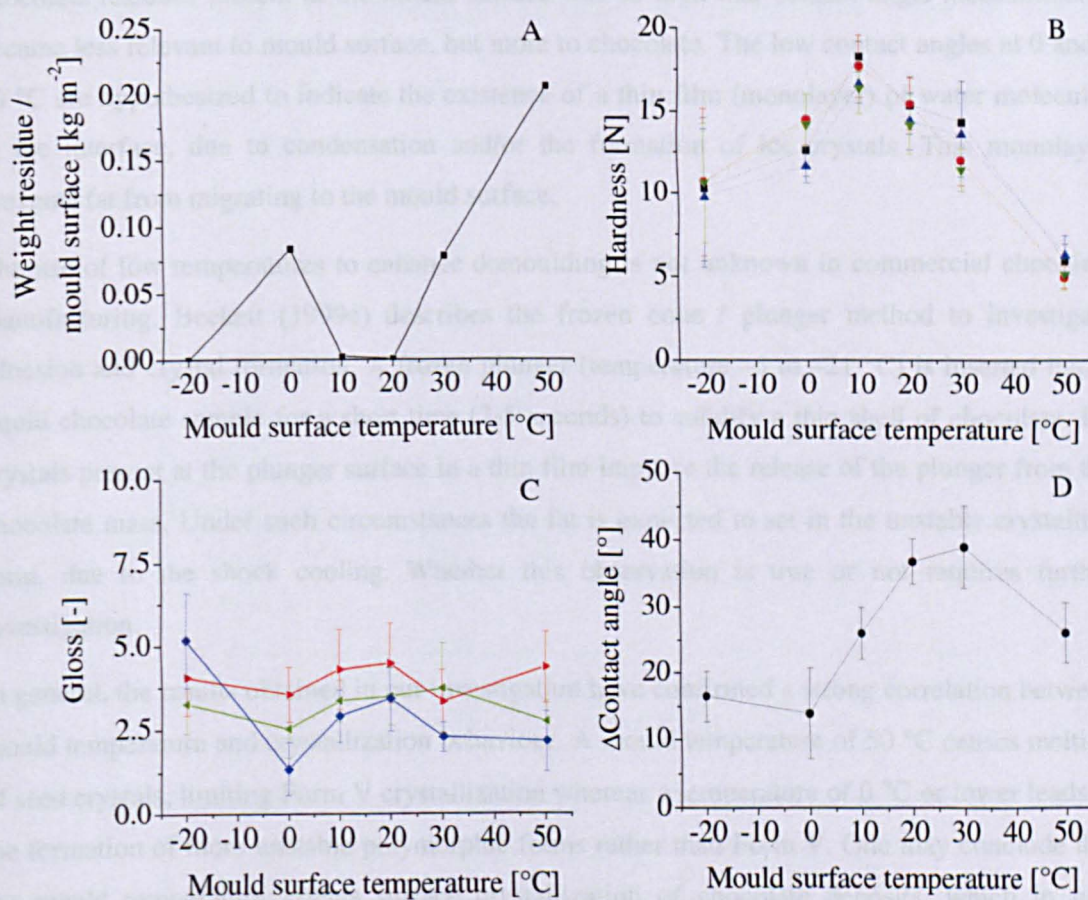


**Figure 5.9** The effect of mould surface temperature on the amount of residues after probe separation (A), the hardness of the solidified chocolate samples (B), the difference of surface glossiness (C) and the difference of contact angle (D) of the polycarbonate mould surface before and after chocolate contact.

In (B) (■) represents the hardness of the bulk at the chocolate–air interface, (●) the bulk at the chocolate–mould interface, (▲) the surface at the chocolate–air interface, and (▼) the surface at the chocolate–mould interface, respectively. In (C) (◆) represents the surface glossiness of the mould surface, (◀) the chocolate–mould interface, and (▶) the chocolate–air interface.

Error bar is representative of the standard deviation.



Taking a closer look at the mould surface after the surface adhesion measurements reveals significant changes in the contact angle of water, whereas the gloss of the different mould surfaces is fairly constant, as can be observed from Figure 5.9C and D, respectively. At intermediate mould temperatures, e.g. 10, 20 and 30 °C, an increase in contact angle can be ascribed to the deposition of a thin film of fat on the mould surface, leading to an increased surface hydrophobicity. A similar effect was described in section 4.3.6.1 (Figure 4.20). Wettability experiments by Luengo et al. (1997) on mica surfaces used for thin film tribology of chocolate also confirmed the presence of a hydrophobic monolayer on the solid (mould) surface after contact with chocolate. At increased surface temperatures, e.g. 50 °C, the amount of chocolate residues present at the mould surface was so high that contact angle measurements became less relevant to mould surface, but more to chocolate. The low contact angles at 0 and -20 °C are hypothesized to indicate the existence of a thin film (monolayer) of water molecules at the interface, due to condensation and/or the formation of ice crystals. This monolayer prevents fat from migrating to the mould surface.

The use of low temperatures to enhance demoulding is not unknown in commercial chocolate manufacturing. Beckett (1999c) describes the frozen cone / plunger method to investigate adhesion and crystal formation. A frozen plunger (temperature -5 to -21 °C) is inserted into a liquid chocolate sample for a short time (2-5 seconds) to solidify a thin shell of chocolate. Ice crystals present at the plunger surface in a thin film improve the release of the plunger from the chocolate mass. Under such circumstances the fat is expected to set in the unstable crystalline form, due to the shock cooling. Whether this observation is true or not requires further investigation.

In general, the results obtained in our investigation have confirmed a strong correlation between mould temperature and crystallization behaviour. A mould temperature of 50 °C causes melting of seed crystals, limiting Form V crystallization whereas a temperature of 0 °C or lower leads to the formation of more unstable polymorphic forms rather than Form V. One may conclude that the mould temperature affects surface crystallization of chocolate deposits, which in turn determines the ease of demoulding, as measured by the force required to pull a mould probe off the solidified chocolate.

#### **5.3.4 Cooling temperature**

The main aim of the cooling step of the chocolate manufacturing process, as discussed in detail in section 2.1.4.2.2, is the removal of specific and latent heat from the liquid chocolate sample. This will enable the crystallization and consequent solidification of the cocoa butter. If the cocoa butter is crystallized in the correct polymorphic form, i.e. Form V, the subsequent contraction aids an easy demoulding. Although it is known that the time required for cooling and solidification depends on the rate of heat transfer from the chocolate product to the air,

which in turn depends on the temperature and flow rate of the cooling air (Beckett, 2008), the cooling time and air flow rate have been kept constant in this part of the research.

The relationship between cooling temperature and surface adhesion is shown in Figure 5.10. A nearly linear inverse correlation is visible. Until a cooling temperature of 15 °C the surface adhesion shows a linear decrease with increasing cooling temperature. A further increase in cooling temperature results in a sharp drop in surface adhesion, as is observed for a cooling temperature of 20 °C (ambient temperature). An important observation is that at almost all cooling temperatures a clean surface separation was observed, as can be seen in Figure 5.11A. This indicates that the cohesive strength of the dark chocolate sample exceeded the surface adhesion force, resulting in a clean break and no fracturing at the chocolate–mould interface.

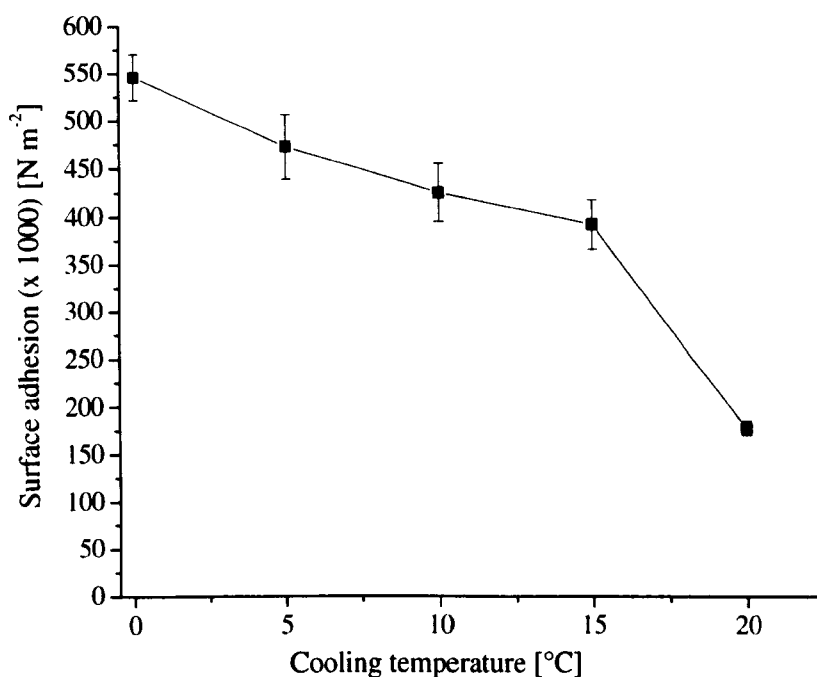


**Figure 5.10** Surface adhesion of dark chocolate as a function of cooling temperature.

Error bar is representative of the standard deviation,  $n = 4$ .

Further investigation of the relationship between cooling temperature and surface adhesion shows a similar nearly linear inverse correlation between the chocolate hardness and surface adhesion force, as can be observed from Figure 5.11B. The temperature difference between the melted, tempered chocolate (30 °C) and the cooling air, at the start of the cooling process, is expected to be responsible for the differences in surface adhesion and hardness obtained in this part of the research. At low cooling temperatures, e.g. 0 °C, the temperature difference between the liquid chocolate and the cooling air is relatively large. Consequently, the heat transfer from the chocolate surface to the cold air is much higher compared to a cooling temperature of 20 °C. Although the air flow rate is constant, the heat removal will be higher at low air temperatures due to the increased temperature difference between the chocolate and cooling air. It is hypothesized that this increased heat transfer is responsible for the formation of a significant

amount of small fat crystals with a dense packing, whereas relatively high cooling temperatures promote the formation of significantly larger crystals because of the faster growth of crystals in comparison to the rate of crystal nucleation.

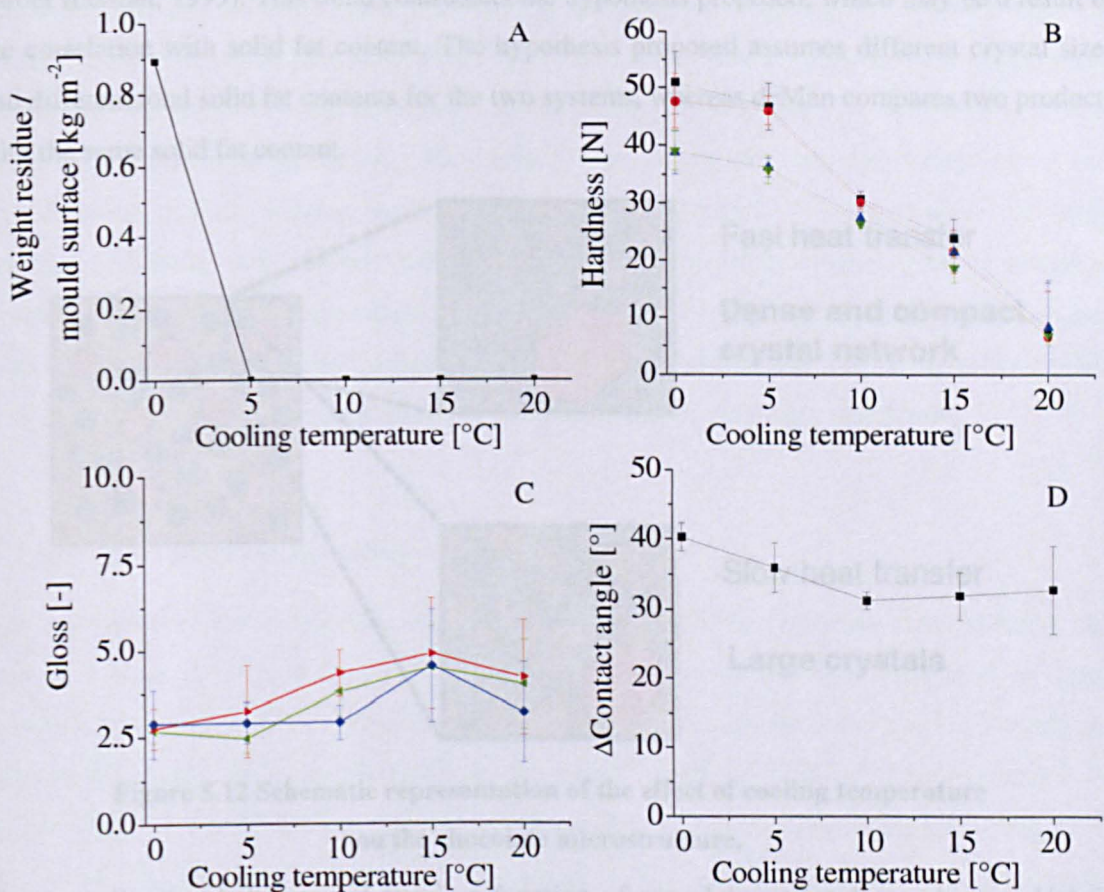


**Figure 5.11** The effect of cooling temperature on the amount of residues after probe separation (A), the hardness of the solidified chocolate samples (B), the difference of surface glossiness (C) and the difference of contact angle (D) of the polycarbonate mould surface before and after chocolate contact.

In (B) (■) represents the hardness of the bulk at the chocolate–air interface, (●) the bulk at the chocolate–mould interface, (▲) the surface at the chocolate–air interface, and (▼) the surface at the chocolate–mould interface, respectively. In (C) (◆) represents the surface glossiness of the mould surface, (◀) the chocolate–mould interface, and (▶) the chocolate–air interface.

Error bar is representative of the standard deviation.

The effect of heat transfer on the microstructure of dark chocolate is visualized in Figure 5.12. A dense and compact fat crystal network is expected to have a high cohesive strength, due to the large number of inter-particle interactions, and consequently a higher surface adhesion. It is furthermore observed that the dense and more compact packing arrangement of the small crystals at low air temperatures evokes an increase in hardness, which can be observed by the almost four times higher penetration force obtained for the chocolate sample solidified at < 5 °C compared to that formed at 20 °C. Fat crystal size is known to influence the hardness of the



cocoa butter system, although this is strongly correlated to the solid fat content of the system. Assuming that the solid fat content is the same for two products, the product with the smaller fat crystals is softer, more plastic, compared to the product with the larger fat crystals, which is harder (deMan, 1999). This trend contradicts the hypothesis proposed, which may be a result of the correlation with solid fat content. The hypothesis proposed assumes different crystal sizes and different total solid fat contents for the two systems, whereas deMan compares two products with the same solid fat content.

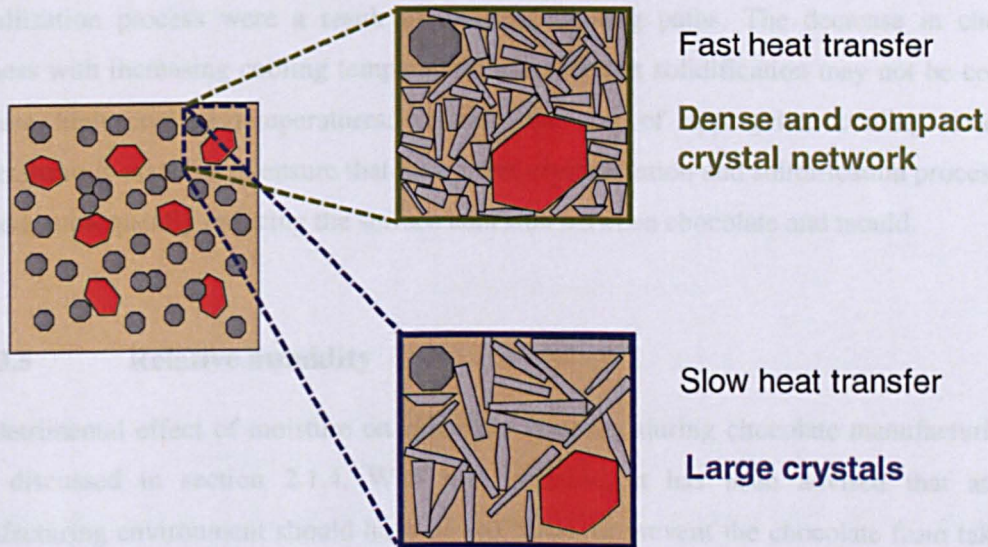


**Figure 5.12 Schematic representation of the effect of cooling temperature on the chocolate microstructure.**

The crystallization behaviour of fats is a function of triacylglycerol polymorphism, which in turn is influenced amongst others by temperature (Sato, 2001). Especially temperature variations were observed to determine whether polymorphic transformations occur through melt-mediation or in a solid state. According to Himawan et al. (2006) both kinetic and thermodynamic factors determine which polymorph will form from the melt. With respect to cooling temperatures and rates, two important observations are made: 1) the formation of  $\alpha$ - or  $\beta'$  polymorphs, respectively, depends on the cooling rate applied, as is shown for the specific case of the binary PPP/SSS system; 2) rapid crystallization enhances the formation of poorly packed crystals, which may persist for years in the absence of a liquid phase. These observations are in good agreement with the hypothesis proposed in this research, where the cooling temperature determines the type of crystals and network formed.

In order for crystal growth to take place, it is essential that molecules diffuse through the chocolate matrix to the surface of the nuclei. A low cooling temperature, or high cooling rate, will decrease the molecular mobility as a result of the solidification front that advances through the chocolate. This will result in a solid product with a crystal network and individual molecules that are not aligned (Pinschower, 2003). Too high a cooling temperature, on the other hand, will



increase the number of lower melting point polymorphs, which are crystallizing at the expense of Form V polymorphs (Tewkesbury et al., 2000).

Even though the exact mechanism responsible for the decrease in surface adhesion with increasing cooling temperature is not fully understood, the importance of kinetics on fat crystallization and subsequent solidification is clear. In a model to predict the temperature distribution within a cooling chocolate, developed by Tewkesbury et al. (2000), it was demonstrated that different polymorphic forms formed during the chocolate solidification and crystallization process were a result of different cooling paths. The decrease in chocolate hardness with increasing cooling temperature indicates that solidification may not be complete at these high cooling temperatures. Overall, the use of appropriate cooling times and temperatures is essential to ensure that the correct crystallization and solidification processes are pursued, subsequently reducing the surface adhesion between chocolate and mould.

### **5.3.5 Relative humidity**

The detrimental effect of moisture on chocolate viscosity during chocolate manufacturing has been discussed in section 2.1.4. With that in mind, it has been advised that an ideal manufacturing environment should have 35–40 %RH, to prevent the chocolate from taking up moisture (Beckett, 2001). In this research, the relative humidity (RH) of the air, which is in contact with the mould surface during the pre-conditioning or thermal equilibrium stage (30 min. at 30 °C), was varied to determine the effect on the surface adhesion force. The results presented in Figure 5.13 show significant differences in surface adhesion with varying RH. Initially, the surface adhesion increases with increasing RH. At approximately 25 %RH the adhesion force stabilizes forming a plateau till ca. 50 %RH. A sharp decrease in surface adhesion is observed at RH > 50%. Similar observations have been made in industry, where the adhesion of chocolate to roll-refiners increased significantly if the air in the factory was 20–25 %RH. Based on these observations the assumption is made that changes in surface adhesion are related to the change of mould surface hydrophilicity due to the adsorption of water vapour on the polycarbonate mould surface. Figure 5.14 shows schematically the effect of water vapour condensation on the mould surface. Water vapour from the air surrounding the mould surface during the thermal equilibrium stage adsorbs onto the polycarbonate surface, creating a hydrophilic surface layer. Depending on the air conditions, it is expected that the water vapour present at the mould surface increases with increasing relative humidity, i.e. initially individual water molecules will be present, but their number will increase with RH subsequently forming a monolayer (thin film) and possibly even a (macroscopic) wetting film at high RH. The presence of water vapour at the mould surface reduces the interactions between chocolate and mould surface, accordingly reducing the adhesion.

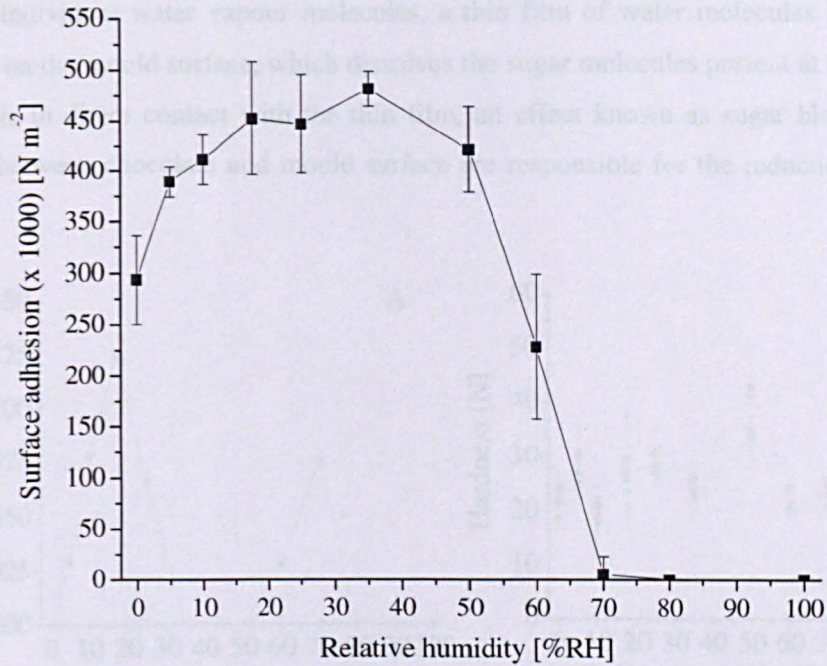


**Figure 5.13** Surface adhesion of dark chocolate as a function of environmental relative humidity.

Error bar is representative of the standard deviation,  $n = 5$ .

Further investigation of the relationship between relative humidity and surface adhesion, as presented in Figure 5.15, shows that the initial increase in surface adhesion observed at low RH coincides with an increase in cohesive–adhesive failure, i.e. the amount of chocolate adhering to the mould surface. At this low RH there is limited water vapour present on the mould surface, and direct contact between chocolate and mould surface is feasible. A high RH, on the other hand, resulted in a reduction of the surface adhesion, but caused a detrimental effect on the chocolate surface gloss, see Figure 5.15C.

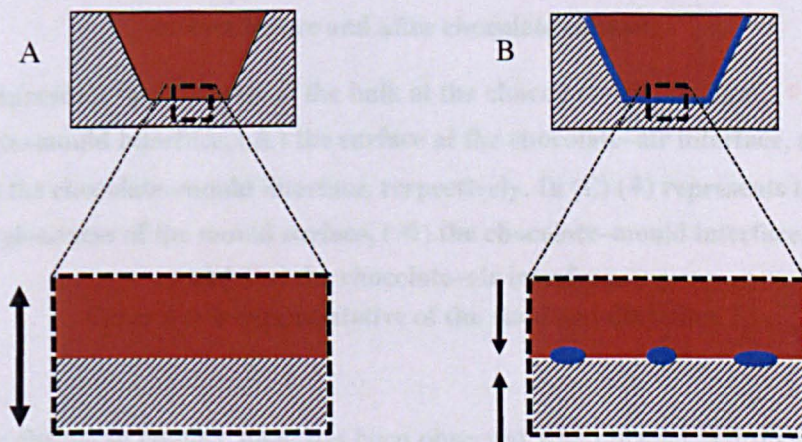


**Figure 5.14** Schematic representation of the effect of vapour adsorption at the mould surface. Image A shows the standard or normal chocolate–mould interface, whereas image B shows the presence of water vapour at the chocolate–mould interface and the subsequent reduction in chocolate–mould interactions and surface adhesion force.



Rather than individual water vapour molecules, a thin film of water molecules is thought to have formed on the mould surface, which dissolves the sugar molecules present at the chocolate surface that is in direct contact with the thin film, an effect known as sugar bloom. Limited interactions between chocolate and mould surface are responsible for the reduction in surface adhesion.

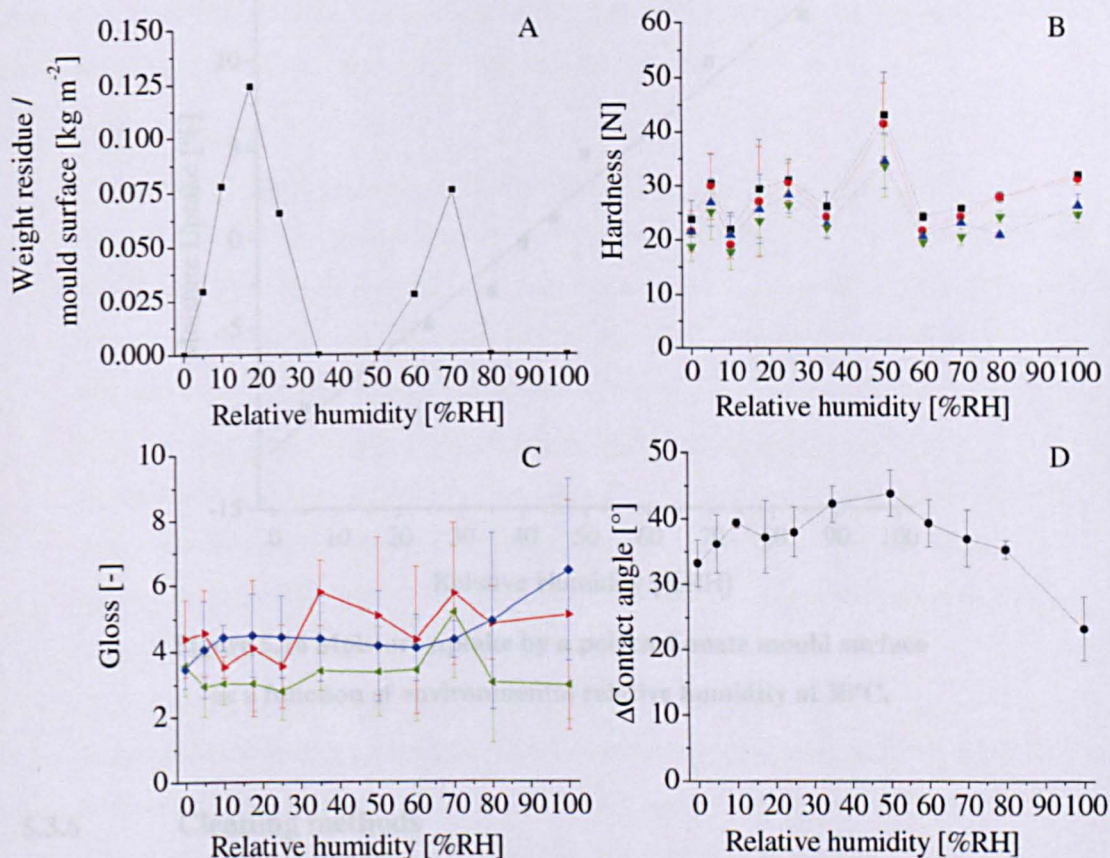


**Figure 5.15** The effect of environmental relative humidity on the amount of residues after probe separation (A), the hardness of the solidified chocolate samples (B), the difference of surface glossiness (C) and the difference of contact angle (D) of the polycarbonate mould surface before and after chocolate contact.

In (B) (■) represents the hardness of the bulk at the chocolate–air interface, (●) the bulk at the chocolate–mould interface, (▲) the surface at the chocolate–air interface, and (▼) the surface at the chocolate–mould interface, respectively. In (C) (◆) represents the surface glossiness of the mould surface, (◄) the chocolate–mould interface, and (►) the chocolate–air interface.

Error bar is representative of the standard deviation.

An interesting change in contact angle has been observed when placing a drop of water on the mould surface after the surface adhesion measurements, shown in Figure 5.15D. At high RH there is a significantly lower change in contact angle observed, indicating that a limited amount of fat is deposited onto the mould surface.



## IMAGING SERVICES NORTH

Boston Spa, Wetherby  
West Yorkshire, LS23 7BQ  
[www.bl.uk](http://www.bl.uk)

**PAGE MISSING IN  
ORIGINAL**

As a result of the increased mould surface hydrophilicity, the adhesion to the hydrophobic chocolate at these air conditions should be lower. The reduction in surface adhesion at high %RH, however, shows an increasingly tacky and dull chocolate surface, with bloom occurring within days.

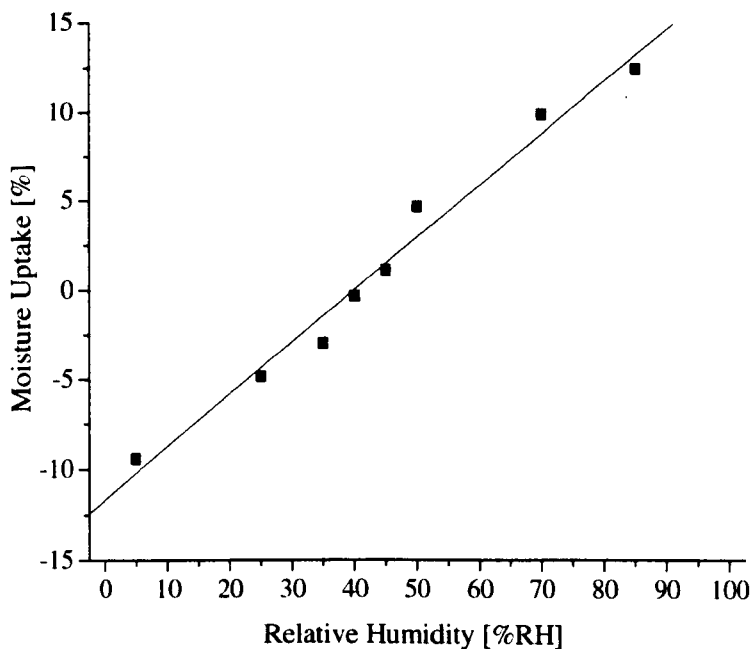


**Figure 5.16 Moisture uptake by a polycarbonate mould surface as a function of environmental relative humidity at 30°C.**

### 5.3.6 Cleaning methods

In commercial chocolate manufacturing the moulds are normally not washed after each production cycle, as a detrimental effect of the use of new and cleaned moulds has been observed. This is expected to be due to the formation of a thin film of fat on the mould surface, caused by fat migrating from the chocolate matrix to the polycarbonate surface upon contact. The increased hydrophobicity of the mould surface enhances demoulding. Results obtained in sections 4.3.6.1 and 5.3.3 have shown the deposition of a very thin layer of chocolate (fat) residues on the mould surface during its contact with chocolate making the surface more hydrophobic and less glossy, and the negative effect of moisture adsorption on the mould surface and on the surface adhesion force, respectively. The aim of this part of the research was to examine the relation between cleaning methods and surface adhesion, in order to increase understanding of the practical observations made in commercial chocolate manufacturing. Cleaning methods can be divided into two distinctly different areas of study, cleaning procedures and non-cleaning. Cleaning procedures refers to the current practices in commercial chocolate manufacturing, with the aim of increasing understanding of the effect of changes in surface chemistry of the mould surface on surface adhesion. Non-cleaning refers to the repeated use of chocolate moulds in several production cycles without any form of cleaning procedure.

### 5.3.6.1 *Cleaning procedures*

Basically, the surface adhesion of four different cleaning procedures is compared to non-cleaning. All samples are cleaned using the standard method for polycarbonate surfaces, i.e. soaking in the respective cleaning solution, rinsing with distilled water and drying using compressed air. The cleaning materials used are obtained from Nestlé PTC (York), where they are used in commercial chocolate manufacturing. Concentrated solutions are used to ensure a significant change in surface chemistry of the mould surfaces.

- Distilled water
- Concentrated detergent solution (Diverwash HD7) (JohnsonDiversey, 2009)  
Diverwash HD7 (JohnsonDiversey) is a mild alkaline (pH 9.2 – 10.0 for 1% solution) liquid detergent that is low foaming, hard water tolerant and suitable for washing plastic trays, e.g. polycarbonate. The main surface active component is tetrasodium ethylenediaminetetraacetate, a synthetic surfactant.
- Concentrated rinsing agent (Suma Rinse A5) (JohnsonDiversey, 2009)  
Suma Rinse A5 (JohnsonDiversy) is a neutral (pH 5.3) rinse aid that is low foaming, and contains a special blend of non-ionic surfactants for rapid, spot and streak free drying. Approximately 5 – 15% non-ionic surfactant is present, with alkyl alcohol alkoxyate representing the main component.
- Combination of a detergent and rinsing agent  
Polycarbonate surface cleaned with 1.0 % (w/w) detergent solution (Diverwash HD7), followed by a rinse using 0.2–0.5 ml l<sup>-1</sup> rinsing agent solution (Suma Rinse A5).  
Concentrations are based on recommendations made by the supplier.

The results presented in Figure 5.17 show significant differences for the cleaning materials or procedures tested. In general it can be observed that the use of a detergent increases the surface adhesion, similar to the observations made in industry. Washing of mould materials with a detergent is necessary on occasions when macroscopic chocolate residues have been deposited on the mould surface. Use of a detergent ensures a clean and fat free mould surface, but often causes problems laminating or wetting, possibly due to the presence of detergent residues (chemicals) on the mould surface after washing. Rinsing of mould materials with a rinsing aid results in a significant reduction in the surface adhesion, especially if compared to the surface adhesion force obtained by using a detergent system. By combining a detergent and rinsing aid, a decrease in surface adhesion is obtained compared to the sole use of a detergent solution. However, non-cleaning is superior over all cleaning materials used for obtaining a low surface adhesion. An important observation is that all cleaning procedures result in a clean separation, with no chocolate or residues adhering to the polycarbonate mould surface, as can be observed in Figure 5.18A.



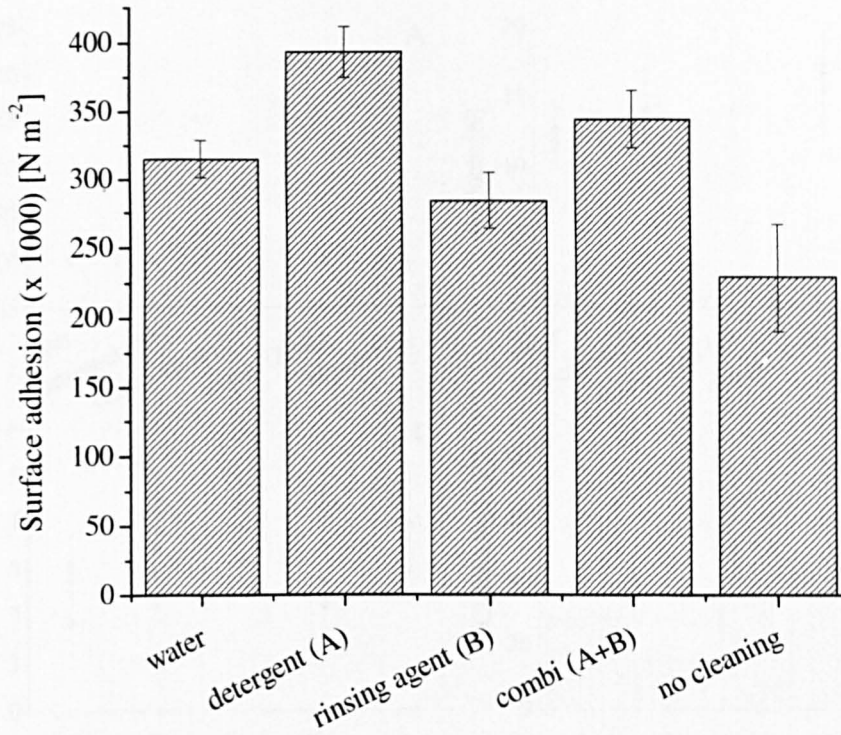


**Figure 5.17** Surface adhesion of dark chocolate as affected by different cleaning procedures. Error bar is representative of the standard deviation,  $n = 4$ .

Further investigation of the relationship between cleaning materials and surface adhesion shows significant changes in the surface chemistry of the polycarbonate mould surface due to treatment with different cleaning materials, as can be observed from Figure 5.18, especially graphs C and D. Although the results may not be significant, the glossiness of polycarbonate surfaces shows distinct differences. Particularly focussing on the rinsing agent, an increase in glossiness for all surfaces, i.e. both chocolate and mould, can be observed. Significant differences are obtained for the difference in contact angle of the polycarbonate mould surface before and after chocolate contact, which indicates that the use of different cleaning materials affects the surface chemistry of a polycarbonate surface in different ways. A more detailed visualization of the differences in contact angle before surface adhesion, i.e. on the clean mould surface, and after surface adhesion measurements, is given in Figure 5.19. Remarkable is the fact that, although the initial contact angle is variable, the contact angle after chocolate contact is largely stable over the range of surface treatments, indicating that a thin film of fat is deposited on all surfaces, irrespective of the cleaning material applied. Minor differences in hardness can be observed in Figure 5.18B, but these are not regarded as significant.



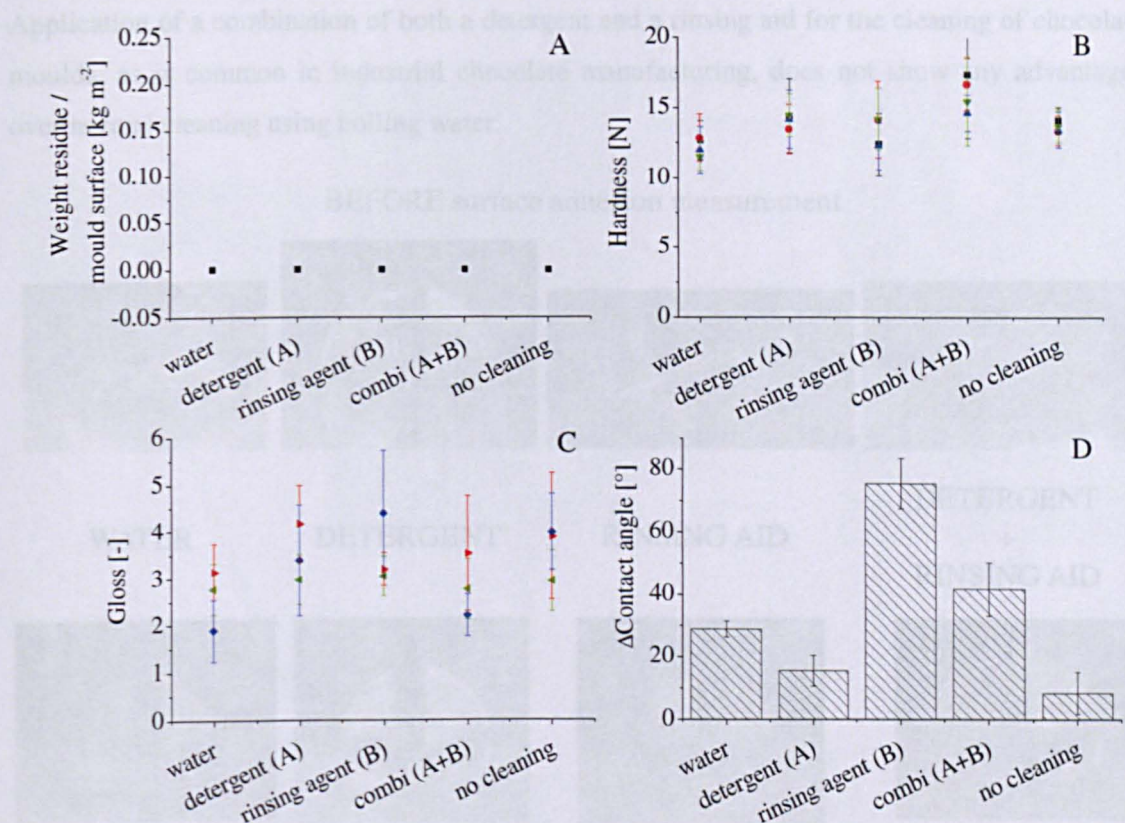


**Figure 5.18** The effect of different cleaning procedures on the amount of residues after probe separation (A), the hardness of the solidified chocolate samples (B), the difference of surface glossiness (C) and the difference of contact angle (D) of the polycarbonate mould surface before and after chocolate contact.

In (B) (■) represents the hardness of the bulk at the chocolate–air interface, (●) the bulk at the chocolate–mould interface, (▲) the surface at the chocolate–air interface, and (▼) the surface at the chocolate–mould interface, respectively. In (C) (◆) represents the surface glossiness of the mould surface, (◀) the chocolate–mould interface, and (▶) the chocolate–air interface.

Error bar is representative of the standard deviation.

The contact angles of water drops deposited on the cleaned mould surfaces, as shown by the top row of images in Figure 5.19, indicate that the application of different cleaning materials affects the surface chemistry and possibly the surface energy of the polycarbonate mould surface. Washing with a detergent creates a more hydrophobic surface, which can be observed by the increase in water contact angle compared to a mould surface cleaned with water. Application of a rinsing aid, on the other hand, makes the surface more hydrophilic, resulting in a water drop that spreads out over the polycarbonate and wets the surface. Relating these observations to the results obtained for the surface adhesion (see Figure 5.17) shows that a lower surface adhesion is obtained with a more hydrophilic mould surface in comparison with an increase in surface adhesion for a more hydrophobic mould surface.



Application of a combination of both a detergent and a rinsing aid for the cleaning of chocolate moulds, as is common in industrial chocolate manufacturing, does not show any advantages over normal cleaning using boiling water.

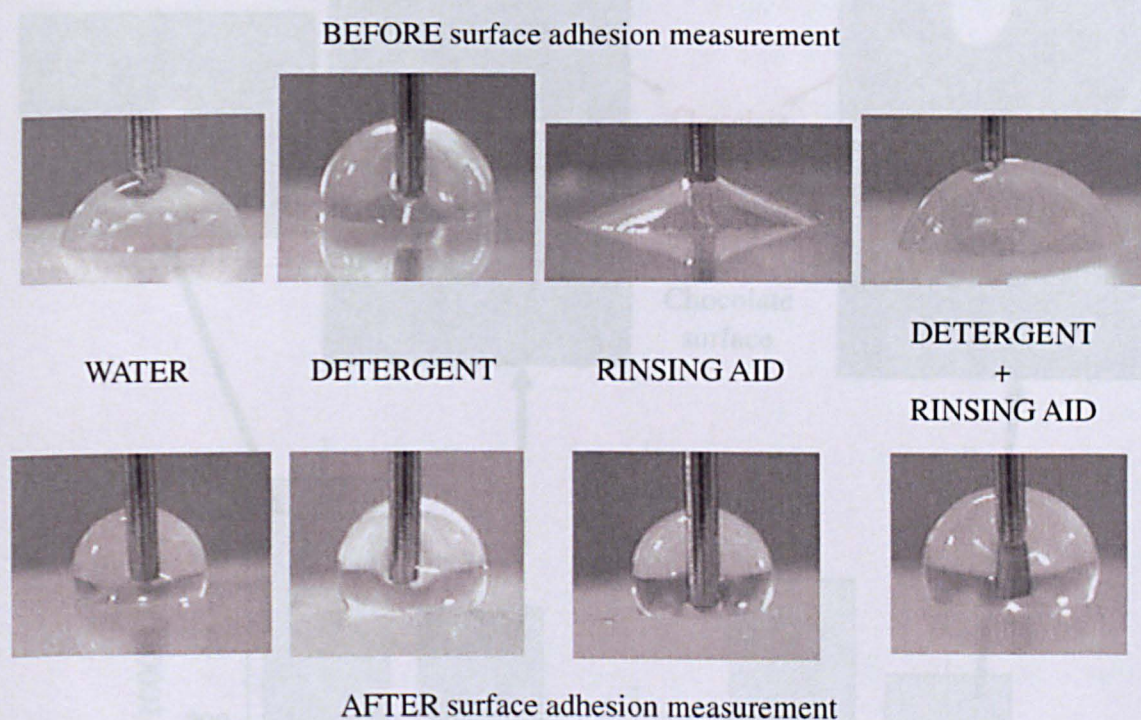


**Figure 5.19** Contact angle of water on polycarbonate mould surfaces treated with water, detergent, rinsing aid or a combination of detergent and rinsing aid, respectively, both before and after contact with a dark chocolate sample.

### 5.3.6.2 *Non-cleaning*

In industrial chocolate manufacturing it is normal that chocolate moulds are not cleaned between production cycles, as long as there are no chocolate residues present on the surface or physical damages visible. The results obtained when repeatedly (4x) re-using the polycarbonate mould surfaces, as seen in Figure 5.20, clearly show a reduction in surface adhesion when the mould is not cleaned in between measurements. The highest adhesion force is obtained with the new or clean mould, and a similar observation is commonly made during commercial chocolate manufacturing where new or cleaned (washed) moulds often show increased adhesion. A high correlation is further known to exist between the increased adhesion of new moulds and the presence of defects at the chocolate surface. Pictures included in Figure 5.20 show the presence of residues at both the chocolate and the mould surfaces after the surface adhesion force determination. Comparison of the 1<sup>st</sup> and the 4<sup>th</sup> repetition clearly shows the build up of a fat layer on the mould surface, which is assumed to be responsible for the decrease in surface adhesion force observed.



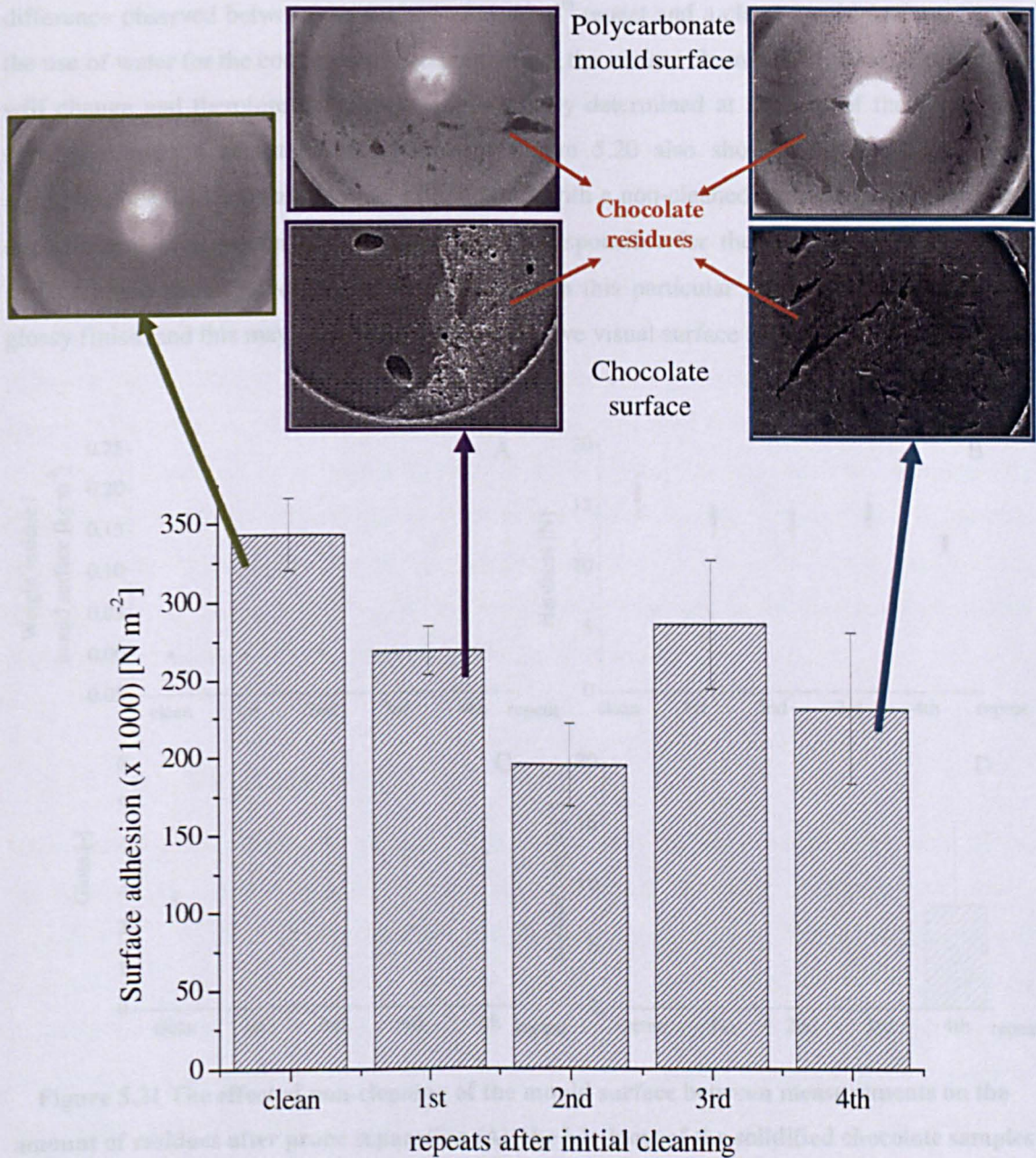


**Figure 5.20** Evolution of the surface adhesion of dark chocolate if the mould surface is not cleaned between measurements, together with a visualization of the mould and chocolate surfaces.

Error bar is representative of the standard deviation,  $n = 4$ .

Further investigation of the relation between non-cleaning and surface adhesion shows that a clean separation is obtained for all repeats, as can be observed from Figure 5.21A. The pictures in Figure 5.20, however, do show the deposition of chocolate residues on the polycarbonate mould surface. These (chocolate) residues have a distinct effect on both the mould and chocolate surface. Comparison of the clean mould surface with the same surface after 4 repeats shows the presence of a thin film covering the whole surface. This film is expected to be fat, as the contact angle of a water drop shows an increase compared to the clean surface, indicating



that the surface is becoming more hydrophobic. Figure 5.21D shows only the contact angle difference observed between the surface after the 4<sup>th</sup> repeat and a clean mould surface. Due to the use of water for the contact angle determination, the surface chemistry of the mould surfaces will change and therefore the contact angle is only determined at the end of the production cycle, i.e. after 4 repeats. The pictures in Figure 5.20 also show the change in surface appearance of the chocolate sample, after contact with a non-cleaned mould surface. Non-ideal experimental process conditions may be partly responsible for these detrimental effects on surface appearance. Polycarbonate surfaces used in this particular study have not received a glossy finish, and this may explain in part the negative visual surface appearance.

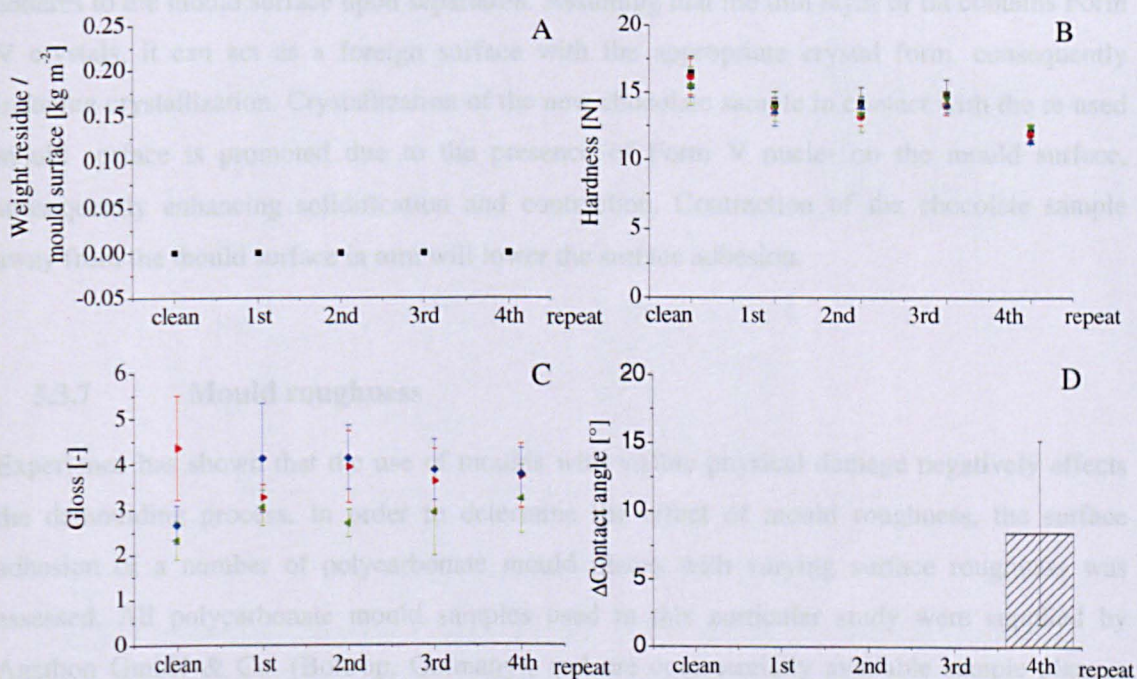


**Figure 5.21** The effect of non-cleaning of the mould surface between measurements on the amount of residues after probe separation (A), the hardness of the solidified chocolate samples (B), the difference of surface glossiness (C) and the difference of contact angle (D) of the polycarbonate mould surface before and after chocolate contact.

In (B) (■) represents the hardness of the bulk at the chocolate–air interface, (●) the bulk at the chocolate–mould interface, (▲) the surface at the chocolate–air interface, and (▼) the surface at the chocolate–mould interface, respectively. In (C) (◆) represents the surface glossiness of the mould surface, (◀) the chocolate–mould interface, and (▶) the chocolate–air interface.

Error bar is representative of the standard deviation.

Based on numerous observations and contact angle experiments the assumption is made that the thin film deposited on the mould surface whilst in contact with chocolate is a fat layer. The microstructure of chocolate has been discussed extensively in section 2.1.3.3.1 where it was proposed that chocolate consists of solid particles, e.g. fat crystals, cocoa and sugar particles,

dispersed in a continuous fat phase. The exact structure of the dispersed particulate network is not fully understood, but evidence exists for a porous structure in which the holes, pores or crevices are partly filled with liquid cocoa butter (Loisel et al., 1997). It has been observed that fat migrating to the surface is partly responsible for the formation of fat bloom upon storage. Further research has investigated whether this migration of liquid fat through the porous matrix happens via diffusion or capillary flow (Aguilera et al., 2004). Either way, the results obtained indicate that not only upon storage but already during chocolate manufacturing liquid fat is transported to the surface. Possibly as a result of the contraction of the tempered chocolate, a limited amount of liquid fat located between the solid particles is propelled to the surface (Quevedo et al., 2005). The thus formed thin layer of fat present on the chocolate surface adheres to the mould surface upon separation. Assuming that the thin layer of fat contains Form V crystals, it can act as a foreign surface with the appropriate crystal form, consequently inducing crystallization. Crystallization of the new chocolate sample in contact with the re-used mould surface is promoted due to the presence of Form V nuclei on the mould surface, subsequently enhancing solidification and contraction. Contraction of the chocolate sample away from the mould surface in turn will lower the surface adhesion.

### **5.3.7 Mould roughness**

Experience has shown that the use of moulds with visible physical damage negatively affects the demoulding process. In order to determine the effect of mould roughness, the surface adhesion of a number of polycarbonate mould pieces with varying surface roughness was assessed. All polycarbonate mould samples used in this particular study were supplied by Agathon GmbH & Co. (Bottrop, Germany), and are commercially available sample plaques produced from Bayer Makrolon 2858 polycarbonate with a variety of textures. The roughness of the different textures is classified as 0 (smooth, highly glossy), 30, 36, 39, 40 and 42, and refers to a grading made by the supplier, where the level of texturing or roughness increases if the number is higher. Results obtained for the surface adhesion of the polycarbonate mould surfaces with different levels of roughness or texturing are shown in Figure 5.22. A clear positive correlation between surface roughness and surface adhesion can be observed, with adhesion increasing significantly with surface roughness. As the differences in surface texture have not been quantified, it is impossible to say whether this correlation is linear. The photographs inserted in Figure 5.22 show the clean mould surfaces with a roughness factor of 30 and 40, respectively. From a macroscopic point of view clear differences are visible in roughness and/or texture of the mould surfaces used. The increase in effective surface area with increasing surface roughness is hypothesized to be responsible for an increase in interactions between chocolate and mould, and subsequently an increase in surface adhesion. With the increase in surface texture, especially as it is at a macroscopic level, the surface area of the mould surface



increases correspondingly. A higher surface area means an increase in the number of attachment sites where the chocolate can adhere to the mould surface. The liquid tempered chocolate spreads out over the polycarbonate mould surface, consequently wetting the whole surface. Through an increase in attachment sites and possibly a limited degree of mechanical interlocking of chocolate in the mould cavities, the adhesion between chocolate and mould surface increases. Viscosity of the chocolate could furthermore affect the surface adhesion in relation to surface roughness, but as the same chocolate type is used for all measurements in this particular part of the research, viscosity can be disregarded.

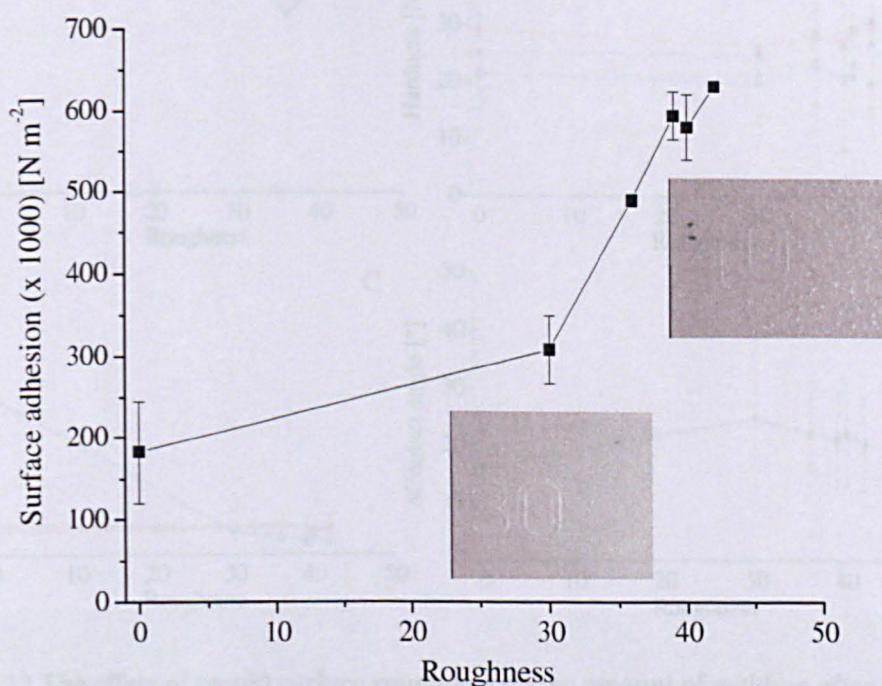


**Figure 5.22** Surface adhesion of dark chocolate as affected by mould surface roughness.

**Error bar is representative of the standard deviation, n = 4.**

Further investigation of the relation between mould surface roughness and surface adhesion does not give any significant or remarkable observations, as can be seen in Figure 5.23. The residue weight adhering to the mould surfaces, see Figure 5.23A, indicates a cohesive–adhesive failure at all roughnesses. A slight reduction in residues is obtained for a surface roughness of 36, but this is not regarded as significant. Except for the high glossiness of the mould surface with a surface texture of 0, there are no differences in surface glossiness. It is expected that the deposition mechanism of fat residues onto the mould surface is oblivious to surface roughness, and as such it is assumed that the surface gloss, Figure 5.23C, and contact angle, Figure 5.23D, are unaffected by changes in surface roughness. Slight differences are observed in contact angle of the clean mould surfaces, showing an increase in contact angle with increasing surface roughness (not shown here). This would indicate that the mould surface becomes more hydrophobic with increasing texture.



However, the presence of a low level of texture means that the surface deviates from the ideal situation, making the use of contact angles relatively unreliable. Overall it can be concluded that surface roughness has a negative impact on surface adhesion, but hardly influences chocolate hardness, glossiness and the amount of residues adhering.

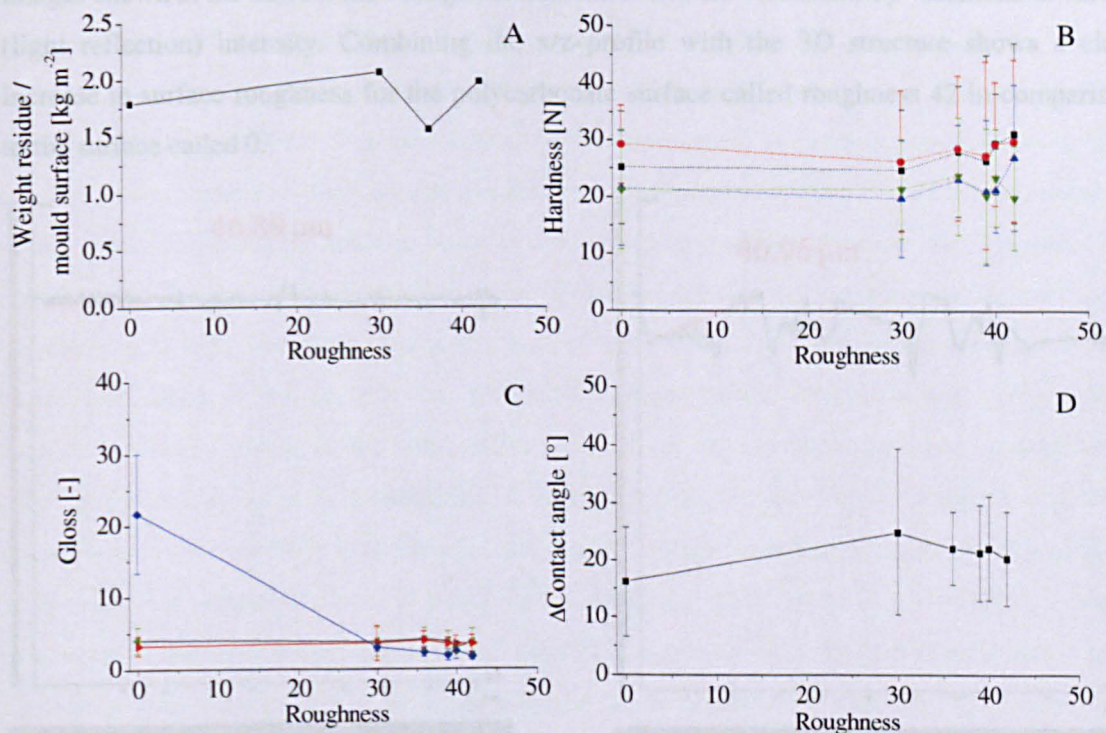


**Figure 5.23** The effect of mould surface roughness on the amount of residues after probe separation (A), the hardness of the solidified chocolate samples (B), the difference of surface glossiness (C) and the difference of contact angle (D) of the polycarbonate mould surface before and after chocolate contact.

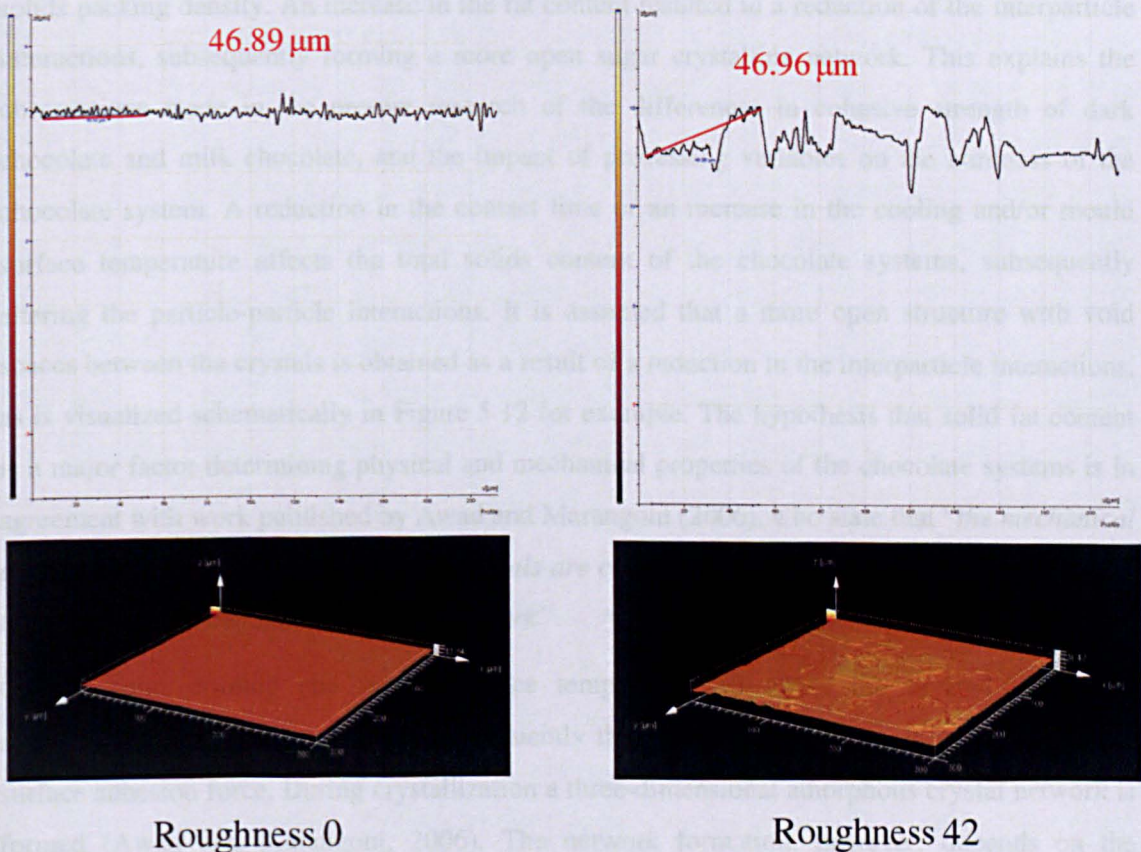
In (B) (■) represents the hardness of the bulk at the chocolate–air interface, (●) the bulk at the chocolate–mould interface, (▲) the surface at the chocolate–air interface, and (▼) the surface at the chocolate–mould interface, respectively. In (C) (◆) represents the surface glossiness of the mould surface, (◀) the chocolate–mould interface, and (▶) the chocolate–air interface.

Error bar is representative of the standard deviation.



## 5.3.7.1 Surface microstructure

In order to quantify the differences in surface roughness, confocal laser scanning microscopy (CLSM) was applied to analyse the microstructure of a set of polycarbonate mould surfaces, as is visualized in Figure 5.24. The  $x/z$ -profiles (top images), indicate the variation in height of the two surfaces studied, one with a roughness of 0 and the other with a roughness of 42. In the 3D images shown at the bottom the changes in microstructure are visualized by variations in colour (light reflection) intensity. Combining the  $x/z$ -profile with the 3D structure shows a clear increase in surface roughness for the polycarbonate surface called roughness 42 in comparison to the surface called 0.



Roughness 0

Roughness 42

**Figure 5.24** Surface microstructure of a polycarbonate mould surface with roughness 0 and with roughness 42.

The trend observed in Figure 5.22 for the surface adhesion shows a sharp increase for the polycarbonate mould material with a roughness of 42 compared to the surface with a roughness of 0. CLSM results confirm that the surface microstructure is significantly different between these two surfaces, and is therefore expected to be responsible for the differences observed in surface adhesion force.



## 5.4 DISCUSSION

Babin (2005) studied the effect of the presence of oil-soluble surface-active components in model sugar-oil systems. Results obtained indicated the partial replacement of inner oil surfactants from the sugar surface after the addition of an emulsifier in high sugar systems, and a reduction in the sediment volume resulting in an increase in the sediment particle packing density of 10 wt% sugar dispersions. It was concluded that the adsorption of surfactants at the sedimenting sugar particle surface reduced the strength of the attractive interparticle interactions between the sugar particles. Similarly, Afoakwa et al. (2009) showed that a dark chocolate system containing 25% fat displayed extensive particle-particle interaction strengths and a high solids packing density. An increase in the fat content resulted in a reduction of the interparticle interactions, subsequently forming a more open sugar crystalline network. This explains the observations made in the present research of the differences in cohesive strength of dark chocolate and milk chocolate, and the impact of processing variables on the hardness of the chocolate system. A reduction in the contact time or an increase in the cooling and/or mould surface temperature affects the total solids content of the chocolate systems, subsequently altering the particle-particle interactions. It is assumed that a more open structure with void spaces between the crystals is obtained as a result of a reduction in the interparticle interactions, as is visualized schematically in Figure 5.12 for example. The hypothesis that solid fat content is a major factor determining physical and mechanical properties of the chocolate systems is in agreement with work published by Awad and Marangoni (2006), who state that “*the mechanical properties of fats and fat-structured materials are controlled by the amount of solids (SFC) and the microstructure of their fat crystal network*”.

Contact time, cooling and mould surface temperature all affect the crystallization and solidification of the cocoa fat, and consequently the ease of demoulding, as measured by the surface adhesion force. During crystallization a three-dimensional amorphous crystal network is formed (Awad and Marangoni, 2006). The network formation, however, depends on the presence of nuclei formed either in the bulk phase, i.e. homogeneous nucleation, or at the surface of existing (foreign) particles, i.e. heterogeneous nucleation (Mullin, 2001). In the present research the assumption is made that the polycarbonate mould surface acts as a foreign body, inducing nucleation and affecting crystal growth. Rousseau and Sonwai (2008) discuss the effect of the dispersed particulate, such as cocoa solids, sugar crystals and milk powder, on the crystallization mechanism. They propose that these particulates act as nucleation sites for the cocoa butter and reduce the free energy of nucleation, as a result of which the supercooling required for chocolate is lower than that for pure cocoa butter. The polycarbonate mould surface in contact with the chocolate surface layer may act in a similar way, subsequently enhancing fat crystal growth at the interface.

Varying the temperature of the mould surface will change its characteristics, consequently affecting the crystal formation of the fat phase at the chocolate–mould interface. Fluctuations in mould temperature may cause crystal nuclei at the surface of the chocolate sample to either melt or crystallize and solidify in another polymorphic form. In general, the processing conditions will alter the crystal growth mechanism and the crystal network formation. As described by Mullin (2001), crystal growth can take place via diffusion as a result of differences in concentration (see section 2.1.3) or via adsorption onto the crystal surface. Changes in temperature will affect especially this latter crystal growth mechanism. Stapley et al. (1999) suggest that chocolate crystallization is correlated with cooling rate, as they observed a relatively uniform crystallization in untempered chocolate at lower cooling rates and the formation of unstable polymorphs in tempered chocolate at higher cooling rates. With respect to chocolate microstructure Rousseau (2007) mentions the presence of pores and hairline cracks in solidified chocolate systems processed with a too fast a cooling rate. In comparison with these results it is expected that in the current research at the higher cooling temperatures, which result in a lower cooling rate, and possibly also at the lower contact times, the amount of higher melting polymorphs formed is increased, whereas the nucleation and growth of unstable or lower melting polymorphs is delayed. Furthermore, melting out of crystals or the presence of ingredients (foreign bodies) or water molecules at the chocolate–mould interface for example will also affect the crystal network formation, either through a change in surface energy, such as observed for the different cleaning methods, or the removal of crystal nuclei at high mould surface temperatures.

Using a specifically developed DSC technique, Baichoo et al. (2006) demonstrated that the cooling conditions affect the kinetics of crystal growth. Within a tempered chocolate the formation of low-melting polymorphs is enhanced when using a fast cooling rate, whereas the formation of higher-melting polymorphs was favoured on slow cooling. According to Loisel et al. (1998) the crystallization of dark chocolate during cooling from 40°C is either via a single sharp crystallization for a chocolate temperature < 26.2 °C or via a two step fractionated crystallization at a temperature > 26.2 °C. Based on these observations it is assumed that changes in cooling temperature within the present research result in the formation of varying polymorphic forms. The formation of different polymorphic forms furthermore influences the crystal packing at the chocolate–mould interface. Schenk and Peschar (2004) discuss the differences in crystal packing of the  $\beta'$  structure, where the layers are packed loosely due to the fatty acid chains being organized perpendicular, compared to that of the  $\beta$  structure, where the chains are organised parallel, consequently forming a much more dense and closed packed structure. The varying crystal packing of different polymorphs is responsible for differences in the degree of contraction obtained on solidification, which in turn affects the demoulding of the solidified chocolate bar (Beckett, 2001).

## 5.5 CONCLUSIONS

The processing conditions during the mould and cooling stages of the chocolate manufacturing process significantly influence the mechanism of adhesion between chocolate and mould surface, consequently affecting the demoulding process. Different processing conditions mainly affect crystallization and solidification of the fat phase of the chocolate. Contact time is assumed to be highly correlated with the number and size of crystals formed, which in turn are correlated with the cohesive strength of the chocolate system. The melting out of crystal nuclei at high mould surface temperatures and the formation of polymorphic forms other than Form V as a result of processing conditions affect the crystal arrangement of the cocoa butter fat. As a result, limited contraction occurs, causing difficulties demoulding. Both cooling temperature and the inclusion of different ingredients influence the total solids content, resulting in a change in interparticle interactions and chocolate microstructure. With respect to the effect of relative humidity, the presence of water vapour leads to the formation of a hydrophilic mould surface, which lowers the surface adhesion, due to limited chocolate–mould interactions. Cleaning conditions alter the surface chemistry of the polycarbonate mould surface and thus affect the surface energy. Overall it can be concluded, based on the results obtained for the different processing conditions, that the ease of demoulding can be optimised by pre-heating the (polycarbonate) mould under controlled environmental conditions, i.e. 0% RH and 25 – 30 °C, and using a cooling temperature of approximately 10 – 15 °C.



## CHAPTER 6

### THE EFFECT OF AERATION ON CHOCOLATE DEMOULDING

#### 6.1 INTRODUCTION

Within the confectionery industry a significant increase in the launch of new mousse and aerated confectionery products has been observed. There has been a sharp rise in both the number of aerated products and aeration techniques, as a result of which the fundamental understanding of bubble mechanics especially in relation to the production of stable aerated products is essential. Aeration is defined by Niranjana (1999) as “*a process in which air or carbon dioxide or any other gaseous mixture is included within a food system, to produce a gas phase and a condensed phase (solid or liquid).*” For an intermediate viscosity system such as chocolate, bubbles can be included in the continuous fat phase via four mechanisms according to Campbell and Mougeot (1999): dough and paste mixing, (cold) expansion extrusion, pressure beating (dissolution of air or gas under pressure), and vacuum expansion (followed by rapid cooling). One of the advantages of this variability in bubble inclusion methods is that it allows the production of a set of aerated chocolate products with slightly varying characteristics. However, a negative aspect is that there is limited correlation between processing parameters and aeration characteristics such as gas hold-up, bubble size and distribution, or more general, bubble formation, behaviour and stability.

Research by Haedelt (2005) investigated effects of ingredients and processing parameters on bubble inclusion, and showed a strong interaction between recipe composition and gas hold up and mean bubble section diameter, respectively. It was proposed that the different fat crystal network formed in a chocolate product containing milk fat was responsible for the decrease in the setting rate, which consequently allowed a higher degree of bubble expansion and coalescence. Furthermore, the type of gas was observed to significantly impact the bubble inclusion, with low soluble gases such as N<sub>2</sub> resulting in micro-aeration, and high soluble gases such as CO<sub>2</sub> giving the chocolate macro-aeration. The present part of this research aimed to reveal the effect of bubble inclusion on the level of adhesion, by correlating the experimental adhesion to the solid surface free energy, chocolate ingredients and bubble size / distribution. This will enhance understanding of adhesion at the chocolate–mould interface and the effect of processing conditions on these interfacial interactions.

## **6.2 METHODS**

The aeration equipment and methodologies of chocolate–mould adhesion and the structural characterisation of the aerated chocolate have been discussed in CHAPTER 3. This section will describe specific materials and analyses or processing conditions applied in adhesion studies of aerated chocolate systems.

### **6.2.1 Materials**

For the determination of the effect of aeration on the experimental surface adhesion force, it is important that both the same chocolate systems and the same mould materials are used as previously applied in CHAPTER 4. Polycarbonate was chosen as the solid mould substrate when determining the importance of bubble size for the same reason as discussed in CHAPTER 4. Milk chocolate (29% cocoa solids) was used as the standard chocolate system, as the commercial AERO (Nestlé) product is based on a milk chocolate system.

### **6.2.2 Methods**

Preliminary investigations focussed on the technique used to melt the aerated chocolate and create contact between a solid mould surface and the aerated chocolate sample. The results of this work have shown that the most appropriate technique is to remove the outer chocolate shell present on commercial aerated chocolate products. For pilot plant products the aerated chocolate mass is deposited directly into a polycarbonate mould, and there is therefore no need to remove the outer shell before adhesion experiments. The aerated chocolate sample is then carefully heated in an oven under controlled temperature conditions, depending on the composition, i.e. dark or milk chocolate. Contact between the aerated chocolate and the mould surface is created using the same methodology previously applied for non-aerated chocolate systems.

## **6.3 RESULTS**

### **6.3.1 Effect of aeration**

An aerated milk chocolate system was compared to a standard or non-aerated milk chocolate system with respect to their effect on the experimental surface adhesion force of a polycarbonate mould surface. The same milk chocolate recipe was used, with a total cocoa solids content of 29%. Figure 6.1 compares the surface adhesion force of both systems, and it clearly shows a significant difference as a result of the aeration process. On average, the inclusion of bubbles into a chocolate system causes an increase in surface adhesion force, irrespective of the chocolate system.

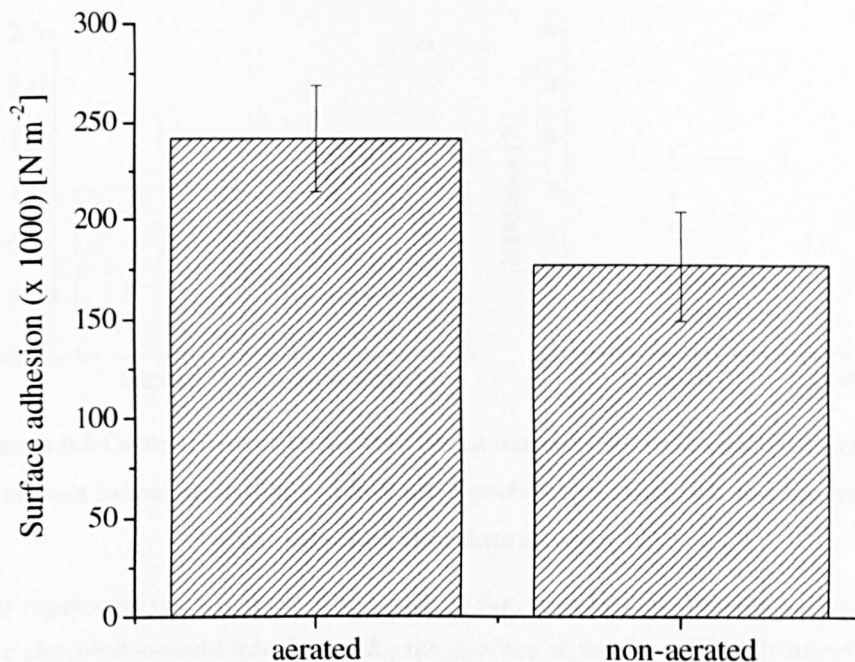


**Figure 6.1 Comparison of the surface adhesion of an aerated and a non-aerated milk chocolate system.**

**Error bar is representative of the standard deviation, n = 4.**

Further investigation of the relationship between aeration and surface adhesion shows that the inclusion of air bubbles results in a significant increase of the amount of milk chocolate residues present on the polycarbonate mould surface after separation, as can be observed from Figure 6.2A. For all measurements, a cohesive failure was observed, indicating that the aeration step affects the cohesive strength of the chocolate system. Not much difference in hardness of the aerated and non-aerated systems is present, although the average value is in all instances lower for the aerated system, as can be observed from Figure 6.2B.

The presence of air bubbles is expected in general to reduce the hardness of the chocolate systems. In relation to that, it is hypothesized that the method used to determine the hardness is giving an indication of the mechanical strength of the chocolate system, rather than the hardness. In any case, the hardness profile (not shown) is affected by the presence of air bubbles, as a result of which the penetration force no longer reaches a constant plateau value. Whenever an air bubble is present, the penetration force shows a drop until the thin film surrounding the air is reached, resulting in a hardness profile with hills and valleys. However, the overall hardness of the milk chocolate system seems not to be affected by the inclusion of air in the system.



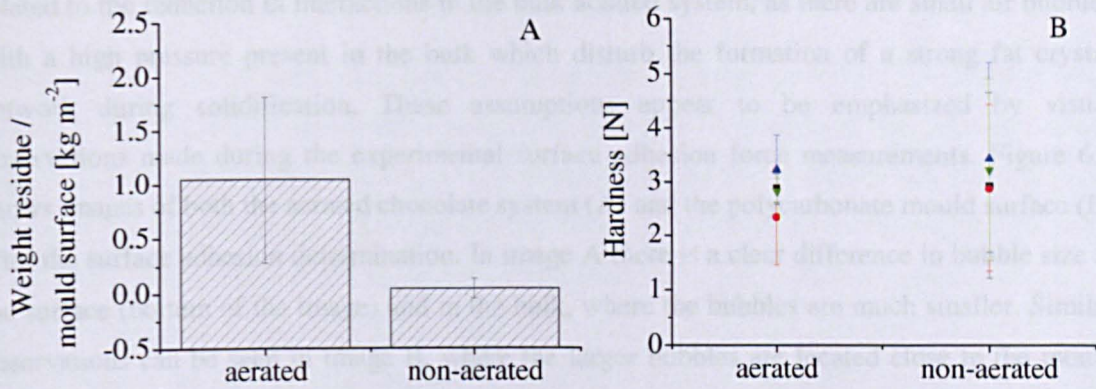


**Figure 6.2 Comparison of an aerated and a non-aerated milk chocolate system with respect to the amount of residues after probe separation (A), and the hardness of the solidified chocolate samples (B).**

In (B) (■) represents the hardness of the bulk at the chocolate–air interface, (●) the bulk at the chocolate–mould interface, (▲) the surface at the chocolate–air interface, and (▼) the surface at the chocolate–mould interface, respectively.

Error bar is representative of the standard deviation.

It can be concluded from the results obtained for the chocolate residues adhering and the hardness that the interfacial chocolate–mould strength is higher than the bulk cohesive strength of the chocolate, resulting in a break within the bulk of the chocolate system rather than at the interface. The reason for the enhanced interfacial strength is not known, but is assumed to be a consequence of an imbalance of the forces at the interface. Surface tension, in combination with the pressure inside and outside a bubble must be in equilibrium; otherwise a bubble will not exist, as is described by the balance of forces (Beckett, 2008):

$$2\pi\gamma + \pi r^2 p_1 = \pi r^2 p_2, \quad [6-1]$$

$$p_2 - p_1 = 2\gamma/r, \quad [6-2]$$

where  $p_1$  is the pressure outside the bubble,  $p_2$  the pressure inside the bubble and  $2\pi\gamma$  refers to the surface tension acting on the circumference of the bubble. During the process of creating the chocolate–mould interface the interactions within the surface layer of the chocolate will change, consequently affecting the surface tension and pressure acting on the bubbles. A restoration of the balance of forces is required for the bubbles to exist, which means that larger bubbles are created at the cost of small bubbles as the gas is moving from high pressure areas (small bubbles) to low pressure areas (large bubbles). This is because lower pressure in the large bubbles means a lower amount of energy is required.

It is suspected that after solidification an increased interfacial strength is obtained, as a result of the imbalance of forces between the bubbles at the interface. The pressure difference across the surface film increases for smaller bubbles, as a result of which a higher amount of energy is available for particle–particle or crystal–crystal interactions in the thin chocolate films, subsequently enhancing the interfacial strength. Similarly, the reduced bulk cohesive strength is



related to the reduction in interactions in the bulk aerated system, as there are small air bubbles with a high pressure present in the bulk which disturb the formation of a strong fat crystal network during solidification. These assumptions appear to be emphasized by visual observations made during the experimental surface adhesion force measurements. Figure 6.3 shows images of both the aerated chocolate system (A) and the polycarbonate mould surface (B) after the surface adhesion determination. In image A there is a clear difference in bubble size at the surface (bottom of the image) and in the bulk, where the bubbles are much smaller. Similar observations can be seen in image B, where the larger bubbles are located close to the mould surface and the smaller bubbles at the line of failure.

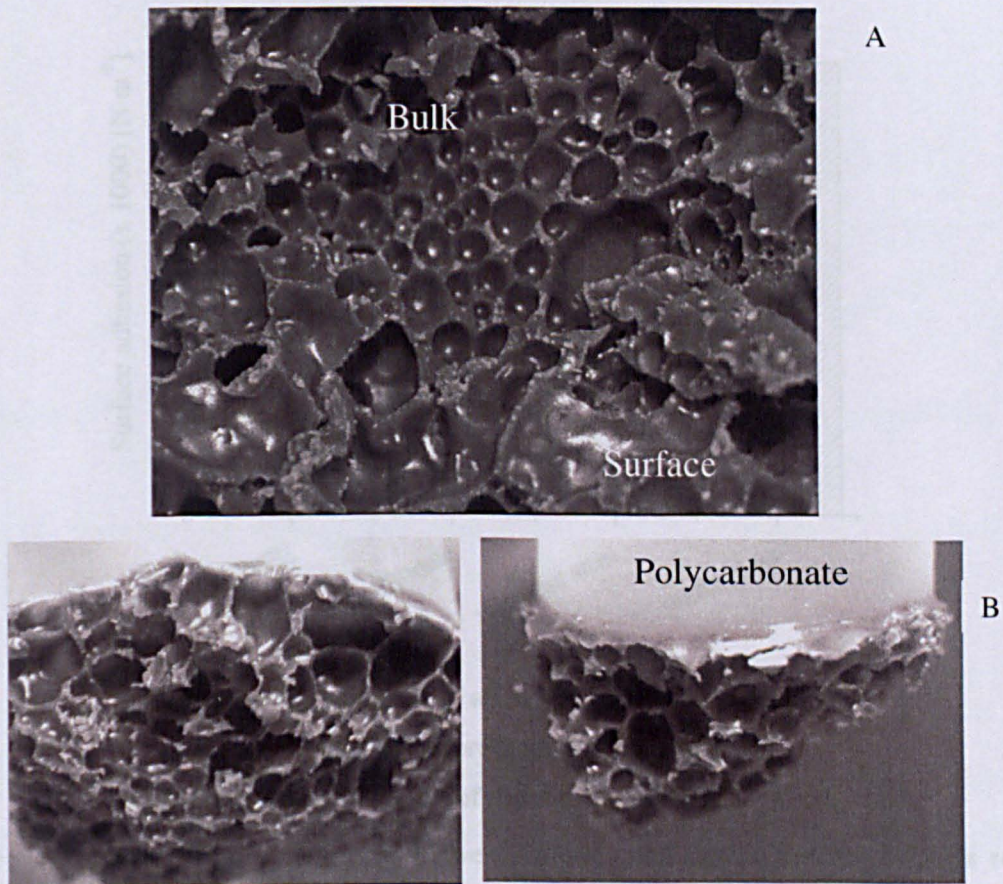


**Figure 6.3 Images (scale 1:0.34) of the aerated chocolate (A) and the mould surface (B) after the experimental surface adhesion force determination.**

The results obtained for the experimental surface adhesion determination are in good agreement with common observations made during commercial manufacturing practices. Aerated chocolate is often observed to adhere to the mould surfaces during production, causing problems demoulding and the presence of defects on the chocolate surface.



### 6.3.2 Effect of different mould materials

In the same way as for dark chocolate and cocoa butter systems (section 4.3.6.1), the surface adhesion of aerated milk chocolate has been investigated in relation to the different mould materials applied in this research. Figure 6.4 shows the experimental surface adhesion force for the four solid mould surfaces. Most outstanding result is that obtained for the surface adhesion of a PTFE surface, which is not significantly different from a polycarbonate surface, whereas a significant difference was previously obtained for non-aerated milk chocolate. Otherwise, the overall trend is the same as that observed previously, with quartz glass having the highest value for the surface adhesion.

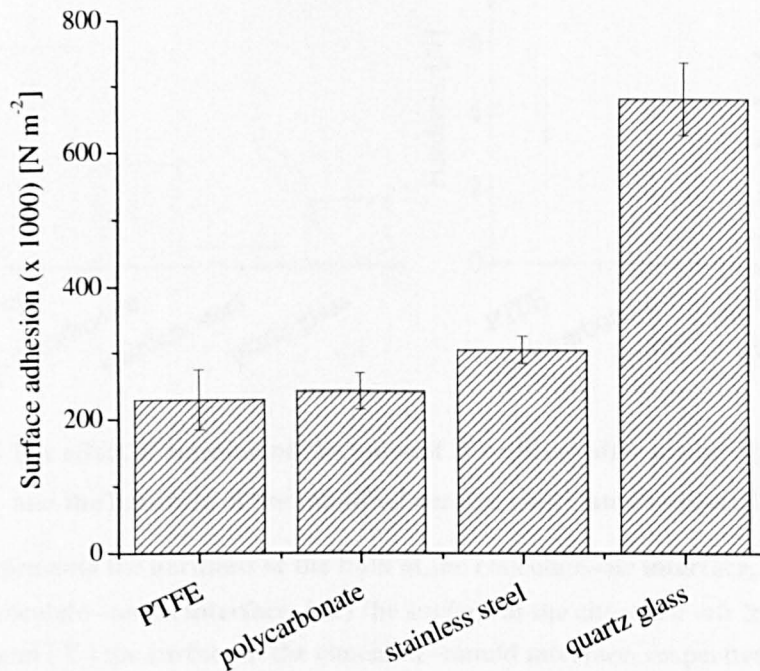


**Figure 6.4** Surface adhesion of an aerated milk chocolate system as affected by different mould materials.

**Error bar is representative of the standard deviation, n = 4.**

Further investigation of the relationship between aeration and mould material displays some very interesting effects on the amount of chocolate residues adhering to the polycarbonate surface after the surface adhesion measurement, as is shown in Figure 6.5A. The largest amount of chocolate residues is present on the PTFE surface, which previously showed an adhesive failure or clean separation for a non-aerated milk chocolate system. Both polycarbonate and quartz glass also show a cohesive failure, with no difference between the amounts of residues adhering. Interestingly, stainless steel shows an adhesive failure with the aerated milk chocolate system, with little or no residues adhering after separation. Significant differences between the mould materials can also be observed for the hardness, see Figure 6.5B. The surface hardness of the milk chocolate system that has been in contact with stainless steel is higher than any of the chocolate samples in contact with the other surfaces.



This indicates a difference in the crystallization / solidification mechanism or the average bubble size as a result of the physical contact with solid mould surfaces with varying surface energies, which is expected to be the main cause for the clean separation of stainless steel.

Visual observations have confirmed that all the milk chocolate systems were aerated, and that the break on separation took place in the bulk of the aerated system, similar to the images shown in Figure 6.3, resulting in a cohesive failure.

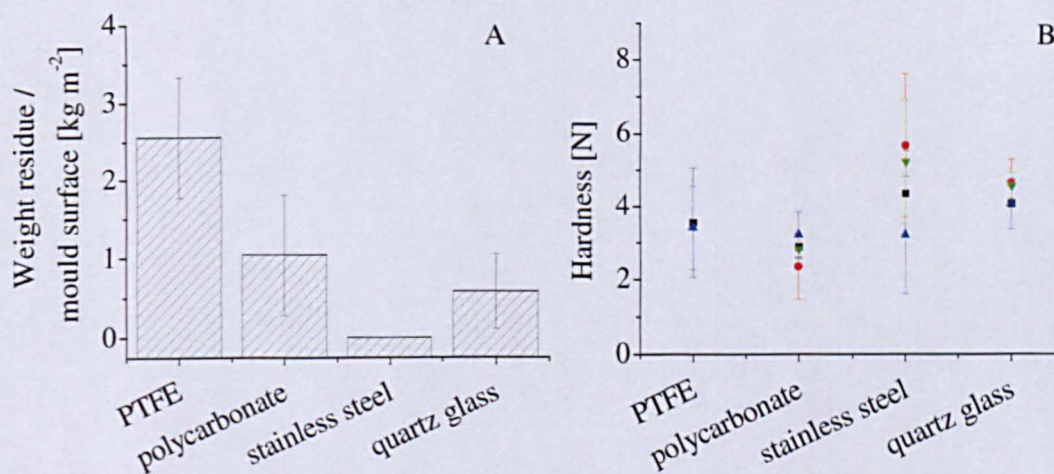


**Figure 6.5** The effect of aeration on the amount of residues after probe separation (A), and the hardness of the solidified aerated chocolate samples (B).

In (B) (■) represents the hardness of the bulk at the chocolate–air interface, (●) the bulk at the chocolate–mould interface, (▲) the surface at the chocolate–air interface, and (▼) the surface at the chocolate–mould interface, respectively.

Error bar is representative of the standard deviation.

A pilot plant trial has been conducted at Nestlé PTC (York) to determine the effect of different mould materials on the demoulding capabilities of aerated milk and dark chocolate systems. Aeration was acquired via the vacuum box method, described in section 3.3.4. The commercial mould materials used were PTFE, polycarbonate and stainless steel. Although they are the same materials as used for the experimental surface adhesion force determination, the composition and physical / chemical characteristics of these respective commercial moulds may differ from those used in this research for adhesion force measurements. Figure 6.6 shows images of the commercial mould surfaces after the demoulding process. All three materials show a cohesive–adhesive or cohesive failure, respectively. Visual observations indicate that the whole PTFE surface is covered with a thin film of milk chocolate (cohesive failure), whereas the stainless steel surface presents only a limited amount of chocolate adhering after demoulding (cohesive–adhesive failure).



These results are not in complete agreement with those obtained for the experimental surface adhesion force, where a clean surface separation was obtained for the stainless steel surface. The overall trend is similar, though. The largest amount of chocolate was present on the PTFE surface, as a result of which the demoulding process of aerated chocolate systems is most difficult for this mould material. A relatively low amount of adhesion is observed for the stainless steel system, consequently showing better demoulding properties.

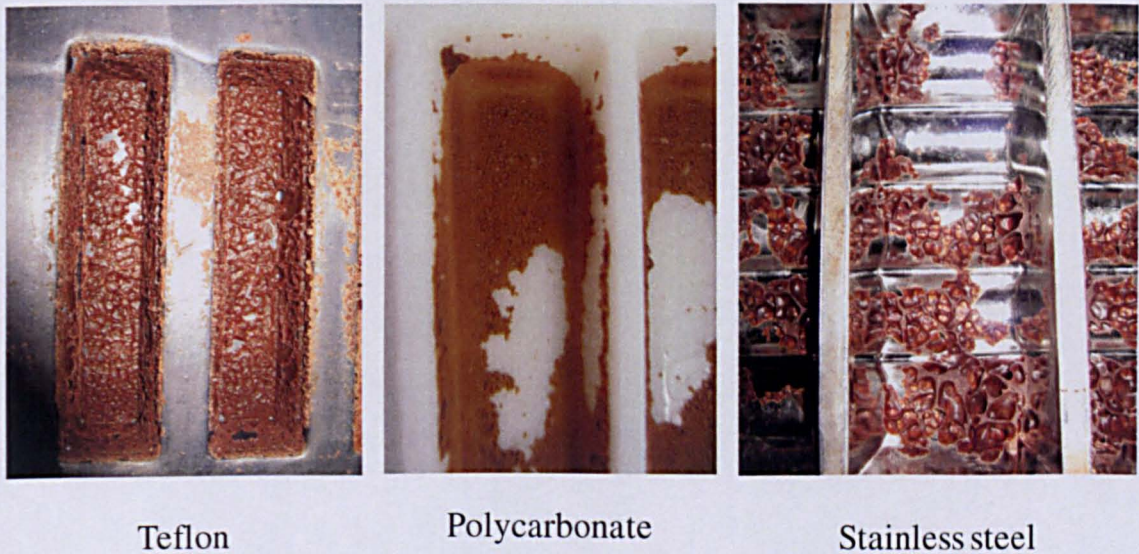


**Figure 6.6 Images showing the surfaces of commercial mould materials after contact with aerated chocolate samples, obtained via the vacuum box aeration.**

Relating the surface adhesion to the surface free energy gives a positive correlation, as can be seen in Figure 6.7. For both an aerated and a non-aerated milk chocolate system the same exponential growth type relation can be observed. Fitting the experimental data to the model shows a higher correlation for the aerated system. The apparent critical surface energy of the mould substrate remains the same for both aerated and non-aerated systems ( $\sim 30 \text{ mN m}^{-1}$ ).

The main issue when comparing the correlation between surface energy and surface adhesion for aerated and standard (non-aerated) chocolate systems is the observed difference in failure. Standard chocolate systems show a break at the chocolate–mould interface, whereas aerated chocolate systems show a cohesive failure within the bulk of the system. This means that Figure 6.7 actually compares surface adhesion of a set of mould surfaces with varying surface energy with the bulk adhesion or cohesive strength of aerated milk chocolate systems. Furthermore, variations in the level of aeration and/or bubble size and distribution between the different samples used will affect the cohesive strength of the aerated milk chocolate systems and consequently reduce the accuracy of the adhesion measurement and the correlation between surface energy and chocolate adhesion for aerated chocolate systems.



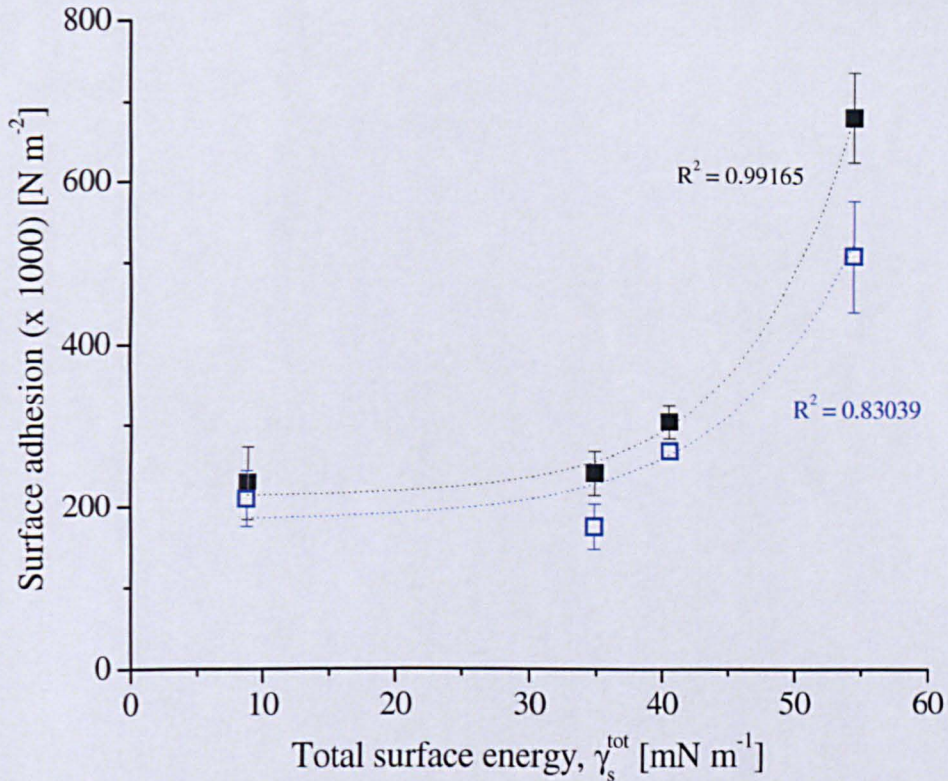


**Figure 6.7** Surface adhesion of an aerated (■) and a non-aerated (□) milk chocolate system as a function of surface energy.

**Gas hold-up of the aerated chocolate system used is approximately 55 %.**

**Error bar is representative of the standard deviation, n = 4.**

The heat transfer capacities of both the solid mould materials and the chocolate system are hypothesized to be responsible for the differences in surface adhesion and type of failure observed for aerated and non-aerated chocolate systems. First of all, the inclusion of bubbles in a chocolate system causes the system to act as insulation, slowing down the heat transfer from the surface to the centre or bulk of the chocolate system (Decker and Ziegler, 2002). Table 6.1 mentions the heat conductivity values of air and butter, amongst others. Taking butter as a replacement for chocolate, and comparing this to the heat conductivity of air, a significant difference is visible. Incorporation of air or another gas, such as CO<sub>2</sub> or N<sub>2</sub> can be observed to significantly reduce the heat conductivity of a fat based system like butter. By acting as an insulator, the aerated chocolate system will normally show a reduced hardness compared to a non-aerated system.

Secondly, the heat transfer rate of the different mould materials is dissimilar, as can be observed from the values reported for the heat conductivity in Table 3.3 (section 3.2.2). Stainless steel has the highest heat conductivity, indicating that it will transfer the largest amount of heat or energy within a specified time period. Polycarbonate and PTFE, on the other hand, show similar values of heat conductivity, and can be observed to be more likely as insulator materials. Relating these data to the surface adhesion of chocolate, it is assumed that the high heat transfer rate from the



stainless steel mould to a chocolate system is responsible for the clean separation and increased hardness that is observed. A high heat transfer is assumed to be responsible for a faster crystallization and solidification, and an increased (bulk) cohesive strength of the chocolate system. This applies not only to aerated but also to non-aerated chocolate samples. Polycarbonate and PTFE, on the other hand, show a much lower heat transfer rate, and the chocolate systems in contact with these materials subsequently take longer to crystallize and solidify. The combined effect of the insulation by the mould material and the aerated chocolate system significantly reduce the cohesive strength of the chocolate systems in contact with these mould materials, causing a cohesive failure, as is visualized in Figure 6.8.

**Table 6.1 Heat conductivity values of a selection of gases and liquids / food systems at 20 °C (Singh and Heldman, 2001).**

	<b>Heat conductivity [W m<sup>-1</sup> K<sup>-1</sup>]</b>
Air (mixture)	0.0251
CO <sub>2</sub>	0.014
N <sub>2</sub>	0.024
Water	0.597
Butter	0.197

A possible solution would be the use of a mould which consists of a thin film of PTFE coated on a stainless steel substrate. This combines the good physical characteristics of stainless steel, such as its conductivity properties, and the anti-adhesion chemical characteristics of PTFE. The thickness of both the PTFE and the stainless steel will be important in relation to the mould functionality. If the PTFE coating is too thick, the positive effect of the stainless steel substrate will be reduced. Similarly, if the stainless steel substrate is relatively thin, the heat conductivity may not be enhanced to a degree that significantly affects the demoulding properties of the aerated chocolate mass.

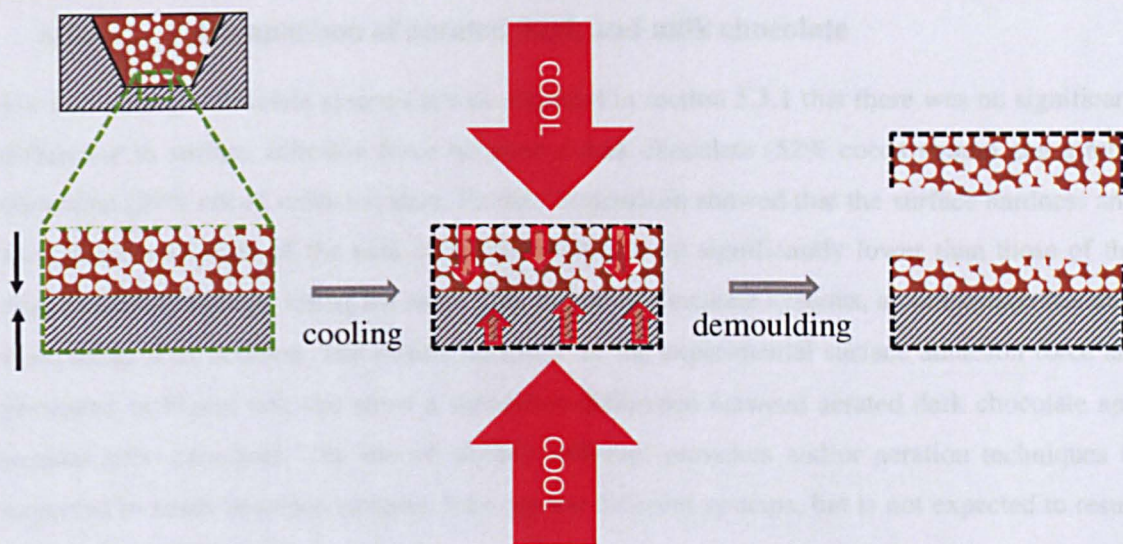


**Figure 6.8 Schematic representation of the relation between heat conductivity and demoulding of aerated chocolate systems.**

**Due to the reduced conductivity of both the aerated chocolate mass and the mould material, crystallization and solidification are delayed, resulting in a cohesive failure upon demoulding.**

Limited solutions are available to enhance the conductivity properties of the aerated chocolate mass, especially as these are reduced by the aeration. As will be discussed in section 6.3.4 the type of gas used affects the aeration, which subsequently impacts on the demoulding characteristics. The use of different ingredients is not expected to significantly impact the heat transfer characteristics of the aerated chocolate mass. Haedelt (2005) investigated the effect of different emulsifiers such as polyglycerol polyricinoleate (PGPR), sorbitan tristearate (STS) and glycerol monostearate (GMS), and fats such as milk fat, hard nonlauric vegetable fat and soft nonlauric vegetable fat, on the aeration of a standard milk chocolate recipe. Main impact was observed for milk fat, which increased both the gas hold-up and mean bubble-section diameter compared to the control recipe. On the other hand, a reduction in gas hold-up was observed for the recipes containing PGPR, or soft or hard vegetable fat. However, as surface adhesion was not measured, no mention was made regarding hardness or cohesive strength of these samples.



### 6.3.3 Comparison of aerated dark and milk chocolate

For non-aerated chocolate systems it was observed in section 5.3.1 that there was no significant difference in surface adhesion force between a dark chocolate (52% cocoa solids) and a milk chocolate (29% cocoa solids) system. Further comparison showed that the surface hardness and the cohesive strength of the milk chocolate system were significantly lower than those of the dark chocolate system. Using the same dark and milk chocolate systems, a comparison has also been made after aeration. The results obtained for the experimental surface adhesion force are presented in Figure 6.9, and show a significant difference between aerated dark chocolate and aerated milk chocolate. The use of slightly different pressures and/or aeration techniques is expected to result in minor variation between the different systems, but is not expected to result in significant differences.

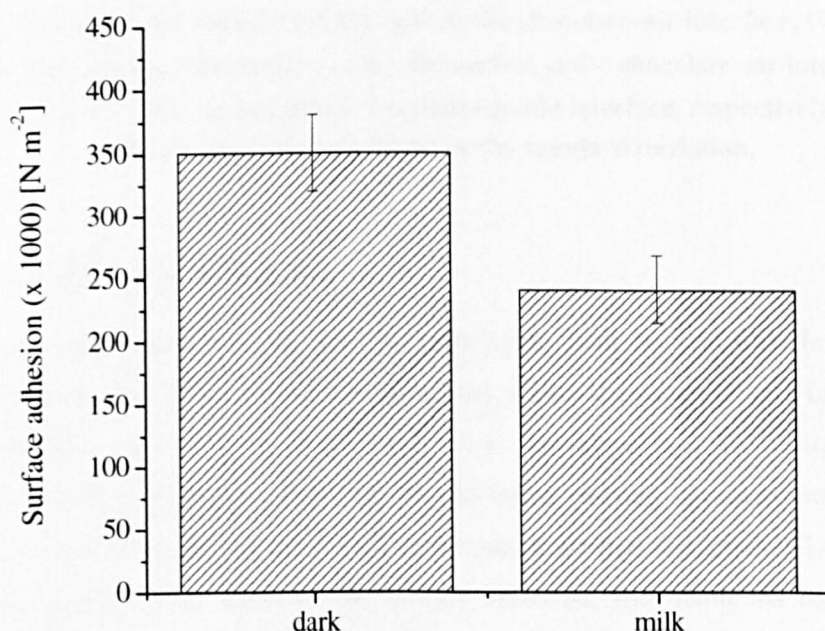


**Figure 6.9 Comparison of the surface adhesion of an aerated dark and an aerated milk chocolate system.**

**Error bar is representative of the standard deviation, n = 4.**

One of the reasons that would explain the differences between dark and milk chocolate would be the same explanation as proposed for the standard non-aerated systems, where the cohesive strength of the milk chocolate system is observed to be much lower. However, from Figure 6.10A it can be observed that significantly more dark chocolate residues adhere to the polycarbonate mould surface after separation. The hardness of the milk chocolate system is lower than that of dark chocolate, as can be seen from Figure 6.10B. This would indicate that the cohesive and/or mechanical strength of the milk chocolate system is lower than that of the dark chocolate system. The increased amount of dark chocolate residues would then result from a difference in crystallization and solidification rather than cohesive strength.



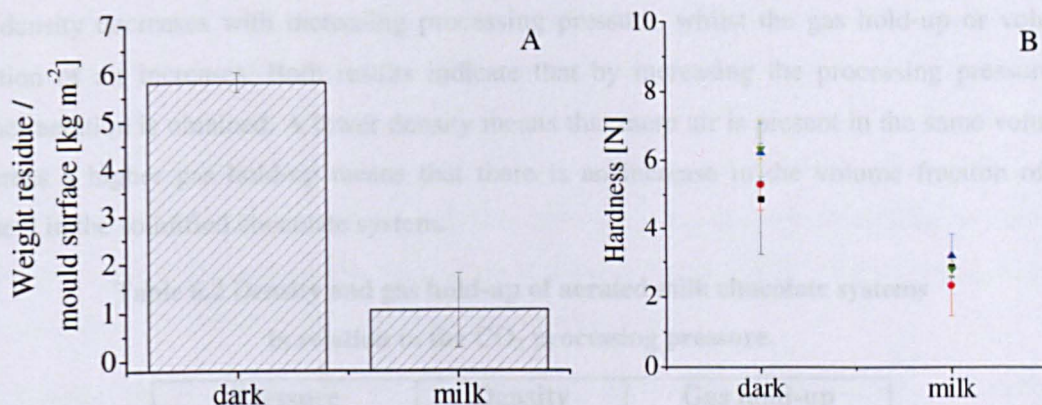


**Figure 6.10** Comparison of an aerated dark and an aerated milk chocolate system on the amount of residues after probe separation (A), and the hardness of the solidified chocolate samples (B).

In (B) (■) represents the hardness of the bulk at the chocolate–air interface, (●) the bulk at the chocolate–mould interface, (▲) the surface at the chocolate–air interface, and (▼) the surface at the chocolate–mould interface, respectively.

Error bar is representative of the standard deviation.

### 6.3.4 Effect of bubble size

A positive pressure batch rig was used to incorporate both N<sub>2</sub> and CO<sub>2</sub> in standard milk chocolate systems. By applying different pressures within the range 0 to 7 bar, a variety of aerated structures was created. Using the same technique as previously applied, the experimental surface adhesion force of the different aerated products was determined. Microstructure was assessed via the C-Cell technique, described in section 3.3.4.3. The results are discussed per gas type used for the surface adhesion, and combined for the structural characterisation.

#### 6.3.4.1 CO<sub>2</sub> gas

Carbon dioxide (CO<sub>2</sub>) is known to give a so called macro-aeration to chocolate systems, with an average gas hold-up value of 68%, as determined by Haedelt (2005). Using x-ray tomography the bubble characteristics of 2-D bubble sections were analyzed, giving average values for the diameter of 0.51 mm, corresponding to a mean bubble volume of 0.18 mm<sup>3</sup>. It was concluded that aeration using CO<sub>2</sub> gas increased bubble inclusion within a confined volume and enhanced coalescence phenomena, as a result of the higher solubility of CO<sub>2</sub> in cocoa butter fat compared to other gas types. The current research investigated the relation between aeration using CO<sub>2</sub> gas at different pressures and the experimental surface adhesion force. Table 6.2 relates the processing pressures used during the CO<sub>2</sub> aeration to the quality of the aerated chocolate systems, as represented by the density,  $\rho$ , and the gas hold-up value,  $\varepsilon$ . It can be observed that

the density decreases with increasing processing pressure, whilst the gas hold-up or volume fraction of air increases. Both results indicate that by increasing the processing pressure, a higher aeration is obtained. A lower density means that more air is present in the same volume, whereas a higher gas hold-up means that there is an increase in the volume fraction of air present in the solidified chocolate system.

**Table 6.2 Density and gas hold-up of aerated milk chocolate systems in relation to the CO<sub>2</sub> processing pressure.**

Pressure [Bar]	Density [g ml <sup>-1</sup> ]	Gas hold-up [%]
0	1.3	0
1.3	1.213	6.69
2	1.16	10.77
3	0.681	47.62
4.2	0.49	62.31
5.2	0.37	71.54
7.2	0.35	73.08

Plotting the experimental surface adhesion force against the CO<sub>2</sub> gas hold-up shows an inverse exponential relationship, as can be observed from Figure 6.11. This indicates that the adhesion or stickiness of chocolate decreases when more air is incorporated in the system.

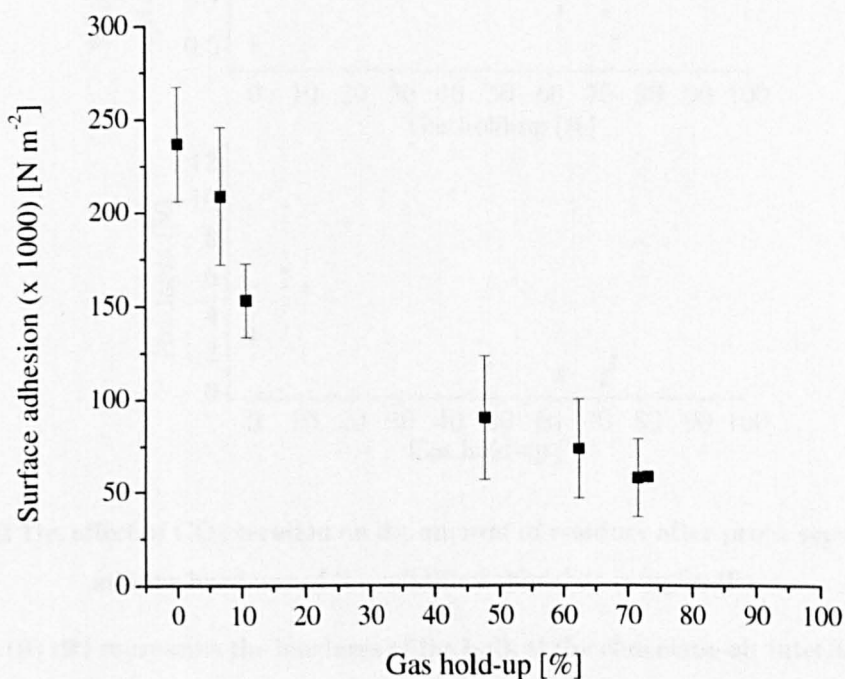


**Figure 6.11 Surface adhesion as a function of CO<sub>2</sub> gas hold-up. Error bar is representative of the standard deviation, n = 4.**



However, the relationship between CO<sub>2</sub> aeration and surface adhesion is not as straight forward as expected. From Figure 6.12A it can be observed that a cohesive failure is present for all aerated systems. Although the amount of chocolate adhering to the mould surface decreases with the CO<sub>2</sub> gas hold-up, this does not mean that the volume of chocolate adhering decreases. The main conclusion is that for all aerated milk chocolate systems a cohesive failure is observed within the aerated chocolate mass, rather than at the chocolate–mould interface, indicating that aeration affects the cohesive strength of the chocolate system.

The surface hardness in Figure 6.12B shows significant differences between the different aerated milk chocolate systems. Due to the cohesive failure, the hardness has only been measured at the chocolate–air interface. No significant differences can be observed between the hardness of the bulk and that of the surface. Compared to the standard non-aerated milk chocolate an increase in surface hardness can be observed at low aeration, whilst at higher gas hold-up values the surface hardness is significantly lower. The initial increase is not significant, and is accompanied by a large error, probably caused by a high degree of non-uniformity. With increasing gas hold-up values the hardness decreases, indicating that the inclusion of air bubbles reduces the hardness of the milk chocolate system.

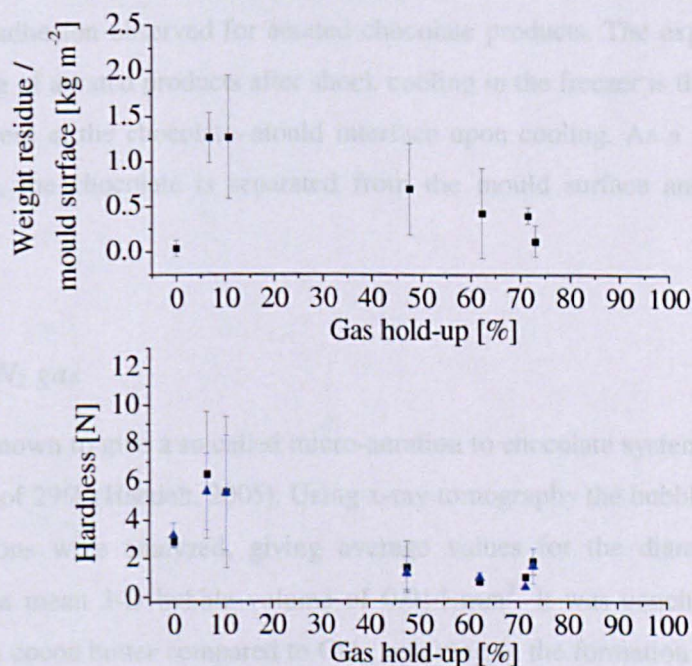


**Figure 6.12** The effect of CO<sub>2</sub> aeration on the amount of residues after probe separation (A), and the hardness of the solidified chocolate samples (B).

In (B) (■) represents the hardness of the bulk at the chocolate–air interface, and (▲) the surface at the chocolate–air interface, respectively.

Error bar is representative of the standard deviation.



The general trend observed for the surface adhesion is in good agreement with observations made during commercial manufacturing of aerated chocolate products as well as pilot plant trials. During this research the products made with CO<sub>2</sub> gas inclusion showed problems during demoulding at pressures above 3 bar. An additional shock-cooling in the freezer (-18 °C) was required to aid demoulding for these products. Besides, a difference in force required to demould the milk chocolate system processed at 2 bar and that at 3 bar was observed, with the latter requiring a higher force.

A good and easy demoulding is observed for the milk chocolate systems with limited CO<sub>2</sub> inclusion (gas hold-up values < 15%), whereas difficulties are obtained at higher CO<sub>2</sub> levels of aeration (gas hold-up values > 35%). The hypothesis proposed is that a combined effect of the CO<sub>2</sub> gas and water vapour present at the chocolate–mould interface together with a reduced contraction is the main cause. As previously discussed in section 5.3.5, results obtained in this research have resulted in the formulation of the hypothesis that water vapour is present at the chocolate–mould interface, subsequently reducing the chocolate–mould interactions and surface adhesion force. This water vapour present at the chocolate–mould interface is assumed to interact with the aerated chocolate mass, by dissolving the CO<sub>2</sub> gas present in the surface layer of the aerated milk chocolate system. In combination with a decrease in the level of contraction, due to the Laplace bubble pressure opposing the contracting forces, these effects are responsible for the increased adhesion observed for aerated chocolate products. The explanation proposed for the demoulding of aerated products after shock cooling in the freezer is the expansion of the water vapour present at the chocolate–mould interface upon cooling. As a result of the water vapour expansion, the chocolate is separated from the mould surface and demoulding can proceed.

### 6.3.4.2 N<sub>2</sub> gas

Nitrogen (N<sub>2</sub>) is known to give a so called micro-aeration to chocolate systems, with an average gas hold-up value of 29% (Haedelt, 2005). Using x-ray tomography the bubble characteristics of 2-D bubble sections were analyzed, giving average values for the diameter of 0.13 mm, corresponding to a mean 3-D bubble volume of 0.014 mm<sup>3</sup>. It was concluded that N<sub>2</sub> has a lower solubility in cocoa butter compared to CO<sub>2</sub>, resulting in the formation of a lower number of bubble nuclei with overall a limited volume. Due to the relatively small and low number of bubbles, the tendency to coalesce is reduced. The current research investigated the relation between aeration using N<sub>2</sub> gas at different pressures with the experimental surface adhesion force. Table 6.3 relates the processing pressures used during the N<sub>2</sub> aeration to the quality of the aerated chocolate systems, as represented by the density,  $\rho$ , and the gas hold-up value,  $\epsilon$ .

**Table 6.3 Density and gas hold-up of aerated milk chocolate systems in relation to the N<sub>2</sub> processing pressure.**

Pressure [Bar]	Density [g ml <sup>-1</sup> ]	Gas hold-up [%]
0	1.3	0
2.4	1.09	16.15
4.4	0.9	30.77
6.2	0.85	34.62

It can be observed that the density decreases with increasing processing pressure, whilst the gas hold-up or volume fraction of air increases, similar to the trend observed for the aeration using CO<sub>2</sub>. The main difference between the two gases is the rate at which the gas hold-up and density increase and decrease, respectively. At a processing pressure of 6 bar, the gas hold-up is above 70% when using CO<sub>2</sub> gas, whereas it is only 34% when using N<sub>2</sub> gas. For both gases a higher aeration is obtained at increasing processing pressures, although the rate of increase is much lower for the N<sub>2</sub> gas. These results indicate that a lower aeration is obtained when using N<sub>2</sub> gas. Based on these results it is expected that N<sub>2</sub> gives a micro-aeration, whereas CO<sub>2</sub> is rather responsible for a macro-aeration of the same chocolate system (Haedelt, 2005).

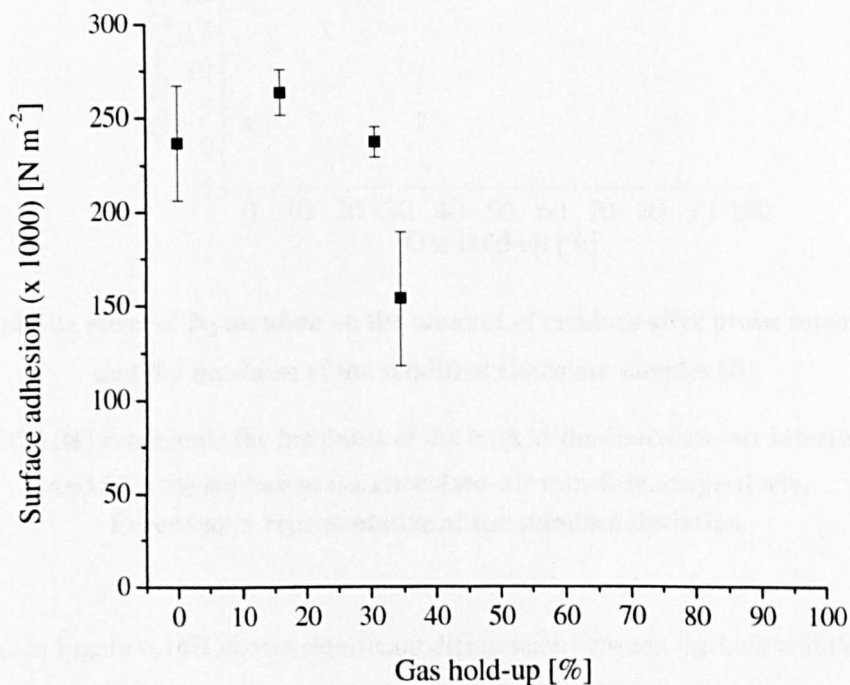


**Figure 6.13 Surface adhesion as a function of N<sub>2</sub> gas hold-up.**  
Error bar is representative of the standard deviation, n = 4.



Plotting the experimental surface adhesion force against the  $N_2$  gas hold-up shows a parabolic relationship (see Figure 6.13). The general trend shows an initial increase in average surface adhesion, followed by a significant decrease of the surface adhesion force with increasing  $N_2$  gas hold-up. In contrast to the results previously obtained for  $CO_2$ , where aeration caused a significant decrease in the cohesive strength, for  $N_2$  a reduction in cohesive strength is only observed at a pressure above 4.4 bar (30% gas hold-up). At lower pressures the micro-aeration obtained when using  $N_2$  gas is assumed to be responsible for a contraction upon cooling, similar to that seen for non-aerated chocolate, subsequently resulting in an adhesive failure or clean break at the chocolate–mould interface. At a higher pressure ( $> 4.4$  bar), the cohesive strength is reduced and a cohesive–adhesive failure is observed, as can be seen in Figure 6.14A. It is concluded that  $N_2$  aeration does not impact the surface adhesion below a certain threshold pressure.

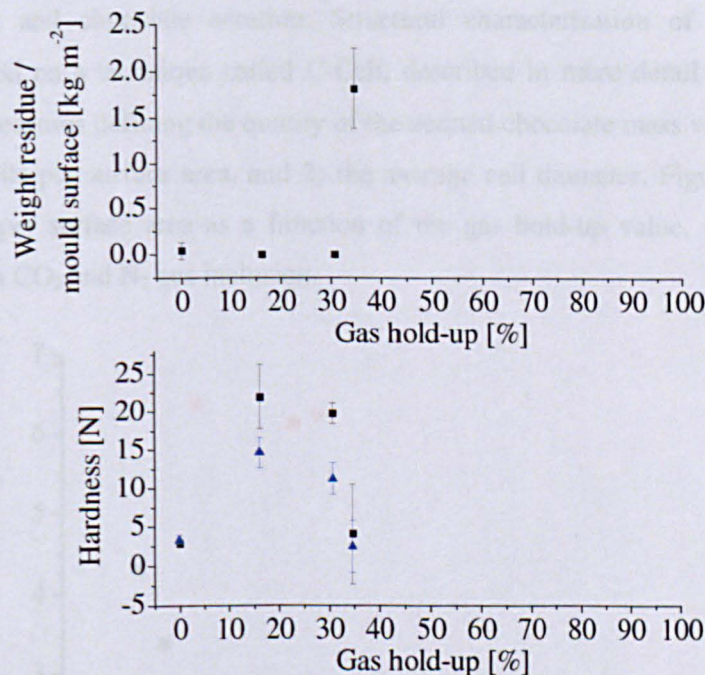


**Figure 6.14** The effect of  $N_2$  aeration on the amount of residues after probe separation (A), and the hardness of the solidified chocolate samples (B).

In (B) (■) represents the hardness of the bulk at the chocolate–air interface, and (▲) the surface at the chocolate–air interface, respectively. Error bar is representative of the standard deviation.

The hardness in Figure 6.14B shows significant differences between the bulk and the surface for gas hold-up values of 15 and 30%, respectively. Both show increased values compared to the non-aerated milk chocolate system (0% gas hold-up), whose hardness is similar to that of the aerated system with a gas hold-up of 35%. Again, a reduction in hardness is observed with increased gas hold-up, although this coincides with a transition of an adhesive failure to a cohesive–adhesive and possibly even cohesive failure. The system showing a failure of the



cohesive strength can also be observed to have a significantly lower hardness. Finally, an increase in the error observed for the latter system is expected to be caused by the enhanced aeration or bubble inclusion.

The general trend observed for the surface adhesion is in good agreement with observations made during the pilot plant trials. During this research the products made with N<sub>2</sub> gas inclusion showed hardly any problems during demoulding. It is assumed that these good demoulding characteristics, i.e. low adhesion or stickiness, are a result of the contraction of the micro-aerated N<sub>2</sub> milk chocolate system, similar to a non-aerated milk chocolate system.

### 6.3.4.3 Microstructure

Chocolate microstructure is an important influencing parameter to the relationship between surface adhesion and chocolate aeration. Structural characterisation of aerated chocolate systems was based on a technique called C-Cell, described in more detail in section 3.3.4.3. Two important measures defining the quality of the aerated chocolate mass were determined: 1) the number of cells per surface area, and 2) the average cell diameter. Figure 6.15 shows the number of cells per surface area as a function of the gas hold-up value, for milk chocolate systems with both CO<sub>2</sub> and N<sub>2</sub> gas inclusion.

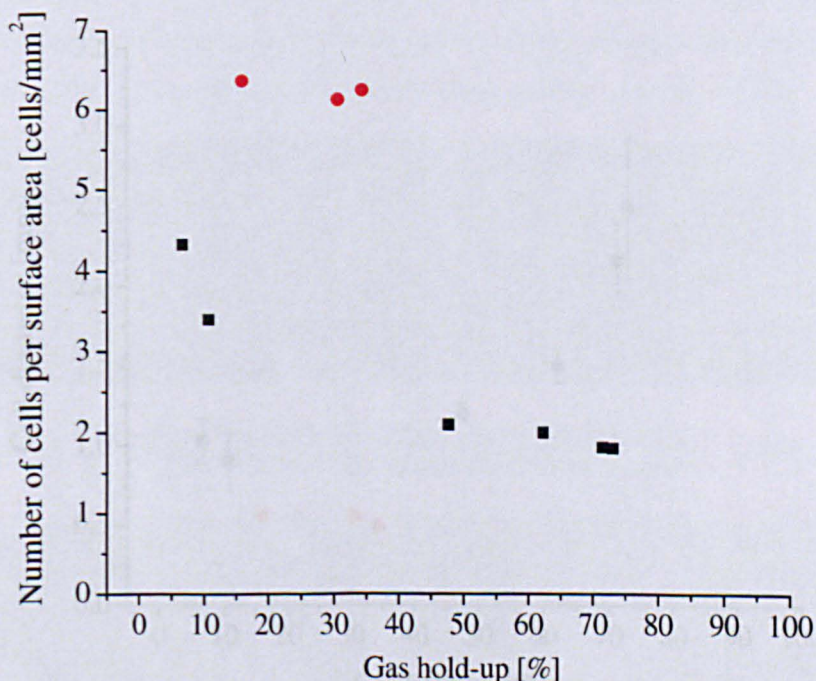


**Figure 6.15** Number of cells per surface area as a function of gas hold-up of both CO<sub>2</sub> (■) and N<sub>2</sub> (●) aerated milk chocolate systems.

The systems containing CO<sub>2</sub> show a negative exponential relationship ( $R^2 = 0.999$ ) with the gas hold up value, indicating that at higher gas hold-up values the impact on the number of cells per surface area is limited. The most significant change can be observed at the initial stages of the



aeration process, i.e. at low pressure and particularly between a pressure of 2 and 3 bar, corresponding to between roughly 11% and 48% gas hold-up, respectively. Within this same pressure range, the most important change in surface adhesion can be observed in Figure 6.11. For the systems containing  $N_2$  (see red dots in Figure 6.15 and Figure 6.16) a more or less linear relationship with the gas hold-up value is obtained, indicating that the microstructure is not significantly affected by inclusion of  $N_2$  gas.

The average cell diameters of above systems are shown in Figure 6.16. Inclusion of  $CO_2$  gas results in a positive exponential relationship ( $R_2 = 0.969$ ) between the average cell diameter and the gas hold-up value of milk chocolate. An increase in processing pressure results in an increase in the average cell diameter of  $CO_2$  gas bubbles. Again, the transition seems to take place between pressures of 2 and 3 bar, corresponding to gas hold-up values of 11% and 48%, respectively. In contrast to the results obtained at higher gas hold-up values for the number of cells per surface area, the cell diameter shows significant differences at these gas hold-up values. Limited differences in average cell diameter are present at the lower end of the scale, below 15 % gas hold-up. For  $N_2$ , on the other hand, a linear relationship can be observed, indicating that the microstructure, as assessed by the average cell diameter, is not significantly affected by the inclusion of  $N_2$  gas.

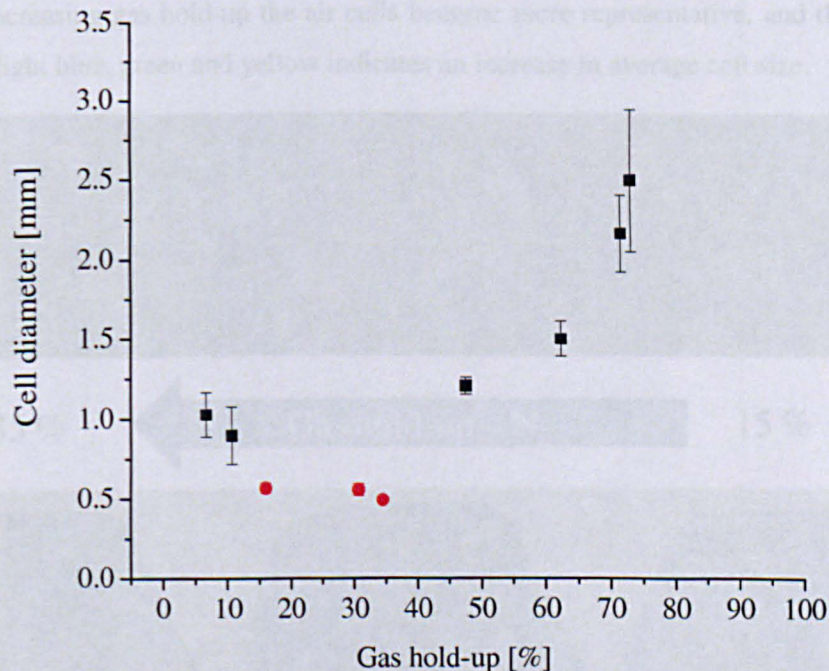


**Figure 6.16** Average cell diameter as a function of gas hold-up of both  $CO_2$  (■) and  $N_2$  (●) aerated milk chocolate systems.

Error bar is representative of the standard deviation,  $n = 5$ .



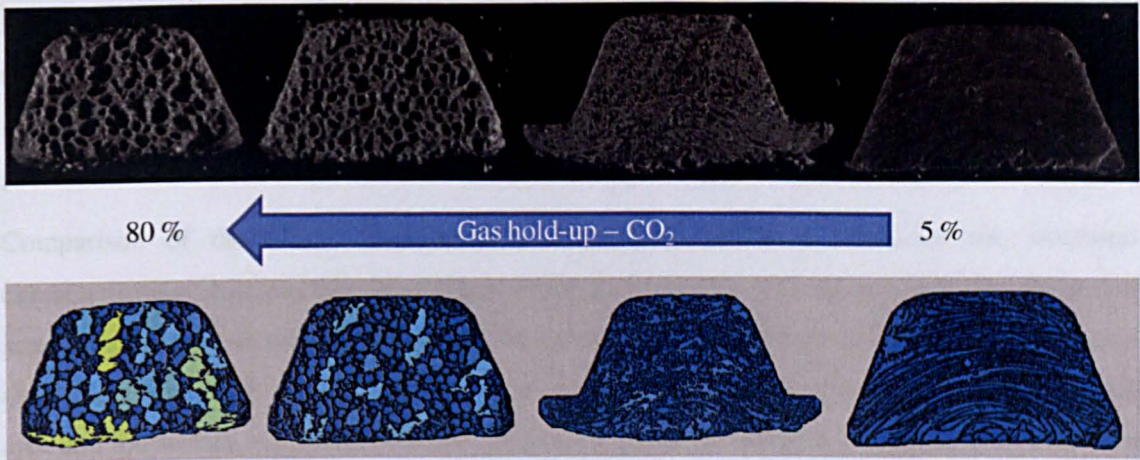


**Figure 6.17** Cross-sections representing the microstructure of milk chocolate samples at varying  $\text{CO}_2$  gas hold-up values.

The grey images (top) represent the raw images, whereas the coloured images (bottom) represent the cell image, in which lighter shades indicate larger cells.

Further investigation of the impact of processing pressure on the microstructure of the aerated milk chocolate systems via the cross-sections shown in Figure 6.17 for the samples containing  $\text{CO}_2$  gas and in Figure 6.18 for the samples containing  $\text{N}_2$  gas shows significant differences, similar to the quantitative results discussed. The images in Figure 6.17 show both a decrease in number of cells and increase in average cell diameter with increasing gas hold-up value for milk chocolate systems containing  $\text{CO}_2$  gas. At a gas hold-up of 7% nearly the whole image is dark blue. With increasing gas hold-up the air cells become more representative, and the change of dark blue to light blue, green and yellow indicates an increase in average cell size.

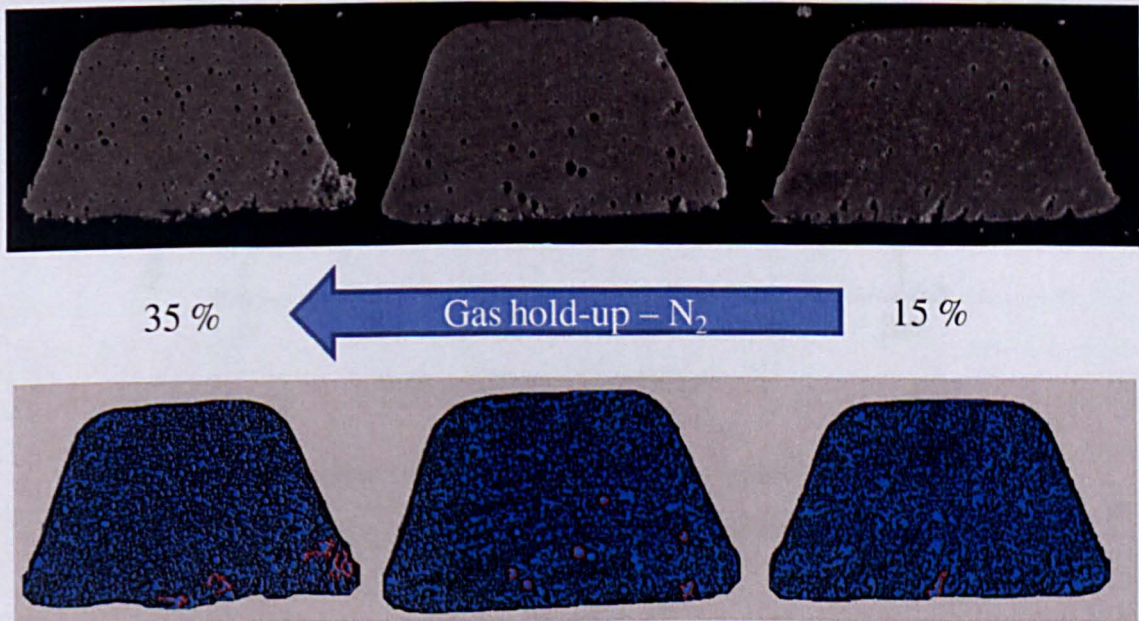


**Figure 6.18** Cross-sections representing the microstructure of milk chocolate samples at varying  $\text{N}_2$  gas hold-up values.

The grey images (top) represent the raw images, whereas the coloured images (bottom) represent the cell image, in which lighter shades indicate larger cells.



Figure 6.18 shows three fairly similar images, indicating limited differences in microstructure of the milk chocolate systems containing  $N_2$  gas. “Micro” air cells are present in all systems, but neither their number nor the average cell size seems to be affected by the variation in processing pressure.

Comparison of the results obtained for the surface adhesion force and the structural characterisation indicates that the surface adhesion decreases with an increase in average cell size and a decrease in the number of cells per surface area for systems containing  $CO_2$  gas, as is shown in Figure 6.19. A linear correlation is observed between the number of cells per surface area and the surface adhesion, whereas a positive exponential relation can be observed between the average cell diameter and the surface adhesion force. For the latter, an increase in processing pressure from 2 to 3 bar is responsible for a significant change in microstructure and surface adhesion force. Contradictory, for systems containing  $N_2$  gas the microstructure does not show any significant changes which coincide with the change in surface adhesion force observed at a gas hold-up value of 35% (see Figure 6.13).

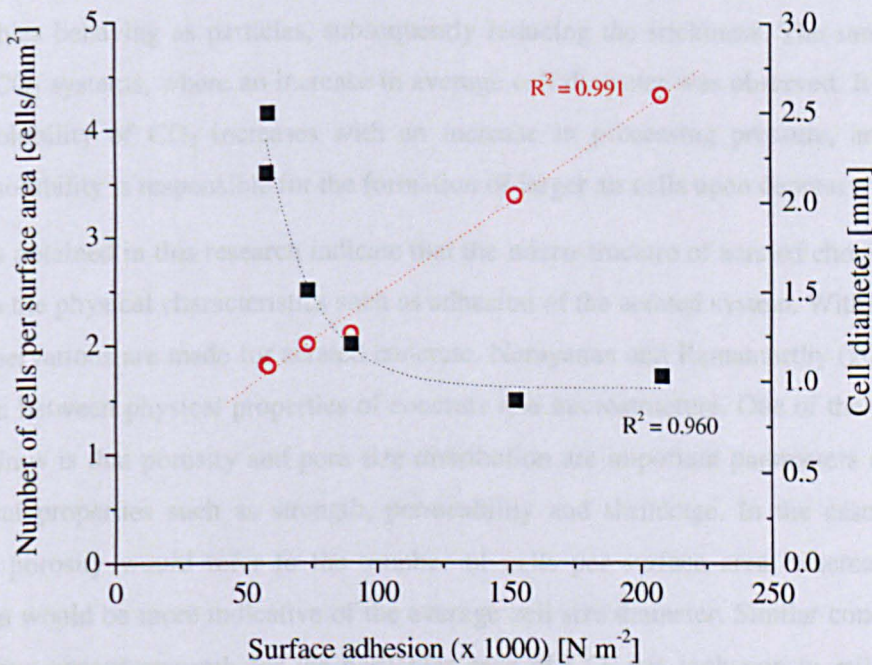


**Figure 6.19** Number of cells per surface area (○) and cell diameter (■) as a function of surface adhesion of  $CO_2$  aerated chocolate systems.

## 6.4 DISCUSSION

Within literature not much attention has been paid to the subject of chocolate aeration and in particular a comparison of aerated and non-aerated samples with respect to mechanical properties. An extensive piece of work was conducted by Haedelt (2005), who investigated the effect of different bubble inclusion techniques, as well as gas and chocolate composition, on the bubble formation mechanism in liquid chocolate. One of the main conclusions was that differences in gas solubility were responsible for the variation in microstructure obtained when applying different gases. Similar to the results obtained in this research, CO<sub>2</sub> gas tended to form larger bubbles and a macro-aeration compared to N<sub>2</sub> gas, which formed smaller bubbles and a micro-aerated structure. It is assumed that the higher solubility of CO<sub>2</sub> causes an increase in the amount of gas released upon depressurisation, resulting in the formation of larger air cells compared to the less soluble N<sub>2</sub>. Microstructural images obtained in the present research show no differences in bubble structure for N<sub>2</sub> systems at different processing pressures. This indicates that the solubility of N<sub>2</sub> is not only lower than that of CO<sub>2</sub>; there is also a maximum level of gas that can dissolve in liquid chocolate, irrespective of the processing pressure. It is furthermore assumed that the reduced adhesion of N<sub>2</sub> compared to CO<sub>2</sub> systems is due to the micro-bubbles behaving as particles, subsequently reducing the stickiness. The same does not apply for CO<sub>2</sub> systems, where an increase in average cell diameter was observed. It is assumed that the solubility of CO<sub>2</sub> increases with an increase in processing pressure, and that this increased solubility is responsible for the formation of larger air cells upon depressurisation.

The results obtained in this research indicate that the microstructure of aerated chocolate in part determines the physical characteristics such as adhesion of the aerated system. Within literature, similar observations are made for aerated concrete. Narayanan and Ramamurthy (2000) discuss the relation between physical properties of concrete and microstructure. One of the conclusions that they draw is that porosity and pore size distribution are important parameters determining the physical properties such as strength, permeability and shrinkage. In the case of aerated chocolate, porosity would refer to the number of cells per surface area, whereas pore size distribution would be more indicative of the average cell size diameter. Similar conclusions are drawn in the current research for the particular case of CO<sub>2</sub> gas inclusion in milk chocolate systems, where a change in number of cells per surface area and average cell size diameter impacts on the cohesive strength of the aerated chocolate system, subsequently affecting the experimental surface adhesion force.

According to Müller-Fisher and Windhab (2005), the Laplace pressure or inner bubble pressure is lower for a larger bubble, which in turn causes this large bubble to have a higher degree of deformability. In correlation with the higher deformability, foams with larger air cells have shown a reduced elastic modulus and shape retention capacity. This is in good agreement with the observations made in this research, with the presence of cohesive failure of aerated milk

chocolate systems in comparison to non-aerated chocolate systems, and the further increase with increasing average cell diameter for systems containing CO<sub>2</sub> gas. Another consideration is the possible change in air cell structure due to contact with the solid mould surface. Especially for large air cells with a higher degree of deformability, it is expected that the structural pattern of the foam may change due to contact with a solid surface. Mancini and Oguey (2005) discussed the surface structure of liquid foam in contact with a solid. A smooth, flat solid surface was observed to promote the formation of circular arcs and 2D foam. Curved solid surfaces and/or non-perpendicular contact, however, deform the 2D foam. This implies that the cell structure at the chocolate–mould interface is different from that of the bulk chocolate system, another parameter complicating interfacial behaviour and surface adhesion.

Both Dutta et al. (2002) and Boerboom (2000) discuss the impact of surfactants on foam formation and stabilization. Dynamic film tension was, in both studies, an important parameter determining the bubble size and the amount of air incorporated during the aeration stage. The presence of a surfactant such as lecithin within the chocolate system is, however, not expected to impact on the mechanical properties of the liquid chocolate foam. It is assumed that solidification of the cocoa butter is the main stabilization mechanism. By using tempered chocolate a fast crystallization and consequently a fast solidification is obtained. Solidification of the fat crystal network could be responsible for the immobilization of the aerated structure and the capacity of the chocolate to hold the gas and bubble structure. A similar conclusion can be drawn from the Stokes equation, which describes moving velocity of a colloidal particle driven by gravity,  $v_s$ :

$$v_s = \frac{g\Delta\rho d^2}{18\eta_c}, \quad [6-3]$$

where  $g$  is the gravity or acceleration,  $\rho$  the density,  $d$  the diameter of the air cell and  $\eta_c$  the viscosity of the continuous phase. Assuming that the bubble diameter and density remain constant, an increase in viscosity would cause the velocity to decrease. So, to prevent creaming and/or coalescence, and to obtain a stable aerated chocolate system, an increase in viscosity would be beneficial. This can be obtained through crystallization and solidification of the cocoa butter.



## 6.5 CONCLUSIONS

Aeration in combination with chocolate composition are the two most important characteristics affecting the cohesive (mechanical) strength of a chocolate system. Milk chocolate is generally regarded as being softer and having a lower cohesive strength compared to dark chocolate. Aeration does not change this observation, and as a result a lower adhesive force is obtained for the aerated milk chocolate system compared to the aerated dark chocolate system. In general, however, the reduced cohesive strength of aerated chocolate systems is responsible for a decrease in the experimental surface adhesion force of aerated samples when compared to non-aerated systems. An increased level of deformability due to the presence of air cells, and an imbalance of forces within the aerated chocolate surface layer all act together in the reduction of both the cohesive strength and surface adhesion of aerated systems.

Comparison of different mould materials has previously shown a significant impact of the surface free energy of the solid mould surfaces. When comparing the same solid surfaces in combination with aerated milk chocolate systems a similar trend is observed. On average, with the higher surface free energy surfaces a higher surface adhesion force is required. The heat transfer coefficient of both the aerated system and the solid mould surface are hypothesized to be responsible for this observation. Aeration causes a decrease in the heat transfer rate, subsequently increasing the time required for crystallization and solidification. If the processing time before demoulding takes place is not prolonged, a cohesive failure is obtained due to the reduced bulk cohesive strength. Simultaneously, the heat transfer coefficient differs depending on the mould material used. A low heat transfer or conductivity coefficient will also prolong the crystallization and solidification processes.

Structural characterisation of the aerated chocolate systems (as assessed by the number of cells per surface area and the average cell diameter) was shown to have a direct impact on the surface adhesion force for systems containing CO<sub>2</sub> gas. For N<sub>2</sub> gas, processing pressure has very limited influence on the microstructure, and, therefore, on surface adhesion of such aerated systems.

## CHAPTER 7

# CHOCOLATE ADHESION TO POLYCARBONATE SURFACES COATED WITH A THIN FILM

### 7.1 INTRODUCTION

The use of edible and/or bio-degradable coatings or films in combination with commercial food products is increasing. Wu et al. (2002) defined an edible film or coating as *“a thin layer of material which can be eaten by the consumer, can be applied on or within foods by wrapping, dipping, brushing, or spraying and function as selective barriers against transmission of gases, vapours and solutes, and also provide mechanical protection”*. One of the main requisites is that the shelf life and quality of food products is guaranteed. Currently new polymeric materials, such as bio-nanocomposites, are used to develop so called multi-functional intelligent packaging, which have stronger mechanical, barrier and thermal performances (Sorrentino et al., 2007) compared to the standard plastic packaging materials. A disadvantage of the use of biodegradable polymers is their performance, processing and cost. Several publications are available which review the use of a large range of biopolymers as a packaging or edible coating in combination with food products.

Over the years many different biopolymers have been used for the formation of an edible film or coating which can be used to inhibit lipid migration in confectionery products. Migration of low melting point lipids from a fat based filling or centre into the chocolate coating negatively impacts on the crystallization behaviour of cocoa butter, resulting in chocolate (fat) bloom. Nelson and Fennema (1991) investigated the resistance of hydrocolloid films to migration of linoleic acid from peanut oil. All films showed good lipid barrier properties. Further investigations by Brake and Fennema (1993) focussed on the use of different sweeteners in combination with hydrocolloids. The coatings were applied at the interface between chocolate and peanut butter for sensory perception testing. Final coating formulation, consisting of a high methoxyl pectin, acacia gum, high fructose corn syrup, dextrose, fructose and sucrose, had good lipid barrier characteristics.

Preliminary research by Mastrantonakis (2004) investigated the use of three different emulsifiers, polyglycerol polyricinoleate (PGPR), sodium dodecyl sulphate (SDS) and soya lecithin, to coat a polycarbonate mould for improved chocolate demoulding. No differences in advancing contact angle of a mixture consisting of cocoa butter, fine sugar and lecithin were observed for the mould surfaces coated with different emulsifiers. A pilot plant trial was conducted to determine the effect of washing of the moulds with a surfactant (Tween 60) solution prior to chocolate–mould contact. However, the Tween 60 coating did not reduce the adhesion between chocolate and mould surface, rather the opposite. Aim of the current part of the research was to investigate the effect of edible coatings placed at the chocolate–mould interface on the level of adhesion of chocolate. This will enhance the understanding of adhesion phenomena at the chocolate–mould interface in relation to the solid mould surface characteristics.

## **7.2 METHODS**

The coating preparation and application techniques have been discussed in CHAPTER 3. Adhesion and surface characterisation parameters have been applied previously in CHAPTER 4, CHAPTER 5 and CHAPTER 6. This section will describe specific materials and coating application techniques applied.

### **7.2.1 Materials**

Polycarbonate was chosen as the solid mould substrate onto which different coating solutions were applied to modify the surface characteristics. Dark chocolate (52% cocoa solids) was chosen as the standard chocolate system, for the same reason as discussed in CHAPTER 4 and CHAPTER 5. Standard milk chocolate (29% cocoa solids) and aerated milk chocolate were used on one instance to assess the impact of chocolate recipe in relation to mould surface modifications.

### **7.2.2 Methods**

Preliminary investigations focussed on the thin film coating preparation and application methodology. The technique described in section 0 is a result of these investigations. Initial results showed that a homogeneous thin film or coating could be prepared by using the operating principle shown in Figure 3.25. Contact between the chocolate and the coated mould surface is created using the same methodology previously applied.



## 7.3 RESULTS

### 7.3.1 One component coatings

To assess the impact of surface modifications through the application of thin films on polycarbonate mould surfaces, two different types of edible coatings were prepared. The first was based on the use of degradable biopolymers or hydrocolloids, whereas the second tested the use of different lipid components. For comparison reasons the two types of coatings are discussed individually per type and the results obtained are compared to the results obtained for a standard polycarbonate mould surface, as discussed in CHAPTER 4.

#### 7.3.1.1 Hydrocolloids

Four hydrocolloid coatings (0.1% solutions) with varying compositions were compared to a clean polycarbonate surface without coating. A hydrocolloid concentration of 0.1% was chosen based on preliminary results which showed that at a concentration of 1.0% high methoxyl (HM) pectin 105 or carboxymethylcellulose (CMC) a so called “stand-alone” coating was formed, as can be seen in Figure 7.1.

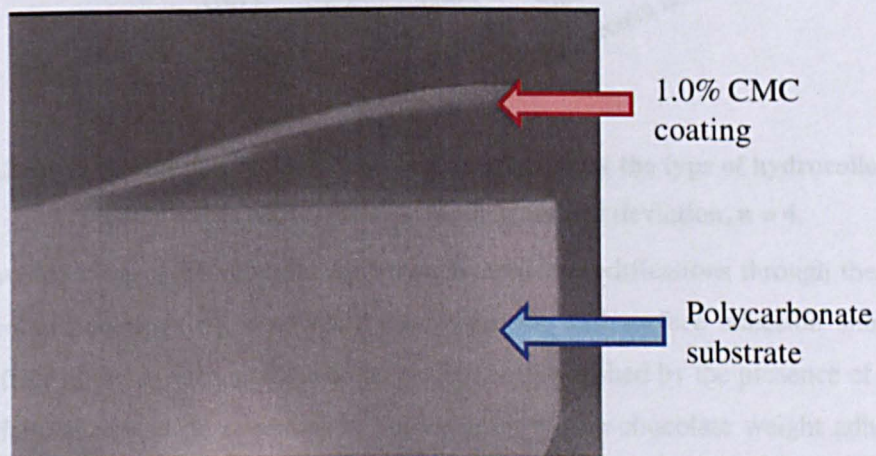


**Figure 7.1 Visualization of a stand-alone 1.0% CMC coating formed on a solid polycarbonate substrate.**

This presents issues when creating contact with the liquid chocolate, which is pulled partly underneath the coating making direct contact with the polycarbonate substrate. As a result of this, the impact of surface modifications on the surface adhesion force is no longer measured. Hydrocolloids coatings with a concentration of 0.1% did not form a stand-alone coating and this concentration was therefore chosen when comparing the impact of different hydrocolloid coatings on the adhesion force.

The results presented in Figure 7.2 show significant differences in surface adhesion of the 0.1% hydrocolloid coatings tested, both individually and if compared to the clean polycarbonate mould surface. Except for the HM pectin 150 and the HM pectin 105 coating that was boiled



prior to application, all hydrocolloids significantly reduced the surface adhesion force. No significant difference was observed between HM pectin 105 and CMC, two hydrocolloids which were chosen based on results reported by Brake and Fennema (1993) and Nelson and Fennema (1991) on their use in combination with chocolate confectionery products.

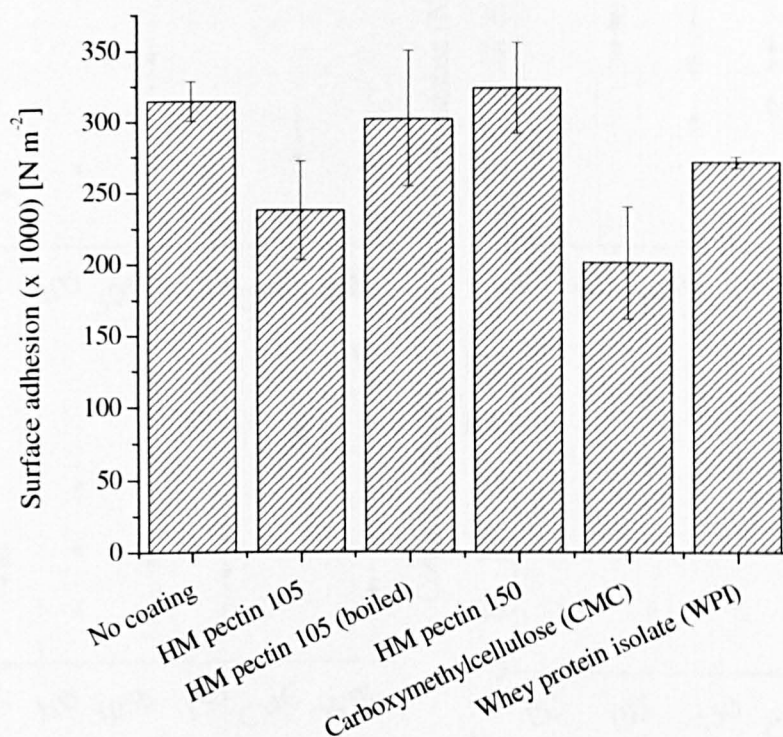


**Figure 7.2** Surface adhesion of dark chocolate as affected by the type of hydrocolloid coating.

Error bar is representative of the standard deviation,  $n = 4$ .

Further investigation of the relationship between surface modifications through the application of hydrocolloid coatings on a polycarbonate substrate and surface adhesion shows that the positive effect of the surface modifications is slightly diminished by the presence of a cohesive–adhesive failure, as can be observed in Figure 7.3A by the chocolate weight adhering to the different surfaces after separation. As can be observed from Figure 7.3B, the hydrocolloid coatings actually increase surface hardness of chocolate samples compared to that from the standard polycarbonate substrate. This can therefore not explain the cohesive–adhesive failure observed for all hydrocolloid coatings. Although the coatings modify the surface chemistry of the polycarbonate substrate, the thickness is limited and is not expected to impact on the heat transfer characteristics of the solid mould material.

Both Figure 7.3C and D show the effectiveness of hydrocolloid coatings in modifying the solid mould surface. Especially for CMC, an increase in surface glossiness of both the mould and the chocolate/mould interface is visible. The water contact angle furthermore is lower for the clean CMC coating compared to the standard polycarbonate surface. This indicates that the CMC coating is responsible for the creation of a mould surface with a higher hydrophilicity.



Again, all surfaces show approximately similar values for the water contact angle after having been in contact with the chocolate system.

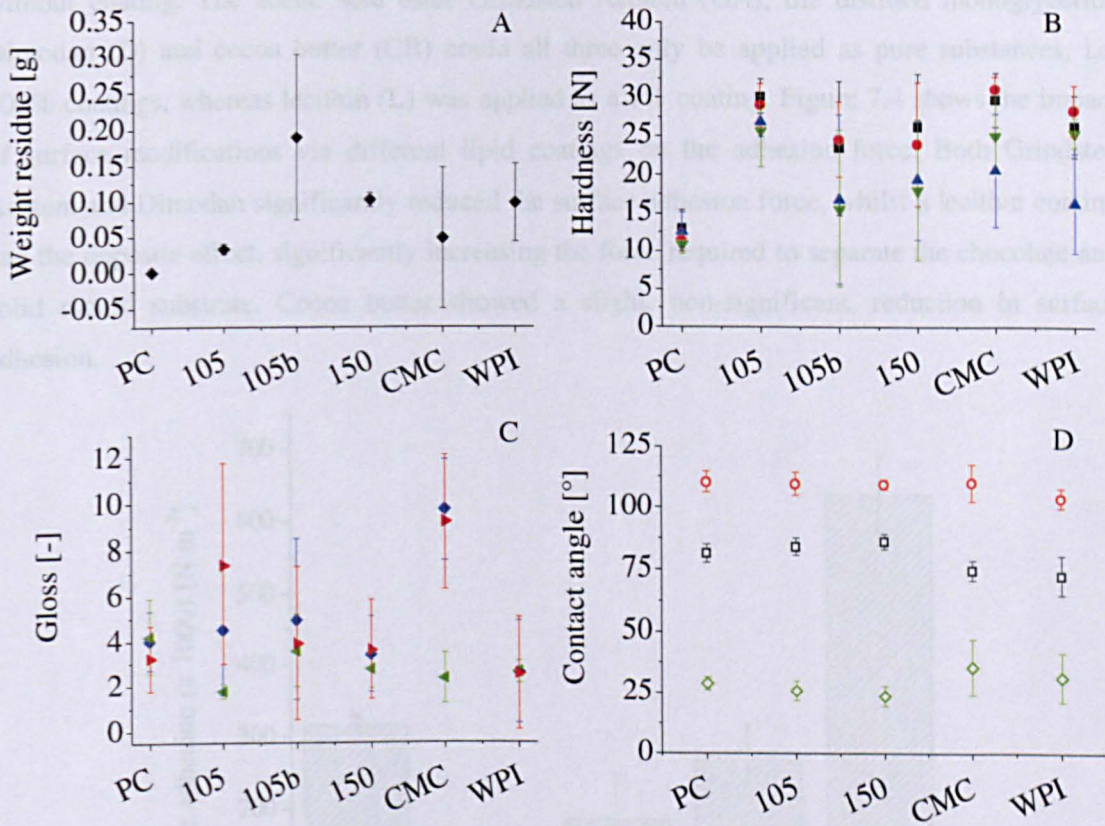


**Figure 7.3** The effect of different types of hydrocolloids on the amount of residues after probe separation (A), the hardness of the solidified chocolate samples (B), the difference of surface glossiness (C) and the water contact angle (D).

In (B) (■) represents the hardness of the bulk at the chocolate–air interface, (●) the bulk at the chocolate–mould interface, (▲) the surface at the chocolate–air interface, and (▼) the surface at the chocolate–mould interface, respectively. In (C) (◆) represents the surface glossiness of the mould surface, (◀) the chocolate–mould interface, and (▶) the chocolate–air interface. In (D) (□) represents the water contact angle before chocolate contact, (○) after chocolate contact, and (◇) the difference in contact angle before and after chocolate contact. Error bar is representative of the standard deviation.

The overall results indicate that it is possible to reduce the surface adhesion between chocolate and a solid mould surface by modifying the substrate with the application of a hydrocolloid coating. Further investigations are required to develop a coating with optimum characteristics. CMC is assumed to be a good candidate, due to its reduction of the experimental surface adhesion force, and its positive effect of the surface glossiness of chocolate after being in contact with a CMC coated polycarbonate surface.



## 7.3.1.2 Lipids

Four lipid coatings with varying compositions were compared to a clean polycarbonate surface without coating. The acetic acid ester Grindsted Acetem (GA), the distilled monoglyceride Dimodan (D) and cocoa butter (CB) could all three only be applied as pure substances, i.e. 100% coatings, whereas lecithin (L) was applied as a 1% coating. Figure 7.4 shows the impact of surface modifications via different lipid coatings on the adhesion force. Both Grindsted Acetem and Dimodan significantly reduced the surface adhesion force, whilst a lecithin coating had the opposite effect, significantly increasing the force required to separate the chocolate and solid mould substrate. Cocoa butter showed a slight, non-significant, reduction in surface adhesion.

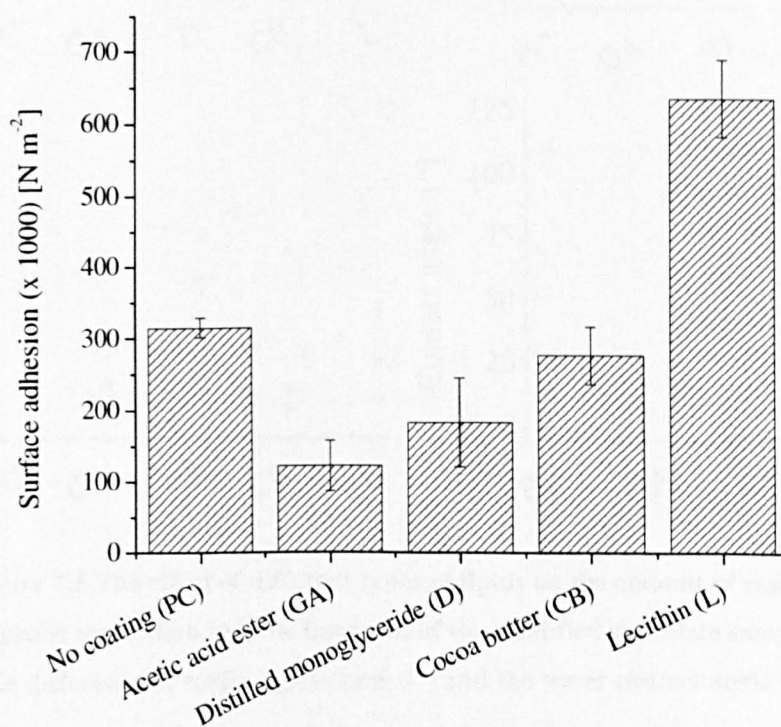


**Figure 7.4** Surface adhesion of dark chocolate as affected by different types of lipid coating.

Error is representative of the standard deviation,  $n = 4$ .

Further investigation of the relationship between surface modifications through the application of lipid coatings on a polycarbonate substrate and surface adhesion shows again a cohesive–adhesive failure at the chocolate–mould interface, except for the Dimodan coating, as can be observed from Figure 7.5A. Similar to the hydrocolloid coatings, the lipid coatings again increase the hardness, as is shown in Figure 7.5B. The observed values for the hardness are slightly lower compared to those obtained for the hydrocolloid coatings, indicating that lipid coatings have a slight softening effect. Still, the hardness is significantly higher compared to that obtained previously after contact with a polycarbonate mould surface.



In contrast to the results obtained for the hydrocolloid coatings, where an increase in chocolate glossiness was observed, the surface glossiness is significantly reduced as a result of contact with the lipid coatings, as can be observed from Figure 7.5C.

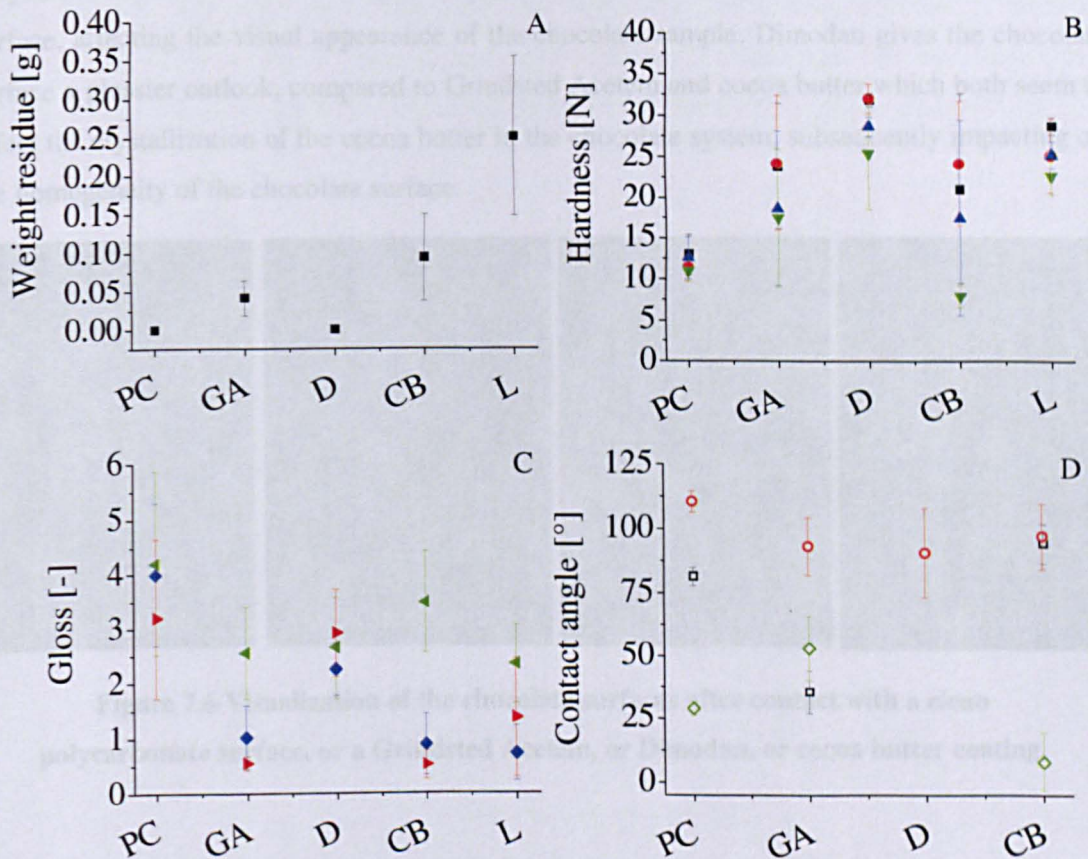


**Figure 7.5** The effect of different types of lipids on the amount of residues after probe separation (A), the hardness of the solidified chocolate samples (B), the difference of surface glossiness (C) and the water contact angle (D).

In (B) (■) represents the hardness of the bulk at the chocolate–air interface, (●) the bulk at the chocolate–mould interface, (▲) the surface at the chocolate–air interface, and (▼) the surface at the chocolate–mould interface, respectively. In (C) (◆) represents the surface glossiness of the mould surface, (◀) the chocolate–mould interface, and (▶) the chocolate–air interface. In (D) (□) represents the water contact angle before chocolate contact, (○) after chocolate contact, and (◇) the difference in contact angle before and after chocolate contact.

Error bar is representative of the standard deviation.

Some contrasting results are obtained for the water contact angle, shown in Figure 7.5D. A Grindsted Acetem coating is observed to be significantly more hydrophilic compared to the standard polycarbonate surface. Cocoa butter, on the other hand, creates a surface with a highly hydrophobic character, similar to that obtained after contact with chocolate. As there is no difference in water contact angle on the cocoa butter surface before and after contact, this confirms the assumption that residues of cocoa butter are deposited on the mould surface during contact with the chocolate.



The detrimental effect of the lipid coatings on the visual outlook of the chocolate surfaces is shown in Figure 7.6, which shows a chocolate surface after contact with lipid-coated polycarbonate. A clean and homogeneous surface is obtained after contact with the standard polycarbonate surface. All three lipid coatings seem to deposit minor residues on the chocolate surface, affecting the visual appearance of the chocolate sample. Dimodan gives the chocolate surface a glossier outlook, compared to Grindsted Acetem and cocoa butter which both seem to affect the crystallization of the cocoa butter in the chocolate system, subsequently impacting on the homogeneity of the chocolate surface.

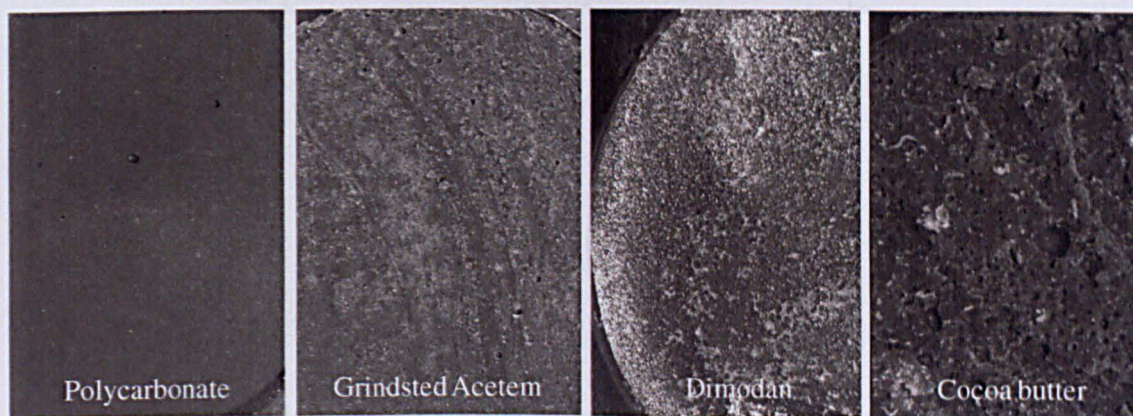


**Figure 7.6 Visualization of the chocolate surfaces after contact with a clean polycarbonate surface, or a Grindsted Acetem, or Dimodan, or cocoa butter coating.**

The overall results indicate that it is possible to reduce the surface adhesion between chocolate and a solid mould surface by modifying the substrate with the application of a lipid coating. However, a negative effect was observed on the chocolate surface glossiness, as a result of which the use of lipid coatings is not recommended. Wu et al. (2002) came to a similar conclusion regarding pure non-polar hydrocarbon-based materials such as lipids. They recommend the combined use of these materials with hydrophilic film-forming agents like polysaccharides and proteins.

### 7.3.2 Effect of concentration

In order to develop the optimum coating with respect to the surface adhesion between chocolate and a mould material, the effect of concentration was further investigated. One hydrocolloid, CMC, and one lipid, Grindsted Acetem, were chosen based on the results obtained in section 7.3.1.1



## 7.3.2.1 CMC concentration

The effect of CMC concentration on the experimental surface adhesion force is shown in Figure 7.7. After an initial decrease in adhesion at low CMC concentrations (0.01 and 0.1%) compared to the standard polycarbonate surface (0%), an increase in the surface adhesion is obtained moving from 0.2% to 0.3% CMC. These results clearly indicate that the optimum CMC concentration for a coating which reduces the surface adhesion force is approximately 0.1%.

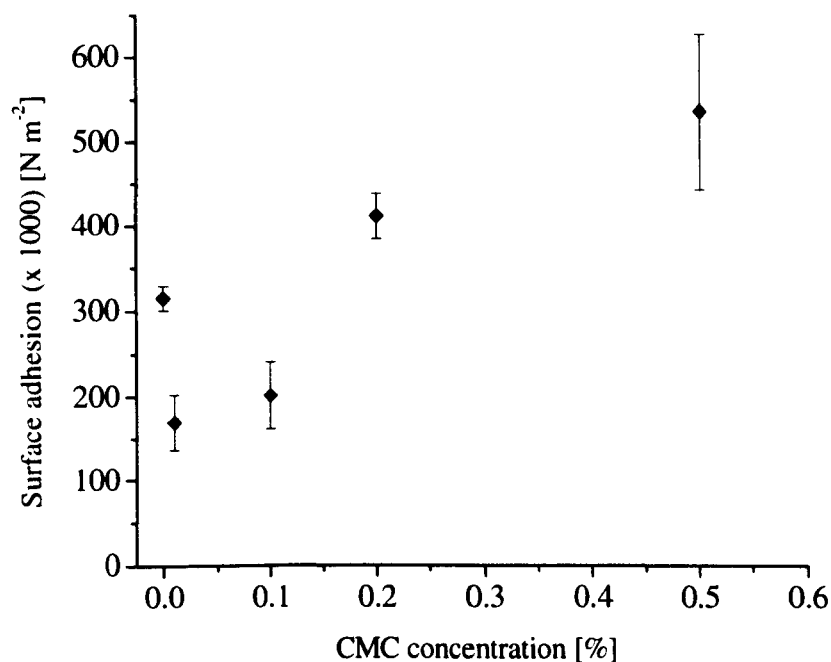


**Figure 7.7** Surface adhesion as a function of CMC concentration.

**Error bar is representative of the standard deviation, n = 4.**

Further investigation of the relationship between CMC concentration and surface adhesion shows a clear trend with the amount of (chocolate) residues present on the mould probe surface after separation. Figure 7.8A shows the transition from a cohesive–adhesive failure with a significant amount of chocolate adhering to an adhesive failure with no chocolate residues adhering. This transition coincides with the transition observed for the adhesion force in the range from 0.1 to 0.2% CMC. The hardness of the chocolate samples, shown in Figure 7.8B is fairly constant across the different CMC concentrations, and the variation seems to reduce with increasing CMC concentration.

A positive effect of CMC concentration on the surface glossiness can be observed in Figure 7.8C. With increasing CMC concentration the surface glossiness of both the mould surface and the chocolate–mould interface increases linearly. The glossiness of the chocolate–air interface stays constant with increasing CMC concentration, which was expected as there is no surface modification involved in the contact. There does not seem to be a correlation between the surface glossiness and the water contact angle.

In Figure 7.8D an initial decrease in water contact angle measured on the surfaces before chocolate contact, i.e. the “clean” surfaces, is observed. However, with increasing CMC concentration the water contact angle does not change. So called stick-slip behaviour, though, hinders the correct measurement of the advancing water contact angle of the CMC coatings. This behaviour is visualized in Figure 7.9.

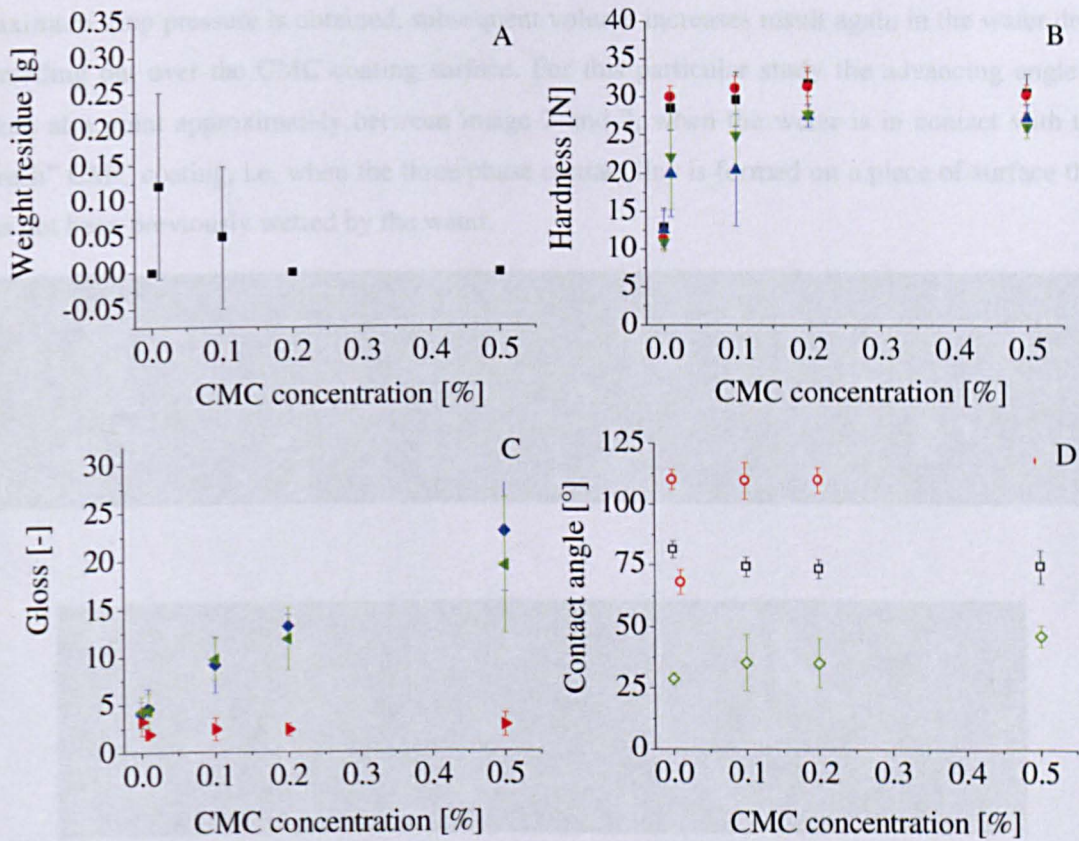


**Figure 7.8** The effect of CMC concentration on the amount of residues after probe separation (A), the hardness of the solidified chocolate samples (B), the difference of surface glossiness (C) and the water contact angle (D).

In (B) (■) represents the hardness of the bulk at the chocolate–air interface, (●) the bulk at the chocolate–mould interface, (▲) the surface at the chocolate–air interface, and (▼) the surface at the chocolate–mould interface, respectively. In (C) (◆) represents the surface glossiness of the mould surface, (◀) the chocolate–mould interface, and (▶) the chocolate–air interface. In (D) (□) represents the water contact angle before chocolate contact, (○) after chocolate contact, and (◇) the difference in contact angle before and after chocolate contact. Error bar is representative of the standard deviation.



Initial contact between water and a 0.5% CMC coating results in the formation of a relatively hydrophobic contact angle ( $> 90^\circ$ ). However, with the increase in volume required for the determination of the advancing angle the drop suddenly spreads out over the surface, forming a rather hydrophilic contact angle ( $< 50^\circ$ ). A second increase in water volume increases the contact angle, but does not cause the drop to spread out over the surface. The surface tension of the water seems to be stronger than the interaction with the coating surface, resulting in the formation of a relatively hydrophobic drop on subsequent volume increases. Once a certain maximum drop pressure is obtained, subsequent volume increases result again in the water drop spreading out over the CMC coating surface. For this particular study the advancing angle is taken at a point approximately between image 2 and 3, when the water is in contact with the “fresh” CMC coating, i.e. when the three phase contact line is formed on a piece of surface that has not been previously wetted by the water.

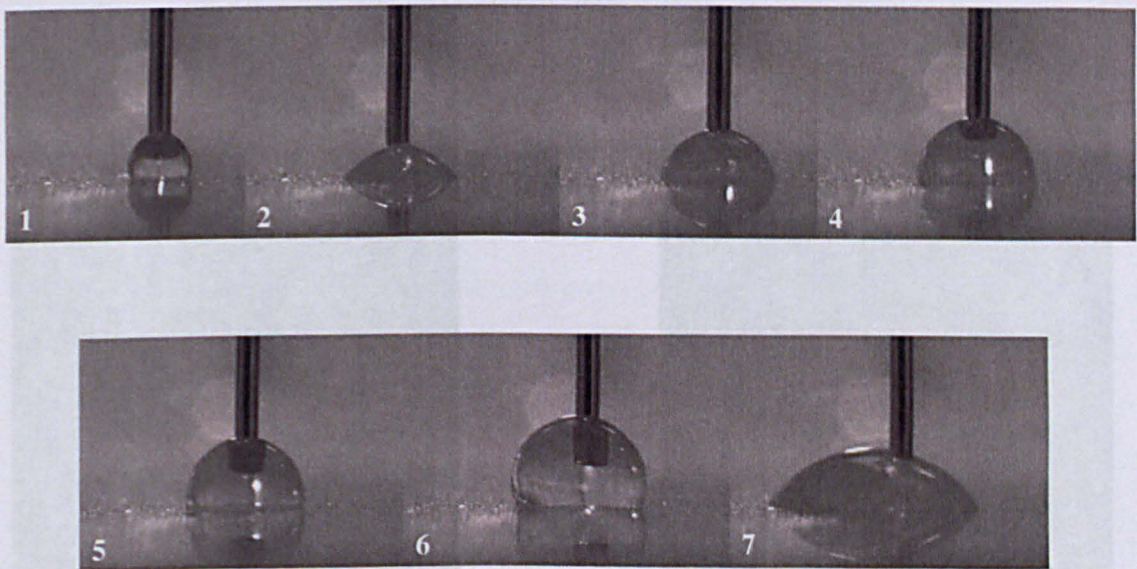


**Figure 7.9 Visualization of the stick-slip behaviour observed when determining the advancing water contact angle on a 0.5% CMC coating.**

**The progression of the water drop with increasing volume in time is represented by the images 1 to 7.**

The overall results indicate that 0.1% CMC is an optimum concentration in relation to minimizing the surface adhesion force. A CMC coating furthermore has a positive effect on the visual appearance of the chocolate by increasing the surface glossiness of the chocolate system. For further investigation it is recommended to use a coating with 0.1% CMC.



**IMAGING SERVICES NORTH**

Boston Spa, Wetherby  
West Yorkshire, LS23 7BQ  
[www.bl.uk](http://www.bl.uk)

**PAGE MISSING IN  
ORIGINAL**

Further investigation of the relationship between GA concentration and surface adhesion does not necessarily show the detrimental effect of GA on the chocolate and mould surfaces, as can be observed from Figure 7.12A. At a GA concentration of 0.1% there are no residues adhering to the mould surface, as determined by weighing the solid mould probe after chocolate contact. However, visual observations as shown in Figure 7.11 clearly show the presence of (chocolate) residues on the coated polycarbonate surface after contact. Figure 7.12C shows the effect of GA concentration on the glossiness, and no distinct differences can be observed between the chocolate–mould interfaces after contact with GA coatings with different concentrations. The surface glossiness of the mould surface with a pure GA coating is lower than that of any of the other samples. Results obtained for the hardness, Figure 7.12B, and the contact angle, Figure 7.12D, are not significantly different and lie in the same range as previously obtained for the lipid coatings.

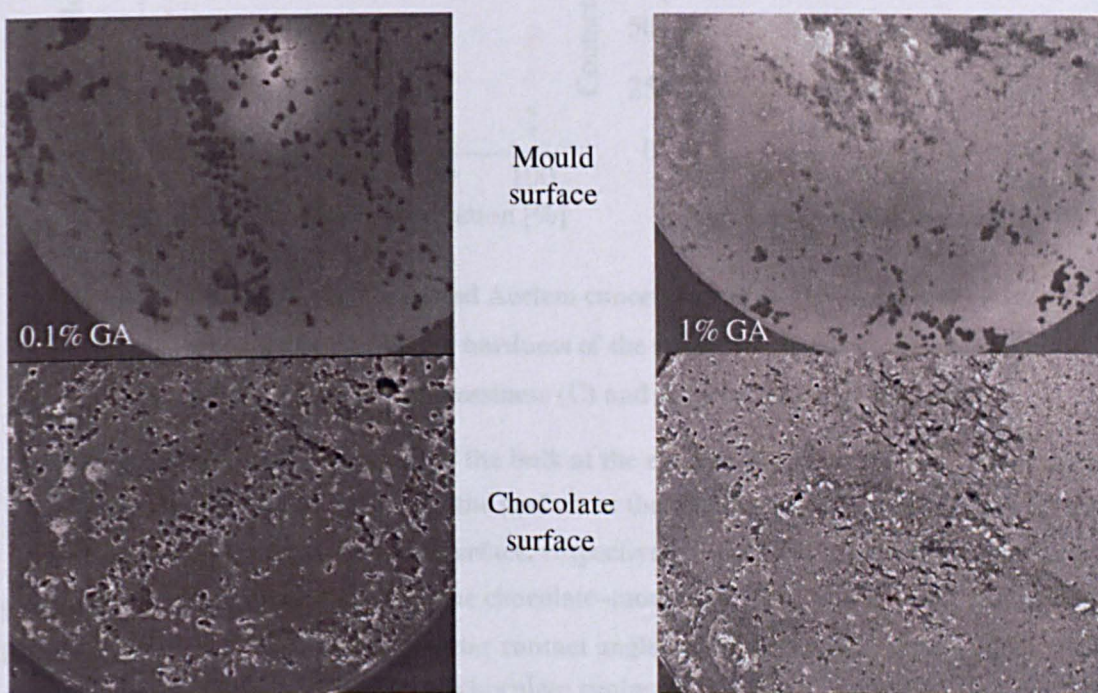


**Figure 7.11** Visualization of the chocolate and mould surfaces coated with GA after contact.

The chocolate surfaces, on the other hand, show defects in the form of irregular surfaces. At the places where residues are adhering to the mould surface, the chocolate surfaces show minor holes, resulting in a relatively rough and irregular surface. With an increase in GA concentration this effect seems to be enhanced.

The overall results indicate that 0.1-1.0% GA is an optimum concentration in relation to minimizing the surface adhesion force and detrimental effects of GA on the visual appearance of both chocolate and mould surfaces. In contrast to the results obtained for CMC coatings, GA coatings have a negative effect on the surface appearance of the chocolate and it is therefore recommended not to use GA as single component coatings. Further investigations are required to test the effect of GA inclusion in 2-component coatings.



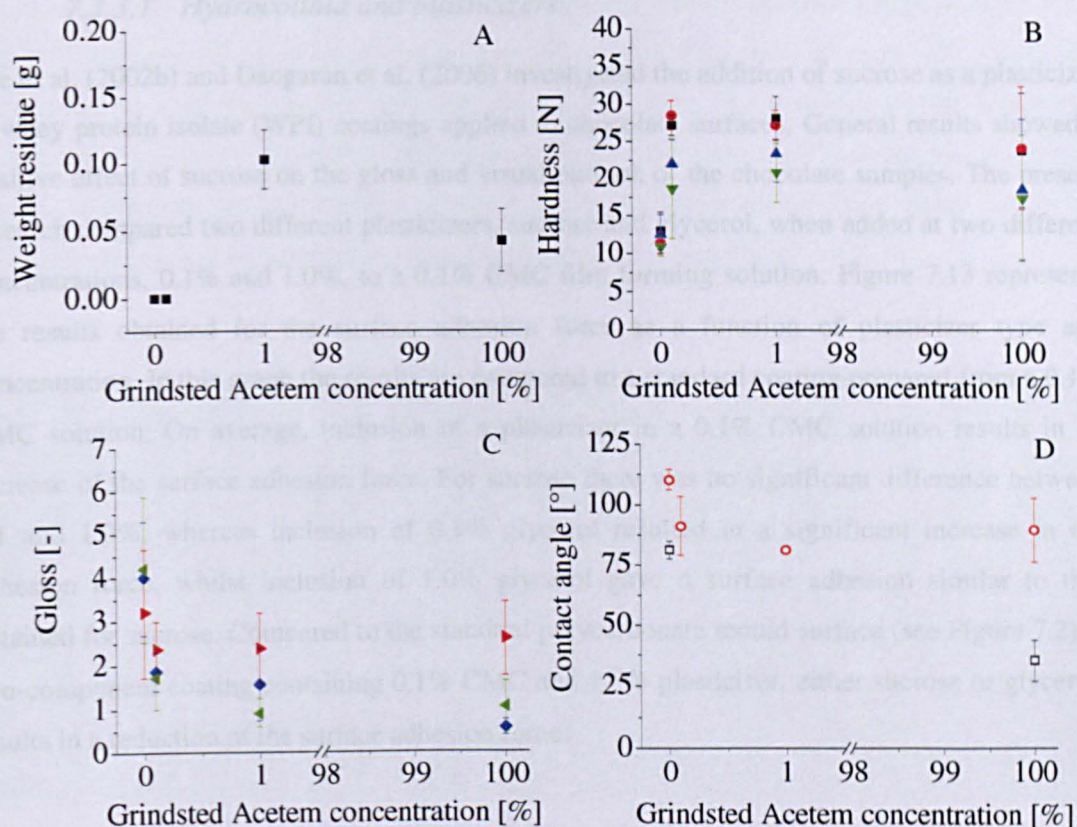


**Figure 7.12** The effect of Grindsted Acetem concentration on the amount of residues after probe separation (A), the hardness of the solidified chocolate samples (B), the difference of surface glossiness (C) and the water contact angle (D).

In (B) (■) represents the hardness of the bulk at the chocolate–air interface, (●) the bulk at the chocolate–mould interface, (▲) the surface at the chocolate–air interface, and (▼) the surface at the chocolate–mould interface, respectively. In (C) (◆) represents the surface glossiness of the mould surface, (◀) the chocolate–mould interface, and (▶) the chocolate–air interface. In (D) (□) represents the water contact angle before chocolate contact, and (○) after chocolate contact.

Error bar is representative of the standard deviation.

### 7.3.3 Two component coatings

Within the literature, many examples exist of the use of two-component coatings to protect food products against physical, chemical or microbiological damage and extend product shelf-life. Plasticizers are additives such as sorbitol, sucrose, glycerol or poly(ethylene glycol), which are generally included in coatings to enhance the physical characteristics of the coating film, e.g. flexibility and extensibility. Barreto et al. (2003) describe the enhanced film forming properties of sodium caseinate solutions after sorbitol addition. A typical rheological Newtonian behaviour was obtained. It was furthermore observed that sorbitol inclusion resulted in the formation of a more ordered structure, assumed to be a result of the hydrogen bonding formation between sorbitol and the amino acid side chain replacing part of the protein–protein interactions.



## 7.3.3.1 Hydrocolloid and plasticizers

Lee et al. (2002b) and Dangaran et al. (2006) investigated the addition of sucrose as a plasticizer to whey protein isolate (WPI) coatings applied to chocolate surfaces. General results showed a positive effect of sucrose on the gloss and visual outlook of the chocolate samples. The present research compared two different plasticizers, sucrose and glycerol, when added at two different concentrations, 0.1% and 1.0%, to a 0.1% CMC film forming solution. Figure 7.13 represents the results obtained for the surface adhesion force as a function of plasticizer type and concentration. In this graph the results are compared to a standard coating prepared from a 0.1% CMC solution. On average, inclusion of a plasticizer in a 0.1% CMC solution results in an increase of the surface adhesion force. For sucrose there was no significant difference between 0.1 and 1.0%, whereas inclusion of 0.1% glycerol resulted in a significant increase in the adhesion force, whilst inclusion of 1.0% glycerol gave a surface adhesion similar to that obtained for sucrose. Compared to the standard polycarbonate mould surface (see Figure 7.2), a two-component coating containing 0.1% CMC and 1.0% plasticizer, either sucrose or glycerol, results in a reduction of the surface adhesion force.

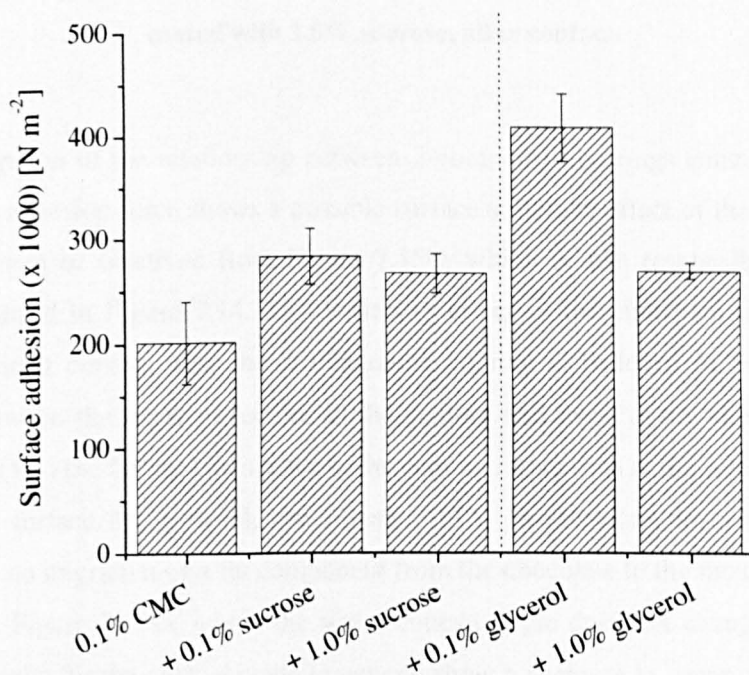


**Figure 7.13** Surface adhesion as affected by plasticizer type and concentration, for a 2-component coating with 0.1% CMC as the 1<sup>st</sup> component.

Error bar is representative of the standard deviation,  $n = 4$ .



An immediate observation made during the experimental surface adhesion determinations is the “sticky” character of the coatings containing plasticizers. Especially at high (1%) plasticizer concentrations a sticky, almost gum-like, elastic behaviour was observed at the chocolate–mould interface. Upon separation bridges were formed between the chocolate and the mould surface, which ruptured as a result of thinning behaviour. The resulting visual appearance of the chocolate and coated polycarbonate mould surfaces is shown in Figure 7.14.

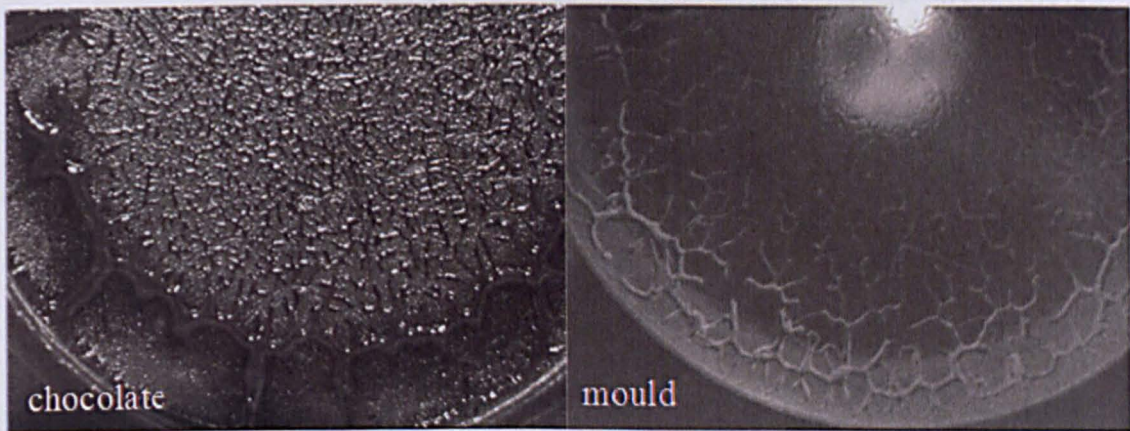


**Figure 7.14 Visualization of a chocolate and mould surface coated with 1.0% sucrose, after contact.**

Further investigation of the relationship between 2-component coatings containing plasticizers and the surface adhesion force shows a possible surface softening effect of the chocolate by the plasticizers, as can be observed from Figure 7.15B, which is also responsible for the sticky character visualized in Figure 7.14. This softening effect of the chocolate surface layer as a result of the direct contact with the 2-component coating is believed to be a result of the interactions between the sugar molecules in the coating and those in the chocolate. At higher concentrations (1%) the failure takes place in the coating rather than at the interface, resulting in a clean mould surface for glycerol, see Figure 7.15A. Furthermore, in contrast to previous results, there is no migration of a fat component from the chocolate to the mould surface, as can be observed in Figure 7.15D, where the water contact angle does not change after chocolate contact. The results for the contact angle in general show a decrease in water contact angle with increasing plasticizer content, indicating that addition of sucrose or glycerol makes the surface more hydrophilic. This observation is in line with the results obtained in section 5.3.6 for a rinsing agent, showing that an increase in surface hydrophilicity reduces the surface adhesion.



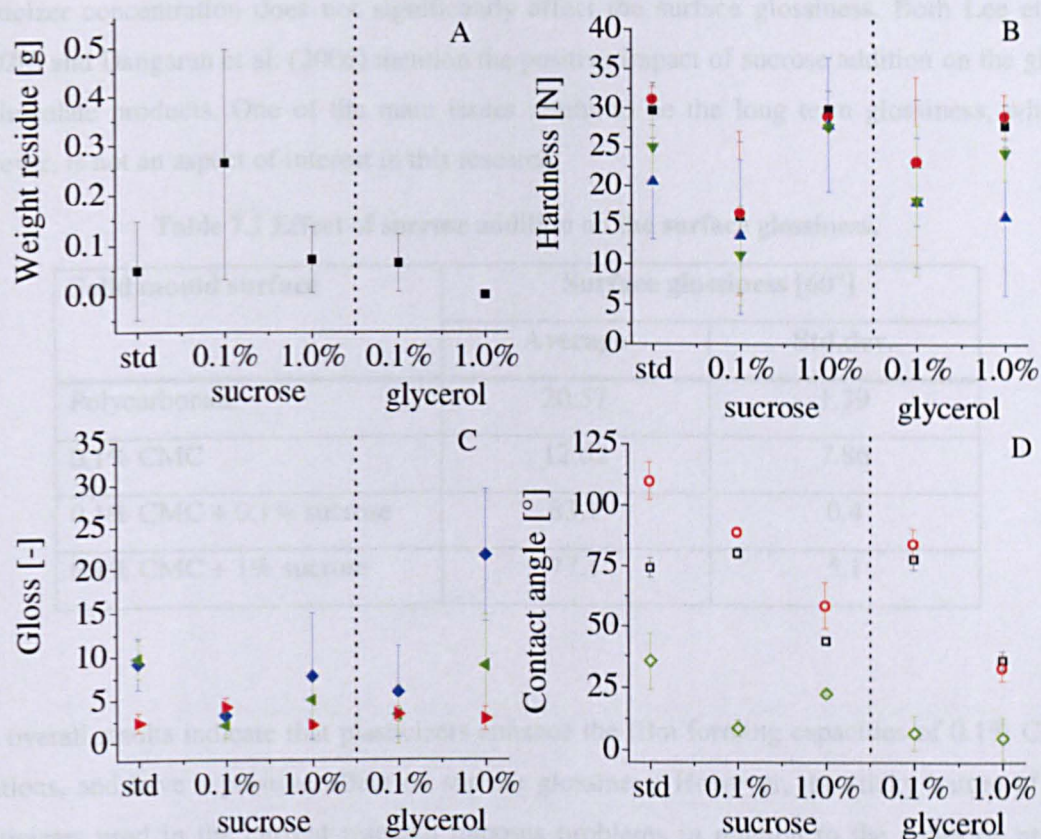


**Figure 7.15** The effect of plasticizer type and concentration of a 2 component coating system with 0.1% CMC on the amount of residues after probe separation (A), the hardness of the solidified chocolate samples (B), the difference of surface glossiness (C) and the water contact angle (D).

In (B) (■) represents the hardness of the bulk at the chocolate–air interface, (●) the bulk at the chocolate–mould interface, (▲) the surface at the chocolate–air interface, and (▼) the surface at the chocolate–mould interface, respectively. In (C) (◆) represents the surface glossiness of the mould surface, (◀) the chocolate–mould interface, and (▶) the chocolate–air interface. In (D) (□) represents the water contact angle before chocolate contact, (○) after chocolate contact, and (◇) the difference in contact angle before and after chocolate contact. Error bar is representative of the standard deviation.

Significant differences can also be observed for the surface glossiness, as shown in Figure 7.15C. The glossiness of the mould surfaces after chocolate contact is reduced by the addition of low (0.1%) concentrations of plasticizer to the standard coating of 0.1% CMC. This is assumed to be a result of the cohesive–adhesive failure taking place at these concentrations. Addition of higher concentrations (1%) of plasticizer significantly increases the surface glossiness of both the mould surface and the chocolate–mould interface. The increased roughness of the surfaces after separation, as can be seen in Figure 7.14, is assumed to be responsible for the large error at these concentrations. Measurement of the surface gloss of the clean coatings prior to chocolate contact shows a sharp increase after addition of sucrose, as can be seen from Table 7.1. The



plasticizer concentration does not significantly affect the surface glossiness. Both Lee et al. (2002b) and Dangaran et al. (2006) mention the positive impact of sucrose addition on the gloss of chocolate products. One of the main issues seems to be the long term glossiness, which, however, is not an aspect of interest in this research.

**Table 7.1 Effect of sucrose addition on the surface glossiness.**

Solid mould surface	Surface glossiness [60°]	
	Average	Std.dev.
Polycarbonate	20.57	1.79
0.1% CMC	12.62	7.86
0.1% CMC + 0.1% sucrose	83.1	0.4
0.1% CMC + 1% sucrose	77.1	5.1

The overall results indicate that plasticizers enhance the film forming capacities of 0.1% CMC solutions, and have a positive effect on surface glossiness. However, the sticky nature of the plasticizers used in the current research imposes problems in relation to the adhesion at the chocolate–mould interface. It is believed that the interactions between plasticizers and chocolate at the interface lead to negative visual effects, from a consumer point of view. From a practical point of view a preference is given to the use of sucrose over glycerol, as the behaviour of sucrose is more consistent than that of glycerol.

### 7.3.3.2 Hydrocolloid and lipid

In imitation of the work done by Lee et al. (2002b), who observed that water-based WPI coatings with a lipid (cocoa butter) component had a higher sensorial value than normal alcohol based shellac coatings, 2-component coatings were prepared by adding Grindsted Acetem at two levels to a standard 0.1% CMC film forming solution. In contrast to the results obtained in section 0, where the 1-component coating systems with Grindsted Acetem significantly reduced the surface adhesion force, addition of Grindsted Acetem at a concentration of 0.1% to 0.1% CMC results in a sharp increase in adhesion, as can be observed from Figure 7.16.

Further addition of GA up to a total concentration of 1% causes the surface adhesion to drop to a similar level as that obtained for the standard coating with 0.1% CMC.

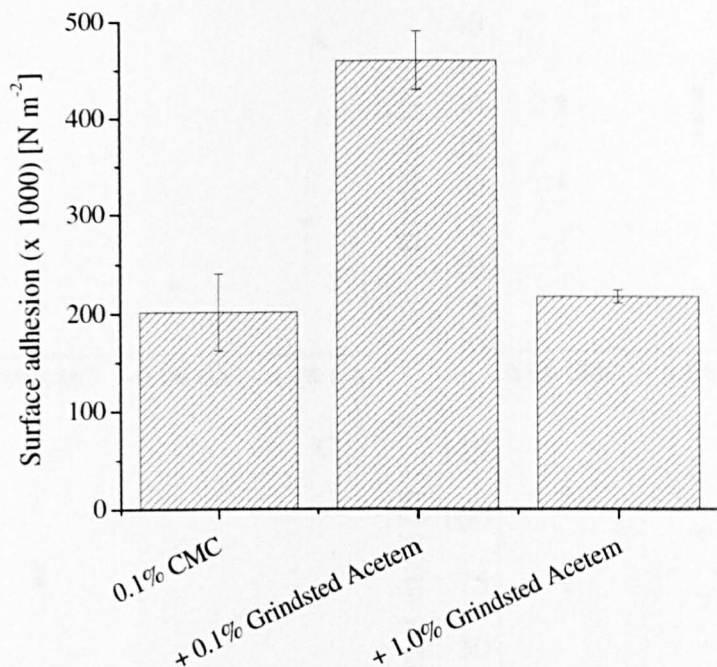


**Figure 7.16** Surface adhesion as a function of Grinsted Acetem concentration, for a 2-component coating with 0.1% CMC as the 1<sup>st</sup> component. Error bar is representative of the standard deviation,  $n = 4$ .

Further investigation of the relationship between 2-component coatings containing Grinsted Acetem as the lipid component and the surface adhesion force shows no significant effect on the type of failure occurring as measured by the amount of chocolate residues adhering or on the hardness of the chocolate systems, as can be observed from Figure 7.17A and B, respectively. Compared to the basic 0.1% CMC coating, the surface glossiness of both the chocolate–mould interface and the mould surface is significantly lower for the 2-component coatings containing Grinsted Acetem, as can be seen in Figure 7.17C. Figure 7.17D shows the water contact angle on the clean surfaces and on the same surfaces after chocolate contact. The results indicate a limited increase in water contact angle after chocolate contact, suggesting that the mould surface is becoming more hydrophobic as a result of the migration of lipid components from the chocolate to the mould surface. However, this effect is not as strong as previously observed for the standard polycarbonate surface. An increase in the amount of GA in the coating furthermore makes the mould surface more hydrophilic. The contact angle difference between before and after chocolate contact is similar for all surfaces.

The overall results indicate that addition of a lipid component in the form of the acetic acid ester Grinsted Acetem to a coating containing 0.1% CMC does not show any positive effect on the surface adhesion force. From a consumer point of view the lipid component negatively affects the visual appearance of the chocolate system, especially the surface gloss. Based on these results such a 2-component coating is not recommendable.



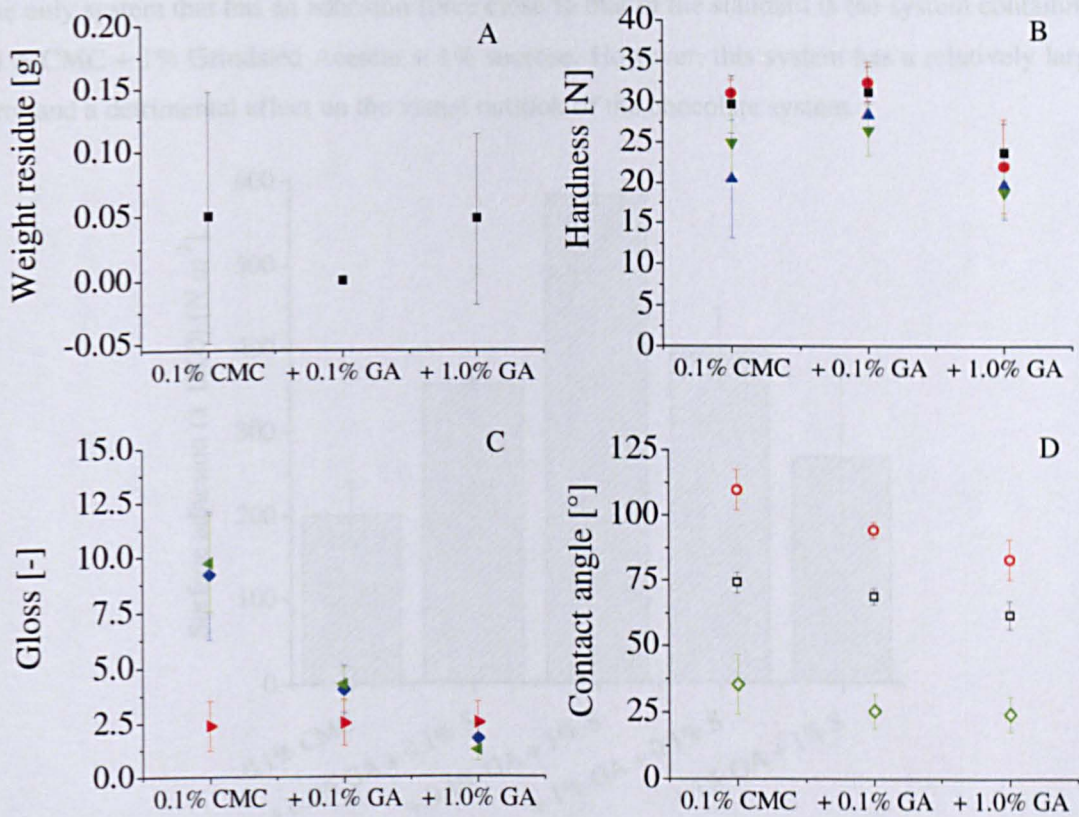


**Figure 7.17** The effect of Grindsted Acetem concentration of a 2-component coating system with 0.1% CMC on the amount of residues after probe separation (A), the hardness of the solidified chocolate samples (B), the difference of surface glossiness (C) and the water contact angle (D).

In (B) (■) represents the hardness of the bulk at the chocolate–air interface, (●) the bulk at the chocolate–mould interface, (▲) the surface at the chocolate–air interface, and (▼) the surface at the chocolate–mould interface, respectively. In (C) (◆) represents the surface glossiness of the mould surface, (◀) the chocolate–mould interface, and (▶) the chocolate–air interface. In (D) (□) represents the water contact angle before chocolate contact, (○) after chocolate contact, and (◇) the difference in contact angle before and after chocolate contact.

Error bar is representative of the standard deviation.

### 7.3.4 Three component coatings

Aim of the present research was to develop a coating based on the results previously obtained for the individual hydrocolloids and lipids and 2-component coating systems. Four different systems were prepared including the hydrocolloid CMC as the basic thin film forming agent, sucrose as the plasticizer and Grindsted Acetem as the lipid emulsifier. The results presented in Figure 7.18 show the experimental surface adhesion force as a function of the four different 3-component coating systems developed. 0.1% CMC was added as the standard coating system for comparison purposes. Compared to the 1-component CMC coating system all 3-component coatings significantly increased the surface adhesion force.



The only system that has an adhesion force close to that of the standard is the system containing 0.1% CMC + 1% Grindsted Acetem + 1% sucrose. However, this system has a relatively large error and a detrimental effect on the visual outlook of the chocolate system.

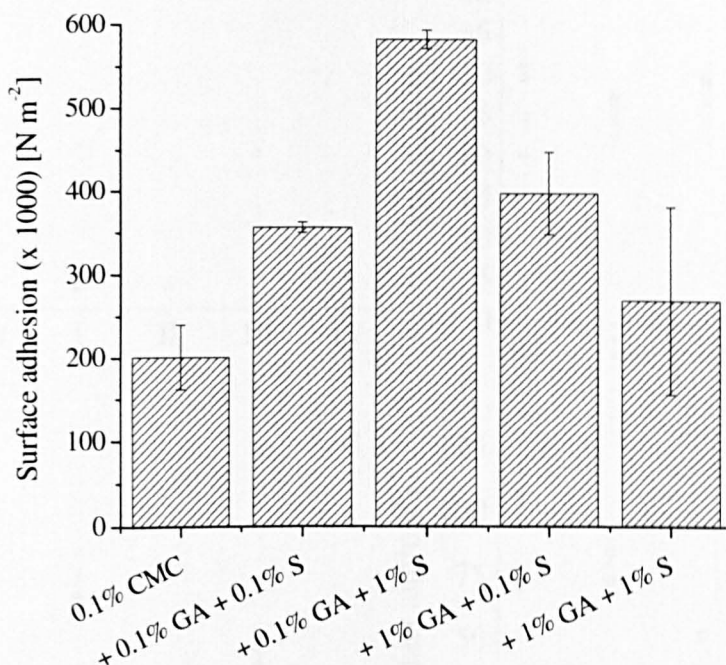


**Figure 7.18** Surface adhesion as affected by the 3-component coating composition.

**GA** stands for Grindsted Acetem and **S** for sucrose.

**Error bar is representative of the standard deviation, n = 4.**

Further investigation of the relationship between 3-component coatings containing a hydrocolloid, plasticizer and lipid component and the surface adhesion force shows a clear distinction in the amount of residues adhering between 0.1% GA and 1.0% GA, as can be observed from Figure 7.19A. With a low lipid concentration an adhesive failure is observed, with no residues adhering to the mould surface after separation. An increase in GA concentration results in a cohesive–adhesive failure. There is no correlation between the type of failure occurring and the hardness of the chocolate systems, shown in Figure 7.19B. A minor softening effect can be observed for the 3-component coating systems, but there is no clear trend. Similarly, the positive effect previously observed for sucrose addition on the surface glossiness is not observed in Figure 7.19C. The interaction between Grindsted Acetem and the sucrose is assumed to be responsible for this effect. Results obtained for the water contact angle, Figure 7.19D, seem to be the inverse of those obtained for the surface adhesion force. The highest adhesion is obtained with the system showing the most hydrophilic character after chocolate contact, whilst the system with the most hydrophobic character has the lowest surface adhesion force. In general, the adhesion force seems to increase when the contact angle after chocolate contact decreases, i.e. the surface is more hydrophilic.

Above results indicate that the 3-component coating systems developed in this research are not capable of reducing the surface adhesion force of a polycarbonate mould surface.

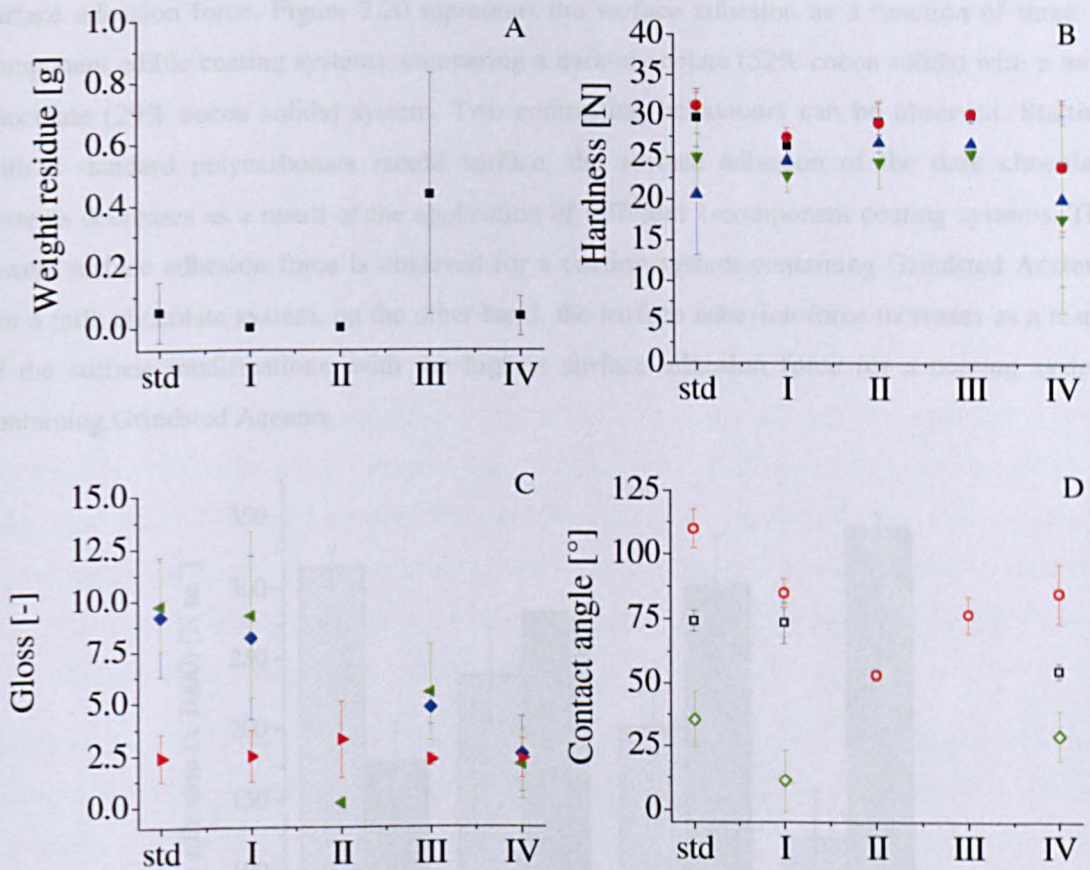


**Figure 7.19** The effect of composition of a 3 component coating system on the amount of residues after probe separation (A), the hardness of the solidified chocolate samples (B), the difference of surface glossiness (C) and the water contact angle (D).

Std refers to a standard coating containing 0.1% CMC, all others samples are based on the standard coating and contain in addition 0.1% GA and sucrose (I), 0.1% GA and 1% sucrose (II), 1% GA and 0.1% sucrose (III), or 1% GA and sucrose (IV), respectively. In (B) (■)

represents the hardness of the bulk at the chocolate–air interface, (●) the bulk at the chocolate–mould interface, (▲) the surface at the chocolate–air interface, and (▼) the surface at the chocolate–mould interface, respectively. In (C) (◆) represents the surface glossiness of the mould surface, (◀) the chocolate–mould interface, and (▶) the chocolate–air interface. In (D) (□) represents the water contact angle before chocolate contact, (○) after chocolate contact, and (◇) the difference in contact angle before and after chocolate contact.

Error bar is representative of the standard deviation.



### 7.3.5 Chocolate composition

A final research study was conducted to determine the impact of chocolate composition on the surface adhesion force. Figure 7.20 represents the surface adhesion as a function of three 1-component edible coating systems, comparing a dark chocolate (52% cocoa solids) with a milk chocolate (29% cocoa solids) system. Two contrasting behaviours can be observed. Starting with a standard polycarbonate mould surface, the surface adhesion of the dark chocolate systems decreases as a result of the application of different 1-component coating systems. The lowest surface adhesion force is observed for a coating system containing Grindsted Acetem. For a milk chocolate system, on the other hand, the surface adhesion force increases as a result of the surface modifications, with the highest surface adhesion force for a coating system containing Grindsted Acetem.

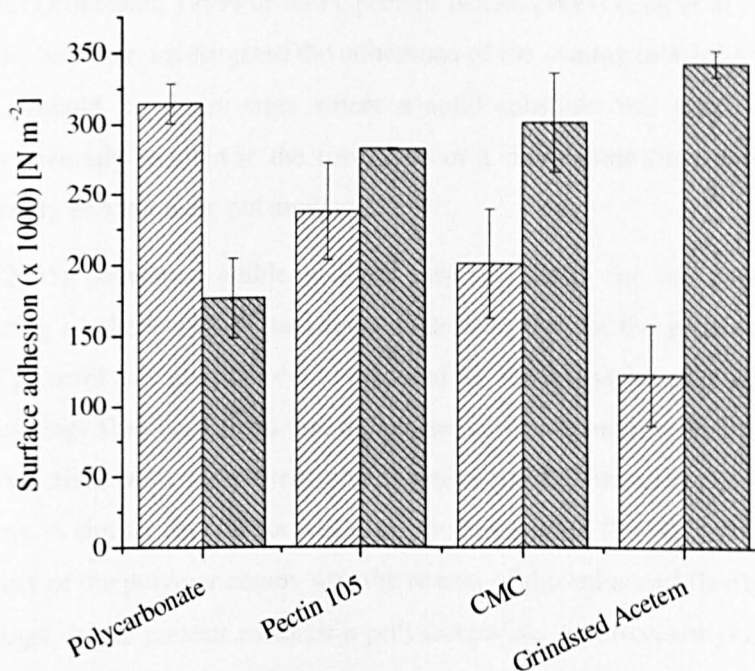


**Figure 7.20** Surface adhesion as affected by different 1-component coating systems in combination with a dark chocolate (▨) or a milk chocolate (■) system.

**Error bar is presentative of the standard deviation, n = 4.**

These results indicate that chocolate composition or ingredients have a strong impact on the surface adhesion force, and that interactions at the chocolate–mould interface should be taken into consideration when developing edible coatings which are applied as surface modifications. A similar test was done using aerated chocolate samples, which showed a cohesive–adhesive failure in all instances and negligible differences in surface adhesion. From these results it can be concluded that edible coatings can only be applied to individual chocolate samples and cannot be used as a generalized surface modification technique.



#### 7.4 DISCUSSION

One of the main issues in this research concerning edible coatings is the level of adhesion. As the coating is edible, there is no preference for the thin film to adhere to the solid mould substrate or the chocolate surface. However, it is important that the coating does not show interactions with both the mould and chocolate surface, as this will commonly result in an increase in the force required to de-mould the chocolate or visual defects. Research done on confectionery products has focussed primarily on the use of edible coatings to inhibit lipid migration by incorporating thin films in the confectionery products as a barrier between the chocolate shell and lipid-based filling (Nelson and Fennema, 1991; Brake and Fennema, 1993). Another area of interest within the confectionery industry is the use of edible coatings to enhance gloss and overall appearance, for example through the use of polyvinyl acetate (Hagenmaier and Grohmann, 1999) or whey protein isolate (WPI) (Lee et al., 2002b). None of these approaches, however, investigated the adherence of the coating to a solid substrate such as a polycarbonate mould. In those cases where a solid substrate was used for the thin film preparation this generally resulted in the formation of a stand-alone film, and the interactions with a confectionery product were not analyzed.

Schou et al. (2005) developed edible sodium caseinate films for the packaging of bread products, replacing synthetic plastic packaging materials. One of the problems observed was that addition of glycerol as a plasticizer was essential for the formation of a film that would not crack during handling. They concluded that the plasticizers competed for hydrogen bonding and electrostatic interactions with the protein chains, subsequently lowering the protein chain-to-chain interactions. A similar conclusion was given by Hong et al. (2004), who assumed that the increased mobility of the polymer chains was the reason of the enhanced flexibility of the WPI-plasticizer coatings. In the present research a polysaccharide, carboxymethyl cellulose (CMC), was chosen for more in-depth investigations over a protein, WPI. First of all, in single component coatings the WPI coating was very brittle, and thus affected the visual appearance of the chocolate surface negatively. Secondly, the CMC coating showed a higher reduction of the experimental adhesion force. Finally, the CMC coating improved the surface gloss of the chocolate samples more than the WPI coating. Even though CMC is not a protein, it is expected that the mechanism responsible for the improvement in film forming properties through the addition of a plasticizer is the same as that discussed for proteins, i.e. an enhanced flexibility and mobility of the polymer chains as a result of the location of the plasticizer molecules in between the polymer chains.

It is generally accepted that plasticizers are essential ingredients to prevent film brittleness and to enhance surface gloss. The type of plasticizer depends to a certain extent on the application. For chocolate products, Lee et al. (2002a) showed that sucrose gave a chocolate surface a higher gloss compared to glycerol, propylene glycol or polyethylene glycol. Dangaran et al. (2006) continued this work and related the loss of gloss of WPI coatings with time to the transformation of amorphous sucrose to crystalline sucrose. Nucleation and crystal growth enhance the surface roughness and subsequently decrease the surface gloss. Addition of a crystallization inhibitor, such as lactose, prevents this loss of gloss. The presence of lactose in milk chocolate is expected to affect the interactions between an edible coating containing sucrose and the chocolate system, which is assumed to be a result of the crystallization inhibitive characteristics of lactose.

The solid substrate is often strongly correlated with the mechanical properties of a thin film, and not the coating (Lee et al., 2007). Primarily because the surface chemistry of the substrate determines the interactions at the interface. Hong et al. (2005) mention the fact that it was almost impossible to apply a homogeneous polysaccharide coating on an untreated non-polar polypropylene (PP) surface. They hypothesized that the solid substrate did not offer enough binding sites for biopolymer coatings. Modification of the PP surface by corona discharge increased the surface energy and enhanced film forming properties. A poly(vinyl chloride) (PVC) substrate, on the other hand, promoted the formation of uniform WPI coatings (Hong et al., 2004), and it was hypothesized that the molecular structure of PVC allowed the formation of enough binding sites between the whey protein and the substrate. Comparing the molecular structure of the solid substrate used in this research, i.e. polycarbonate, with that of the main coating component, i.e. CMC, leads to the formulation of the hypothesis that there are enough binding sites which would promote adhesion of a CMC coating to a polycarbonate mould surface. Similar to observations made by Hong et al. (2004), it was observed in the current research that CMC concentration did not affect the surface energy of the edible films. The water contact angle is independent of the CMC concentration of the coating, see Figure 7.8D. It is not independent of plasticizer type though, and the water contact angle is shown to decrease with increasing molecular weight of the plasticizers. The current research does not show an explicit difference between glycerol and sucrose, but clearly shows a reduction in solid surface energy as a result of the inclusion of a plasticizer in the coating. In contrast to the results obtained in CHAPTER 4, where a reduction in the solid surface free energy caused a decrease in the surface adhesion force, the results obtained in the current research showed a slight increase in surface adhesion force. Interactions at the chocolate–mould (coating) interface as a result of the presence of sugar in both systems are believed to be responsible for this increase in adhesion.

## 7.5 CONCLUSIONS

Film structure and composition impact the optical, e.g. surface gloss, properties of a coating, and these characteristics can be transferred from the coating to a chocolate system upon direct contact. The quality attributes of the thin film need to be high in order to deliver a high quality surface finish to the chocolate system. Plasticizers have generally been observed to have a positive influence on the surface gloss of chocolate samples.

The results presented in this chapter have shown that it is possible to reduce the surface adhesion force by modifying the solid mould surface, especially through the use of hydrocolloid coatings. Further optimisations are required to develop an edible coating that is capable of lowering the surface adhesion force, without a cohesive–adhesive failure. However, this indicates that a combined action might be required, i.e. a solid surface modification to alter the surface energy of the mould material, and a chocolate modification increasing the cohesive strength of the chocolate system, possibly through addition of an emulsifier or surfactant to the chocolate system.



## CHAPTER 8

### CONCLUDING REMARKS

#### 8.1 SUMMARY OF THE MAIN RESULTS

Aim of this research study was to gain understanding of the mechanisms that cause the sticking (adhesion) of (aerated) chocolate to the mould materials and to reveal determining factors. An experimental method was developed to determine the force required to pull a probe off a solidified chocolate sample, imitating the chocolate demoulding process. By establishing relationships between the surface adhesion force, i.e. the level of adhesion of chocolate to the mould surface during demoulding, and the solid surface free energy of a range of mould materials, as well as processing conditions, understanding of the interactions taking place at the chocolate–mould interface was enhanced.

Measurement of the surface tension,  $\gamma$ , of a set of probe liquids and the contact angle,  $\theta$ , of each individual probe liquid when placed on a solid surface, allows the determination of the solid surface free energy,  $\gamma_s$ . The surface tension of liquid chocolate was found to vary depending on the chocolate composition, and in particular the presence of surface active molecules such as lecithin. Fatty acid composition of cocoa butter was hypothesized to be the main factor determining the value obtained for the surface tension. Similar results were obtained for the total solid surface energy,  $\gamma_s^{\text{tot}}$ , of chocolate systems, with milk chocolate showing a significantly higher dispersive component of the surface energy,  $\gamma_s^{\text{d}}$ , than dark chocolate. With respect to the solid mould materials results obtained for  $\gamma_s^{\text{tot}}$  were in good agreement with those observed in literature, i.e. PTFE < polycarbonate < stainless steel < quartz glass. Main differentiating factor amongst these solid surfaces is the electron donor contribution to the surface free energy,  $\gamma_s^-$ .

Correlating the surface energy results with the experimental surface adhesion force shows an exponential growth relationship, with an apparent critical surface free energy of the mould substrate of  $\sim 30 \text{ mN m}^{-1}$ . For solid materials with a surface energy above this value a pronounced increase in surface adhesion could be seen. A similar exponential growth relationship was established between the electron donor component,  $\gamma_s^-$ , and the surface adhesion force, with a critical value of the electron donor component of  $\sim 15 \text{ mN m}^{-1}$  below which the chocolate–mould adhesion was minimized. Based on a review of literature it is proposed that the surface energy of solid mould materials affects the crystallization and solidification mechanisms of the cocoa butter present within the surface region of the chocolate system. A low surface energy substrate is assumed to promote the formation of a loose and porous structure with limited crystal–crystal and crystal–mould interactions and subsequently a relatively low surface adhesion force.

Particular processing conditions generally applied during the moulding and demoulding stages in commercial chocolate manufacturing plants were investigated in relation to their effect on the experimental surface adhesion force using a set-up specifically developed in this research. Variation of the contact time, i.e. the time from the moment of chocolate–mould interface creation up to the measurement of the surface adhesion force, affected the crystallization and solidification mechanisms. A low contact time is assumed to correlate to low total solids content. With increasing contact time the total solids content increases through crystallization of liquid fat, resulting in an increase in the cohesive strength of the chocolate system and an increase in the resistance against separation. Based on these results a contact time  $\geq 60$  minutes is recommended, in combination with the cooling conditions applied in this research. A strong correlation with crystallization was also observed for the mould surface temperature, which is in good agreement with observations made in literature. High mould temperatures ( $\sim 50$  °C) at the time of chocolate–mould interface creation are responsible for the melting out of the seed crystals present in the surface region, subsequently limiting the formation of Form V crystals. Low mould temperatures ( $\leq 0$  °C) lead to the formation of polymorphic forms other than Form V. Cooling temperature is thought to affect the rate of heat transfer and subsequently the rate of crystallization, rather than the polymorphic transition. A high heat transfer rate, i.e. low cooling temperature, is proposed to promote the formation of a relatively dense packing with small fat crystals. The subsequent increase in crystal–crystal and crystal–mould interactions is expected to be related to the observed increase in surface adhesion force, similar to the observations made for high surface energy mould materials. A recommendation was made to pre-heat the mould materials under controlled environmental conditions, i.e. 0 %RH, 25–30 °C, prior to the moulding stage, and to use a cooling temperature of 10–15 °C in order to improve demoulding.

The negative interaction of chocolate with moisture is well-known. According to the results obtained in this research an optimal relative humidity that gives minimum surface adhesion and maximum chocolate quality, is 0 % RH. Moisture sorption experiments have confirmed the adsorption of water molecules on the polycarbonate mould surface at high relative humidity. Desorption was observed at low humidities, and the transition from desorption to adsorption coincided almost perfectly with the sharp decrease in surface adhesion at 40 – 50 %RH. The formation of a wetting film by the water molecules is assumed to limit the number of attachment sites at the chocolate–mould interface, creating a more hydrophilic mould surface. A similar observation was made when comparing the effect of different cleaning methods. Application of a rinsing aid after cleaning with water enhanced mould surface hydrophilicity and decreased the surface adhesion. Application of a detergent made the surface more hydrophobic and significantly enhanced the surface adhesion force. The best result, i.e. lowest surface adhesion force, was obtained for polycarbonate surfaces which were not cleaned between measurements. Migration of fat residues from the chocolate to the solid mould surface is assumed to be responsible for this reduction in surface adhesion.

A similar correlation between solid surface energy and surface adhesion as obtained for normal chocolate systems was found for aerated chocolate systems. With increasing solid surface energy the surface adhesion increases. The main difference between the aerated and standard or non-aerated systems is the reduced cohesive strength of aerated chocolate systems. All aerated systems show a cohesive failure within the aerated chocolate mass, rather than a failure at the chocolate–mould interface. This may be caused by a combined insulation effect of the mould material and the aerated chocolate system, resulting in a reduction in the heat transfer rate and consequently a reduction in the crystallization and solidification rates.

The gas used for the aeration step significantly affected the aeration and microstructure of chocolate systems, CO<sub>2</sub> giving a so-called macro-aeration and N<sub>2</sub> a micro-aeration. This is expected to be a result of the differences in solubility. Structural characterization of the microstructure of aerated chocolate using C-Cell allowed the quantitative measurement of the number of cells per surface area and the average cell diameter. A linear correlation of the surface adhesion force with the number of cells per surface area was obtained for systems containing CO<sub>2</sub> gas, whereas no significant correlation was found for systems containing N<sub>2</sub> gas. Based on these results the hypothesis is that N<sub>2</sub> inclusion in chocolate systems does not affect the contraction, and therefore shows good demoulding properties, whereas CO<sub>2</sub> inclusion negatively affects demoulding at higher concentrations. It is assumed that the CO<sub>2</sub> gas dissolves in the water vapour present at the chocolate–mould interface, subsequently increasing the stickiness. Upon (shock) cooling the expansion of water vapour is thought to be responsible for the demoulding of the aerated chocolate system.

A variety of edible thin film coatings was prepared using either individual hydrocolloids or lipids, or a combination of two- or three-components. For the single-component coatings it was observed that hydrocolloids in general possessed better surface adhesion reduction capabilities. Advantage of hydrocolloids over lipids was primarily their positive effect on the surface appearance of the chocolate system. Disadvantage of the use of hydrocolloids was the preparation of a stand-alone coating at higher concentrations, as a result of which the surface adhesion force could not be determined. The use of plasticizers such as sucrose or glycerol positively influenced the film forming capacities of 0.1% CMC solutions, and enhanced the surface glossiness of the chocolate surface. Softening of the coating after plasticizer addition negatively affected the stickiness at the chocolate–mould interface, resulting in a cohesive–adhesive failure. It was concluded that further optimisations are required, but edible coatings appear useful as a surface modification technique.



## **8.2 PRACTICAL APPLICATION**

The results obtained in this research have shown that the surface adhesion of different chocolate systems is not necessarily linearly correlated with their composition or with processing conditions. From a practical point of view this basically means that the mould material should be optimized for each specific application, i.e. chocolate type or product. Low surface energy materials such as PTFE are recommended for reduced surface adhesion, but are unfavourable for aerated chocolate systems due to their relatively low heat transfer capabilities. Optimization of the mould material is therefore recommended, possibly by applying a thin PTFE film on a stainless steel base. The relationship between the surface free energy of solid mould surfaces and the surface crystallization of chocolate systems implies the possible use of particular surfaces as a crystallization enhancer. Complete replacement of the tempering stage is not recommended though as the formation of crystal nuclei is still required.

Until now, observations made during commercial chocolate manufacturing with respect to the effect of processing conditions on chocolate manufacturing often were not reported. This research increased the scientific understanding of problems during the moulding and demoulding stages of the chocolate manufacturing process. This understanding can be used for the future optimisation of the processing guidelines, to avoid surface defects and product recalls.

### 8.3 FUTURE WORK

Future work recommended based on the results obtained in this research:

- Development of a surface with a non-adhesive character:
  - Surface modification through the application of an edible coating. Both surface chemistry and surface energy of solid surfaces can be controlled via this technique. The use of edible or biodegradable compounds allows the coating to adhere to either the mould or the chocolate or both upon demoulding;
  - Surface modification through the inclusion of additives in the cleaning process, especially in combination with a rinsing aid;
  - Chemical or physical modifications of mould surfaces, such as ion beam irradiation, synchrotron radiation under CO<sub>2</sub> gas atmosphere, plasma irradiation or corona discharge. These surface modifications are aimed at obtaining a material with a low surface energy and a high heat transfer coefficient.
- Determining the relationship between chocolate composition and the stickiness or adhesion of chocolate to mould surface:
  - Research into the use of atomic force microscopy (AFM) to measure the adhesion between chocolate and solid mould surfaces, especially in relation to the ingredients used;
  - The effect of different emulsifiers and/or surfactants on the cohesive forces of chocolate, especially in combination with aeration.
- Understanding of the interactions taking place at the chocolate–mould interface:
  - Application of the extended DVLO theory (named after Derjaguin, Landau, Verwey and Overbeek) in combination with surface thermodynamics to predict the adhesion behaviour of chocolate;
  - Investigation of the composition of deposits or residues present on the mould surface after demoulding using surface characterization techniques such as confocal laser scanning microscopy (CLSM) and/or scanning electron microscopy (SEM);
  - Investigation of the effect of solid surface energy and processing conditions on cocoa butter crystallization via differential scanning calorimetry (DSC).

---

**REFERENCES**

- Acros Organics (2009). *Technical Support – Material Safety Data Sheet (MSDS)*. Available from the World Wide Web: [http://www.acros.com/portal/alias\\_Rainbow/lang\\_en-US/tabID\\_41/DesktopDefault.aspx](http://www.acros.com/portal/alias_Rainbow/lang_en-US/tabID_41/DesktopDefault.aspx) [January 2006].
- Adamson, A.W. & Gast, A.P. (1997). *Physical Chemistry of Surfaces*, John Wiley & Sons, Inc., New York.
- ADAS (2007). Research into UK Food and Drink Manufacturing – Final Report (Desk Research). Food and Drink Federation, UK.
- Adhikari, B., Howes, T., Bhandari, B.R. & Truong, V. (2001). Stickiness in foods: a review of mechanisms and test methods. *International Journal of Food Properties*, 4(1), 1-33.
- Adhikari, B., Howes, T., Bhandari, B.R. & Truong, V. (2003). In-situ characterization of stickiness of sugar-rich foods using a linear actuator driven stickiness testing device. *Journal of Food Engineering*, 58, 11-22.
- Adhikari, B., Howes, T., Shrestha, A. & Bhandari, B.R. (2007). Effect of surface tension and viscosity on the surface stickiness of carbohydrate and protein solutions. *Journal of Food Engineering*, 79, 1136-1143.
- Afoakwa, E.O., Paterson, A. & Fowler, M. (2007). Factors influencing rheological and textural qualities in chocolate – a review. *Trends in Food Science & Technology*, 18, 290-298.
- Afoakwa, E.O., Paterson, A., Fowler, M. & Vieira, J. (2009). Microstructure and mechanical properties related to particle size distribution and composition in dark chocolate. *International Journal of Food Science & Technology*, 44, 111-119.
- Aguilera, J.M., Michel, M. & Mayor, G. (2004). Fat migration in chocolate: Diffusion or capillary flow in a particulate solid? – A hypothesis paper. *Journal of Food Science*, 69, 167-174.
- Allen, C.A.W., Watts, K.C & Ackman, R.G. (1999). Predicting the surface tension of biodiesel fuels from their fatty acid composition. *Journal of the American Oil Chemists Society*, 76, 317-323.
- Anonymous (2002). Popol Vuh. In G.M. Joseph and T.J. Henderson (Eds.), *The Mexico Reader: History, Culture, Politics* (pp. 79-85). Duke University Press, USA.
- Arishima, T. & Sato, K. (1989). Polymorphism of POP and SOS III. Solvent crystallization of  $\beta_2$  and  $\beta_1$  polymorphs. *Journal of the American Oil Chemists Society*, 66, 1614-1617.
- Atkins, P.W. (1994). *Physical Chemistry (5<sup>th</sup> ed)*. Oxford University Press, Oxford, UK.



## References

---

- Awad, T.S. & Marangoni, A.G. (2006). Ingredient interactions affecting texture and microstructure of confectionery chocolate. In A.G. Gaonkar & A. McPherson (Eds.), *Ingredient interactions: Effects on food quality* (2<sup>nd</sup> ed.) (pp. 423-475). CRC Press / Taylor & Francis Group, London, UK.
- Babin, H. (2005). *Colloidal properties of sugar particle dispersions in food oils with relevance to chocolate processing*. PhD Thesis, The University of Leeds.
- Baichoo, N., MacNaughtan, W., Mitchell, J.R. & Farhat, I.A. (2006). A STEPSCAN differential scanning calorimetry study of the thermal behaviour of chocolate. *Food Biophysics*, 1, 169-177.
- Balkenende, A.R., van den Boogaard, H.J.A.P., Scholten, M. & Willard, N.P. (1998). Evaluation of different approaches to assess the surface tension of low-energy solids by means of contact angle measurements. *Langmuir*, 14 (20), 5907-5912.
- Barreto, P.L.M., Roeder J., Crespo, J.S., Maciel, G.R., Terenzi, H., Pires, A.T.N. & Soldi, V. (2003). Effect of concentration, temperature and plasticizer content on rheological properties of sodium caseinate and sodium caseinate/sorbitol solutions and glass transition of their films. *Food Chemistry*, 82, 425-431.
- Bateup, B.O. (1981). Surface chemistry and adhesion. *International Journal of Adhesion and Adhesives*, 1, 233-239.
- Bayer MaterialScience (2004). Makrolon<sup>®</sup> 2805, 2865, 2807, 2867 and 2858. *Makrolon<sup>®</sup> Technical Information*.
- Beckett, S.T. (1999a). Traditional chocolate making. In S.T. Beckett (Ed), *Industrial Chocolate Manufacture and Use* (pp. 1-7). Blackwell Science, Oxford.
- Beckett, S.T. (1999b). Conching. In S.T. Beckett (Ed), *Industrial Chocolate Manufacture and Use* (pp. 153-181). Blackwell Science, Oxford.
- Beckett, S.T. (1999c). Non-conventional machines and processes. In S.T. Beckett (Ed), *Industrial Chocolate Manufacture and Use* (pp. 405-428). Blackwell Science, Oxford.
- Beckett, S.T. (2001). Milling, mixing and tempering – an engineering view of chocolate. *Proceedings of the Institution of Mechanical Engineers. Part E, Journal of Process Mechanical Engineering*, 215, 1-8.
- Beckett, S.T. (2008). *The Science of Chocolate* (2<sup>nd</sup> ed). The Royal Society of Chemistry, Cambridge, UK.
- Belitz, H.-D., Grosch, W. & Schieberle, P. (2004). *Food Chemistry* (3<sup>rd</sup> revised ed). Springer-Verlag, Berlin, Germany.

## References

---

- Bhandari, B. & Howes, T. (2005). Relating the stickiness property of foods undergoing drying and dried products to their surface energetic. *Drying Technology*, 23, 781-797.
- Blaurock, A.E. (1999). Fundamental understanding of the crystallization of oils and fats. In N. Widlak (Ed), *Physical Properties of Fats, Oils and Emulsifiers* (pp. 1-32). AOCS Press, Champaign.
- Bobe, U. Hofmann, J., Sommer, K., Beck, U. & Reiners, G. (2007). Adhesion – where cleaning starts. *Trends in Food Science & Technology*, 18, S36-S39.
- Boerboom, F.J.G. (2000). *The influence of dynamic surface properties on the creation and stability of foams*. PhD Thesis, Wageningen Universiteit.
- Bott, T.R. (1995). *Fouling of Heat Exchangers*. Elsevier Science b.v., Amsterdam.
- Boulangé-Petermann, L., Gabet, C. & Baroux, B. (2006). On the respective effect of the surface energy and micro-geometry in the cleaning ability of bare and coated steels. *Colloids and Surfaces A – Physicochemical and Engineering Aspects*, 272, 56-62.
- Brake, N.C. & Fennema, O.R. (1993). Edible coatings to inhibit lipid migration in a confectionery product. *Journal of Food Science*, 58, 1422-1425.
- British Stainless Steel Association (2007). Chemical composition of stainless steels to BS EN 10088-2. Available from the World Wide Web: <http://www.bssa.org.uk/topics.php?article=44> [13 June 2009].
- Brunello, N., McGauley, S.E. & Marangoni, A. (2003). Mechanical properties of cocoa butter in relation to its crystallization behavior and microstructure. *Lebensmittel-Wissenschaft und -Technology*, 36, 525-532.
- Brydson, J.A. (1999). *Plastics Materials* (7<sup>th</sup> ed). Butterworth-Heinemann, Oxford, UK.
- Butt, H.J., Graf, K. & Kappl, M. (2003). *Physics and Chemistry of Interfaces*. Wiley-VCH, Weinheim.
- Campbell, G.M. & Mougeot, E. (1999). Creation and characterisation of aerated food products. *Trends in Food Science & Technology*, 10, 283-296.
- CAOBISCO (2006). *Ranking of Consumption – Chocolate Confectionery*. Statistical Bulletin, CAOBISCO and ICA, Belgium.
- Chattoraj, D.K. (2001). Thermodynamics of adsorption at interfaces and the Gibbs surface excess. *Proceedings of the Indian National Science Academy*, 67 –A (6), 663-685.
- Chen, J. (2007). Surface texture of foods: perception and characterization. *CRC Critical Reviews of Food Science and Nutrition*, 47, 583-598.

## References

---

- Chen, J., Feng, M., Gonzalez, Y. & Pugaloni, L.A. (2008). Application of probe tensile method for quantitative characterisation of the stickiness of liquid foods. *Journal of Food Engineering*, 87, 281-290.
- Chevalley, J. (1999). Chocolate flow properties. In S.T. Beckett (Ed), *Industrial Chocolate Manufacture and Use* (pp. 182-200). Blackwell Science, Oxford.
- Cho, K., Kim, D & Yoon, S. (2003). *Effect of substrate energy on transcrystalline growth and its effect on interfacial adhesion of semicrystalline polymers*. *Macromolecules*, 36 (20), 7652-7660.
- Chumpitaz, L.D.A., Coutinho, L.F. & Meirelles, A.J.A. (1999). Surface tension of fatty acids and triglycerides. *Journal of the American Oil Chemists Society*, 76 (3), 379-382.
- Codex Alimentarius (2003). *Codex standard for chocolate and chocolate products* (Codex Stan 87-1981, Rev. 1 – 2003). FAO / WHO Food Standards.
- Comyn, J. (1997). *Adhesion Science*. RSC Paperbacks, The Royal Society of Chemistry, Cambridge, UK.
- Cruickshank, D. (2005). Chocolate cooling and demoulding. *The Manufacturing Confectioner*, 85(6), 79-82.
- Dangaran, K.L., Renner-Nantz, J. & Krochta, J.M. (2006). Whey protein-sucrose coating gloss and integrity stabilization by crystallization inhibitors. *Journal of Food Science*, 71, 152-157.
- Dann, J. R. (1970). Forces involved in adhesive process. 1 - Critical surface tensions of polymeric solids as determined with polar liquids. *Journal of Colloid and Interface Science*, 32 (2), 302-320.
- Decker, N.R. & Ziegler, G.R. (2002). The structure of aerated confectionery. *The Manufacturing Confectioner*, September, 101-108.
- Della Volpe, C., Maniglio, D., Brugnara, M., Siboni, S. & Morra, M. (2004). The solid surface free energy calculation - I. In defence of the multicomponent approach. *Journal of Colloid and Interface Science*, 271 (2), 434-453.
- Della Volpe, C. & Siboni, S. (2004). *Calculations of Acid-Base Surface Tension Components*. Available from the World Wide Web: <http://devolmac.ing.unitn.it:8080/> [03 February 2006].
- DeMan, J.M. (1999). Relationship among chemical, physical, and textural properties of fats. In N. Widlak (Ed), *Physical Properties of Fats, Oils and Emulsifiers* (pp. 79-95). AOCS Press, Champaign.
- De Zaan (2006). The de Zaan<sup>®</sup> cocoa manual. *Archer Daniels Midland Company*.



## References

---

- Dhoedt, A. (2008). "Food of the Gods" – The rich history of chocolate. *AgroFOOD*, 19 (3), 4-6.
- Dhonsi, D. & Stapley, A.G.F. (2006). The effect of shear rate, temperature, sugar and emulsifier on the tempering of cocoa butter. *Journal of Food Engineering*, 77, 936-942.
- Dimick, P.S. (1999). Compositional effect on crystallization of cocoa butter. In N. Widlak (Ed), *Physical Properties of Fats, Oils and Emulsifiers* (pp. 140-164). AOCS Press, Champaign.
- Dimick, P.S. & Hoskin, J.C. (1999). The chemistry of flavour development in chocolate. In S.T. Beckett (Ed), *Industrial Chocolate Manufacture and Use* (pp. 137-152). Blackwell Science, Oxford.
- Dunnewind, B., Janssen, A.M., van Vliet, T. & Weenen, H. (2004). Relative importance of cohesion and adhesion for sensory stickiness of semisolid foods. *Journal of Texture Studies*, 35, 603-620.
- Dutta, A., Chengara, A. Nikolov, A. Wasan, D.T., Chen, K. & Campbell, B. (2002). Effect of surfactant composition on aeration characteristics and stability of foams in aerated food products. *Journal of Food Science*, 67 (8), 3080-3086.
- Ebewele, R.O. (2000). *Polymer Science and Technology*. CRC Press, Boca Raton.
- Erbil, H.Y. (2006). *Surface Chemistry of Solid and Liquid Interfaces*. Blackwell Publishing, Oxford.
- Förster M., & Bohnet M. (1999). Influence of the interfacial free energy crystal/heat transfer surface on the induction period during fouling. *International Journal of Thermal Science*, 38, 944-954.
- Förster M., & Bohnet M. (2000). Modification of molecular interactions at the interface crystal/heat transfer surface to minimize heat exchanger fouling. *International Journal of Thermal Science*, 39, 697-708.
- Fowkes, F.M. (1964). Attractive forces at interfaces. *Industrial and Engineering Chemistry*, 56(12), 40-52.
- Fowler, M.S. (1999). Cocoa beans: From tree to factory. In S.T. Beckett (Ed), *Industrial Chocolate Manufacture and Use* (pp. 8-35). Blackwell Science, Oxford.
- Fox, H.W. & Zisman, W.A. (1950). The spreading of liquids on low-energy surfaces, 1. Polytetrafluoroethylene. *Journal of Colloid Science*, 5, 514-531.
- Fox, H.W. & Zisman, W.A. (1952a). The spreading of liquids on low-energy surfaces, 2. Modified tetrafluoroethylene polymers. *Journal of Colloid Science*, 7, 109-121.
- Fox, H.W. & Zisman, W.A. (1952b). The spreading of liquids on low-energy surfaces, 3. Hydrocarbon surfaces. *Journal of Colloid Science*, 7, 428-442.

## References

---

- Fryer, P. & Pinschower, K. (2000). The materials science of chocolate. *MRS Bulletin*, 25(12), 25-29.
- Galet, L., Vu, T.O., Oulahna, D. & Fages, J. (2004). The wetting behaviour and dispersion rate of cocoa powder in water. *Food and Bioproducts Processing*, 82(C4), 298-303.
- Garbassi, F., Morra, M. & Occhiello, E. (1994). *Polymer Surfaces: From Physics to Technology*. John Wiley and Sons, Oxford.
- Gindl, M., Sinn, G. Gindl, W., Reiterer, A. & Tschegg, S. (2001). A comparison of different methods to calculate the surface free energy of wood using contact angle measurements. *Colloids and Surfaces A: Physicochemical and Engineering Aspects*, 181, 279-287.
- Good, R.J. (1979). Contact angles and the surface free energy of solids. In R.J. Good & R.R. Stromberg (Eds.), *Surface and Colloid Science*, Plenum Press, New York.
- Good, R.J. (1992). Contact angle, wetting, and adhesion – a critical review. *Journal of Adhesion Science and Technology*, 6 (12), 1269-1302.
- Götz, J., Balzer, H. & Hinrichs, R. (2005). Characterisation of the structure and flow behaviour of model chocolate systems by means of NMR and rheology. *Applied Rheology*, 15(2), 98-111.
- Greener Donhowe, I. & Fennema, O. (1994). Edible films and coatings: characteristics, formation, definitions, and testing methods. In J.M. Krochta, E.A. Baldwin & M.O. Nisperos-Carriedo (Eds.), *Edible Coatings and Films to Improve Food Quality*, CRC Press, Boca Raton.
- Güleç, H.A., Sarioğlu, K. & Mutlu, M. (2006). Modification of food contact surfaces by plasma polymerisation technique, Part I: Determination of hydrophilicity, hydrophobicity and surface free energy by contact angle method. *Journal of Food Engineering*, 75, 187-195.
- Haedelt (2005). *An Investigation into Bubble Inclusion into Liquid Chocolate*. PhD Thesis, University of Reading.
- Hagenmaier, R.D. & Grohmann, K. (1999). Polyvinyl acetate as a high-gloss edible coating. *Journal of Food Science*, 64 (6), 1064-1067.
- Harbecke, P.M. (2005). Designing and developing chocolate moulds. *The Manufacturing Confectioner*, 85(6), 85-90.
- Harkins, W.D. (1941). A general thermodynamic theory of the spreading of liquids to form duplex films and of liquids or solids to form monolayers. *Journal of Chemical Physics*, 9, 552-568.

## References

---

- Harkins, W.D. & Feldman, A. (1922). Films, the spreading of liquids and the spreading coefficient. *Journal of the American Chemical Society*, 44, 2665-2685.
- Hartel, R.W. (2001). *Crystallization in Foods*. Springer, Berlin, Germany.
- Haylock, S.J. & Dodds, T.M. (1999). Ingredients from milk. In S.T. Beckett (Ed), *Industrial Chocolate Manufacture and Use* (pp. 57-77). Blackwell Science, Oxford.
- Heemskerck, R.F.M. (1999). Cleaning, roasting and winnowing. In S.T. Beckett (Ed), *Industrial Chocolate Manufacture and Use* (pp. 78-99). Blackwell Science, Oxford.
- Hiemenz, P.C. (1986). *Principles of Colloid and Surface Chemistry*. Dekker, New York.
- Himawan, C., Starov, V.M. & Stapley, A.G.F. (2006). Thermodynamic and kinetic aspects of fat crystallization. *Advances in Colloid and Interface Science*, 122, 3-33.
- Hoare, B. (2007). *Assessment of the Surface Energy of Chocolate; Effects of Crystallization and Aeration*. BSc Thesis, University of Leeds.
- Hong, S-I, Han, J.H. & Krochta, J.M. (2004). Optical and surface properties of whey protein isolate coatings on plastic films as influenced by substrate, protein concentrations, and plasticizer type. *Journal of Applied Polymer Science*, 92, 335-343.
- Hong, S-I, Lee, J-W. & Son, S-M. (2005). Properties of polysaccharide-coated polypropylene films as affected by biopolymer and plasticizer types. *Packaging Technology and Science*, 18, 1-9.
- Hoseney, R.C. & Smewing, J. (1999). Review paper – Instrumental measurement of stickiness of doughs and other foods. *Journal of Texture Studies*, 30 (2), 123-36.
- Jackson, K. (1999). Recipes. In S.T. Beckett (Ed), *Industrial Chocolate Manufacture and Use* (pp. 323-346). Blackwell Science, Oxford.
- Janczuk, B. & Zdziennicka, A. (1994). A study on the components of surface free energy of quartz from contact angle measurements. *Journal of Materials Science*, 29, 3559-3564.
- Janssen, D., De Palma, R. Verlaak, S. Heremans, P. & Dehaen, W. (2006). Static solvent contact angle measurements, surface free energy and wettability of various self-assembled monolayers on silicon dioxide. *Thin Solid Films*, 515, 1433-1438.
- JohnsonDiversey (2009). *Where practicality meets innovation*. Product information and material safety data sheet for Diverwash HD7 and Suma Rinse A5. Available from the World Wide Web: <http://www.johnsondiversey.com/Cultures/en-GB/OpCo/Products+and+Systems/Products/203.htm> [October 2006].
- Johnston, G.M. (1972). Fats and processes used in manufacturing chocolate and confectionery coatings. *Journal of the American Oil Chemists Society*, 49, 462-467.



## References

---

- Jowitt, R. (1974). The terminology of food texture. *Journal of Texture Studies*, 5, 351-358.
- Karbowiak, T., Debeaufort, F. & Voilley, A. (2006). Importance of surface tension characterization for food, pharmaceutical and packaging products: a review. *Critical Reviews in Food Science and Nutrition*, 46, 391-407.
- Keijbets, E.L., Chen, J., Dickinson, E. & Vieira J. (2009). Surface energy investigation of chocolate adhesion to solid mould materials. *Journal of Food Engineering*, 92 (2), 217-225
- Kendall, K. (2001). *Molecular Adhesion and its Applications – the Sticky Universe*. Kluwer Academic / Plenum Publishers, New York.
- Keogh, M.K., Murray, C.A. & O’Kennedy, B.T. (2003). Effects of selected properties of ultrafiltered spray-dried milk powders on some properties of chocolate. *International Dairy Journal*, 13, 719-726.
- Khwaldia, K., Perez, C., Banon, S., Desobry, S. & Hardy, J. (2004). Milk proteins for edible films and coatings. *Critical Reviews in Food Science and Nutrition*, 44, 239-251.
- Kilcast, D. & Roberts, C. (1998), Perception and measurement of stickiness in sugar-rich foods. *Journal of Texture Studies*, 29 (1), 81-100.
- Kinloch, A.J. (1980). The science of adhesion. Part 1. Surface and interfacial aspects. *Journal of Materials Science*, 15, 2141-2166.
- Kinta, Y. & Hatta, T. (2007). Composition, structure and color of fat bloom due to the partial liquefaction of fat in dark chocolate. *Journal of the American Oil Chemists Society*, 84, 107-115.
- Kloubek, J. (1992). Development of methods for surface free energy determination using contact angles of liquids on solids. *Advances in Colloid and Interface Science*, 38, 99-142.
- Krisdhasima V., McGuire J. & Sproull R. (1992). *Surface hydrophobic influences on beta-lactoglobulin adsorption-kinetics*. *Journal of Colloid and Interface Science* 154, 337-350.
- Krüger, Ch. (1999). Sugar and bulk sweeteners. In S.T. Beckett (Ed), *Industrial Chocolate Manufacture and Use* (pp. 36-56). Blackwell Science, Oxford.
- KRÜSS GmbH (2009). *Measuring methods*. Available from the World Wide Web: <http://www.kruss.de/en/theory/measurements.html> [November 2005].
- Kwok, D.Y. & Neumann, A.W. (1999). Contact angle measurement and contact angle interpretation. *Advances in Colloid and Interface Science*, 81, 167-249.
- Kwok, D. & Neumann, A.W. (2000a). Contact angle interpretation: combining rule for solid-liquid intermolecular potential. *Journal of Physical Chemistry B*, 104, 741-746.

## References

---

- Kwok, D. & Neumann, A.W. (2000b). Contact angle interpretation in terms of solid surface tension. *Colloids and surfaces A – Physicochemical and Engineering Aspects*, 161, 31-48.
- Larsson, K. (1966). Classification of glyceride crystal forms. *Acta Chemica Scandinavica*, 20, 2255-2260.
- Lawler, P.J. & Dimick, P.S. (2002). Crystallization and polymorphism of fats. In C.C. Akoh and D.B. Min (Eds), *Food Lipids – Chemistry, Nutrition and Biotechnology* (2<sup>nd</sup> ed.) (pp. 245-266). Marcel Dekker, New York.
- Lee, L.-H. (1993). Roles of molecular interactions in adhesion, adsorption, contact angle and wettability. *Journal of Adhesion Science and Technology*, 7 (6), 583-634.
- Lee, S.-Y., Danganan, K.L., Krochta, J.M. (2002a). Gloss stability of whey protein/plasticizer coating formulations on chocolate surface. *Journal of Food Science*, 67 (3), 1121-1125.
- Lee, S.-Y., Danganan, K.L., Guinard, J.-X. & Krochta, J.M. (2002b). Consumer acceptance of whey-protein-coated as compared with shellac-coated chocolate. *Journal of Food Science*, 67, 2764-2769.
- Lee, J.-W., Son, S.-M., Hong, S.-I. (2007). Characterization of protein-coated polypropylene films as a novel composite structure for active food packaging application. *Journal of Food Engineering*, 86, 484-493.
- Lewin, M., Mey-Arom, A. & R. Frank (2005). Surface free energies of polymeric materials, additives and minerals. *Polymers for Advanced Technologies*, 16, 429-441.
- Li, D. & Neumann, A.W. (1990). A reformulation of the equation of state for interfacial tensions. *Journal of Colloid and Interface Science*, 137, 304-307.
- Li, D. & Neumann, A.W. (1992a). Equation of state for interfacial tensions of solid-liquid systems. *Advances in Colloid and Interface Science*, 39, 299-345.
- Li, D. & Neumann, A.W. (1992b). Contact angles on hydrophobic solid-surfaces and their interpretation. *Journal of Colloid and Interface Science*, 148, 190-200.
- Liang, B. & Hartel, R.W. (2004). Effects of milk powders in milk chocolate. *Journal of Dairy Science*, 87, 20-31.
- Liu, W., Zhang, Z. & Fryer, P.J. (2006a). Identification and modelling of different removal modes in the cleaning of a model food deposit. *Chemical Engineering Science*, 61(22), 7528-7534.
- Liu, W., Fryer, P.J., Zhang, Z., Zhao, Q., & Liu, Y. (2006b). Identification of cohesive and adhesive effects in the cleaning of food fouling deposits. *Innovative Food Science & Emerging Technologies*, 7, 263-269.

## References

---

- Loisel, C., Lecq, G., Ponchel, G., Keller, G. & Ollivon, M. (1997). Fat bloom and chocolate structure studied by mercury porosimetry. *Journal of Food Science*, 62, 781-788.
- Loisel, C., Keller, G., Lecq, G., Bourgaux, C. & Ollivon, M. (1998a). Phase transitions and polymorphism of cocoa butter. *Journal of the American Oil Chemists Society*, 75, 425-439.
- Loisel, C., Lecq, G., Keller, G. & Ollivon, M. (1998b). Dynamic crystallization of dark chocolate as affected by temperature and lipid additives. *Journal of Food Science*, 63, 73-79.
- Lonchampt, P. & Hartel, R.W. (2006). Surface bloom on improperly tempered chocolate. *European Journal of Lipid Science and Technology*, 108, 159-168.
- Luengo, G., Tsuchiya, M., Heuberger, M. & Israelachvili, J. (1997). Thin film rheology and tribology of chocolate. *Journal of Food Science*, 62, 767-812.
- Lyklema, J. (1991). *Fundamentals of Interface and Colloid Science. Volume I: Fundamentals*. Academic Press, London.
- Lyklema, J. (1995). *Fundamentals of Interface and Colloid Science. Volume II: Solid-liquid interfaces*. Academic Press, London.
- Lyklema, J. (2000). *Fundamentals of Interface and Colloid Science. Volume III: Liquid-fluid interfaces*. Academic Press, London.
- Mancini, M. & Oguey, C. (2005). Equilibrium conditions and symmetries for foams in contact with solid surfaces. *Colloids and Surfaces A: Physicochemical and Engineering Aspects*, 263, 33-38.
- Mangel, A. (2007). *Cisorp Water Sorption Analyser – User Manual*. CI Electronics Ltd., Salisbury, UK
- Mars Incorporated (US) (1999). Improved molding process. International Patent WO 99/34685.
- Mastrantonakis, K. (2004). *An Investigation on the Surface Properties of Moulds and the Effect of Emulsifiers on the Demoulding of Aerated Chocolate*. MSc Thesis, University of Leeds.
- Mazzanti, G., Guthrie, S.E., Sirota, E.B., Marangoni, A.G. & Idziak, S.H.J. (2004). Communications – Novel shear-induced phases in cocoa butter. *Crystal Growth & Design*, 4, 409-411.
- McGauley, S.E. & Marangoni, A.G. (2002). Static crystallization behaviour of cocoa butter and its relationship to network microstructure. In A.G. Marangoni and S.S. Narine (Eds.), *Physical Properties of Lipids*. Marcel Dekker, New York.



## References

---

- McGuire, J. (2005). Surface properties. In M.A. Rao, S.S.H. Rizvi and A.K. Datta (Eds.), *Engineering Properties of Foods* (3<sup>rd</sup> ed), Taylor & Francis, London, UK.
- Meiron, T.S. & Saguy, I.S. (2007). Wetting properties of food packaging. *Food Research International*, 40, 653-659.
- Meursing, E.H. & Zijderveld, J.A. (1999). Cocoa mass, cocoa butter and cocoa powder. In S.T. Beckett (Ed), *Industrial Chocolate Manufacture and Use* (pp. 101-114). Blackwell Science, Oxford.
- Michalski, M.C., Desobry, S. & Hardy, J. (1997). Food materials adhesion: a review. *Critical Reviews in Food Science and Nutrition*, 37, 591-619.
- Michalski, M.C., Desobry, S., Pons, MN. & Hardy, J. (1998a). Adhesion of edible oils to food contact surfaces. *Journal of the American Oil Chemists Society*, 75, 447-454.
- Michalski, M.C., Desobry, S. & Hardy, J. (1998b). Adhesion of edible oils and food emulsions to rough surfaces. *Lebensmittel-Wissenschaft und -Technology*, 31, 495-502.
- Michalski, M.C., Desobry, S., Babak, V. & Hardy, J. (1999). Adhesion of food emulsions to packaging and equipment surfaces. *Colloids and Surfaces A – Physicochemical and Engineering Aspects*, 149, 107-121.
- Michalski, M.C. & Briard, V. (2003). Fat-related surface tension and wetting properties of milk. *Milchwissenschaft*, 58 (1/2), 26-28.
- Minifie, B.W. (1989). *Chocolate, Cocoa and Confectionery: Science and Technology* (3<sup>rd</sup> ed). Van Nostrand Reinhold, New York.
- Müller-Steinhagen, N. & Windhab, E.J. (2005). Influence of process parameters on microstructure of food foam whipped in a rotor-stator device within a wide static pressure range. *Colloids and Surfaces A: Physicochemical and Engineering Aspects*, 263, 353-362.
- Mullin, J.W. (2001). *Crystallization* (4<sup>th</sup> ed.). Elsevier, Oxford, UK.
- Myers, D. (1999), *Surfaces, Interfaces and Colloids: Principles and Applications* (2<sup>nd</sup> ed.). Wiley & Sons, Inc., New York.
- Narayanan, N. & Ramamurthy, K. (2000). Structure and properties of aerated concrete: a review. *Cement & Concrete Composites*, 22, 321-329.
- Narine, S.S. & Marangoni, A.G. (1999). Relating structure of fat crystal networks to mechanical properties: a review. *Food Research International*, 32, 227-248.
- Narine, S.S. & Marangoni, A.G. (2005). Microstructure. In A.G. Marangoni (Ed.), *Fat Crystal Networks* (pp. 179-254). Marcel Dekker, New York.

## References

---

- Nelson, R.B. (1999). Enrobers, moulding equipment and coolers. In S.T. Beckett (Ed), *Industrial Chocolate Manufacture and Use* (pp. 259-286). Blackwell Science, Oxford.
- Nelson, K.L. & Fennema, O.R. (1991). Methylcellulose films to prevent lipid migration in confectionery products. *Journal of Food Science*, 56, 504-509.
- Neumann, A.W. & Good, R.J. (1979). Techniques of measuring contact angles. In R.J. Good and R.R. Stromberg (Eds), *Surface and Colloid Science* (pp. 31-91). New York, Plenum Press.
- Neumann, A.W., Good, R.J., Hope, C.J. & Sepal, M. (1974). Equation of state approach to determine surface tensions of low-energy solids from contact angles. *Journal of Colloid and Interface Science*, 49, 291-304.
- Nice, G. (2005). Chocolate moulding – soup to nuts. *The Manufacturing Confectioner*, 85(6), 71-77.
- Niranjan, K. (1999). Introduction to bubble mechanics in food. In G.M. Campbell, C. Webb, S.S. Pandiella and K. Niranjan (Eds), *Bubbles in Food* (pp. 3-8). Eagen Press.
- Norberg, S. (2006). Chocolate and confectionery fats. In F. Gunstone (Ed.), *Modifying Lipids for Use in Food* (pp. 488-516). Woodhead Publishing Limited, Cambridge.
- Norde, W. (2003). *Colloids and Interfaces in Life Sciences*. Marcel Dekker, New York.
- Nussinovitch, A. (2003). *Water-Soluble Polymer Applications in Foods*. Blackwell Science Ltd., Oxford, UK.
- NVON-commissie (1998). *Binas – Informatieboek vwo/havo voor het onderwijs in de natuurwetenschappen*. Wolters-Noordhoff, Groningen, the Netherlands.
- Oláh, A. & Vancso, G.J. (2005). Characterization of adhesion at solid surfaces: development of an adhesion-testing device. *European Polymer Journal*, 41, 2803-2823.
- Owens, D.K. & Wendt, R.C. (1969). Estimation of surface free energy of polymers. *Journal of Applied Polymer Science*, 13, 1741-1747.
- Padday, J.F. (1969). Theory of surface tension. In E. Matijevic (Ed), *Surface and Colloid Science*, John Wiley & Sons, Inc., New York.
- Padley, F.B. (1997). Chocolate and confectionery fats. In F.D. Gunstone and F.B. Padley (Eds.), *Lipid Technologies and Applications* (pp. 391-432). Marcel Dekker, New York.
- Pereni, C.I., Zhao, Q., Liu, Y. & Abel, E. (2006). Surface free energy effect on bacterial retention. *Colloids and Surfaces B – Biointerfaces*, 48, 143-147.
- Pinschower, K. (2003). *Direct Measurement of the Contraction of Chocolate during Solidification*. Ph.D. Thesis, University of Birmingham.

## References

---

- PRODCOM (2008). PRA15840 Product Sales and Trade: Cocoa, Chocolate and Sugar Confectionery. National Statistics, UK.
- Pucciarelli, D.L. & Grivetti, L.E. (2008). Review – The Medicinal Use of Chocolate in Early North America. *Mol. Nutr. Food Res.*, 52, 1215-1227.
- Quevedo, R., Brown, C., Bouchon, P. & Aguilera, J.M. (2005). Surface roughness during storage of chocolate: fractal analysis and possible mechanisms. *Journal of the American Oil Chemists' Society*, 82(6), 457-462.
- Quezado Gallo, J.-A., Debeaufort, F., Callegarin, F. & Voilley, A. (2000). Lipid hydrophobicity, physical state and distribution effects on the properties of emulsion-based edible films. *Journal of Membrane Science*, 180, 37-46.
- Rodríguez, M., Osés, J., Ziani, K. & Maté, J.I. (2006). Combined effect of plasticizers and surfactants on the physical properties of starch based edible films. *Food Research International*, 39, 840-846.
- Rosmaninho, R., Visser, H. & Melo, L. (2004). Influence of surface tension components of stainless steel on fouling caused by calcium phosphate. *Progress in Colloid and Polymer Science*, 123, 203-209.
- Rosmaninho, R. & Melo, L.F. (2006). Calcium phosphate deposition from simulated milk ultrafiltrate on different stainless steel-based surfaces. *International Dairy Journal*, 16, 81-87.
- Rosmaninho (2007), R., Santos, O., Nylander, T., Paulsson, M., Beuf, M., Benezech, T., Yiantsios, S. Andritsos, N., Karabelas, A., Rizzo, G., Müller-Steinhagen, H. & Melo, L.F. (2007). Modified stainless steel surfaces targeted to reduce fouling – Evaluation of fouling by milk components. *Journal of Food Engineering*, 80, 1176-1187.
- Rousseau, D. (2007). The microstructure of chocolate. In D.J. McClements (Ed), *Understanding and Controlling the Microstructure of Complex Foods* (pp. 648-690). Woodhead Publishing Limited, Cambridge.
- Rousseau, D. & Sonwai, S. (2008). Influence of the dispersed particulate in chocolate on cocoa butter microstructure and fat crystal growth during storage. *Food Biophysics*, 3, 273-278.
- Rusanov, A.I. (1996). Thermodynamics of solid surfaces. *Surface Science Reports*, 23, 173-247.
- Saikhwan, P., Geddert, T., Augustin, W. Scholl, S., Paterson, W.R. & Wilson, D.I. (2006). Effect of surface treatment on cleaning of a model food soil. *Surface and Coatings Technology*, 201 (3-4), 943-951.



## References

---

- Sato, K. (1993). Polymorphic transformations in crystal growth. *Journal of Physics, D. – Applied Physics*, 26, B77-B84.
- Sato, K. (2001). Crystallization behaviour of fats and lipids – a review. *Chemical Engineering Science*, 56, 2255-2265.
- Sato, K. & Koyano, T. (2001). Crystallization properties of cocoa butter. In N. Garti & K. Sato (Eds.), *Crystallization Processes in Fats and Lipid Systems* (pp. 429-456). CRC Press, Boca Raton.
- Saunders, S.R., Hamann, D.D. & Lineback, D.R. (1992). A systems approach to food material adhesion. *Lebensmittel-Wissenschaft & Technologie*, 25 (4), 309-15.
- Schantz, B., Linke, L. & Rohm, H. (2005). Effects of different emulsifiers on rheological and physical properties of chocolate. *Proceedings of the 3th International Symposium on Food Rheology and Structure*, Proceedings Lectures II, 329-333.
- Schenk, H. & Peschar, R. (2004). Understanding the structure of chocolate. *Radiation Physics and Chemistry*, 71, 829-835.
- Schou, M., Longares, A., Montesinos-Herrero, C., Monahan, F.J., O’Riordan, D. & O’Sullivan (2005). *Properties of edible sodium caseinate films and their application as food wrapping*. *Lebensmittel-Wissenschaft und –Technologie*, 38, 605-610.
- Schrader, M. E. (2003). Effect of adsorbed vapour on liquid–solid adhesion. In K.L. Mittal (Ed.), *Contact Angle, Wettability and Adhesion*, Vol. 3, 67-91.
- Sharma, P.K. & Rao, K.H. (2002). Analysis of different approaches for evaluation of surface energy of microbial cells by contact angle goniometry. *Advances in Colloid and Interface Science*, 98, 341-463.
- Shaw, D.J. (1992). *Introduction to Colloid and Surface Chemistry*. Butterworth-Heinemann, Oxford.
- Sheen Instruments (2003). *Gloss & Appearance*. Product data sheet. Available from the World Wide Web: <http://www.sheeninstruments.com/products/gloss/glossmaster.htm> [May 2006].
- Siboni, S., Della Volpe, C., Maniglio, D. & Brugnara, M. (2004). The solid surface free energy calculation - II. The limits of the Zisman and of the "equation-of-state" approaches. *Journal of Colloid and Interface Science*, 271 (2), 454-472.
- Sigma-Aldrich (2009). *Product Safety Center – Material Safety Data Sheet (MSDS)*. Available from the World Wide Web: <http://www.sigmaaldrich.com/safety-center.html> [January 2006].

## References

---

- Singh, P. & Heldman, D.R. (2001). *Introduction to Food Engineering (3<sup>rd</sup> ed)*. Academic Press, London.
- Sonwai, S. & Mackley, M.R. (2006). The effect of shear on the crystallization of cocoa butter. *Journal of the American Oil Chemists Society*, 83, 583-596.
- Sonwai, S. & Rousseau, D. (2008). Fat crystal growth and microstructural evolution in industrial milk chocolate. *Crystal Growth & Design*, 8(9), 3165-3174.
- Sorrentino A., Gorrasi, G. & Vittoria V. (2007). Potential perspectives of bio-nanocomposites for food packaging applications. *Trends in Food Science & Technology*, 18, 84-95.
- Stalder, A.F., Kulik, G., Sage, D., Barbieri, L. & Hoffmann, P. (2006). A snake-based approach to accurate determination of both contact points and contact angles. *Colloids and Surfaces A – Physicochemical and Engineering Aspects*, 286, 92-103.
- Stapley, A.G.F., Tewkesbury, H. & Fryer, P.J. (1999). The effects of shear and temperature history on the crystallization of chocolate. *Journal of the American Oil Chemists Society*, 76, 677-685.
- Talbot, G. (1999a). Chocolate temper. In S.T. Beckett (Ed), *Industrial Chocolate Manufacture and Use* (pp. 218-230). Blackwell Science, Oxford.
- Talbot, G. (1999b). Vegetable fats. In S.T. Beckett (Ed), *Industrial Chocolate Manufacture and Use* (pp. 307-322). Blackwell Science, Oxford.
- Tang, D. & Marangoni, A.G. (2007). Structure and function fat crystals and their role in microstructure formation in complex foods. In D.J. McClements (Ed), *Understanding and Controlling the Microstructure of Complex Foods* (pp. 67-88). Woodhead Publishing Limited, Cambridge.
- Tewkesbury, H., Stapley, A.G.F. & Fryer, P.J. (2000). Modelling temperature distributions in cooling chocolate moulds. *Chemical Engineering Science*, 55, 3123-3132.
- Timms, R.E. (1997). Fractionation. In F.D. Gunstone and F.B. Padley (Eds.), *Lipid Technologies and Applications* (pp. 199-222). Marcel Dekker, New York.
- Toro-Vazquez, J.F., Pérez-Martínez, D., Dibildox-Alvarado, E., Charó-Alonso, M. & Reyes-Hernández, J. (2004). Rheometry and polymorphism of cocoa butter during crystallization under static and stirring conditions. *Journal of the American Oil Chemists Society*, 81, 195-202.
- Tscheuschner, H.-D. & Markov, E. (1989). Instrumental texture studies on chocolate. II. Compositional factors influencing texture. *Journal of Texture Studies*, 20, 335-345.
- Tsibouklis, J. & Nevell, T.G. (2003). Ultra-low surface energy polymers: the molecular design requirements. *Advanced Materials*, 15 (7-8), 647-650.

## References

---

- Tsibouklis, J., Stone, M., Thorpe, A.A., Graham, P., Peters, V., Heerlien, R., Smith, J.R., Green, K.L. & Nevell, T.G. (1999). Preventing bacterial adhesion onto surfaces: the low-surface-energy approach. *Biomaterials*, 20 (13), 1229-1235.
- Van Malssen, K, van Langevelde, A., Peschar, R. & Schenk, H. (1999). Phase behavior and extended phase scheme of static cocoa butter investigated with real-time X-ray powder diffraction. *Journal of the American Oil Chemists Society*, 76, 669-676.
- Van Oss, C.J. (2006). *Interfacial Forces in Aqueous Media* (2<sup>nd</sup> ed.). CRC Press, New York.
- Van Oss, C.J. and Good, R.J. (1989). Surface tension and the solubility of polymers and biopolymers: the role of polar and apolar interfacial free-energies. *Journal of Macromolecular Science – Part A*, 26 (8), 1183-1203.
- Van Oss, C.J., Good, R.J. & Chaudhury, M.K. (1986). The role of van der Waals forces and hydrogen-bonds in hydrophobic interactions between bio-polymers and low energy surfaces. *Journal of Colloid and Interface Science*, 111, 378-390.
- Van Oss, C.J., Good, R.J. & Chaudhury, M.K. (1988a). Additive and nonadditive surface tension components and the interpretation of contact angles. *Langmuir*, 4, 884-891.
- Van Oss, C.J., Good, R.J. & Chaudhury, M.K. (1988b). Interfacial Lifshitz–van der Waals and polar interactions in macroscopic systems. *Chemical Reviews*, 88, 927-941.
- Walstra, P. (1996). Dispersed systems: basic considerations. In O.R. Fennema (Ed.), *Food Chemistry* (3<sup>rd</sup> ed.) (pp. 95-155). Marcel Dekker, New York.
- Walstra, P. (2003). *Physical Chemistry of Foods*. Marcel Dekker, New York.
- Walstra, P., Kloek, W. & van Vliet, T. (2001). Fat crystal networks. In N. Garti and K. Sato (Eds.), *Crystallization Processes in Fats and Lipid Systems* (289-328). Marcel Dekker, New York.
- Werner, S.R.L., Jones, J.R. & Paterson, A.H.J. (2007a). Stickiness of maltodextrins using probe tack test during in-situ drying. *Journal of Food Engineering*, 80, 859-868.
- Werner, S.R.L., Jones, J.R. & Paterson, A.H.J. (2007b). Stickiness during drying of amorphous skin-forming solutions using a probe tack test. *Journal of Food Engineering*, 81, 647-656.
- Wille, R.L. & Lutton, E.S. (1966). Polymorphism of cocoa butter. *Journal of the American Oil Chemists Society*, 43, 942.
- Wu, Y., Weller, C.L., Hamouz, F., Cuppett, S.L. & Schnepf, M. (2002). Development and application of multicomponent edible coatings and films: a review. *Advances in Food and Nutrition Research*, 44, 347-394.



## References

---

- Wyatt, L.M., Coveney, V., Riddlford, C. & Sharpe R. (1998). Materials, properties and selection. In E.H. Smith (Ed.), *Mechanical Engineer's Reference Book* (12<sup>th</sup> ed) (pp. 330-). Elsevier Butterworth-Heinemann, Oxford, UK.
- Zhao, Q. (2004). Effect of surface free energy of graded NI-P-PTFE coatings on bacterial adhesion. *Surface and Coatings Technology*, 185 (2-3), 199-204.
- Zhao, Q., Liu, Y. & Abel, E.W. (2004a). Effect of temperature on the surface free energy of amorphous carbon films. *Journal of Colloid and Interface Science*, 280, 174-183.
- Zhao, Q., Wang, S. & Müller-Steinhagen, H. (2004b). Tailored surface free energy of membrane diffusers to minimize microbial adhesion. *Applied Surface Science*, 230 (1-4), 371-378.
- Zhao, Q., Liu, W., Wang, C. Wang, S. & Muller-Steinhagen, H. (2005). Effect of surface free energy on the adhesion of biofouling and crystalline fouling. *Chemical Engineering Science*, 60, 4858-4865.
- Ziegler, G. & Hogg, R. (1999). Particle size reduction. In S.T. Beckett (Ed), *Industrial Chocolate Manufacture and Use* (pp. 115-136). Blackwell Science, Oxford.
- Ziegler, G.R., Garbolino, C. and Coupland, J.N. (2003). The influence of surfactants and moisture on the colloidal and rheological properties of model chocolate dispersions. *Proceedings of the 3th International Symposium on Food Rheology and Structure*, Proceedings Lectures II, 335-338.

## PUBLICATIONS

1. Keijbets, E.L., Chen, J. Dickinson, E. & Vieira, J. (2009). Surface energy investigation of chocolate adhesion to solid mould materials. *Journal of Food Engineering*, 92 (2), 217-225.
2. Keijbets, E.L., Chen, J. & Vieira, J. (2010). Chocolate demoulding and effects of processing conditions. *Journal of Food Engineering*, 98 (1), 133-140.